Terms and Conditions of Use of Digitised Theses from Trinity College Library Dublin

Copyright statement

All material supplied by Trinity College Library is protected by copyright (under the Copyright and Related Rights Act, 2000 as amended) and other relevant Intellectual Property Rights. By accessing and using a Digitised Thesis from Trinity College Library you acknowledge that all Intellectual Property Rights in any Works supplied are the sole and exclusive property of the copyright and/or other IPR holder. Specific copyright holders may not be explicitly identified. Use of materials from other sources within a thesis should not be construed as a claim over them.

A non-exclusive, non-transferable licence is hereby granted to those using or reproducing, in whole or in part, the material for valid purposes, providing the copyright owners are acknowledged using the normal conventions. Where specific permission to use material is required, this is identified and such permission must be sought from the copyright holder or agency cited.

Liability statement

By using a Digitised Thesis, I accept that Trinity College Dublin bears no legal responsibility for the accuracy, legality or comprehensiveness of materials contained within the thesis, and that Trinity College Dublin accepts no liability for indirect, consequential, or incidental, damages or losses arising from use of the thesis for whatever reason. Information located in a thesis may be subject to specific use constraints, details of which may not be explicitly described. It is the responsibility of potential and actual users to be aware of such constraints and to abide by them. By making use of material from a digitised thesis, you accept these copyright and disclaimer provisions. Where it is brought to the attention of Trinity College Library that there may be a breach of copyright or other restraint, it is the policy to withdraw or take down access to a thesis while the issue is being resolved.

Access Agreement

By using a Digitised Thesis from Trinity College Library you are bound by the following Terms & Conditions. Please read them carefully.

I have read and I understand the following statement: All material supplied via a Digitised Thesis from Trinity College Library is protected by copyright and other intellectual property rights, and duplication or sale of all or part of any of a thesis is not permitted, except that material may be duplicated by you for your research use or for educational purposes in electronic or print form providing the copyright owners are acknowledged using the normal conventions. You must obtain permission for any other use. Electronic or print copies may not be offered, whether for sale or otherwise to anyone. This copy has been supplied on the understanding that it is copyright material and that no quotation from the thesis may be published without proper acknowledgement.

Identification, Isolation and Validation of Ovarian Cancer Stem Cells.

Ph. D. 2013

Brendan Ffrench

Declaration

I declare that this thesis has not been submitted as an exercise for a degree at this or any other university and it is entirely my own work.

I agree to deposit this thesis in the University's open access institutional repository or allow the library to do so on my behalf, subject to Irish Copyright Legislation and Trinity College Library conditions of use and acknowledgement.

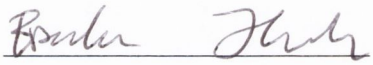

Brendan Ffrench

Abstract

Ovarian cancer is often diagnosed at a late stage. Even so, it often responds (~73 %) to first-line therapies. However, the five year survival rate for late stage ovarian cancer is poor (~27 %). It is hypothesised that recurrent chemoresistant ovarian cancer is driven by a small residual population of ovarian cancer stem cells (OvCSCs), which have adapted to chemotherapy. This project aims to isolate and characterise OvCSCs with the long-term intention of identifying therapeutically targetable pathways within OvCSCs. Such therapies could minimise the cases of recurrent ovarian cancer and bring the five year survival rate back in line with the first-line therapy response rates.

CSCs must be isolated to a high degree of purity before the can be studied. Here six models of ovarian malignancy and one model of non-malignant ovarian surface epithelium were screened for the presence of OvCSCs and somatic stem cells respectively. These models include pair matched chemosensitive and chemoresistant cell lines as well as cell lines established from metastatic ascites and solid tumour sources. This enables the study of the role of CSCs in chemoresistance and metastasis.

Putative ovarian CSCs were successfully identified using; ALDEFLUOR™ (ALDH), Hoechst Side-Population (HSP) and Cell Surface Protein (CSP) Assays (CD44, CD117, CD133, CXCR4) and isolated via fluorescence-assisted cell sorting (FACS). Putative CSCs (pCSCs) were successfully validated in NOD.SCID mouse tumourgenicity assays and single cell self-renewal and differentiation assays.

The results presented indicate the presence of multiple pCSC populations within several of the model systems. A sub-set of 12 pCSCs and non-pCSCs were isolated from multiple cell lines via FACS, including a pair of cisplatin sensitive and cisplatin adapted cell lines. The pCSCs and non-pCSCs were validated as CSCs and non-CSCs in a pair of ovarian cancer models. Analysis of these CSC and non-CSC sub-populations identified a potential cancer stemness hierarchy in ovarian cancer (ALDH_NegA → ALDH+ → ALDH_NegB). The data and materials produced in this project enables the future work of the laboratory to establish stable OvCSC model systems and identify the molecular mechanisms of differentiation in OvCSCs, which can be targeted therapeutically.

The data and materials produced have taken another step forward toward the development of CSC directed cancer therapies, which are not susceptible to CSC driven relapse, metastasis and acquired chemoresistance.

Table of Contents

Declaration....i
Abstract....ii
Table of Contents....iii
Index of Figures....xi
Index of Tables....xiii
List of Abbreviations....xiv
List of Presentations and Publications....xvi
Acknowledgements....xvii

1.0 General Introduction
1.1Introduction:....1
1.2Premise of this Study:....2
1.3Stem Cell Biology forms the Basis of CSC Research:....2
1.4CSC Research is the Application of Stem Cell Principles to the Study of Cancer:....5
1.5Cancer Stem Cells:....7
1.6Ovarian Cancer:....11
1.7Ovarian Cancer Stem Cells:....14
1.8Developmental Biology of the Ovary:....16
1.9Modelling Ovarian Cancer:....17
1.9.1Modelling Chemoadaptation:....18
1.9.2Modelling Metastasis:....19
1.9.3Modelling Normal Ovarian Surface Epithelium:....19
1.10 Identification of CSCs:....19
1.10.1ALDEFLUORTM Assay:....20
1.10.2 Hoechst Side Population Assay:....22
1.10.3Cell Surface Protein Assay:....23
1.10.3.1CD44:....24
1.10.3.2CD117:....24
1.10.3.3CD133:....25
1.10.3.4CXCR4:....25
1.11FACS is the Best Method for Isolation of Cancer Stem Cells:....26
1.11.1Spheroid Growth:....26
1.11.2 Holoclones, Meroclones and Paraclones:....27
1.11.3 Magnetic-Activated Cell Sorting:....28
1.11.4 Fluorescence-Activated Cell Sorting:....29
1.12Flow Cytometry:....30
1.12.1Flow Cytometry Overview:....30
1.12.2Flow Cytometry Analysis:....30
1.12.3Fluorescence-activated Cell Sorting (FACS):....32
1.13CSCs Provide Avenues for Novel Therapeutic Approaches:....32
1.14Summary:....34
1.15References:....37

2.0 Materials and Methods
2.1Culture and Sub-Culture....36
2.2All-Trans-Retinoic acid (RA) differentiation of NT2 cells....38
2.3Cell Counting....39
2.4Flow Cytometry based pCSC screen....39
2.4.1ALDH Assay....39

Table of Contents

2.4.2HSP Assay....40
2.4.3CSP Assay....40
2.4.4Dead Cell Staining....42
2.4.5Cyan ADP Flow Cytometric Analysis....42
2.4.6Multi-parametric Analysis....43
2.5Fluorescence-activated Cell Sorting....44
2.5.1ALDH Assay....44
2.5.2HSP Assay....44
2.5.3CSP Assay....45
2.5.4Post Cell Sorting....45
2.6Mouse Tumourgenicity Assay....45
2.6.1Ethics....46
2.6.2Housing....47
2.6.3Handling Mice....47
2.6.4Ear Punching....47
2.6.5Shaving....47
2.6.6Injecting....48
2.6.7Euthanasia....48
2.6.8Post-mortem Inspection....49
2.6.8.1i) Identifying and recording the tumour....49
2.6.8.2v) Fixing, embedding and staining....50
2.7Single Cell Self-renewal and Differentiation (SD) Assay....50
2.7.1Plating Single Cells....50
2.7.2Passaging the Colonies....50
2.7.3Retesting for Cancer Stemness Markers....51

3.0 Optimisations

3.1Introduction....52
3.1.1Flow Cytometry Based Screening and Isolation:....52
3.1.1.1ALDH Assay Optimisations:....53
3.1.1.2HSP Assay Optimisations:....54
3.1.1.3CSP Assay Optimisations:....54
3.1.1.3.1Antibody and Fluorochrome Selection....54
3.1.2Validation....55
3.1.2.1Tumourgenicity Assay....56
3.1.2.1.1Cell Vehicle....56
3.1.2.1.2Proof of Principle....57
3.1.2.2SD Assay....57
3.1.2.2.1Serial Dilution....57
3.1.2.2.2FACS Validated by High Throughput Imaging....58
3.1.2.2.3FACS of Pure Populations – No Visual Validation, Statistical Approach....58
3.1.3Aims....59
3.2Materials and Methods....60
3.2.1Cell Culture and Sub-Culture:....60
3.2.2Differentiation of NTera2 Cells....60
3.2.3Cell Dissociation Techniques....60
3.2.4Flow cytometry....60
3.2.4.1Technical Controls....60
3.2.4.2ALDH Assay....60
3.2.4.3HSP Assay....61

Table of Contents

3.2.4.4CSP Assay....61
3.2.5FACS....61
3.2.6In Vivo Mouse Tumourgenicity Assay....61
3.2.7SD Assay....61
3.2.7.1Serial dilution....61
3.2.7.2InCELL Analyser....61
3.3Data....62
3.3.1Flow Cytometry
....62
3.3.1.1Establishing the ALDH CSC Screening Assay:....62
3.3.1.2Establishing the ALDH CSC Isolation Procedure:....64
3.3.1.2.1Scaling the ALDH Assay....64
3.3.1.2.2Identifying the Positive/Negative Threshold....65
3.3.1.3Establishing the HSP CSC Screening Assay:....67
3.3.1.4CSP Assay Optimisations....72
3.3.1.4.1Establishing the CSP CSC Screening Assay – antiCD44 Staining....72
3.3.1.4.2Establishing the CSP CSC Screening Assay – antiCD117 Staining....73
3.3.1.4.3Establishing the CSP CSC Screening Assay – CD133....74
3.3.1.4.4Establishing the CSP CSC Screening Assay – antiCXCR4 Staining....75
3.3.1.5Summary of the Flow Cytometry Optimisations....76
3.3.2Establishing the In Vivo Mouse Tumourgenicity CSC Validation Assay:....76
3.3.2.1CSC Proof of Principle....78
3.3.3Establishing the SD CSC Validation Assay:....86
3.3.3.1Approaches to Single Cell plating....86
3.3.3.1.1Serial Dilution and Light Microscope....86
3.3.3.1.2FACS and High Content Analysis....88
3.3.3.1.3Pre-purify and FACS....88
3.3.3.2Summary of SD Assay Optimisations....89
3.4Discussion....90
3.4.1Positive and negative controls were central to the establishment of flow cytometry based identification and isolation of pCSCs....90
3.4.1.1The scaling of the ALDH assay staining reaction and the inclusion of an additional gating control enables the use of the ALDH assay in the identification and isolation of pCSC regardless of the ALDH+ population size....91
3.4.1.2HSP Assay....92
3.4.1.3Positive and Negative Controls Established:....92
3.4.2UndiffNT2 and diffNT2SSEA4- cells demonstrate that the in vivo tumourgenicity assay established in this project is fit for the purpose of CSC validation....93
3.4.3SD Assay is not only a Validation Assay but has the power to identify further sub-populations within purified samples:....94
3.4.4Summary....96
3.5References....97

4.0 Identification of Putative Cancer Stem Cells.

4.1Introduction:....98
4.1.1The Difference between Screening and Selection....98
4.1.2pCSC Markers....98
4.1.3The pCSC marker panel....99
4.1.4The Model Systems Screened....99
4.1.5The Approach to Screening....100

Table of Contents

4.1.6Ranking pCSCs....100
4.1.7Aims....101
4.1.8Hypotheses....102
4.2Materials and Methods:....103
4.2.1Cell Culture and Sub-Culture....103
4.2.2Flow Cytometry....103
4.2.2.1ALDH Assay....103
4.2.2.2HSP Assay....103
4.2.2.3CSP Assay....103
4.2.2.4Multi-parametric staining....103
4.2.2.4.1Multi-marker CSP Assay Staining....103
4.2.2.4.2ALDH Assay and CSP Assay Staining....104
4.2.2.4.3HSP Assay, ALDH Assay and CSP Assay Staining....104
4.3Data:....105
4.3.1ALDH Assay....106
4.3.2The HSP Assay....107
4.3.3The CSP Assay....108
4.3.3.1Summary of single parametric CSP Screen....110
4.3.4pCSC Hierarchies....111
4.3.4.1IGROV-1 Multi-Parametric Staining....111
4.3.4.2IGROV-CDDP Multi-Parametric Staining....113
4.3.5Ranking the pCSC Populations Identified....116
4.3.5.1Statistical Ranking....116
4.3.5.2Hypothesis Based Ranking....119
4.3.6pCSC screen Summary....122
4.4Discussion:....123
4.4.1Screening for OvCSC:....123
4.4.2The OvCSC Field:....124
4.4.3The Advantages and Disadvantages of Large Flow Cytometry Based pCSC Screens:
....125
4.4.4Furthering the Understanding of OvCSC Biology:....127
4.4.4.1Novel pCSCs and pSSCs have been identified:....127
4.4.4.2Poor Correlation between OvCSC markers:....129
4.4.4.3Hierarchical OvCSCs:....131
4.4.4.3.1A2780 Hierarchies....131
4.4.4.3.2A2780cis Hierarchies....132
4.4.4.3.3IGROV-1 Hierarchies....132
4.4.4.3.4IGROV-CDDP Hierarchies....132
4.4.4.3.5SK-OV-3 Hierarchies....133
4.4.4.3.659M Hierarchies....133
4.4.4.3.7HIO-80 Hierarchies....134
4.4.4.4Comparison of pCSCs between models....134
4.4.4.4.1Cisplatin Sensitive and Cisplatin Resistant pCSCs....134
4.4.4.4.2The Role of pCSCs in Metastasis....135
4.4.4.4.3The Role of the CD133+ pCSC....136
4.4.5Future Directions:....138
4.4.6Summary:....139
4.5References:....140

Table of Contents

5.0 Isolation of Putative Cancer Stem Cells.

5.1Introduction:....140
5.1.1The Role of Cell Sorting in Cancer Biology:....140
5.1.2Approaches to CSC Isolation:....141
5.1.3Prioritisation of pCSC for Isolation:....142
5.1.4Summary:....142
5.2Materials and Methods:....143
5.2.1Cell Culture and Sub-Culture....143
5.2.2Flow Cytometry....143
5.2.2.1ALDH Assay....143
5.2.2.2HSP Assay....143
5.2.2.3CSP Assay....143
5.2.3FACS....143
5.3Data:....144
5.3.1A2780....145
5.3.2A2780cis....148
5.3.3IGROV-1....152
5.3.4IGROV-CDDP....156
5.3.5SK-OV-3....159
5.3.659M....162
5.4Discussion....165
5.4.1Isolation of Sub-populations:....165
5.4.1.1The CSCs' Role in Therapeutic Evasion and Acquired Chemoresistance:....166
5.4.1.1.1Probing the intrinsic resistance of CSCs:....166
5.4.1.1.2Identifying the molecular pathways behind intrinsic and/or acquired chemoresistance:....167
5.4.1.1.3Investigating the hereditary changes associated with acquired chemoresistance in ovarian cancer:....168
5.4.1.2The CSCs' Role in Metastatic Ascites:....169
5.4.2Stability of the isolated sub-populations:....171
5.4.3Summary:....172
5.5References....174

6.0 Validation of Cancer Stem Cells.

6.1Introduction:....167
6.1.1Predefined Xenograft Mouse Assay Parameters:....168
6.1.1.1.1Strain of Mouse....168
6.1.1.1.2Mode of Injection....169
6.1.2Principles of the Xenograft Mouse Assay:....170
6.1.3Principles of the SD Assay:....171
6.1.4Tumourgenicity based versus SD based validation:....172
6.1.5Aims:....173
6.1.6Hypothesis....173
6.2Materials and Methods:....174
6.2.1Cell Culture and Sub-Culture:....174
6.2.2Mouse Tumourgenicity Assay:....174
6.2.2.1Housing....174
6.2.2.2Handling....174
6.2.2.3Ear-punching....175
6.2.2.4Shaving....175

Table of Contents

6.2.2.5Injecting....175
6.2.2.6Euthanasia....175
6.2.2.7Post-mortem Inspection....175
6.2.3Single Cell Self-renewal and Differentiation Assay....175
6.2.4Flow Cytometry:....175
6.2.4.1ALDH Assay....175
6.2.4.2HSP Assay....175
6.2.4.3CSP Assay....175
6.3Data:....176
6.3.1Primary Ovarian Cancer A2780 CSC Assay Data:....178
6.3.1.1Mouse Tumourgenicity Assay:....178
6.3.1.1.1Size and Latency:....178
6.3.1.1.2Histopathology:....180
6.3.1.2Single Cell Self-renewal and Differentiation Assay:....182
6.3.1.2.1A2780 ALDH- non-pCSC clones:....182
6.3.1.2.2A2780 ALDH+pCSC clones:....185
6.3.2Cisplatin-Adapted Primary Ovarian Cancer A2780cis CSC Assay Data:....187
6.3.2.1Mouse Tumourgenicity Assay:....187
6.3.2.1.1Size and Latency:....187
6.3.2.1.2Histopathology:....188
6.3.2.2Single Cell Self-renewal and Differentiation Assay:....190
6.3.2.2.1A2780cis ALDH- non-pCSC clones:....190
6.3.2.2.2A2780cis ALDH+ pCSC clones:....192
6.3.3Primary Ovarian Cancer IGROV-1 CSC Assay Data:....193
6.3.3.1Mouse Tumourgenicity Assay:....193
6.3.3.2Single Cell Self-renewal and Differentiation Assay:....195
6.3.4Cisplatin-adapted Primary Ovarian Cancer IGROV-CDDP CSC Assay Data:....197
6.3.4.1Mouse Tumourgenicity Assay:....197
6.3.4.2Single Cell Self-renewal and Differentiation Assay:....199
6.3.5SK-OV-3:....201
6.3.5.1Single Cell Self-renewal and Differentiation Assay:....201
6.3.659M:....203
6.3.6.1Single Cell Self-renewal and Differentiation Assay:....203
6.4Discussion:....206
6.4.1Outcomes of the Functional Validations....206
6.4.1.1The A2780 and A2780cis cell lines contains more than one CSC sub-population:....207
6.4.1.2The HSP+ sub-populations of IGROV-1 and IGROV-CDDP cell lines are non-apical CSCs/progenitors in a stem cell hierarchy: 208
6.4.1.3The SK-OV-3 and 59M CD117+ pCSCs and non-pCSCs are not well suited to SD based CSC validation:....210
6.4.2Cancer stem cell populations in the A2780 and A2780cis models....211
6.4.2.1Malignant potential:....211
6.4.2.2Differentiation and self-renewal potential:....211
6.4.2.3A Revised Hypothesis:....213
6.4.3Two hypotheses regarding the CSC and non-CSC biology of acquired cisplatin resistance in Ovarian Cancer....216
6.4.4Tumourgenicity based validation of the IGROV-1 and IGROV-CDDP pCSC and non-pCSC sub-populations:....217

Table of Contents

6.4.5SD based validation of the SK-OV-3, 59M and A2780 pCSC and non-pCSC sub-populations:....218
6.4.6Summary:....220
6.5References:....222

7.0 Investigating the Predictions of the Revised ALDH_NegA/B Hypothesis.
7.1Introduction:....222
7.1.1Predictions of the revised ALDH_NegA/B Hypothesis:....222
7.1.2Aims:....224
7.1.3Hypotheses:....224
7.2Materials and Methods:....225
7.2.1Cell Culture and Sub-Culture:....225
7.2.2Mouse Tumourgenicity Assay:....225
7.2.2.1Housing....226
7.2.2.2Handling....226
7.2.2.3Ear-punching....226
7.2.2.4Shaving....226
7.2.2.5Injecting....226
7.2.2.6Euthanasia....226
7.2.2.7Post-mortem Inspection....226
7.2.3Single Cell Self-renewal and Differentiation Assay....226
7.2.4Flow Cytometry:....226
7.2.4.1ALDH Assay....226
7.2.4.2HSP Assay....226
7.2.4.3CSP Assay....226
7.3Data:....227
7.3.1A2780 ALDH_NegB Malignant Potential:....227
7.3.2A2780cis ALDH_NegB Malignant Potential....232
7.4Discussion:....236
7.4.1A2780 and A2780cis ALDH_NegB experiments:....236
7.4.2Testing the Predictions of the Revised ALDH_A/B Hypothesis:....238
7.4.2.1Identification of ALDH_NegA and ALDH_NegB markers:....238
7.4.2.2ALDH_NegA cells are predicted to differentiate to produce both ALDH+ and ALDH_NegB cells:....239
7.4.2.3ALDH+ cells are predicted to differentiate to produce ALDH_NegB but not ALDH_NegA cells:....239
7.4.2.4ALDH_NegB Cells are predicted to have a reduced malignant potential when compared to ALDH+ and ALDH_NegA cells:....240
7.4.2.5It is predicted that ALDH_NegA and ALDH+ cells can be force differentiated to produce ALDH_NegB:....241
7.4.3Summary:....242
7.5References:....243

8.0 General Discussion
8.8Introduction:....241
8.9Viewing tumours as a malignant form of organogenesis can improve our understanding of the disease:....241
8.10 The experimental system established for this project systematically isolates ovarian CSCs and is readily transferable to patient samples and other malignancies:....244

Table of Contents

8.11The data and materials produced in the screening and validation phases of this study identified models systems in which to study hierarchial cancer stemness and enabled the mapping of self-renewal and differentiation pathways within cancer stem cell hierarchies: 245
8.12 CSC Hierarchies as opposed to CSC sub-populations may be better candidates for therapeutic targeting:.....247
8.13 A 'Clonal Cancer Stemness' model of cancer predicts the failure of unilateral therapeutic approaches and suggests that alternative, multifaceted therapeutic approaches should be more successful:.....248
8.14Summary:.....251
8.15References:.....252

9.0 Appendix DVD
Appendix Table of Contents
Appendix A
Appendix B
Appendix C

Index of Figures

Section 1.0 – General Introduction:
Figure 1.1: Stem Cell Potency....4
Figure 1.2: SSC Origin of Cancer....9
Figure 1.3: The Ovary....12
Figure 1.4: ALDH Staining....21
Figure 1.5: HSP Staining....22
Figure 1.6: Technical Flow Cytometry Controls....31

Section 3.0 – Optimisations:
Figure 3.1: A2780cis is a positive control for the ALDH assay....63
Figure 3.2: 59M is a negative control for the ALDH assay....63
Figure 3.3: ALDH Assay Cell Densities....64
Figure 3.4: Increasing the DEAB inhibitor concentration increases cell death....66
Figure 3.5: Increasing the DEAB inhibitor concentration did not decrease the fluorescence of the inhibited sample....66
Figure 3.6: ALDH Mixed Populations Control....67
Figure 3.7: IGROV-1-CDDP is a positive control for the HSP assay....68
Figure 3.8: A2780cis is a negative control for the HSP assay....68
Figure 3.9: The CyAn™ and MoFlo™ produce slightly different profiles for the HSP assay....70
Figure 3.10: SP and non-SP cells sorted on the MoFlo™ correspond to SP and non-SP populations identified on the CyAn™....71
Figure 3.11: SK-OV-3 is a positive control for antiCD44 staining....72
Figure 3.12: A2780cis is a negative control for anti CD44 staining....72
Figure 3.13: SK-OV-3 is a positive staining control for anti-CD117 staining....73
Figure 3.14: A2780cis is a negative control for anti-CD117 staining....73
Figure 3.15: UndiffN2 is a positive staining control for anti-CD133 staining....74
Figure 3.16: A2780cis is a negative staining control for anti-CD133 staining....74
Figure 3.17: Hela is a positive staining control for anti-CXCR4 staining....75
Figure 3.18: A2780cis is a negative staining control for anti-CXCR4 staining....75
Figure 3.19: Comparison of the tumourgenicity of 5 x 10^6 undifferentiated and differentiated cells....78
Figure 3.20: UndiffNT2 cells can escape differentiation....79
Figure 3.21: The diffNT2 tumour was made up of both diffNT2 and undiffNT2 cells....80
Figure 3.22: diffNT2 cells do not de-differentiate in the absence of RA....80
Figure 3.23: Comparison of the tumourgenicity of 5 x 10^4 undifferentiated and differentiated NT2 cells....82
Figure 3.24: There were no sign of atypical cells in the 5 x 10^4 diffNT2 s.c. regions....82
Figure 3.25: Hematoxylin and eosin stained undiffNT2 xenograft tumour....83
Figure 3.26: SSEA4- cells were purified from diffNT2 cells via FACS....84
Figure 3.27: Tumourgenicity CSC Validation Assay, Proof of Principle....85
Figure 3.28: Initial analysis of Serial Dilution Single cell plating....87
Figure 3.29: Analysis of Serial Dilution Single cell plating 18 days post-plating....87

Section 4.0 – Identification of Putative Cancer Stem Cells:
Figure 4.1: IGROV-1 multi-parametric CD44 staining....112
Figure 4.2: IGROV-CDDP multi-parametric CD133/ALDH Staining....113
Figure 4.3: IGROV-CDDP multi-parametric ALDH/HSP/CD133 Staining....115

Section 5.0 – Isolation of Putative Cancer Stem Cells:
Figure 5.1: ALDH+/- Cell Sorting of the A2780 Cell Line....146
Figure 5.2: Second round A2780 ALDH+ purification....147

Index of Figures

Figure 5.3: ALDH+/- Cell Sorting of the A2780cis Cell Line....148
Figure 5.4: Second round A2780cis ALDH+ purification....149
Figure 5.5: HSP+/- Cell Sorting of the IGROV-1 Cell Line....150
Figure 5.6: HSP+/- Cell Sorting of the IGROV-CDDP Cell Line....152
Figure 5.7: CD117+/- Cell Sorting of the SK-OV-3 Cell Line....154
Figure 5.8: Second round SK-OV-3 CD117+ purification....155
Figure 5.9: The CD117- and CD117+ sub-populations of SK-OV-3 have a different morphology in tissue culture....155
Figure 5.10: CD117+/- Cell Sorting of the 59M Cell Line....157
Figure 5.11: The 59M CD117+ Enriched Cells lost the CD117+ Phenotype....158

Section 6.0 – Validation of CSCs:
Figure 6.1: A2780 ALDH+ versus ALDH- Mouse Tumourgenicity Experiments....179
Figure 6.2: Hematoxylin and eosin stained of the A2780 ALDH+ and ALDH- derived tumours....181
Figure 6.3: A2780 ALDH_NegB Single Cell Asymmetric Division Assay....184
Figure 6.4: A2780 ALDH_NegA Single Cell Asymmetric Division Assay....184
Figure 6.5: A2780 ALDH- (Unclassified) Single Cell Asymmetric Division Assay....185
Figure 6.6: A2780 ALDH+ Single Cell Asymmetric Division Assay....186
Figure 6.7: A2780cis ALDH+ versus ALDH- Mouse Tumourgenicity Experiments....188
Figure 6.8: Hematoxylin and eosin stained of the A2780cis ALDH+ and ALDH- derived tumours....189
Figure 6.9: A2780cis ALDH- ALDH_NegA Single Cell Asymmetric Division Assay....191
Figure 6.10: A2780cis ALDH- (Unclassified) Single Cell Asymmetric Division Assay....191
Figure 6.11: A2780cis ALDH+ Single Cell Asymmetric Division Assay....192
Figure 6.12: IGROV-1 HSP+ versus HSP- Mouse Tumourgenicity Experiments....194
Figure 6.13: IGROV-1 HSP- Single Cell Asymmetric Division Assay....196
Figure 6.14: IGROV-1 HSP+ Single Cell Asymmetric Division Assay....196
Figure 6.15: IGROV-CDDP HSP+ versus HSP- Mouse Tumourgenicity Experiments....198
Figure 6.16: IGROV-CDDP HSP- Single Cell Asymmetric Division Assay....200
Figure 6.17: IGROV-CDDP HSP+ Single Cell Asymmetric Division Assay....201
Figure 6.18: SK-OV-3 CD117- Single Cell Asymmetric Division Assay....202
Figure 6.19: SK-OV-3 CD117+ Single Cell Asymmetric Division Assay....202
Figure 6.20: 59M CD117- Single Cell Asymmetric Division Assay....204
Figure 6.21: 59M CD117+ Single Cell Asymmetric Division Assay....205
Figure 6.22: A Revised Hierarchical CSC Hypothesis....214
Figure 6.23: A Stochastic De-differentiation Hypothesis....215

Section 7.0 – Investigating the Predictions of the Revised ALDH_NegA/B Hypothesis:
Figure 7.1: A2780 ALDH_NegB versus A2780 ALDH+ and A2780 ALDH- Mouse Tumourgenicity Experiments....229
Figure 7.2: A2780cis ALDH_NegB versus A2780cis ALDH+ and A2780cis ALDH- Mouse Tumourgenicity Experiments....232

Index of Tables

Section 2.0 – Materials and Methods:
Table 2.1: Origins of each cell line....36
Table 2.2: Cell Culture media used for each cell line....37
Table 2.3: Passaging information for each cell line....38
Table 2.4: Samples included in the CSP Assay....41
Table 2.5: CyAnTM ADP detector set-up for each of the pCSC screens....43

Section 4.0 – Identification of Putative Cancer Stem Cells:
Table 4.1: A Description of the Models Screened and the High Ranking pCSC Populations Identified....105
Table 4.2: An Overview of the ALDH assay defined pCSCs within Malignant and Normal Ovarian Epithelial cell lines....107
Table 4.3: An Overview of the HSP assay defined pCSCs within Malignant and Normal Ovarian Epithelial cell lines....108
Table 4.4: An Overview of the CSP assay defined pCSCs within Malignant and Normal Ovarian Epithelial cell lines....110
Table 4.5: ALDH assay defined pCSCs within Malignant and Normal Ovarian Epithelial cells. 117
Table 4.6: HSP assay defined pCSCs within Malignant and Normal Ovarian Epithelial cells. 117
Table 4.7: CD44 assay defined pCSCs within Malignant and Normal Ovarian Epithelial cells. 117
Table 4.8: CD117 assay defined pCSCs within Malignant and Normal Ovarian Epithelial cells. 118
Table 4.9: CD133 assay defined pCSCs within Malignant and Normal Ovarian Epithelial cells. 118
Table 4.10: CXCR4 assay defined pCSCs within Malignant and Normal Ovarian Epithelial cells....118
Table 4.11: pCSC sub-populations which passed the 99 % confidence test....119
Table 4.12: Acquired cisplatin resistance, significantly alters the size of all pCSC sub-populations identified....120
Table 4.13: pCSC and non-pCSC sub-populations which were selected to be brought forward for isolation and downstream analysis....122
Table 4.14: Summary of the possible sub-populations present in the IGROV-CDDP cell line.133

Section 5.0 – Isolation of Putative Cancer Stem Cells:
Table 5.1: pCSC sub-populations which were brought forward for isolation:....144

Section 6.0 – Validation of Putative Cancer Stem Cells:
Table 6.1: A comparison of immune cell deficiencies across three common mouse strains....168
Table 6.2: A summary of the sub-populations used in this chapter....174

Section 7.0 – Investigating the Predictions of the Revised ALDH_NegA/B Hypothesis:
Table 7.1: A2780 Tumourgenicity Assay – Comparison of Tumour Latency and Sizes....230
Table 7.2: A2780cis Tumourgenicity Assay – Comparison of Tumour Latency and Sizes....233

List of Abbreviations

3D3	–	Dimensional.
3Rs	–	Replacement, Reduction and Refinement.
ABC	–	Adenosine Triphosphate-Binding Cassette.
ALDH	–	ALDEFLUORTM™.
AML	–	Acute Myeloid Leukemia.
AML	–	Acute Myeloid Leukemia.
APC	–	Allophycocyanin.
APL	–	Acute Promyelocytic Leukemia.
ATCC	–	American Type Culture Collection.
B Cells	–	Bursa of Fabricius Cells.
BAAA	–	BODIPY-aminoacetaldehyde.
BCRP	–	Breast Cancer Resistance Protein.
BMP	–	Bone Morphogenic Protein.
CD	–	Cluster of Differentiation.
CPCs	–	Cancer Progenitor Cells.
CSCs	–	Cancer Stem Cells.
CSP	–	Cell Surface Protein.
DCV	–	Vybrant® DyeCycleTM Violet.
DEAB	–	Diethylaminobenzaldehyde.
dH20	–	Distilled water.
DMEM	–	Dulbecco's modified Eagle Medium.
ECACC	–	European Collection of Cell Cultures.
EDTA	–	Ethylene Diaminetetraacetic Acid.
ES	–	Embryonic Stem.
FACS	–	Fluorescence-Activated Cell Sorting
FBS	–	heat-inactivated Foetal Bovine Serum.
FIGO	–	The International Federation of Gynaecology and Obstetrics
FITC	–	Fluorescein.
FMO	–	Fluorescence Minus One.
FTE	–	Fallopian Tube Epithelium.
H342	–	Hoechst 33342.
HCDM	–	Human Cell Differentiation Molecules.
HE	–	Haematoxylin and Eosin.
HLDA	–	Human Leukocyte Differentiation Antigen.
HSCs	–	Haematopoetic Stem Cells.
HSP	–	Hoechst Side-Population.
i.p.	–	Intraperitoneal.
IgG	–	Immunoglubulin G.
KLH	–	keyhole Limpet Hemocyanin.
LAST	–	Laboratory Animal Science and Training.
LIF	–	Leukaemia Inhibitory Factor.
LSCs	–	Leukaemic Stem Cells.
MACS	–	Magnetic-Activated Cell Sorting.
MTT	–	Dimethylthiazol-Diphenyltetrazolium Bromide.
NK Cells	–	Natural Killer Cells.
NOD.SCID	–	Non-Obese Diabetic Severe Combined Immunodeficiency.
NOSE	–	Normal Ovarian Surface Epithelium.
NT2	–	NTera2.
OSE	–	Ovarian Surface Epithelium.
OvCSCs	–	Ovarian Cancer Stem Cells.

List of Abbreviations

P/S	–	Penicillin-Streptomycin.
PBS	–	Phosphate Buffered Saline.
pCSC	–	Putative Cancer Stem Cells.
PE	–	Phycoerythrin.
PI	–	Propidium Iodide.
RA	–	Retinoic Acid.
Rb	–	Retinoblastoma.
RPMI	–	Roswell Park Memorial Institute media.
RT-PCR	–	Real-Time Polymerase Chain Reaction.
s.c.	–	Sub-Cutaneous.
SCF	–	Stem Cell Factor.
SDF-1	–	Stromal Cell Derived Factor-1.
SD assay	–	self-renewal and differentiation assay.
SSCs	–	Somatic Stem Cells.
T Cells	–	Thymus Cells.
ToF	–	Time of Flight.
UV	–	Ultra-Violet.
VEGF	–	Vascular Endothelial Growth Factor.

Acknowledgements

I would like to acknowledge the support and guidance of my supervisor Prof. John O'Leary and my co-supervisor Dr. Michael Gallagher. Their mentorship was invaluable during the course of this project.

I would like to acknowledge Dr. Louise Kehoe, who processed the slides produced from the mouse tumourgenicity studies facilitating their histological analysis.

I would like to acknowledge Dr. Brendan Doyle, the pathologist who analysed the slides produced from the mouse tumourgenicity studies.

I would like to acknowledge Ann Atzberger and Barry Moran, the flow cytometry technicians who facilitated the isolation of the cell populations described in this thesis.

I would like to acknowledge the bioresources technicians who facilitated the in vivo mouse tumourgenicity assay described in this thesis.

I would also like to acknowledge the support of all my colleagues in the molecular pathology lab, Coombe Women's Hospital, as well as those based in the central pathology lab, St. James Hospital.

List of Presentations and Publications

Conference Poster Presentations:

2013: Poster Presentation – **Isolation and Interrogation of Ovarian Cancer Stem Cells.** Brendan Ffrench, Michael Gallagher, Aoife Cooke, Britta Stordal, Sharon O'Toole, Cara Martin, Orla Sheils, John O'Leary. USCAP 2013.

2013: Poster Presentation – **Inhibition of Human Embryonal Carcinoma Cancer Stem Cells by Co-Culture with Their Differentiated Progeny.** Michael F Gallagher, Brendan Ffrench, Claudia Gasch, Aoife Cooke, John J O'Leary. USCAP 2013.

2013: Poster Presentation – **Ovarian Cancer Stem Cells, Identification, isolation and characterisation.** B Ffrench, B Stordal, S O'Toole, O Shiels, M Gallagher and J O'Leary. IACR 2013.

2012: Poster Presentation – **A systematic approach to the study of cancer stem cells applied to ovarian cancer.** Brendan Ffrench, Aoife Cooke, Britta Stordal, Sharon O'Toole, Orla Shiels, Michael Gallagher, John O'Leary. AACR 2012

2012: Poster Presentation – **Isolation and Interrogation of Ovarian Cancer Stem Cells.** B Ffrench, B Stordal, S O'Toole, O Shiels, M Gallagher and J O'Leary. USCAP 2012

2012: Poster Presentation – **Ovarian Cancer Stem Cells, Identification, isolation and characterisation.** Brendan Ffrench, B Stordal, S O'Toole, O Shiels, M Gallagher and J O'Leary. IACR 2012.

2011: Poster Presentation – **Differentiated cells inhibit the proliferation of the pluripotent cancer stem cell pool. Ffrench** B, Gallagher M, McEneaney V, Cooke A, O'Leary J. Rediscovering Pluripotency: From Teratocarcinomas to Embryonic Stem Cells

Published Papers:

Platelet adhesion and degranulation induce pro-survival and pro-angiogenic signalling in ovarian cancer cells.
Egan K, Crowley D, Smyth P, O'Toole S, Spillane C, Martin C, Gallagher M, Canney A, Norris L, Conlon N, McEvoy L, **Ffrench B**, Stordal B, Keegan H, Finn S, McEneaney V, Laios A, Ducrée J, Dunne E, Smith L, Berndt M, Sheils O, Kenny D, O'Leary J.
PLoS One. 2011;6(10):e26125. doi: 10.1371/journal.pone.0026125. Epub 2011 Oct 12.

Suppression of cancer stemness p21-regulating mRNA and microRNA signatures in recurrent ovarian cancer patient samples.
Gallagher MF, Heffron CC, Laios A, O'Toole SA, **Ffrench B,** Smyth PC, Flavin RJ, Elbaruni SA, Spillane CD, Martin CM, Sheils OM, O'Leary JJ.
J Ovarian Res. 2012 Jan 19;5(1):2. doi: 10.1186/1757-2215-5-2.

General Introduction

Section 1.0 – General Introduction:

1.1 Introduction:

This thesis will describe the identification, isolation and validation of cancer stem cells (CSCs) from ovarian cancer sources. This thesis will approach the study of cancer from the viewpoint that cancer is a malignant form of organogenesis and tissue homoeostasis, initiated and propagated through acquired genetic mutations.

Cancer research strives to elucidate the biology of cancer, so that effective therapies can be developed and directed towards the treatment of patients with this terrible spectrum of disease. Cancer research often focuses on the genetic mutations that correlate with oncogenesis or the molecular pathways associated with malignant growth and invasion. Such studies have greatly contributed to the understanding, screening and treatment of cancer. Although cancer has its origins in genetic mutations and dysfunctional molecular pathways, it is not a disease of molecules but rather a disease of tissues. It is important to understand how the various genetic mutations and dysfunctional molecular pathways contribute to the functioning of the cells which make up the malignant tissue. It is hypothesised that through such understanding, novel ovarian cancer therapies can be developed which are not susceptible to chemoresistant recurrence.

Identification, isolation and study of different sub-populations of cells within cancerous tissues forms the foundation for investigating how different cell types contribute to the different aspects of malignancy, such as proliferation, invasion and metastasis. This project focuses on the study of CSCs, which are believed to be the root population, from which all the other cell types in the malignancy stem.

Ovarian cancer is infamous for its metastasis, recurrence rates and acquired chemoresistance. CSCs are also closely linked with these characteristics. It looks increasingly likely that CSCs are at least partly responsible for these lethal traits in ovarian cancer. CSCs offer a new therapeutic avenue to the treatment of ovarian cancer. To study ovarian CSCs (OvCSCs), they must first be identified and isolated from heterogeneous sources.

Section 1.0 – General Introduction:

1.2 Premise of this Study:

Women with ovarian cancer are often responsive (~73 %) to first line therapies (McGuire et al. 1996). However, chemoresistant recurrence is common (Lengyel 2010). Many studies have looked at the difference between chemosensitive and chemoresistant ovarian cancer (Brown et al. 1993; Woods et al. 1995; Perego et al. 1996). Such studies have identified glutathione and metallothionein levels as well as increased DNA repair/p53 mutation status as being associated with cisplatin resistance. Paclitaxel resistance has been found to be p53 mutation independent and associated with alterations in β-tubulin isotypes. However, little progress has been made in the treatment of ovarian cancer in the past 17 years, since it was discovered that cisplatin/paclitaxel combination therapy had a better response rate than cisplatin/cyclophosphamide combination therapy (McGuire et al. 1996).

As will be discussed throughout this section (Section 1.0), targeting of CSCs is an avenue through which ovarian cancer treatment may be improved. However, this is hindered by an absence of ovarian CSC models. Robust ovarian CSC models are required to identify targetable mechanisms such as those described in the previous paragraph. The first steps in developing such models is to identify, isolate and validate ovarian CSCs from primary and recurrent, chemosensitive and chemoresistant ovarian cancers. The basis of this thesis is the hypothesis that recurrent chemoresistant ovarian cancer is driven by a small residual population of ovarian cancer stem cells, which have adapted to chemotherapy. It is also hypothesised that metastatic tumours are seeded by metastatic ovarian cancer stem cells. Therefore, the aim of this project is to identify, isolate and validate ovarian CSCs from models of each of these stages of malignancy. Subsequent, analysis and characterisation of these models is likely to lead to the identification of targetable mechanisms. Highlighting of such mechanisms could have substantial positive impact on the treatment of ovarian cancer patients.

1.3 Stem Cell Biology forms the Basis of CSC Research:

CSC research is based on the application of stem cell principles to the growth and development of cancer. This sub-section will describe the basic principles of stem cell biology, to establish the basis of the CSC hypothesis. This sub-section will be referring specifically to human stem cell biology.

Section 1.0 – General Introduction:

Stem cell biology is the study of the cellular origins of the cells which make up the various tissues of an individual. As stem cell biology is the study of cellular origins, this introduction will begin with the fertilised egg. The fertilised egg is formed via the fusion of the male and female gametes. This single cell has the potential to form all of the cells that make up an individual. The generation of new types of cells from the fertilised egg is achieved via a process called differentiation. Stem cells are defined by the amount of cell lineages they can differentiate into. This is referred to as potency (Figure 1.1). Stem cells that can produce all the cells of an organism are called totipotent stem cells. Pluripotent stem cells can differentiate into many different lineages derived from each of the three embryonic germ layers (endoderm, mesoderm and ectoderm). However, a pluripotent stem cell can not differentiate into all the cell types that are required to form a complete individual. A multipotent stem cell is further limited in its differentiation potential: it is only able to differentiate into the cells required to make a given tissue.

Although a totipotent stem cell can give rise to all the cell types of an individual, it cannot do so directly. Instead, it produces its diverse progeny in a stepwise fashion, through the production of pluripotent stem cells, which in turn produce the multipotent stem cells, such as neural, lung and hematopoietic stem cells (HSCs; Figure 1.1). This stepwise differentiation is associated with a loss of differentiation potential, as each stage of differentiation produces a cell type with a restricted differentiation potential. As will be discussed in Section 1.7, many different protein markers have been associated with ovarian CSCs. It is hypothesised that a similar pattern of hierarchical stemness may be the cause of the diversity of OvCSC protein markers reported in the literature.

Section 1.0 – General Introduction:

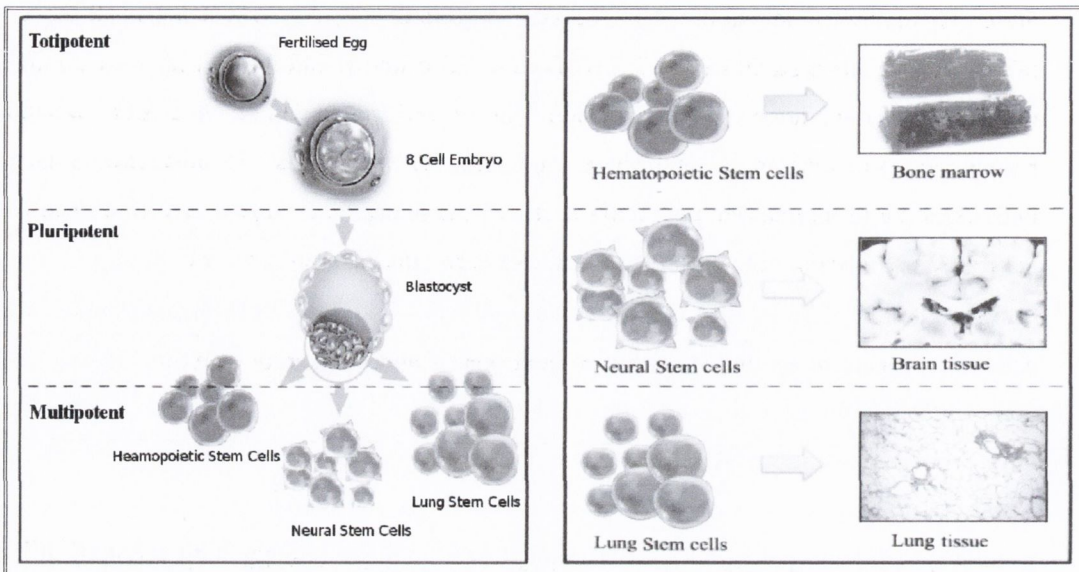

Figure 1.1: Stem Cell Potency – Potency is the primary way in which stem cells are identified. Totipotent and pluripotent stem cells are most commonly associated with the early embryo. Multipotent stem cells are more commonly associated with adult tissues and somatic stemness. Images are adapted from Chen et al. 2011 and "*www.csa.com/discoveryguides/stemcell/overview.php*".

In addition to their differentiation potential, stem cells are defined by their unlimited proliferative potential. The act of cellular division without 'ageing' or differentiation is called self-renewal. All stem cells, from totipotent and pluripotent embryonic stem (ES) cells to multipotent somatic stem cells (SSCs) are capable of self renewing cell division to increase the number of cells in the stem cell pool. Self-renewing divisions are attributable largely to the expression of telomerase (Blasco 2005). Telomerase repairs the protective ends of tandem repeats (telomeres) at the ends of the chromosomes, which are shortened via imperfect DNA replication during cell division (Allsopp et al. 1995).

Human ES cells were first isolated from the inner cell mass of a blastocyst by Thomson et al. (1998). The differentiation potential of the these isolated ES cells was demonstrated via intra-muscular injection into 'non-obese diabetic severe combined immunodeficiency' (NOD.SCID) mice. The xenografted cells formed a benign teratoma, with tissues that represented derivatives of all three germ layers (Thomson et al. 1998). Later Takahashi et al. (2007) demonstrated that fibroblasts could be re-programmed to generate induced pluripotent stem cells via the transfection of four transcription factors: Oct3/4, Sox2, klf4 and c-Myc. In a similar fashion to Thomson et al. (1998), Takahashi et al. (2007) validated the pluripotency of

these iPS cells via their ability to functionally generate tissues derived from all three germ layers, via teratoma studies in NOD.SCID mice. The knowledge gained through ES research provided the foundation for the development of iPS cells, which have great potential in regenerative medicine and novel drug testing. Stem cell research is now positioned to aid in the understanding of tumourigenesis, metastases and post-treatment relapse. The CSC hypothesis is the result of overlapping the principles of the cancer and stem cell research.

The key points to remember from this introduction to stem cell biology are;

- Stem cells are defined by their ability to differentiate and self-renew.
- Differentiation is achieved in a stepwise fashion.
- To prove stemness, stem cells must be functionally validated, for their ability to reconstitute the tissue from which there were originally isolated.

These same principles apply to both SSCs and CSCs.

1.4 CSC Research is the Application of Stem Cell Principles to the Study of Cancer:

Hanahan and Weinberg (2011) describe cancer as having six 'hallmarks': i) sustained proliferative potential, ii) evasion of growth suppressor signals, iii) replicative immortality, iv) resistance to cell death signals, v) angiogenesis and vi) metastases.

As described in Section 1.3, stem cells are the driving force behind the growth of normal tissues. Stem cells usually reside in a quiescent state unless induced to proliferate through external signals (Fortunel et al. 2000; Trumpp et al. 2010). Hanahan and Weinberg's (2011) hallmark of 'sustained proliferative potential' suggest that tumours have overcome the requirement for external factors to induce cell proliferation. There are three mechanisms believed to contribute to this self sufficiency: autocrine/paracrine growth factor signalling within the tumour, up-regulation of growth factor receptors on cancer cells and mutations, which mimic the down stream effects of constitutive proliferation signals (Hanahan and Weinberg 2011; Davies and Samuels 2010).

The cell cycle itself, is a highly regulated, unidirectional change of state progressing towards cell division (Elledge 1996). Cyclin proteins and their cyclin dependent kinases are key regulators of the cell cycle (Nigg 1995). These families of regulators are the gatekeepers which

allow the cell to progress through cell division or prevent its progress via the activation of pathways which induce senescence or apoptosis. Hanahan and Weinberg's (2011) hallmarks suggest that tumours have overcome the 'growth suppressor' and 'cell death' process. Retinoblastoma (Rb) and p53 are among the most well studied proteins which contribute to the evasion of tumour suppression and cell death. Primarily, Rb is associated with the G_1 cell-cycle checkpoint (Weinberg 1995). Mutations and dysregulation of Rb machinery are associated with evasion of tumour suppressor activity in many cancers (Dick 2007). p53 is associated with both tumour suppression and apoptosis (Goodsell 1999). Mutations in p53 are associated with both evasion of tumour suppression and evasion of cell death (Rivlin et al. 2011).

As described in Section 1.3, stem cells have an unlimited proliferative potential associated with active telomerase. Hanahan and Weinberg's (2011) 'hallmarks' suggest that tumours acquire a stem-like 'replicative immortality'. This is believed to be acquired via the malignant activation of telomerase (Blackburn 2005). The hypothesis that cancer may originate from oncogenic transformation of stem cells (described in Section 1.5), would suggest that replicative immortality is an intrinsic characteristic of cancer formation, rather than an acquired characteristic.

The growth and development of normal and cancerous tissues requires access to nutrients and the removal of waste excretions. These requirements are met by the circulatory system. Hanahan and Weinberg's (2011) 'hallmarks' suggest that tumours must recruit and develop a vasculature in order to support the growth and development of the cancerous tissue. Vascular endothelial growth factor (VEGF) is among the most studied molecules involved in the recruitment of blood vessels (angiogenesis) to the developing tumour. Tumours are known to malignantly over-express VEGF, among other angiogenic factors, such as FGF, resulting in the recruitment of tumour associated vasculature (Donovan and Kummar 2006). A growing body of evidence is also contributing to the hypothesis that cancer cells themselves (presumably CSCs) are contributing via transdifferentiation to the development of *de novo* vasculature within the tumours (Soda et al. 2011; Ricci-Vitiani et al. 2010; Wang et al. 2010; Kusumbe et al. 2009; Alvero et al. 2009). This observation is relevant to some of the findings presented in this thesis and will be discussed further in Section 4.4.4.4.3.

Hanahan and Weinberg's (2011) sixth hallmark is 'metastasis'. One of the defining properties of cancer is its ability to invade local tissue and to metastasise to distal locations. Distal metastasis is believed to be attributed to intravasation of the circulatory system (Perlikos et al. 2013). It is believed that platelet cloaking, plays a role in the facilitating the migration of cancer cells

within the circulatory system (Camerer et al. 2004; Gasic et al. 1968). Work published by this laboratory demonstrated that platelets do adhere to ovarian cancer cells. Microarray analysis showed that such platelet adhesion did up-regulate anti-apoptotic and anti-autophagy pathways, suggesting the platelet adhesion could induce pro-survival mechanisms in circulating tumour cells (Egan et al. 2011).

As the cells which establish distal metastases have the malignant potential to generate a new tumour and can differentiate and self-renew to produce a tissue that resembles the tissue of origin (primary tumour), they fit the functional characteristics of CSCs (described in Section 1.5). Therefore, it is likely that CSCs play a central role in metastasis. Furthermore, Shiozawa et al. (2011) showed that metastatic prostate cancer cells migrate directly to the HSC niche in the bone marrow. These findings have further implications for the understanding of dormant micro-metastases. If dormant micro-metastases are CSCs which have occupied SSC niches, then the SSC niche micro-environment may be exerting sufficient control to return the CSC to a more regulated state. A similar effect has been demonstrated in mice: (Mintz and Illmensee 1975) demonstrated that chimeric mice formed from a mixture of murine ES cells and murine pluripotent CSCs grew to develop viable mice, with complete tissues derived from both ES cells and CSCs.

1.5 Cancer Stem Cells:

The 2006 American association for cancer research workshop on CSCs arrived at a consensus definition for CSCs:

"... a cell within a tumour that possess the capacity to self-renew and [differentiate] to cause the heterogeneous lineages of cancer that comprise the tumour"

– Clarke et al. (2006)

This definition outlines the three functional characteristics of CSCs: self-renewal, differentiation and malignant potential. CSCs were first studied in germ cell tumours by Kleinsmith and Pierce (1964), who showed the multipotentiality of embryonal carcinoma cell via single cell mice xenografts which lead to the production of teratocarcinomas which contained up to 14 differentiated somatic tissues. Stable pluripotent CSC cell lines were derived from germ cell tumours and differentiation morphogens (e.g. retinoic acid) had been identified by 1984 (Andrews 1984). In a similar fashion to stem cells (Section 1.3), CSCs can only be

validated through functional analysis. ES cells can form benign teratomas, with tissue derivatives of all three germ layers in immunocompromised mice (Thomson et al. 1998). Similarly, pluripotent CSCs can form malignant teratocarcinomas with tissue derivatives of all three germ layers in immunocompromised mice (Kleinsmith and Pierce 1964). The same validation studies have been applied to the study of HSCs. Morrison and Weissman (1994) validated putative HSCs as the stem cells of the hematopoietic system by demonstrating that they could recover the depleted hematopoietic system of lethally irradiated mice. These findings form the basis of one of the CSC validation assays used in this study: the *in vivo* mouse tumourgenicity assay.

The first CSCs isolated from somatic tumours were validated in a similar fashion. Bonnet and Dick (1997) showed that acute myeloid leukemia (AML) CSCs could be identified and purified via the expression of cell surface markers. They showed that only the AML CSC sub-population, with a CD34+/CD38- expression profile, could transplant the malignancy from human patients to immunodeficient NOD.SCID mice. Subsequent publications have demonstrated the isolation of CSCs from many other somatic tumours (Breast: Al-Hajj et al. 2003; Brain: Singh et al. 2003; Prostate: Collins et al. 2005; Pancreatic: Li et al. 2007; Colon: (O'Brien et al. 2007); Ovary: Zhang et al. 2008). Ovarian CSCs (OvCSCs) will be described in further detail in Section 1.7.

The origins of CSCs are not known. Li et al. (2006) argue that de-differentiation of committed mature cells is not very plausible as there are multiple pathways that would need to be reactivated via multiple mutations. They also point out that SSCs are quite rare when compared to progenitors and more mature cells suggesting that their rarity would make it less likely for them to be targets of oncogenic mutations. They suggest that oncogenic mutations tend to strike progenitor cells as they are not as far down the differentiation path (thus requiring less de-differentiation) and are far more abundant than stem cells. On the other hand Reya et al (2001) argue that progenitors are less likely to be targets of oncogenic mutations as they proliferate for a much shorter period of time than stem cells, before they terminally differentiate (Reya et al. 2001).

Similarities between CSCs and their SSC counterparts (Reya et al. 2001; Pardal et al. 2003), support the hypothesis that SSCs are the target of malignant transformation (Figure 1.2). This hypothesis relates back to the 'hallmarks' of cancer (Section 1.4). If a SSC was the original carcinogenic clone, then 'replicative immortality' could be looked upon as an intrinsic characteristic rather than a property acquired via stochastic mutations. There is evidence to

suggest, that in some cases cancers may also arise from progenitor cells. Huntly et al. (2004) showed that uncommitted hematopoietic stem cells, committed common myeloid progenitor and granulocyte macrophage progenitor cells virally transduced with the MOZ-TIF2 oncogene both produced phenotypically similar, transplantable leukemias. This suggests that CSCs can arise from cells of varying potency. On the other hand, Flesken-Nikitin et al. (2013) identified SSCs of the ovarian surface epithelium (OSE) rather than the more differentiated cells of the OSE as a source of ovarian cancers. They showed that only the SSC compartment showed transformation potential following Cre-loxP mediated conditional knock-out of p53 and Rb1: whose pathways are commonly mutated in high grade epithelial ovarian carcinomas (Cancer Genome Atlas Research Network 2011). It is most likely that several possible routes to tumourgenicity exist.

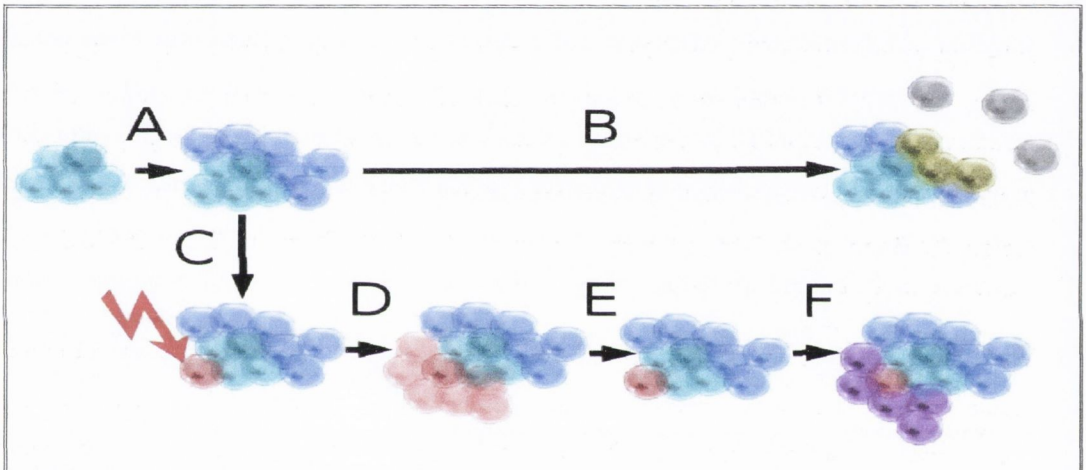

Figure 1.2: SSC Origin of Cancer - A) Normal stem cells (light blue) develop into healthy tissue (dark blue). B) As old cells die (grey) the stem cells replenish the tissue with new cells (yellow). C) An oncogenic transformation occurs in a stem cell (red arrow). D) This CSC (dark red) grows into cancerous tissue (light red). E) Chemotherapy/surgery can initially de-bulk the tumour. F) CSCs can survive the initial treatment and often go on to regenerate a tumour containing more resilient cells (purple).

The CSC hypothesis suggests that if CSCs can be eliminated, the malignant potential of the tumour will be ablated. It is also thought that properties inherited from SSCs may confer chemoresistance to CSCs. SSCs are long lived cells that are responsible for the integrity of entire tissues. As such, it is believed that they possess mechanisms which make them resistant to environmental insults. 'Hoechst dye efflux' is a pCSC marker across multiple malignancies (Breast: Hirschmann-Jax et al. 2004; Blood: Patrawala et al. 2005; Ovarian: Szotek et al. 2006) that is largely attributed to the action of adenosine triphosphate-binding cassette (ABC)

transporters (Golebiewska et al. 2011). Breast cancer resistance protein (BCRP) is a member of the ABC transporter protein family. The ABC transporter family along with the multi-drug efflux proteins are thought to be partially responsible for chemoresistance of somatic and cancerous stem cells. BCRP was found to be responsible for preventing the accumulation of chemotherapeutic drugs in the chemoresistant MCF-7/AdrVp cell line. RNA fingerprinting found the BCRP transcript to be over-expressed in MCF-7/AdrVp compared to its parent cell line MCF-7 (Doyle et al. 1998). CSCs may use similar mechanisms to avoid the effects of chemotherapeutics.

SSCs tend not to divide as quickly as more mature cells and can enter states of quiescence until they are stimulated to divide again by repair or growth signals (Sherley 2002; Watt 2002). This slow cell-cycling can confer resistance to treatments that target rapidly proliferating cells. Harrison and Lerner (1991) demonstrated that a single dose of 5-fluorouracil was not able to ablate the reconstituting ability of HSCs. 5-fluorouracil is an anti-metabolite believed to interfere with RNA and DNA synthesis, which leads to apoptosis in fast cycling cells (Longley et al. 2003). If a single dose is administered, it can cause the HSCs to enter the cell cycle, to replenish the lost cells. A second dose, is then successful at killing the now faster cycling HSCs (Harrison and Lerner 1991). This supports the idea of a slow cell cycle protecting stem cells from the toxic effects of chemotherapeutic agents. If a population of CSCs are not actively dividing they can evade therapies directed at fast cycling cells. Therapeutically targeting CSCs presents challenges, as similar mechanisms are employed by both SSCs and CSCs to maintain the undifferentiated self-renewing state and to facilitate differentiation (Reya et al. 2001; Pardal et al. 2003). Therapeutic approaches to targeting CSCs will be described in Section 1.13.

Although initially responsive to therapy, ovarian cancer frequently relapses and is refractory to additional therapy (Kikkawa et al. 2006). As described above, CSCs may play a role in this relapse and chemoresistance. Targeting OvCSCs could greatly improve the prognosis for ovarian cancer patients. The targeting of CSCs will be discussed in further detail in Section 1.13.

Section 1.0 – General Introduction:

1.6 Ovarian Cancer:

Ovarian Cancer in usually responsive to first line therapy, but is prone metastases relapse and acquired chemoresistance. CSCs are also closely linked with these characteristics. This makes ovarian cancer a good system in which to study CSCs.

Ovarian cancer is a gynaecological malignancy with a poor long term prognosis. Early disease can be asymptomatic or only present vague symptoms such as abdominal discomfort. Therefore, ovarian cancer is generally in a late stage of progression before it is diagnosed, which greatly reduces the probability of a successful cure. There are an estimated 225,000 new cases of ovarian cancer world-wide each year, which is associated with 140,000 deaths per annum. This incidence and death rate represent 1.8% of all cancers evaluated worldwide (Ferlay et al. 2010).

There are three major classes of ovarian cancer; epithelial, specialised and germ cell. Epithelial is by far the most common class of ovarian cancer, representing approximately 90% of all ovarian cancer cases. Specialised and germ cell are far less common, each representing about 5% (Bapat 2010). Epithelial cancers arise from the ovarian surface epithelium (OSE; Figure 1.3). Specialised tumours develop from the cells that make up the ovarian stroma and are responsible for some of the hormone production of the ovaries (Figure 1.3). Germ cell tumours arise from the cells that are destined to form oocytes (Figure 1.3). Germ cell tumours are more common among younger women while epithelial tumours generally strike older, post-menopausal women (Yancik 1993). Within each of these classes there are many different types of disease. For example, epithelial can be of a serous, mucinous, endometrioid or clear cell type, while specialised can be stromal cell or granulosa cell, and germ cell can produce teratomas of various stages of maturity.

The ovary is wrapped in a smooth layer of epithelial cells, one cell thick called the OSE. This layer of cells forms a boundary between the ovaries and the rest of the body and is thus responsible for the transport of materials in and out of the ovaries. Normal OSE is kept separate from the stroma of the ovary by a layer of cells called tunica albuginea. The developmental biology of the OSE is described in Section 1.8. This layer buffers the OSE from any deleterious effects of inter-cellular signalling by the stromal cells. The OSE is generally smooth, but ageing results in it becoming distorted causing an increase in the number of inclusion cysts. Such cysts may form through the pinching off of invaginations in the distorted OSE or by trapping of epithelial cells in the stroma during post-ovulatory repair (Auersperg et al. 2001). Inclusion

cysts are thought to be pre-malignant lesions which have the potential to progress into malignant carcinoma. Ovarian carcinomas, of cyst origin, are generally of low grade while independently arising malignancies are typically of higher grade (Horiuchi et al. 2003).

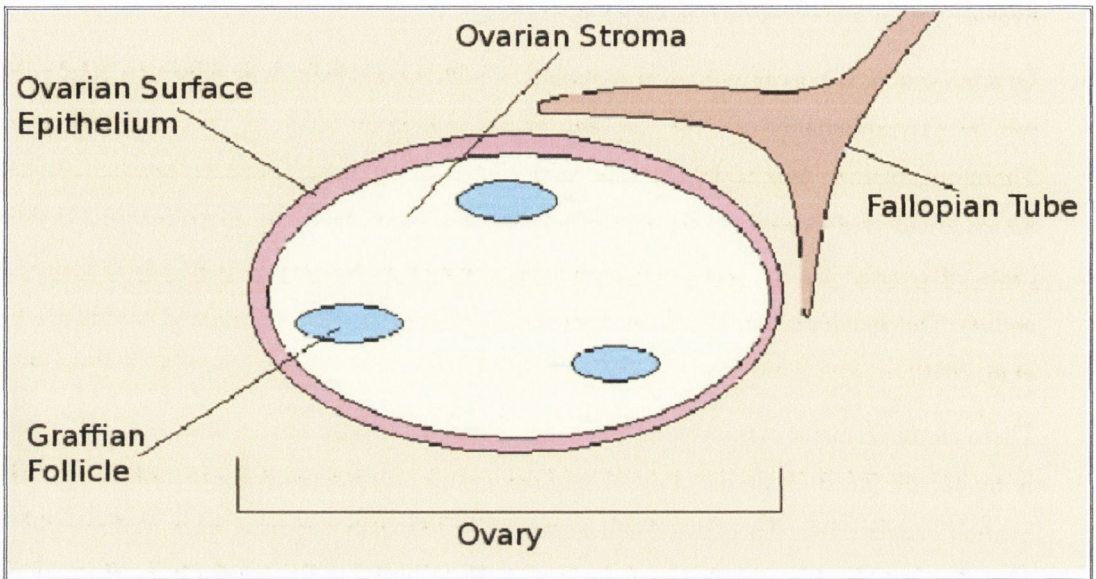

Figure 1.3: The Ovary - Schematic representation of ovary, showing the germ cells (blue), which are responsible for the formation of the oocytes, the stroma (yellow), which is responsible for some of the hormone production of the ovaries, and the epithelium (pink), which is a single layer of cells that surrounds the entire ovary.

Each case of ovarian cancer is assigned a 'stage' and a 'grade'. This is achieved through biopsies of various high risk sites with subsequent histological evaluation. The stage is effectively a measure of how far the cancer has spread from the initial site in the ovary. The International Federation of Gynaecology and Obstetrics (FIGO) standard is the most widely used system. Stages range from *I* to *IV*, with *I* being still localised to the ovaries and *IV* having spread beyond the abdominal cavity e.g. to lungs. Grade is more a gauge of the aggressiveness of the tumour and is dictated by what sort of cells the tumour is made up of i.e. how differentiated it is. A higher grade tumour is more undifferentiated and more aggressive. A lower grade tumour is more differentiated and less aggressive.

Horiuchi et al. (2003) carried out a retrospective study of ovarian cancer cases, where women had received ultrasounds up to 12 months prior to detection of cancer, which indicated that there may be a dual origin to ovarian cancers. It was found that approximately half of the ovarian cancer patients presented with a benign ovarian cyst prior to development of cancer. This suggested a stepwise progression from inclusion cyst to cancer. The other half appeared to develop cancer *de novo* from the surface epithelium with no detectable pre-existing cyst. It was

found that the higher grade invasive cancers appeared to arise *de novo*, while the lower grade, borderline cancers more commonly had a benign cyst origin. This data would suggest that low grade disease does not necessarily develop into high grade tumours and rather that each may have its own unique origin (Horiuchi et al. 2003).

As malignancy progresses to later stages, abdominal distension becomes common: this is known as ascites. Ascites is characterised by an accumulation of fluid in the peritoneal cavity (Martin 2005). Ovarian cancer spheroids are often found in ascitic fluid (Zhang et al. 2008). These are often used as a source of ovarian cancer cells for the establishment of ovarian cancer cell lines (Hills et al. 1989). Ascitic fluid is routinely drained to alleviate discomfort – as such is it is a minimally invasive way of obtaining patient samples. However, it is important to bare in mind that the cells that have progressed to form ascitic anchorage independent spheroids may not actually be completely representative of the original tumour mass.

Ovarian cancer typically responds well to chemotherapy and cytoreductive surgery (Kikkawa et al. 2006). Unfortunately, the majority of individuals who respond well initially, go on to develop recurrent disease, which is often non-responsive to current therapies. In a publication generated from this laboratory, Laios et al. (2008) compared gene expression data between primary and recurrent ovarian cancer samples. It was found that the differential gene expression profiles of all the cancers tested clustered unambiguously into defined primary and recurrent groups. These substantial differences in expression profiles for primary and recurrent tumours faithfully reflect the differences seen in responsiveness of primary and recurrent tumours to therapy. It would appear that the small population of cells that survive the initial treatment either have a different expression profile or adapt their expression profile upon recurrence to generate a new tumour mass that can allow them to tolerate the chemotherapeutic drugs used. Laios et al. (2008) suggest a model of recurrence: tumour cells which survive the initial treatment up-scale the production of adhesion molecules augmenting: attachment, cytokines and inflammatory mediators to improve survival and an array of growth factors and receptors to facilitate proliferation which impose cancerous regulation on the immediate micro-environment giving the cancer cells the advantage they need to re-establish themselves and form a recurrent tumour.

As described in Section 1.2, CSCs are suspected to be the cells which survive initial treatments and these may be the mechanisms through which they adapt to form chemoresistant recurrent disease.

1.7 Ovarian Cancer Stem Cells:

Ovarian Cancer in usually responsive to first line therapy, but is prone to chemoresistant relapse (Herzog 2004). The CSC hypothesis suggests that the reason for such relapses are due to CSCs evading first line therapy, adapting to the environmental conditions and regrowing the tumour in a state that is refractory to therapy.

There has been substantial data published in the literature to support the presence of CSCs in ovarian cancer. Bapat et al. (2005) were the first to isolate stem-like clones from ovarian cancer patients ascites. Szotek et al. (2006) were the first to isolate OvCSCs via marker based screening. They Isolated HSP+ and HSP- cells form genetically engineered murine cell lines and demonstrated increased tumourgenicity in the HSP+ cells. Interestingly, they identified that the CSCs compartment and not the non-CSC compartment was resistant to Doxorubicin (a chemotherapeutic agent), showing a 30 % reduction in cell viability in the CSCs compared to an 80 % reduction in the non-CSCs. They postulated that is due to the presence of drug efflux pumps – specifically BCRP1: a membrane transporter largely responsible for the Hoechst Side Population (HSP) CSC phenotype. In Section 4.0, data will be presented suggesting that the putative drug resistant phenotype of HSP+ cells is conferred a selective advantage when a cell line is chemo-adapted to cisplatin. Identifying and predicting the response of such cell populations in patients may become central to the development of treatment strategies.

Zhang et al. (2008) were the first to suggest putative OvCSC markers based on differential surface marker expression between isolated OvCSCs and the parent population. They identified OvCSCs as expressing a CD44+/CD117+ phenotype. Baba et al. (2008) were the first to isolate and validate OvCSCs from human derived ovarian cancer cell lines. They demonstrated that CD133+ cells isolated from the A2780 cell line were more tumourigenic in mouse xenograft experiments. They were also the first to utilise a single cell self-renewal and differentiation (SD) assay, within an OvCSC context, to validate the differentiation potential of the isolated cells. Furthermore, Baba et al. were able to generate a gene expression signature by examining data for 100 genes in 41 established ovarian cancer cell lines. This gene expression signature was used to successfully segregate CD133+ containing ovarian cancers from completely CD133- cancers. The false positive rate of this segregation was 4.7 % (2 in 42), while the false negative rate was 7.1 % (3 in 42). Such gene signature approaches to the identification of CSC populations could prove especially powerful in the triaging of ovarian cancer patients. Curley et al. (2009) showed that CD133+ cells, isolated from patient samples, demonstrated OvCSC characteristics. Kusumbe et al (2009) called the CD133+ OvCSC marker into question, with

findings that suggested that CD133+ cells were endothelial precursors cells rather than OvCSCs, suggesting that efficient xenograft uptake was due to augmented vasculature via CD133+ cells.

Deng et al. (2010) carried out a large study, across many normal and cancerous tissue types. They identified ALDH+ pCSC sub-populations across a wide range of ovarian cancer cell lines, including the A2780 and SK-OV-3 cell lines. They did not carry out any functional validations on the putative OvCSCs. They showed a correlation to acquired platinum resistance and an increased ALDH+ sub-population size, within the A2780 [0.7 % +/- 0.06 %] and its platinum resistant daughter cell lines (A2780/CP70 [0.2 % +/- 0.00 %], A2780/C200 [1.0 % +/- 0.28 %] and A2780/C30 [2.1 % +/- 0.42 %]). This directly supports some of the findings which will be presented later in this thesis (Section 4.3.1.2). Furthermore, they demonstrated an increase in the size of the ALDH+ population of A2780 xenograft tumours, when mice inoculated with 5×10^6 A2780 cells, were treated with cisplatin. Untreated control mice had a ALDH+ population of 0.09 %. Mice treated with 2 mg/kg cisplatin (½ the maximum tolerated dose) had a ALDH+ population of 0.76 %. Mice treated with 4 mg/kg cisplatin had a ALDH+ population of 0.42 %. These findings suggest that if a patient is found to have an ALDH+ sub-population a directed anti-ALDH+ therapy would be needed in conjunction with cisplatin therapy. Silva et al. (2011) validated ALDH+ cells as OvCSCs. They were among the first to use a large panel of putative OvCSC markers to screen a wide range of patient samples and cell lines. Most of the earlier OvCSC studies used a focused panel of markers often using only 1 or 2 markers. Silva et al. screened for ALDH, CD133, CD44, CD117, CD90 and CD24 across patient tumours, patient ascites and cell lines. They found that only ALDH identified pCSC sub-populations across all samples, with the other pCSC markers identifying pCSCs in only 52 % - 92 % of the samples. While ALDH+ cells were shown to be more stem-like with augmented tumourgenicity when compared to ALDH- cells, Silva et al. found that ALDH+/CD133+ cells grew tumours more efficiently than ALDH+/CD133- cells. This was the first publication to identify sub-populations (CD133+/-) within a OvCSC population (ALDH+).

As seen in the above synopsis, to date there are no definitive OvCSC markers which identify OvCSC across all populations tested. There is no consensus as to how each of the validated OvCSC markers (ALDH+/CD133+: Silva et al. 2011; HSP+: Szotek et al. 2006; CD44+/CD117+: Zhang et al. 2008; CD133+: Curley et al. 2009) relate to each other. As described in Section 1.6, ovarian cancer is believed to be derived from the OSE. At first it may appear counter-intuitive that there should be such CSC diversity originating from such simple

epithelial sources. However, the developmental origins of the OSE and fallopian tube epithelium (FTE) may have a role to play in the spectrum of cell lineages (serous, endometrioid, mucinous, clear cell) observed within ovarian cancer. This is described further in Section 1.8.

The ultimate goal of studying OvCSCs is to develop methods of targeting therapies against them. Current therapies are generally able to send the malignancy into remission but relapse is common (Kikkawa et al. 2006). If OvCSCs were targeted directly, in conjunction with first line therapies, the incidence of relapse should decrease greatly as no cells should remain with the malignant potential to regenerate the tumour.

1.8 Developmental Biology of the Ovary:

The study of CSCs is the application of stem cell principles to the study of cancer. CSCs are cancerous cells with stem-like properties. CSCs may arise from cancerous mutations which strike SSCs or may arise from cancerous mutations which strike more differentiated cells and confer them with more stem-like characteristics. This project will focus on the study of OvCSCs. Historically, ovarian cancer is believed to arise from the OSE (Auersperg et al. 2001). More recent studies suggest that the FTE may be another source of ovarian cancer (Zheng and Fadare 2012).

Unlike the hematopoietic system, which leads the SSC and CSC fields, there is very little information on the stem cell lineages of the OSE and the FTE. However, there is information on the developmental biology of the coelomic epithelium and OSE.

The OSE and FTE are both derived from the coelomic epithelium. The coelomic epithelium is a mesodermal-derived layer of cells which lines the internal body cavity in the developing foetus. This lining covers the presumptive ovaries of the urogenital ridge. The region of the coelomic epithelium covering the presumptive ovaries is the destined to become the OSE (Auersperg et al. 2001).

Beginning at approximately 10 weeks gestation the OSE changes from a squamous-cuboidal epithelium with a fragmented basement membrane to a multi-stratified papillary epithelium with a well defined basement membrane (Auersperg et al. 2001). It is believed that during this stage of development the OSE contributes to the production of granulosa cells which form part of the primordial ovarian follicles. (Auersperg et al. 2001). The OSE looses much of its multi-

stratified layers by week 14 of gestation and is a monolayer by term (Auersperg et al. 2001). This monolayer of OSE is separated from the ovarian stroma by a single layer of cells called the tunica albuginea.

The OSE is continuous with the coelomic epithelium throughout embryonic development. However, there are clear differences in the development of the OSE and the extra-ovarian coelomic epithelium. It is believed that these differences arise from local factors as the extra-ovarian coelomic epithelium and OSE arises from the same source and are both exposed to the one pelvic cavity (Auersperg et al. 2001). One of the most notable differences between extra-ovarian coelomic epithelium and OSE is the lack of CA125 expression on the OSE (Jacobs and Bast 1989). CA125 expression is an epithelial differentiation marker and an ovarian cancer marker. Other coelomic derivatives such as the FTE, endometrial epithelium, endocervix epithelium, pleura and the pericardium all express CA125 (Jacobs and Bast 1989). The lack of CA125 expression on the OSE suggests that it is a less differentiated region of the coelomic epithelium compared to the rest of the coelomic epithelium derived tissues. Furthermore, the expression of CA125 in ovarian cancer suggests the OSE has retained the ability to differentiate into some of these different tissue types (Auersperg et al. 2001). This suspected lack of differentiation of the OSE, may be a contributing factor to the OvCSCs marker heterogeneity described in the literature (Section 1.7). Furthermore, this suspected differentiation potential may contribute to the multiple different foci of cells observed within ovarian tumours (Serous, Mucinous, Endometrioid and clear cell), as well as the multiple overlapping pCSC sub-populations identified within this project and other publications in the literature (Silva et al. 2011).

1.9 Modelling Ovarian Cancer:

As described in Section 1.5, substantial data has been published supporting the presence of CSCs in Cancer. Similarly, multiple studies have demonstrated the presence of CSCs within ovarian cancer (Section 1.7). CSCs have also been demonstrated to be present within cancer cell lines (Rappa et al. 2008; Deng et al. 2010; Zhou et al. 2012). Ovarian cells lines have also been demonstrated to contain CSCs (Baba et al. 2008; Silva et al. 2011).

This thesis describes the identification, isolation and validation of OvCSCs. Prior to the commencement of this project, the laboratory had little experience in the use of flow cytometry to screen for, identify and isolate pCSCs. There were no CSC validation assays, such as the

mouse tumourgenicity assay and the single cell SD assay (described in Section 6.1), established in the laboratory. As such, these techniques had to be established and optimised during the course of this project. It was decided that ovarian cancer cell line models would provide a more stable and scalable supply of material, with which to establish and optimise these techniques. As such, ovarian cancer cell lines were used instead of ovarian cancer patient samples, to model ovarian cancer within this project. Now that these techniques have been established, the laboratory is well placed to progress the findings of this project into the study of ovarian cancer patient samples, as well as other malignancies.

Six models of ovarian cancer and one model of normal OSE were used to model ovarian cancer in this project. Four of these models (A2780/A2780cis and IGROV-1/IGROV-CDDP) formed pairs of cisplatin sensitive/resistant parent/daughter cell lines. Two models (SK-OV-3 and 59M) were derived from metastatic ascites samples. This selection of ovarian cancer models enables the comparison of CSCs from cisplatin sensitive and cisplatin resistant ovarian cancer. The use of two models enables the detection of conserved and/or divergent CSC roles in the acquired cisplatin resistance of ovarian cancer. The selection of ascites derived models and solid tumour derived models allows for investigation into of CSC roles in ascites formation. The characteristics of these models will be described in Sections 1.9.1 – 1.9.3.

1.9.1 Modelling Chemoadaptation:

The A2780 cell line was derived from an ovarian tumour prior to the patient receiving any treatment (Godwin et al. 1992). The histology of the original tumour from which it was derived is unknown (Molthoff et al. 1991). However, A2780 cells have been shown to produce poorly differentiated high grade tumours (Molthoff et al. 1991; Shaw et al. 2004). This cell line has been used to model cisplatin sensitive ovarian cancer (Godwin et al. 1992; van Jaarsveld et al. 2012; Xiang et al. 2013). The A2780cis cell line was derived via chronic exposure of the A2780 cell line (Section 1.9.1) to increasing doses of cisplatin (Egan et al. 2011). This cell line has been used to model cisplatin resistant ovarian cancer (Laios et al. 2013; Kalayda et al. 2012; Schneider et al. 2012).

The IGROV-1 cell line was derived from a tumour sample of a 47 year old patient with Stage III ovarian cancer. Prior to surgery the tumour was mistaken for cervical cancer and was treated topically with 'cobalt therapy'. The histology of the tumour was described as a glandular and polymorphous ovarian epithelioma. It consisted predominantly of endometrioid tissue with some serous, clear cell and undifferentiated foci (Bénard et al. 1985). IGROV-1 has been used

to model cisplatin sensitive ovarian cancer (Ma et al. 1998; Gatti et al. 2012; Stordal et al. 2012). The IGROV-CDDP cell line was derived from the IGROV-1 cell line via intermittent exposure to increasing concentrations of cisplatin, for 9 months (28 passages; Ma et al. 1998). IGROV-CDDP has been used to model cisplatin resistant ovarian cancer. (Ma et al. 1998; Stordal et al. 2012).

1.9.2 Modelling Metastasis:

The SK-OV-3 cell line was derived from the ascites of a patient with an ovarian adenocarcinoma. The ascites sample was taken from the patient after the patient had undergone treatment with thiotepa (Hills et al. 1989). SK-OV-3 has been used to model metastatic ovarian cancer (Egan et al. 2011; Wu et al. 2012; Lu et al. 2013). The 59M cell line was derived from the ascites of a patient with an ovarian adenocarcinoma. The ascites sample was taken from the patient prior to the receipt of any treatment. The histology of the ovarian tumour was described as endometrioid with clear cell components (Hills et al. 1989). 59M has been used to model metastatic ovarian cancer (Egan et al. 2011).

1.9.3 Modelling Normal Ovarian Surface Epithelium:

The HIO-80 cell line was derived from the ovarian surface epithelium of patients undergoing prophylactic oophorectomy. OSE cells were transfected with 'SV40 early' genes to prevent proliferative senescence (Auersperg et al. 1995). The HIO-80 cell line has been used as a model of normal OSE (Yang et al. 2004; Egan et al. 2011).

These seven model systems were used in conjunction with the pCSC marker panel (Section 1.10.1) to study the role of CSCs in acquired chemoresistance and metastasis of ovarian cancer, as well as attempt to further the understanding of how the diversity of OvCSC sub-populations published in the literature relate to one another.

1.10 Identification of CSCs:

As described in Section 1.5, it is believed that CSCs provide a new therapeutic avenue for the treatment of ovarian cancer. CSCs need to be identified and isolated to facilitate their study. The identification of OvCSCs is central to the work presented in this thesis. Through the data published in the literature, several markers have been demonstrated to be capable of isolating OvCSCs (ALDH+: Silva et al. 2011 [0.4 % to 9 %]; HSP+: Szotek et al. 2006 [1.33 % to 19.1 %]; CD44+: Zhang et al. 2008 [0.2 % to 0.16 %]; CD117+: Zhang et al. 2008 [0.2 % to 0.16 %]; CD133+: Curley et al. 2009 [0.3 % to 35 %]). These markers will now be described

(Sections 1.10.1 – 1.10.3.3). A marker of metastasis was also included in the screening panel in an attempt to identify a sub-population of OvCSCs with metastatic potential (CXCR4+: Hermann et al. 2007 [9.58 %]; Section 1.10.3.4).

The size of the CSC population within tumours can often be very small (less than 1 %). This makes it very challenging to study CSCs. Such small populations must be isolated to a high degree of purity to facilitate their study. Having said this, there is a wide range in the size of the CSC population detected between patients: as illustrated by the above references. A similar trend will also be presented in Section 4.0 with respect to the model systems screened for this project. When trying to tackle the problem of chemoresistant recurrent ovarian cancer, the central question is: how does the small population of cells (presumable CSCs as they have the tumourigenic potential to reconstitute the original tumour) evade and adapt to first line therapies? The size of the original CSC population, is not as important as how the CSC pool or a sub-population thereof adapts to first-line therapies generating recurrent tumours that are refractory to further therapy.

1.10.1 ALDEFLUOR™ Assay:

The ALDH assay was developed to identify ALDH expressing HSCs (Storms et al. 1999). This SSC marker was also successfully used to identify and isolate CSCs from a range of malignancies (Breast: Charafe-Jauffret et al. 2009; Colon: Huang et al. 2009; Brain: Corti et al. 2006; Liver: Ma et al. 2008; Ovary: Silva et al. 2011; Lung: Sullivan et al. 2010). Interestingly, it has been shown that lentivirus-mediated siRNA knock-down of ALDH1A1 and ALDH1A3 reduces the clonogenic efficiency and wound repair (scratch assay) of ALDH+ non-small cell lung cancer cell lines, suggesting that ALDH may represent a good target for anti-CSC therapies. However, Alison et al. (2010) make the point that while some strategies for blocking ALDH activity appear to have therapeutic beneficial outcomes it also has the potential to increase the CSC pool within tumours, as it has been linked to a retinoic acid mediated differentiation.

The ALDH Assay identifies CSCs based on their ability to metabolise a synthetic Aldehydrogenase 1 substrate, BODIPY-aminoacetaldehyde (BAAA), to produce a brightly fluorescing substance: BODIPY-aminoacetate. The addition of BAAA to a cell suspension, allows the CSCs to metabolise the BAAA to BODIPY-aminoacetate, causing the CSCs to fluoresce brightly. The non-CSCs cannot metabolise BAAA and therefore do not fluoresce (Figure 1.4).

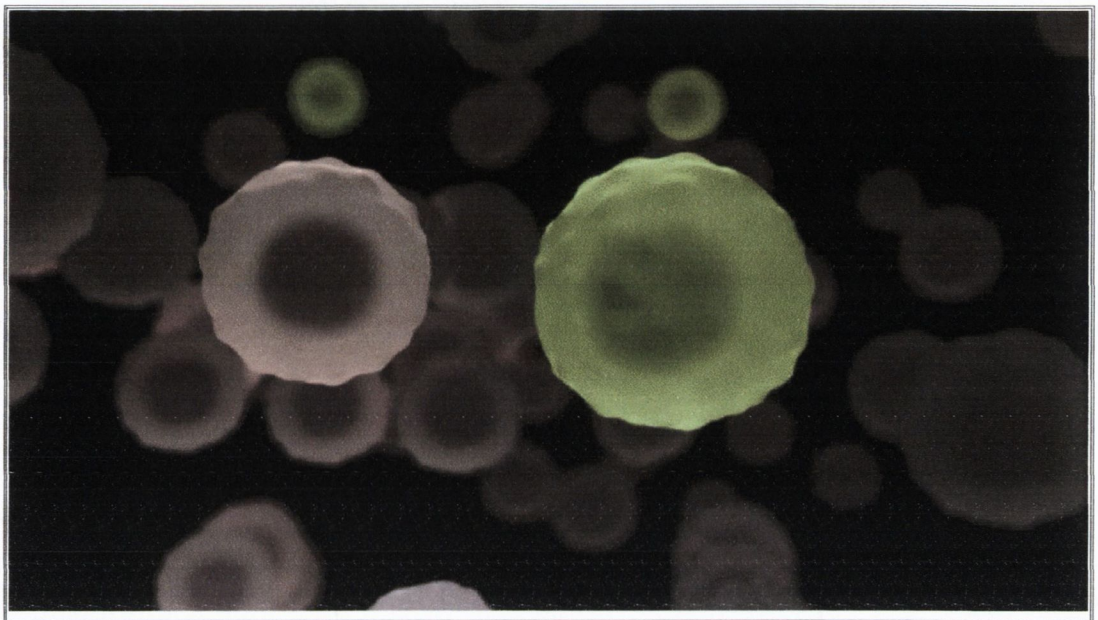

Figure 1.4: ALDH Staining – BAAA is added to a cell suspension, CSCs within that population are able to metabolise BAAA to BODIPY-aminoacetate, which fluoresces brightly when excited by a laser (green). Non-CSCs can not metabolise BAAA and therefore, do not fluoresce (cream). This image was adapted from "http://www.stemcell.com/".

Diethylaminobenzaldehyde (DEAB) is an aldehydrogenase inhibitor and prevents the CSCs from metabolising BAAA. When DEAB is included with BAAA no cells fluoresce. When screening for CSCs using the ALDH assay, two samples are needed. One sample is incubated with BAAA and DEAB together. This was used as a negative control. The other sample is incubated with BAAA only. This is the experimental sample. Subtraction of the negative control data from the experimental sample date allows for the identification and quantification of the ALDH+ pCSCs.

1.10.2 Hoechst Side Population Assay:

The HSP assay was originally found to identify HSCs (Goodell et al. 1996). This SSC marker was also successfully used to identify and isolate CSCs from a range of malignancies (Brain: Bleau et al. 2009 Colon: Haraguchi et al. 2006; Lung: Ho et al. 2007; Liver: Chiba et al. 2006; Ovary: Szotek et al. 2006).

The HSP Assay identifies CSCs based on their ability to exclude the DNA staining dye Hoechst 33342 (H342) from the cell. H342 is cell membrane permeable. When added to a cell suspension it diffuses into the cell and causes the cells to fluoresce when excited by a laser. CSCs, through the expression of drug efflux pumps (ABCB1, ABCC1-5, ABCG2; Golebiewska et al. 2011) and active transport, can exclude H342 from the cell. This results in a reduction in the fluorescent intensity of the CSCs relative to the non-CSCs (Figure 1.5).

Verapamil inhibits the active transport which allows CSCs to efflux H342from the cell (Golebiewska et al. 2011). When Verapamil is included with H342 all the cells fluoresce. When screening for CSCs using the HSP assay, two samples are needed. One sample is incubated with H342 and Verapamil together. This is the negative control. The other sample is incubated with H342 only. This is the experimental sample. Subtraction of the negative control data from the experimental sample date allows for the identification and quantification of the HSP+ pCSCs.

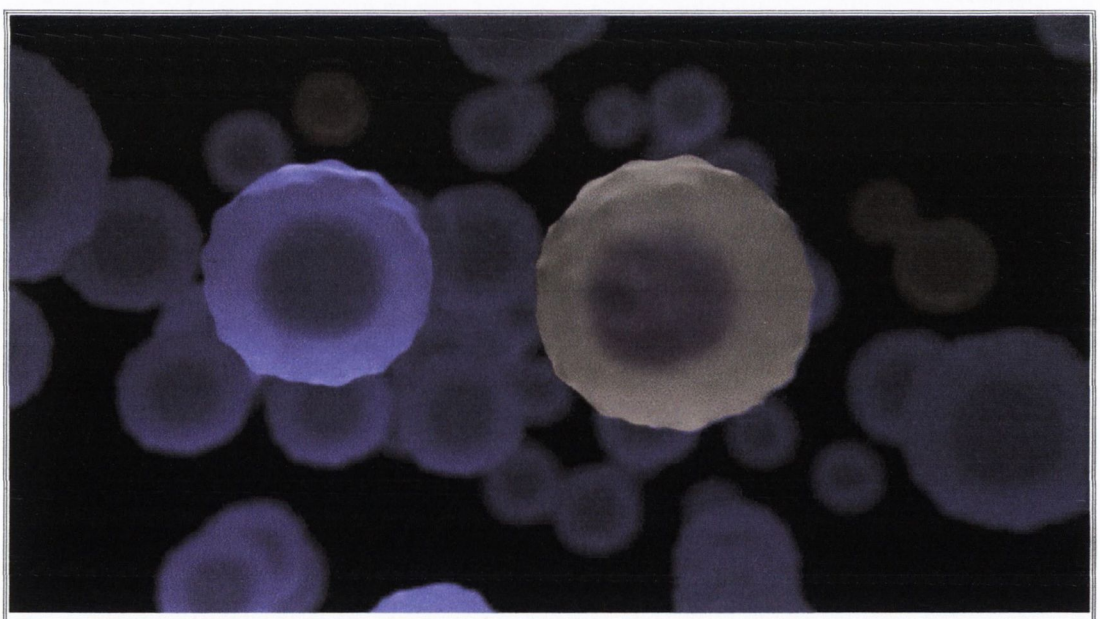

Figure 1.5: HSP Staining – H342 is added to a cell suspension. This cell membrane permeable DNA binding dye diffuses into the cell and causes the cells to fluoresce when excited by a laser. CSCs through the expression of drug efflux pumps and active transport can exclude H342 from the cell. This results in a reduction in the fluorescent intensity of the CSCs (cream) relative to the non-CSCs (purple). This image was adapted from "http://www.stemcell.com/".

1.10.3 Cell Surface Protein Assay:

Cell surface proteins are used to identify the different cell types which make up the hematopoietic system (http://hcdm.org/). 'Human Cell Differentiation Molecules' (HCDM) is the organisation which runs the 'Human Leukocyte Differentiation Antigens' (HLDA) workshops and names and characterises 'Cluster of Differentiation' (CD) molecules. The CD nomenclature is built up around cell surface markers that are associated with various stages of leukocyte differentiation as established at HLDA workshops. CD markers are used to define the cell phenotypes at the various stages of differentiation along the multiple lineages that make up the hematopoietic system.

The CSP Assay identifies CSCs based on their expression of cell surface antigens associated with cancer stemness. These antigens are often CD markers. The CSP assay is based upon antibodies directed against the CSC associated antigen, which have fluorescent fluorochromes conjugated to their heavy chains. When such antibodies are added to a cell suspension, the CSCs, which express the target antigens, are tagged with the fluorochrome via the antibody, allowing them to fluoresce when excited by a laser. The fluorescence signal produced by antibody bound CSCs is then quantified by flow cytometry with respect to two controls. An autofluorescence control is a sample of cells with no antibody present. This control is used to set a threshold of fluorescence, attributable to background fluorescence of the cell. An isotype control is a sample of cells stained with the same immunoglobulin class of antibody, conjugated to the same type of fluorochrome as the CSC detecting antibody. This isotype antibody is directed against an antigen which is not expressed on human cells. This control is used to estimate any non-specific staining caused by the CSC detecting antibody. CSCs are identified by subtracting the autofluorescence control data from the experimental sample. All CSCs identified are analysed with respect to the non-specific staining identified within the isotype control, which is usually negligible.

Morrison and Weissman (1994) used a panel of ten antibodies to identify the first HSC cells. Since then CSP assay based approaches have been used to identify CSCs from a diverse range of malignancies (Prostate: Patrawala et al. 2006; Brain: Singh et al. 2003; Pancreatic: Hermann et al. 2007; Liver: Yin et al. 2007; Ovarian: Curley et al. 2009). Three OvCSC associated antigens were used in this project: CD44, CD117 and CD133 (described in Sections 1.10.3.1 – 1.10.3.3). One metastasis associated antigen was used: CXCR4. The metastasis associated

antigen was included to probe the role of CSCs in metastatic ascites, in conjunction with the two ascites derived models (SK-OV-3 and 59M; Section 1.9).

1.10.3.1 CD44:

Cell surface expression of CD44 has been identified as a marker of CSCs. Prostate cancer was found to have a group of CD44 positive cells that were better able to form tumours in NOD/SCID mice (Patrawala et al. 2006). Collins et al. (2005) had earlier linked the CD44/CD133/α2β1 integrin expressing phenotype, isolated from prostate cancer patient as being more clonogenic and able to sustain anchorage independent growth *in vitro*. Zhang et al. (2008) were the first to link CD44 expression to OvCSCs. They reported that the OvCSCs isolated via spheroid growth had a CD44+/CD117+ phenotype.

The CD44 surface protein is a molecule with many structural variants and functions. The variety associated with CD44 comes from the gene and transcript level. It is encoded be a 20 exon long gene found on chromosome 11 (Rodríguez-Rodríguez et al. 1998). The first five and last five exons are included in every splice variant of the protein, with the central 10 exons being subject to many different combinations of alternate splicing (Rodriguez-Rodriguez et al. 1998). CD44s is the standard form of the protein containing only the first and last five exons (Rodriguez-Rodriguez et al. 1998). The various isoforms created by alternate splicing of the transcript are named CD44v and reference the exons that have been added to the 10 constitutively expressed exons (Rodriguez-Rodriguez et al. 1998). For example; the CD44 variant CD44v8-10 contains the last three exons of the variable region as well as the 10 constitutively expressed exons. Primarily, CD44 is considered a receptor for hyaluronic acid (Lesley and Hyman 1998), CD44 has been linked to a large amount of cellular and tissue functions from cell migration (Faassen et al. 1992), to cell proliferation (Naor et al. 2002) and cytokine, chemokine regulatory functions (Bennett et al. 1995).

An antibody directed against the CD44s variant was used to detect CD44+ pCSCs in this project. This means that the antibody is directed against an epitope expressed in the in the region of the CD44 protein included in all splice variants.

1.10.3.2 CD117:

Although not as widely used as other CSC markers, CD117 has been shown to be expressed on CSCs (Blood: Guibal et al. 2009; Bone: Adhikari et al. 2010;Ovarian: Zhang et al. 2008). Zhang et al. (2008) first linked CD117 expression to OvCSCs. As described above, the OvCSCs

isolated via spheroid growth and functionally validated as CSCs, were found to be CD44+/CD117+.

CD117 is a type III receptor tyrosine kinase (Ashman 1999). Its has five extracellular immunoglobulin like domains and a cytoplasmic region with a tyrosine kinase domain (Ashman, 1999). The gene encoding CD117 is composed of 21 exons spanning approximately 80kb. It's primarily known as a cell membrane receptor protein for Stem Cell Factor (SCF), and is purposed to have anti-apoptotic effects (Canonico et al. 2001). An antibody directed against the CD117 was used to detect CD117+ pCSCs in this project.

1.10.3.3 CD133:

CD133 expression has been used to identify and isolate CSCs across several malignancies (Colon: O'Brien et al. 2007; Prostate: Collins et al. 2005; Liver: Yin et al. 2007, Brain: Singh et al. 2003; Pancreatic: Hermann et al. 2007). Curley et al. (2009) demonstrated that CD133 expression marked OvCSCs by demonstrating that CD133+ but not CD133- cells had the malignant, self-renewal and differentiation potential to form tumours via serial propagation in immunodeficient mice. Baba et al. (2008) also isolated CD133+ OvCSCs from both ovarian cancer patient samples and cell lines, showing the CD133+ population to be more tumourigenic and chemoresistant than both the CD133- and parent populations.

As described in Section 1.4, an increasing body of evidence is suggesting that cancer cells may be capable of trans-differentiating into endothelial-like cells to facilitate angioneogenesis. Kusumbe et al. (2009) demonstrated that an ovarian cancer CD133+ population was not intrinsically more tumourigenic but rather facilitated angioneogenesis within the xenograft tumours, which augmented the malignant potential of the cell inoculum. This will be discussed further in Section 4.4.4.4.3 with respect to findings presented in this thesis.

CD133 is a cell membrane protein glycoprotein with five transmembrane regions, which is coded for by a gene located on chromosome 4 (Corbeil et al. 2000). Although widely used as a CSC marker, the function of CD133 is not yet known. An antibody directed against the CD133 was used to detect CD133+ pCSCs in this project.

1.10.3.4 CXCR4:

CXCR4 appears to play a major role in the regulation of the migration of both normal and cancer stem cells (Kucia et al. 2005; Miki et al. 2007). Hermann et al. (2007) demonstrated that a CD133+ population of cells in pancreatic cancer exhibited increased tumourigenicity relative

to CD133- cells. It was shown that this CD133+ population could be further subdivided into CD133+/CXCR4+ and CD133+/CXCR4- populations. It was demonstrated that while both of these sub-populations of CD133+ cells had similar tumourgenicity, only the CD133+/CXCR4+ population were capable of generating metastasis in a xenograft mouse model (Hermann et al. 2007).

CXCR4 is a cell membrane protein with seven transmembrane regions; its extracellular domain forms a chemokine receptor with affinity for stromal cell-derived factor-1 (SDF-1). The gene encoding CXCR4 is located on chromosome 2. It is composed of two exons; 103bp and 1562bp long and interrupted by a 2132 bp long intron (Wegner et al. 1998).

CXCR4 is a regulator of migration in the haematopoietic system (Tavor et al. 2004). Its regulation of cell trafficking also extends to both normal and cancer stem cells (Kucia et al. 2005). In ovarian cancer it was shown that a small peptide that inhibits CXCR4 was able to prevent CXCR4+ cells from migrating to a SDF-1 source. Prolonged incubation with this inhibitor caused cell death in CXCR4+ cells (Kucia et al. 2005). An antibody directed against CXCR4 was used in an attempt detect CXCR4+ pCSCs associated metastasis.

1.11 FACS is the Best Method for Isolation of Cancer Stem Cells:

Isolation of CSCs is central to the work carried out in this project. Three main methods have been described for the isolation of CSCs from various malignancies: spheroid growth, magnetic-activated cell sorting (MACS) and fluorescent-activated cell sorting (FACS). These approaches will be described (Sections 1.11.1 – 1.11.4) with the intention of explaining why FACS was considered the best approach for the isolation of CSCs in this project.

1.11.1 Spheroid Growth:

Spheroid growth was first introduced to the field of CSC research via the work of Hemmati et al. (2003) and Singh et al. (2003). In these studies, neural CSC populations were enriched by culturing cells isolated from patient samples in low serum media, supplemented with a combination of growth factors: leukemia inhibitory factor, fibroblast growth factor, epithelial growth factor and insulin. These growth conditions were selected based upon the work of Svendsen et al. (1998), who used similar conditions for the *in vitro* propagation of normal neural progenitor cells in an 'undifferentiated' state. Subsequently, spheroid growth has been utilised to enrich for CSC populations across several malignancies (Brain: Hemmati et al. (2003); Mammary and Melanoma: Rappa et al. (2008); Ovarian: Zhang et al. (2008)).

It is believed that spheroid growth is a method of CSC enrichment, rather than isolation. There is no physical separation of the CSC or non-CSC component from the heterogeneous population. Rather, it is believed that the altered culture conditions select for the dominant growth of the CSC population. Although widely used, spheroid growth selection of CSCs is not well understood. It has just been consistently demonstrated that such growth conditions select for CSC characteristics (Hemmati et al. 2003; Rappa et al. 2008; Zhang et al. 2008). It is possible that the growth conditions are inducing a stem-like state in the cells as opposed to selecting for CSCs. However, Rappa et al (2008) demonstrated that only the cells which formed spheroids and not the cells which remained adherent, under spheroid conditions, could be returned to exponential growth under normal culture conditions, and back to spheroid conditions to reform spheroids. This would suggest that spheroid growth is a selective, rather than a transformative process.

Spheroid Growth has the major advantage of not requiring any knowledge of CSC markers prior to isolation. However, it has two main disadvantages; Downstream comparisons of CSCs and non-CSCs often have to be made between cells propagated in different culture conditions (Spheroid versus Adherent growth): The purity of the isolated CSC population cannot be quantified.

However, it has disadvantages; spheroid selective conditions are thought to deplete non-CSCs and enrich for CSCs (Zhang et al. 2008). Such an approach lacks the ability to compare isolated pCSCs to non-pCSCs in the downstream analysis, which was a primary aim of this project. Selective conditions may affect the molecular signature of the isolated CSCs. As selection isolated CSCs can only be compared back to cells that were not maintained under selective conditions it is not possible to normalise out the changes due to selective conditions alone. These limitations reduce the power to identify therapeutically targetable pathways upon characterisation.

1.11.2 Holoclones, Meroclones and Paraclones:

Holoclone selective conditions can produce holoclones, meroclones and paraclones. These are considered to be clones produced from cells of reducing differentiation potential, ranked from high in holoclones to low in paraclones (Tan et al. 2011). In theory, this allows for downstream comparison of pCSCs to non-pCSCs. However, the selective pressures which selected for the growth of these holoclones, meroclones and paraclones may have altered the phenotype of the cells which were selected for. Such alterations, could produce artefacts in the downstream

analysis of the resulting holoclones, meroclones and paraclones. Additionally, there is variability in the viability of the clones post-selection, making them a high risk approach when considering downstream mouse xenograft work.

1.11.3 Magnetic-Activated Cell Sorting:

MACS is a method of cell sorting which can be applied to the isolation of CSCs from heterogeneous populations. The technology utilises antibodies which are conjugated to magnetic micro-beads. A heterogeneous suspension of cells is 'tagged' with magnetic micro-beads, conjugated to an antibody, which has been raised against an antigen that is only expressed on CSCs (a CSCs marker). As the cell suspension is passed through a column, a magnetic field traps the cells that are tagged with micro-beads in the column, while untagged cells are free to pass through. The cells of interest are then eluted from the column, in the absence of a magnetic field and can be returned to tissue culture.

MACS has been used to isolate CSCs from patient samples and cell lines (Pandey et al. 2012; Lee et al. 2011). MACS is not a quantitative process: it cannot provide data on the purity of the relative size of the CSC sub-population. For this reason MACS is often paired with flow cytometry. Flow cytometry is used to identify and quantify the CSCs within the heterogeneous population. MACS is then used to sort the different cell populations and flow cytometry is used post-sort to assess the purity. MACS sorts cells *en masse* as opposed to a cell by cell basis. This makes it a fast and scalable cell sorting technique. MACS is often used to enrich small sub-populations of cells prior to high purity sorting via FACS. When used in combination with FACS, MACS can greatly increase the speed and scale of cell sorting.

MACS is limited by its inability to produce data on the sizes and purity of the cell populations to be sorted. It is also limited by its dependence on antibodies to discriminate between cell types of heterogeneous populations. For example there is no MACS equivalent to the ALDH and HSP assay (described in Sections 1.10.1 and 1.10.2). The major advantage of MACS is its speed and scalability.

MACS was not used in the isolation of CSCs in this project. However, its speed and scalability would have been useful in the sorting of the small sub-populations identified within the A2780 and A2780cis cell lines identified via the ALDH assay. Unfortunately, there is no method to use MACS in conjunction with the ALDH assay, as it is an enzyme based fluorescence assay, rather than an antigen detection assay.

1.11.4 Fluorescence-Activated Cell Sorting:

FACS is a method of cell sorting which can be applied to the isolation of CSCs from heterogeneous populations. FACS is the most widely used method for the isolation of CSCs (ALDH: Silva et al. 2011; HSP: Szotek 2006; CSP: Baba et al. 2008). FACS is based on the principles of flow cytometry, which are described in detail in Section 1.12.

A wide range of fluorescent staining techniques, used in combination with flow cytometers, capable of multi-parametric staining analysis, makes FACS a very powerful method for the detection and isolation of CSCs. The main advantage of FACS is that it can isolate CSCs and non-CSCs into highly pure populations of cells. It is also capable of quantifying the relative size of the CSC and non-CSCs within the heterogeneous population. Furthermore, FACS is capable of quantifying the post-sort purity of the isolated CSC and non-CSC sub-populations. The main disadvantages are its speed and scalability. FACS sorts cells on a cell by cell basis. Therefore, the length of the cell sorting procedure scales linearly with time. To sort sufficient numbers of cells from a small sub-population can take a long time. As described in Section 1.11.3, MACS is often used to enrich such small sub-populations as it is a more scalable protocol. FACS is then used immediately afterwards to isolate this enriched population to a high degree of purity.

FACS was used to isolate the CSC and non-CSC populations identified in this project. It was selected over the other methods described, as it is capable of isolating both CSCs and non-CSCs, which allows for down stream comparisons. It also has the ability to identify and sort based on a wide range of fluorescent assays. Furthermore, it is capable of quantifying the purity of the isolated populations post-sort.

In a similar fashion to ES cells (described in Section 1.3), which were validated as pluripotent stem cells by producing tissues derived from the three germ layers, CSCs must be validated for their functional characteristics described in Section 1.3 (malignant, differentiation and self-renewal potential). The validation of CSCs will be described further in Section 6.0. Until validated, isolated populations based on marker expression can only be considered putative CSCs (pCSCs) and non-CSCs.

1.12 Flow Cytometry:

A large proportion of the work described in thesis is based upon flow cytometric analysis. The basic principles of flow cytometry will be described in Section 1.12.1. The analysis of flow

cytometric data will be described in Section 1.12.2. The application of flow cytometry to cell sorting will be introduced in Section 1.12.3. Cell sorting will be described in further detail in Section 5.1.

1.12.1 Flow Cytometry Overview:

Flow cytometry is the analysis of fluorescent light emitted by stained cells, as they are passed, in single file, past a series of lasers and detectors. Flow cytometry builds a fluorescent profile of a cell suspension by analysing the fluorescent properties of the cell suspension on a cell by cell basis. Cells can be stained using fluorochrome conjugated antibodies or other fluorescent reagents to assay for the desired biological properties. Each of the staining techniques used in this project were described in detail in Section 1.10. Flow cytometry is a robust approach for the analysis sub-populations of cells, with 1000s of papers reporting the successful use of flow cytometry for stem cell analysis.

1.12.2 Flow Cytometry Analysis:

The data generated via flow cytometry can be plotted as a histogram (one parameter), or a dot plot (two parameters). Each individual cell produces a data point (event). Multiple histograms and dot plots allow one to compare and contrast a large amount of data easily and to graphically select the cells of interested. These graphical selections are termed gates. Gating is a very powerful tool allowing the exclusion of all other confounding data, focusing only on the data collected from the cells of interest. Together these data points produce population profiles.

There were three technical controls applied to all flow cytometry experiments in this project (Figure 1.6). These controls allowed for the identification and analysis of events generated from viable single cells. Events generated from debris, doublets and dead cells were excluded from analysis via gates.

The first technical control discriminates cells from debris. As described above (Section 1.12.1) forward scatter and side scatter can be used to infer the size and granularity of an event (cell). Debris are smaller than cells and scatter less light. Plotting forward scatter against side scatter scatter allows for discrimination of cells from debris (Figure 1.6A). Points which appear below the line (gate) represent debris, while those above the line represent cells (Figure 1.6A).

The second technical control discriminates single cells from doublets. A doublet is two cells combined as a single event. Doublets can effect the accurate enumeration of the cells present in each population. Doublets were identified and removed from analysis via the pulse width of the

events generated (Figure 1.6B). Pulse width is a measurement of an event's time of flight (ToF) through the laser. Due to the shear forces of the stream, doublets will flow in a streamline fashion. This means that doublets will have longer ToF than single cells.

The third technical control discriminates live cells from dead cells. Dead cells were identified and removed from analysis via staining with propidium iodide (PI; Figure 1.6C). Dead cells can lead to false negatives in the ALDH and HSP assays. These assays depend upon viable cell membranes to retain and efflux (respectively) the fluorescent dyes. Dead cells can lead to false positives in the antibody based CSP assay, through increased non-specific binding. PI is a membrane impermeable, fluorescent, DNA staining dye. Live cells have an intact cellular membrane that exclude PI from the cell. The damaged cellular membrane of dead cells allows PI to gain access to the nuclear material and fluorescently stain the cell. Therefore, dead cells will have a brighter fluorescent profile than live cells and can be removed from analysis.

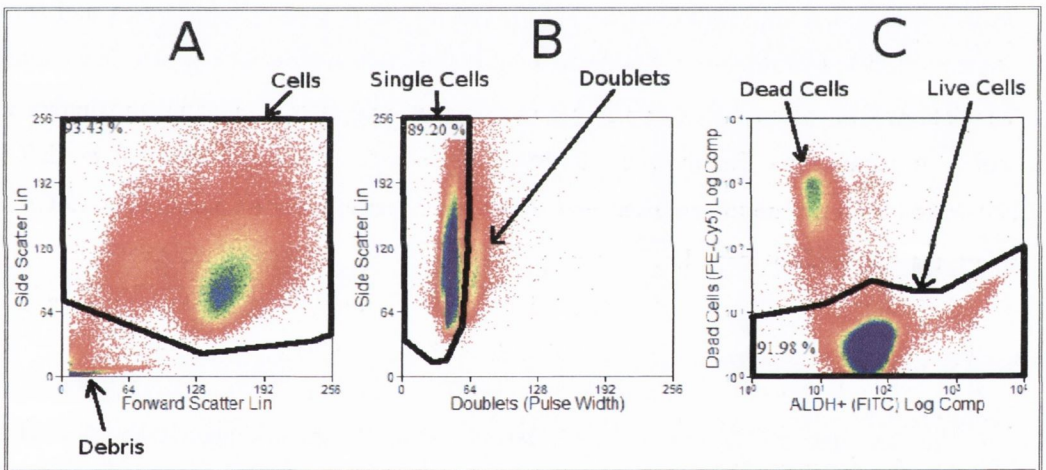

Figure 1.6: Technical Flow Cytometry Controls – These diagrams illustrate the three technical controls applied to all flow cytometry analysis in this project. A) Discrimination of cells from debris. B) Discrimination of single cells from doublets or clusters. C) Discrimination of live cells from dead cells.

The individual assay specific controls are described in Sections 1.10.1, 1.10.2 and 1.10.3. While the above technical controls are used to refine the data being analysed within each sample, the assay specific controls are used to establish positive/negative thresholds (gates) between samples. For example; the autofluorescence negative control sample is used to determine what proportion of fluorescence is due to background fluorescence as opposed to fluorochrome

fluorescence. When the autofluorescence sample has been run, a gate is drawn to mark the limit of fluorescence attributable to autofluorescence. When the experimental sample is run this gate sets the positive/negative thresholds. Events with a fluorescence greater than this threshold are considered positive for the fluorochrome. Events with a fluorescence less than this threshold are considered negative for the fluorochrome. As the proportion of fluorochrome present on a cell is proportional to the biological trait being assayed, these fluorochrome positive/negative cells are considered to be positive/negative for that biological trait.

1.12.3 Fluorescence-activated Cell Sorting (FACS):

FACS is a method of sorting a heterogeneous mix of cells based on flow cytometry technology. It sorts a cell suspension into multiple collection tubes on a cell by cell basis. Cell sorting is achieved by breaking the single file stream of cells into droplets after it has been scanned by the lasers. These droplets are created in such a way that there is a high probability that any droplet only contains one cell. These droplets are given an electrostatic charge based and sorted via magnetic fields into the desired collection tube. The operator decides which characteristics to sort the cells by. The type of charge placed on each droplet is dependent on whether the cell within the droplet has the desired characteristics or not. This method of cell by cell sorting allows for the high purity isolation of CSCs from a heterogeneous population. FACS will be described further in Section 5.1.

1.13 CSCs Provide Avenues for Novel Therapeutic Approaches:

The ultimate goal of CSC research is to develop novel therapeutic approaches to treat cancer, which are not susceptible to CSC driven chemoresistance and relapse. However, in a similar fashion to conventional chemotherapy and radiotherapy, it is hard to target cancerous cells without off target effects on the healthy cell populations. Many of the molecular mechanisms that regulate the undifferentiated state of CSCs also regulate that of the normal SSCs (Reya et al. 2001; Pardal et al. 2003). However, through the study of CSCs and SSCs, differential dependencies have been identified between the two cell types. Yilmaz et al. (2006) demonstrated a targetable dependence of CSCs on mTOR in a mouse leukaemia model. They showed that conditional deletion of *Pten* in adult haematopoietic stem cells (HSCs) led to transplantable leukaemias. The *Pten* deletion was also associated with hyper-proliferation of HSCs which led to their depletion. The leukaemic stem cells (LSC) suffered no such depletion. Yilmaz et al. showed the LSC's resistance to depletion via proliferation was dependent on

mTOR. They showed that treatment with the mTOR inhibitor Rapamycin led to the depletion of the LSC pool and concurrently rescued the HSC pool. This study demonstrated that it was possible to selectively target CSCs without damage to the SSC populations.

Current thinking suggests two approaches to targeting CSCs. One approach suggests that if CSCs are selectively killed the cancer will have lost its malignant potential and thus limited proliferative potential of the non-CSCs would result in the gradual diminishment of tumour burden. Additional chemotherapy could also be used to aggressively reduce the tumour burden. The second approach suggests that forced differentiation of CSCs could deplete the stem cell pool within tumours and therefore diminish its malignant potential. Again limited proliferative potential and/or additional chemotherapy could reduce the residual tumour burden. As both approaches have eliminated the CSC pool, CSC driven relapse and chemoresistance should be circumvented.

Such stem cell based approaches are already proving successful in the clinic. Foster et al. (2009) demonstrated that the treatment of a patient with a 'B-CLL tumour vaccine' elicited a transient immune response which selectively and completely removed the pCSC sub-population of the cancer. This was demonstrated through the loss of HSP+ pCSCs in post-therapy samples isolated from the patient. Although this treatment completely eliminated the CSC population, it did not reduce the total tumour burden. Continued follow-up examinations over an 18 month period demonstrated a continuing decline in the tumour burden, presumably as the 'committed' cells reached the end of their proliferative lifespan. This study demonstrated the it is possible to treat cancer by eliminating the CSC pool, as non-CSCs do not have the malignant potential to perpetuate the tumour. As described in Section 1.7, it is possible that ovarian cancer has multiple CSC populations. It would most likely require the ablation of all such populations to effect a similar treatment in ovarian cancer.

An approach based on differentiation of CSCs has also had some success in the clinic. Retinoic acid (RA) is used in the clinic to induce complete remission of patients with acute promyelocytic leukemia (APL; Degos and Wang 2001). This remission is believed to occur via the differentiation of APL blasts (Castaigne et al. 1990). This demonstrates that differentiation based therapy can be used to remove the proliferative potential form cancer. However, relapse was common with RA therapy. This was believed to be due to RA treatment only differentiating the progenitor cells (APL blasts) and not the true leukemic CSC clone (Degos and Wang 2001). RA used in combination with chemotherapy has a much better outcome, presumably due to the elimination of the leukemic CSC clone (Degos and Wang 2001).

With the advent of the CSC hypothesis comes the opportunity to attack cancer at its root, rather than just targeting the fast dividing cells, with agents that disrupt the cell cycle and induce apoptosis. These stem cell based approaches have the potential to overcome the obstacles posed by chemoresistant and recurrent cancers, paving the way for better more specific therapies.

1.14Summary:

This thesis will describe the identification, isolation and validation of CSCs form ovarian cancer sources. This chapter introduced the key concepts upon which the work presented in this thesis is based. The principles of stem cell biology and cancer biology were presented in Section 1.3 and 1.4 respectively. A review of the published data supporting the presence of CSCs and specifically OvCSCs in cancer was presented in Sections 1.5 and 1.7 respectively. A description of ovarian cancer model systems, pCSCs markers and isolation techniques was given in Sections 1.9, 1.10 and 1.11 respectively. Finally, some of the possible CSC based therapeutic avenues were discussed with the support of the published literature (Section 1.14). The rest of this thesis will now go on to describe the materials and methods used (Section 3.0), and the establishment and optimisation of several of the core methodologies used through out this project. The identification (Section 4.0), isolation (Section 5.0) and validation (Section 6.0) of OvCSCs will then be described. After which further experiments investigating OvCSC hierarchies will be described (Section 7.0). The thesis will conclude with a general discussion regarding the CSC biology field, the findings presented in this chapter and the future directions of the work presented in this project and the CSC biology field in general (Section 8.0).

Section 1.0 – General Introduction:

General Introduction:- Key Points

- In a similar fashion to ES cells and SSCs, CSCs are defined by their differentiation, self-renewal potential. They are also defined by their capacity to reconstitute the tissue from which they were derived (malignant potential).
- Six models of ovarian cancer and one model of OSE were used in this project:
  - Ovarian Cancer: A2780, A2780cis, IGROV-1, IGROV-CDDP, SK-OV-3 and 59M.
  - OSE: HIO-80
- Three fluorescent based assays (ALDH, HSP and CSP) were used to screen for pCSCs and CSCs and metastatic cells. There were six markers used in total:
  - Stemness markers: ALDH, HSP, CD44, CD117 and CD133.
  - Metastatic markers: CXCR4
- Cells were isolated via FACS.
- All isolated cells are only considered pCSCs and non-pCSCs until validation experiments establish them as CSCs and non-CSCs.

1.15References:

Adhikari, Amit S., Neeraj Agarwal, Byron M. Wood, Constance Porretta, Bernardo Ruiz, Radhika R. Pochampally, and Tomoo Iwakuma. 2010. "CD117 and Stro-1 Identify Osteosarcoma Tumor-Initiating Cells Associated with Metastasis and Drug Resistance." *Cancer Research* 70 (11) (June 1): 4602–4612. doi:10.1158/0008-5472.CAN-09-3463.

Al-Hajj, Muhammad, Max S Wicha, Adalberto Benito-Hernandez, Sean J Morrison, and Michael F Clarke. 2003. "Prospective Identification of Tumorigenic Breast Cancer Cells." *Proceedings of the National Academy of Sciences of the United States of America* 100 (7) (April 1): 3983–3988. doi:10.1073/pnas.0530291100.

Alison, Malcolm R, Naomi J Guppy, Susan M L Lim, and Linda J Nicholson. 2010. "Finding Cancer Stem Cells: Are Aldehyde Dehydrogenases Fit for Purpose?" *The Journal of Pathology* 222 (4) (December): 335–344. doi:10.1002/path.2772.

Allsopp, R C, E Chang, M Kashefi-Aazam, E I Rogaev, M A Piatyszek, J W Shay, and C B Harley. 1995. "Telomere Shortening Is Associated with Cell Division in Vitro and in Vivo." *Experimental Cell Research* 220 (1) (September): 194–200. doi:10.1006/excr.1995.1306.

Alvero, A. B., H. H. Fu, J. Holmberg, I. Visintin, L. Mor, C. C. Marquina, J. Oidtman, D. A. Silasi, and G. Mor. 2009. "Stem-Like Ovarian Cancer Cells Can Serve as Tumor Vascular Progenitors." *Stem Cells* 27 (10): 2405–2413.

Andrews, P W. 1984. "Retinoic Acid Induces Neuronal Differentiation of a Cloned Human Embryonal Carcinoma Cell Line in Vitro." *Developmental Biology* 103 (2) (June): 285–293.

Ashman, L K. 1999. "The Biology of Stem Cell Factor and Its Receptor C-kit." *The International Journal of Biochemistry & Cell Biology* 31 (10) (October): 1037–1051.

Auersperg, N, A S Wong, K C Choi, S K Kang, and P C Leung. 2001. "Ovarian Surface Epithelium: Biology, Endocrinology, and Pathology." *Endocrine Reviews* 22 (2) (April): 255–288.

Auersperg, N., S. Maines-Bandiera, J. H. Booth, H. T. Lynch, A. K. Godwin, and T. C. Hamilton. 1995. "Expression of Two Mucin Antigens in Cultured Human Ovarian Surface Epithelium: Influence of a Family Hostory of Ovarian Cancer." *American Journal of Obstetrics and Gynecology* 173 (2): 558–565.

Baba, T., P. A. Convery, N. Matsumura, R. S. Whitaker, E. Kondoh, T. Perry, Z. Huang, R. C. Bentley, S. Mori, and S. Fujii. 2008. "Epigenetic Regulation of CD133 and Tumorigenicity of CD133+ Ovarian Cancer Cells." *Oncogene* 28 (2): 209–218.

Bapat, S. A., A. M. Mali, C. B. Koppikar, and N. K. Kurrey. 2005. "Stem and Progenitor-like Cells Contribute to the Aggressive Behavior of Human Epithelial Ovarian Cancer." *Cancer Research* 65 (8): 3025–3029.

Bapat, Sharmila A. 2010. "Human Ovarian Cancer Stem Cells." *Reproduction (Cambridge, England)* 140 (1) (July): 33–41. doi:10.1530/REP-09-0389.

Bénard, J., J. Da Silva, M. C. De Blois, P. Boyer, P. Duvillard, E. Chiric, and G. Riou. 1985. "Characterization of a Human Ovarian Adenocarcinoma Line, IGROV1, in Tissue Culture and in Nude Mice." *Cancer Research* 45 (10): 4970–4979.

Bennett, K L, D G Jackson, J C Simon, E Tanczos, R Peach, B Modrell, I Stamenkovic, G Plowman, and A Aruffo. 1995. "CD44 Isoforms Containing Exon V3 Are Responsible for the Presentation of Heparin-binding Growth Factor." *The Journal of Cell Biology* 128 (4) (February): 687–698.

Blackburn, Elizabeth H. 2005. "Telomerase and Cancer Kirk A. Landon - AACR Prize for Basic Cancer Research Lecture." *Molecular Cancer Research* 3 (9) (September 1): 477–482. doi:10.1158/1541-7786.MCR-05-0147.

Blasco, Maria A. 2005. "Telomeres and Human Disease: Ageing, Cancer and Beyond." *Nature Reviews Genetics* 6 (8) (August 1): 611–622. doi:10.1038/nrg1656.

Bleau, Anne-Marie, Dolores Hambardzumyan, Tatsuya Ozawa, Elena I Fomchenko, Jason T Huse, Cameron W Brennan, and Eric C Holland. 2009. "PTEN/PI3K/Akt Pathway Regulates the Side Population Phenotype and ABCG2 Activity in Glioma Tumor Stem-like Cells." *Cell Stem Cell* 4 (3) (March 6): 226–235. doi:10.1016/j.stem.2009.01.007.

Bonnet, D, and J E Dick. 1997. "Human Acute Myeloid Leukemia Is Organized as a Hierarchy That Originates from a Primitive Hematopoietic Cell." *Nature Medicine* 3 (7) (July): 730–737.

Section 1.0 – General Introduction

Brown, R, C Clugston, P Burns, A Edlin, P Vasey, B Vojtěsek, and S B Kaye. 1993. "Increased Accumulation of P53 Protein in Cisplatin-resistant Ovarian Cell Lines." *International Journal of Cancer. Journal International Du Cancer* 55 (4) (October 21): 678–684.

Camerer, Eric, Aisha A Qazi, Daniel N Duong, Ivo Cornelissen, Rommel Advincula, and Shaun R Coughlin. 2004. "Platelets, Protease-activated Receptors, and Fibrinogen in Hematogenous Metastasis." *Blood* 104 (2) (July 15): 397–401. doi:10.1182/blood-2004-02-0434.

Cancer Genome Atlas Research Network. 2011. "Integrated Genomic Analyses of Ovarian Carcinoma." *Nature* 474 (7353) (June 30): 609–615. doi:10.1038/nature10166.

Canonico, B, C Felici, and S Papa. 2001. "CD117." *Journal of Biological Regulators and Homeostatic Agents* 15 (1) (March): 90–94.

Castaigne, S, C Chomienne, M T Daniel, P Ballerini, R Berger, P Fenaux, and L Degos. 1990. "All-trans Retinoic Acid as a Differentiation Therapy for Acute Promyelocytic Leukemia. I. Clinical Results." *Blood* 76 (9) (November 1): 1704–1709.

Charafe-Jauffret, E., C. Ginestier, F. Iovino, J. Wicinski, N. Cervera, P. Finetti, M.-H. Hur, et al. 2009. "Breast Cancer Cell Lines Contain Functional Cancer Stem Cells with Metastatic Capacity and a Distinct Molecular Signature." *Cancer Research* 69 (4) (February 3): 1302–1313. doi:10.1158/0008-5472.CAN-08-2741.

Chiba, Tetsuhiro, Kaoru Kita, Yun-Wen Zheng, Osamu Yokosuka, Hiromitsu Saisho, Atsushi Iwama, Hiromitsu Nakauchi, and Hideki Taniguchi. 2006. "Side Population Purified from Hepatocellular Carcinoma Cells Harbors Cancer Stem Cell-like Properties." *Hepatology (Baltimore, Md.)* 44 (1) (July): 240–251. doi:10.1002/hep.21227.

Clarke, Michael F, John E Dick, Peter B Dirks, Connie J Eaves, Catriona H M Jamieson, D Leanne Jones, Jane Visvader, Irving L Weissman, and Geoffrey M Wahl. 2006. "Cancer Stem Cells--perspectives on Current Status and Future Directions: AACR Workshop on Cancer Stem Cells." *Cancer Research* 66 (19) (October 1): 9339–9344. doi:10.1158/0008-5472.CAN-06-3126.

Collins, Anne T, Paul A Berry, Catherine Hyde, Michael J Stower, and Norman J Maitland. 2005. "Prospective Identification of Tumorigenic Prostate Cancer Stem Cells." *Cancer Research* 65 (23) (December 1): 10946–10951. doi:10.1158/0008-5472.CAN-05-2018.

Corbeil, D, K Röper, A Hellwig, M Tavian, S Miraglia, S M Watt, P J Simmons, B Peault, D W Buck, and W B Huttner. 2000. "The Human AC133 Hematopoietic Stem Cell Antigen Is Also Expressed in Epithelial Cells and Targeted to Plasma Membrane Protrusions." *The Journal of Biological Chemistry* 275 (8) (February 25): 5512–5520.

Corti, Stefania, Federica Locatelli, Dimitra Papadimitriou, Chiara Donadoni, Sabrina Salani, Roberto Del Bo, Sandra Strazzer, Nereo Bresolin, and Giacomo P Comi. 2006. "Identification of a Primitive Brain-derived Neural Stem Cell Population Based on Aldehyde Dehydrogenase Activity." *Stem Cells (Dayton, Ohio)* 24 (4) (April): 975–985. doi:10.1634/stemcells.2005-0217.

Curley, M. D., V. A. Therrien, C. L. Cummings, P. A. Sergent, C. R. Koulouris, A. M. Friel, D. J. Roberts, M. V. Seiden, D. T. Scadden, and B. R. Rueda. 2009. "CD133 Expression Defines a Tumor Initiating Cell Population in Primary Human Ovarian Cancer." *Stem Cells* 27 (12): 2875–2883.

Curley, M.D., V.A. Therrien, C.L. Cummings, P.A. Sergent, C.R. Koulouris, A.M. Friel, D.J. Roberts, M.V. Seiden, D.T. Scadden, B.R. Rueda, et al. 2009. "CD133 Expression Defines a Tumor Initiating Cell Population in Primary Human Ovarian Cancer." *Stem Cells* 27 (12): 2875–2883.

Davies, MA, and Y Samuels. 2010. "Analysis of the Genome to Personalize Therapy for Melanoma." *Oncogene* 29 (41) (October 14): 5545–5555. doi:10.1038/onc.2010.323.

Degos, L, and Z Y Wang. 2001. "All Trans Retinoic Acid in Acute Promyelocytic Leukemia." *Oncogene* 20 (49) (October 29): 7140–7145. doi:10.1038/sj.onc.1204763.

Deng, S., X. Yang, H. Lassus, S. Liang, S. Kaur, Q. Ye, C. Li, L. P. Wang, K. F. Roby, and S. Orsulic. 2010. "Distinct Expression Levels and Patterns of Stem Cell Marker, Aldehyde Dehydrogenase Isoform 1 (ALDH1), in Human Epithelial Cancers." *PLoS One* 5 (4): e10277.

Dick, Frederick A. 2007. "Structure-function Analysis of the Retinoblastoma Tumor Suppressor Protein – Is the Whole a Sum of Its Parts?" *Cell Division* 2 (1) (September 13): 26. doi:10.1186/1747-1028-2-26.

Donovan, Erin A., and Shivaani Kummar. 2006. "Targeting VEGF in Cancer Therapy." *Current Problems in Cancer* 30 (1) (January): 7–32. doi:10.1016/j.currproblcancer.2005.11.001.

Section 1.0 – General Introduction

Doyle, L A, W Yang, L V Abruzzo, T Krogmann, Y Gao, A K Rishi, and D D Ross. 1998. "A Multidrug Resistance Transporter from Human MCF-7 Breast Cancer Cells." *Proceedings of the National Academy of Sciences of the United States of America* 95 (26) (December 22): 15665–15670.

Egan, Karl, Darragh Crowley, Paul Smyth, Sharon O'Toole, Cathy Spillane, Cara Martin, Michael Gallagher, et al. 2011. "Platelet Adhesion and Degranulation Induce Pro-Survival and Pro-Angiogenic Signalling in Ovarian Cancer Cells." Edited by Pan-Chyr Yang. *PLoS ONE* 6 (10) (October 12): e26125. doi:10.1371/journal.pone.0026125.

Elledge, Stephen J. 1996. "Cell Cycle Checkpoints: Preventing an Identity Crisis." *Science* 274 (5293) (December 6): 1664–1672. doi:10.1126/science.274.5293.1664.

Faassen, A E, J A Schrager, D J Klein, T R Oegema, J R Couchman, and J B McCarthy. 1992. "A Cell Surface Chondroitin Sulfate Proteoglycan, Immunologically Related to CD44, Is Involved in Type I Collagen-mediated Melanoma Cell Motility and Invasion." *The Journal of Cell Biology* 116 (2) (January): 521–531.

Ferlay, Jacques, Hai-Rim Shin, Freddie Bray, David Forman, Colin Mathers, and Donald Maxwell Parkin. 2010. "Estimates of Worldwide Burden of Cancer in 2008: GLOBOCAN 2008." *International Journal of Cancer. Journal International Du Cancer* 127 (12) (December 15): 2893–2917. doi:10.1002/ijc.25516.

Flesken-Nikitin, Andrea, Chang-Il Hwang, Chieh-Yang Cheng, Tatyana V Michurina, Grigori Enikolopov, and Alexander Yu Nikitin. 2013. "Ovarian Surface Epithelium at the Junction Area Contains a Cancer-prone Stem Cell Niche." *Nature* 495 (7440) (March 14): 241–245. doi:10.1038/nature11979.

Fortunel, N, J Hatzfeld, S Kisselev, M N Monier, K Ducos, A Cardoso, P Batard, and A Hatzfeld. 2000. "Release from Quiescence of Primitive Human Hematopoietic Stem/progenitor Cells by Blocking Their Cell-surface TGF-beta Type II Receptor in a Short-term in Vitro Assay." *Stem Cells (Dayton, Ohio)* 18 (2): 102–111. doi:10.1634/stemcells.18-2-102.

Foster, N. E., K. S. Dziedzic, D. A. W. M. Windt, J. M. Fritz, and E. M. Hay. 2009. "Research Priorities for Non-pharmacological Therapies for Common Musculoskeletal Problems: Nationally and Internationally Agreed Recommendations." *BMC Musculoskeletal Disorders* 10 (1): 3.

Gasic, G J, T B Gasic, and C C Stewart. 1968. "Antimetastatic Effects Associated with Platelet Reduction." *Proceedings of the National Academy of Sciences of the United States of America* 61 (1) (September): 46–52.

Gatti, Laura, Valentina Benedetti, Michelandrea De Cesare, Elisabetta Corna, Raffaella Cincinelli, Nadia Zaffaroni, Franco Zunino, and Paola Perego. 2012. "Synergistic Interaction Between the Novel Histone Deacetylase Inhibitor ST2782 and the Proteasome Inhibitor Bortezomib in Platinum-sensitive and Resistant Ovarian Carcinoma Cells." *Journal of Inorganic Biochemistry* 113 (August): 94–101. doi:10.1016/j.jinorgbio.2012.04.007.

Godwin, A K, A Meister, P J O'Dwyer, C S Huang, T C Hamilton, and M E Anderson. 1992. "High Resistance to Cisplatin in Human Ovarian Cancer Cell Lines Is Associated with Marked Increase of Glutathione Synthesis." *Proceedings of the National Academy of Sciences of the United States of America* 89 (7) (April 1): 3070–3074.

Golebiewska, A., N. H. C. Brons, R. Bjerkvig, and S. P. Niclou. 2011. "Critical Appraisal of the Side Population Assay in Stem Cell and Cancer Stem Cell Research." *Cell Stem Cell* 8 (2): 136–147.

Goodell, M A, K Brose, G Paradis, A S Conner, and R C Mulligan. 1996. "Isolation and Functional Properties of Murine Hematopoietic Stem Cells That Are Replicating in Vivo." *The Journal of Experimental Medicine* 183 (4) (April 1): 1797–1806.

Goodsell, David S. 1999. "The Molecular Perspective: P53 Tumor Suppressor." *The Oncologist* 4 (2) (April 1): 138–139.

Guibal, Florence C, Meritxell Alberich-Jorda, Hideyo Hirai, Alexander Ebralidze, Elena Levantini, Annalisa Di Ruscio, Pu Zhang, et al. 2009. "Identification of a Myeloid Committed Progenitor as the Cancer-initiating Cell in Acute Promyelocytic Leukemia." *Blood* 114 (27) (December 24): 5415–5425. doi:10.1182/blood-2008-10-182071.

Hanahan, Douglas, and Robert A Weinberg. 2011. "Hallmarks of Cancer: The Next Generation." *Cell* 144 (5) (March 4): 646–674. doi:10.1016/j.cell.2011.02.013.

Haraguchi, Naotsugu, Tohru Utsunomiya, Hiroshi Inoue, Fumiaki Tanaka, Koshi Mimori, Graham F Barnard, and Masaki Mori. 2006. "Characterization of a Side Population of Cancer Cells from Human Gastrointestinal System." *Stem Cells (Dayton, Ohio)* 24 (3) (March): 506–513. doi:10.1634/stemcells.2005-0282.

Harrison, D E, and C P Lerner. 1991. "Most Primitive Hematopoietic Stem Cells Are Stimulated to Cycle Rapidly after Treatment with 5-fluorouracil." *Blood* 78 (5) (September 1): 1237–1240.

Hemmati, H. D., I. Nakano, J. A. Lazareff, M. Masterman-Smith, D. H. Geschwind, M. Bronner-Fraser, and H. I. Kornblum. 2003. "Cancerous Stem Cells Can Arise from Pediatric Brain Tumors." *Proceedings of the National Academy of Sciences* 100 (25): 15178–15183.

Hermann, Patrick C, Stephan L Huber, Tanja Herrler, Alexandra Aicher, Joachim W Ellwart, Markus Guba, Christiane J Bruns, and Christopher Heeschen. 2007. "Distinct Populations of Cancer Stem Cells Determine Tumor Growth and Metastatic Activity in Human Pancreatic Cancer." *Cell Stem Cell* 1 (3) (September 13): 313–323. doi:10.1016/j.stem.2007.06.002.

Herzog, Thomas J. 2004. "Recurrent Ovarian Cancer How Important Is It to Treat to Disease Progression?" *Clinical Cancer Research* 10 (22) (November 15): 7439–7449. doi:10.1158/1078-0432.CCR-04-0683.

Hills, C. A., L. R. Kelland, G. Abel, J. Siracky, A. P. Wilson, and K. R. Harrap. 1989. "Biological Properties of Ten Human Ovarian Carcinoma Cell Lines: Calibration in Vitro Against Four Platinum Complexes." *British Journal of Cancer* 59 (4): 527.

Hirschmann-Jax, C, A E Foster, G G Wulf, J G Nuchtern, T W Jax, U Gobel, M A Goodell, and M K Brenner. 2004. "A Distinct 'Side Population' of Cells with High Drug Efflux Capacity in Human Tumor Cells." *Proceedings of the National Academy of Sciences of the United States of America* 101 (39) (September 28): 14228–14233. doi:10.1073/pnas.0400067101.

Ho, Maria M, Alvin V Ng, Stephen Lam, and Jaclyn Y Hung. 2007. "Side Population in Human Lung Cancer Cell Lines and Tumors Is Enriched with Stem-like Cancer Cells." *Cancer Research* 67 (10) (May 15): 4827–4833. doi:10.1158/0008-5472.CAN-06-3557.

Horiuchi, Akiko, Kazuko Itoh, Motohiko Shimizu, Ikuko Nakai, Teruyuki Yamazaki, Kaoru Kimura, Akihiko Suzuki, Isao Shiozawa, Noritane Ueda, and Ikuo Konishi. 2003. "Toward Understanding the Natural History of Ovarian Carcinoma Development: a Clinicopathological Approach." *Gynecologic Oncology* 88 (3) (March): 309–317.

Huang, Emina H, Mark J Hynes, Tao Zhang, Christophe Ginestier, Gabriela Dontu, Henry Appelman, Jeremy Z Fields, Max S Wicha, and Bruce M Boman. 2009. "Aldehyde Dehydrogenase 1 Is a Marker for Normal and Malignant Human Colonic Stem Cells (SC) and Tracks SC Overpopulation During Colon Tumorigenesis." *Cancer Research* 69 (8) (April 15): 3382–3389. doi:10.1158/0008-5472.CAN-08-4418.

Huntly, Brian J P, Hirokazu Shigematsu, Kenji Deguchi, Benjamin H Lee, Shinichi Mizuno, Nicky Duclos, Rebecca Rowan, et al. 2004. "MOZ-TIF2, but Not BCR-ABL, Confers Properties of Leukemic Stem Cells to Committed Murine Hematopoietic Progenitors." *Cancer Cell* 6 (6) (December): 587–596. doi:10.1016/j.ccr.2004.10.015.

Jacobs, I, and R C Bast Jr. 1989. "The CA 125 Tumour-associated Antigen: a Review of the Literature." *Human Reproduction (Oxford, England)* 4 (1) (January): 1–12.

Kalayda, Ganna V, Christina H Wagner, and Ulrich Jaehde. 2012. "Relevance of Copper Transporter 1 for Cisplatin Resistance in Human Ovarian Carcinoma Cells." *Journal of Inorganic Biochemistry* 116 (November): 1–10. doi:10.1016/j.jinorgbio.2012.07.010.

Kikkawa, Fumitaka, Akihiro Nawa, Kazuhiko Ino, Kiyosumi Shibata, Hiroaki Kajiyama, and Seiji Nomura. 2006. "Advances in Treatment of Epithelial Ovarian Cancer." *Nagoya Journal of Medical Science* 68 (1-2) (January): 19–26.

Kleinsmith, Lewis J., and G. Barry Pierce. 1964. "Multipotentiality of Single Embryonal Carcinoma Cells." *Cancer Research* 24 (9) (October 1): 1544–1551.

Kucia, M., R. Reca, K. Miekus, J. Wanzeck, W. Wojakowski, A. Janowska-Wieczorek, J. Ratajczak, and M. Z. Ratajczak. 2005. "Trafficking of Normal Stem Cells and Metastasis of Cancer Stem Cells Involve Similar Mechanisms: Pivotal Role of the SDF-1–CXCR4 Axis." *Stem Cells* 23 (7): 879–894.

Kusumbe, A. P., A. M. Mali, and S. A. Bapat. 2009. "CD133-Expressing Stem Cells Associated with Ovarian Metastases Establish an Endothelial Hierarchy and Contribute to Tumor Vasculature." *Stem Cells* 27 (3): 498–508.

Laios, A., S. A. O'toole, R. Flavin, C. Martin, M. Ring, N. Gleeson, T. D'Arcy, E. McGuinness, O. Sheils, and B. L. Sheppard. 2008. "An Integrative Model for Recurrence in Ovarian Cancer." *Molecular Cancer* 7 (1): 8.

Laios, Alexandros, Bashir Mohamed, Lynn Kelly, Richard Flavin, Stephen Finn, Lynda McEvoy, Michael Gallagher, et al. 2013. "Pre-Treatment of Platinum Resistant Ovarian Cancer Cells with

an MMP-9/MMP-2 Inhibitor Prior to Cisplatin Enhances Cytotoxicity as Determined by High Content Screening." *International Journal of Molecular Sciences* 14 (1) (January 22): 2085–2103. doi:10.3390/ijms14012085.

Lee, Eun-Kyung, Hyungdon Cho, and Chan-Wha Kim. 2011. "Proteomic Analysis of Cancer Stem Cells in Human Prostate Cancer Cells." *Biochemical and Biophysical Research Communications* 412 (2) (August 26): 279–285. doi:10.1016/j.bbrc.2011.07.083.

Lengyel, Ernst. 2010. "Ovarian Cancer Development and Metastasis." *The American Journal of Pathology* 177 (3) (September): 1053–1064. doi:10.2353/ajpath.2010.100105.

Lesley, J, and R Hyman. 1998. "CD44 Structure and Function." *Frontiers in Bioscience: a Journal and Virtual Library* 3 (July 1): d616–630.

Li, Chenwei, David G Heidt, Piero Dalerba, Charles F Burant, Lanjing Zhang, Volkan Adsay, Max Wicha, Michael F Clarke, and Diane M Simeone. 2007. "Identification of Pancreatic Cancer Stem Cells." *Cancer Research* 67 (3) (February 1): 1030–1037. doi:10.1158/0008-5472.CAN-06-2030.

Li, F., B. Tiede, J. Massagué, and Y. Kang. 2006. "Beyond Tumorigenesis: Cancer Stem Cells in Metastasis." *Cell Research* 17 (1): 3–14.

Longley, Daniel B., D. Paul Harkin, and Patrick G. Johnston. 2003. "5-Fluorouracil: Mechanisms of Action and Clinical Strategies." *Nature Reviews Cancer* 3 (5) (May 1): 330–338. doi:10.1038/nrc1074.

Lu, Yan-Ming, Meng-Li Rong, Chao Shang, Ning Wang, Xiang Li, Yan-Yan Zhao, and Shu-Lan Zhang. 2013. "Suppression of HER-2 via siRNA Interference Promotes Apoptosis and Decreases Metastatic Potential of SKOV-3 Human Ovarian Carcinoma Cells." *Oncology Reports* 29 (3) (March): 1133–1139. doi:10.3892/or.2012.2214.

Ma, J, M Maliepaard, H J Kolker, J Verweij, and J H Schellens. 1998. "Abrogated Energy-dependent Uptake of Cisplatin in a Cisplatin-resistant Subline of the Human Ovarian Cancer Cell Line IGROV-1." *Cancer Chemotherapy and Pharmacology* 41 (3): 186–192.

Ma, Stephanie, Kwok Wah Chan, Terence Kin-Wah Lee, Kwan Ho Tang, Jana Yim-Hung Wo, Bo-Jian Zheng, and Xin-Yuan Guan. 2008. "Aldehyde Dehydrogenase Discriminates the CD133 Liver Cancer Stem Cell Populations." *Molecular Cancer Research: MCR* 6 (7) (July): 1146–1153. doi:10.1158/1541-7786.MCR-08-0035.

Martin, Virginia R. 2005. "Straight Talk About Ovarian Cancer." *Nursing* 35 (4) (April): 36–41; quiz 42.

McGuire, W P, W J Hoskins, M F Brady, P R Kucera, E E Partridge, K Y Look, D L Clarke-Pearson, and M Davidson. 1996. "Cyclophosphamide and Cisplatin Compared with Paclitaxel and Cisplatin in Patients with Stage III and Stage IV Ovarian Cancer." *The New England Journal of Medicine* 334 (1) (January 4): 1–6. doi:10.1056/NEJM199601043340101.

Miki, J., B. Furusato, H. Li, Y. Gu, H. Takahashi, S. Egawa, I. A. Sesterhenn, D. G. McLeod, S. Srivastava, and J. S. Rhim. 2007. "Identification of Putative Stem Cell Markers, CD133 and CXCR4, in hTERT–Immortalized Primary Nonmalignant and Malignant Tumor-Derived Human Prostate Epithelial Cell Lines and in Prostate Cancer Specimens." *Cancer Research* 67 (7): 3153–3161.

Mintz, B, and K Illmensee. 1975. "Normal Genetically Mosaic Mice Produced from Malignant Teratocarcinoma Cells." *Proceedings of the National Academy of Sciences of the United States of America* 72 (9) (September): 3585–3589.

Molthoff, C F, J J Calame, H M Pinedo, and E Boven. 1991. "Human Ovarian Cancer Xenografts in Nude Mice: Characterization and Analysis of Antigen Expression." *International Journal of Cancer. Journal International Du Cancer* 47 (1) (January 2): 72–79.

Morrison, S J, and I L Weissman. 1994. "The Long-term Repopulating Subset of Hematopoietic Stem Cells Is Deterministic and Isolatable by Phenotype." *Immunity* 1 (8) (November): 661–673.

Naor, David, Shlomo Nedvetzki, Itshak Golan, Lora Melnik, and Yoram Faitelson. 2002. "CD44 in Cancer." *Critical Reviews in Clinical Laboratory Sciences* 39 (6) (November): 527–579. doi:10.1080/10408360290795574.

Nigg, E A. 1995. "Cyclin-dependent Protein Kinases: Key Regulators of the Eukaryotic Cell Cycle." *BioEssays: News and Reviews in Molecular, Cellular and Developmental Biology* 17 (6) (June): 471–480. doi:10.1002/bies.950170603.

O'Brien, Catherine A, Aaron Pollett, Steven Gallinger, and John E Dick. 2007. "A Human Colon Cancer Cell Capable of Initiating Tumour Growth in Immunodeficient Mice." *Nature* 445 (7123) (January 4): 106–110. doi:10.1038/nature05372.

Section 1.0 – General Introduction

Pandey, P R, F Xing, S Sharma, M Watabe, S K Pai, M Iiizumi-Gairani, K Fukuda, S Hirota, Y-Y Mo, and K Watabe. 2012. "Elevated Lipogenesis in Epithelial Stem-like Cell Confers Survival Advantage in Ductal Carcinoma in Situ of Breast Cancer." *Oncogene* (December 3). doi:10.1038/onc.2012.519.

Pardal, Ricardo, Michael F Clarke, and Sean J Morrison. 2003. "Applying the Principles of Stem-cell Biology to Cancer." *Nature Reviews. Cancer* 3 (12) (December): 895–902. doi:10.1038/nrc1232.

Patrawala, L., T. Calhoun, R. Schneider-Broussard, H. Li, B. Bhatia, S. Tang, J. G. Reilly, D. Chandra, J. Zhou, and K. Claypool. 2006. "Highly Purified CD44+ Prostate Cancer Cells from Xenograft Human Tumors Are Enriched in Tumorigenic and Metastatic Progenitor Cells." *Oncogene* 25 (12): 1696–1708.

Patrawala, Lubna, Tammy Calhoun, Robin Schneider-Broussard, Jianjun Zhou, Kent Claypool, and Dean G Tang. 2005. "Side Population Is Enriched in Tumorigenic, Stem-like Cancer Cells, Whereas ABCG2+ and ABCG2- Cancer Cells Are Similarly Tumorigenic." *Cancer Research* 65 (14) (July 15): 6207–6219. doi:10.1158/0008-5472.CAN-05-0592.

Perego, P, M Giarola, S C Righetti, R Supino, C Caserini, D Delia, M A Pierotti, T Miyashita, J C Reed, and F Zunino. 1996. "Association Between Cisplatin Resistance and Mutation of P53 Gene and Reduced Bax Expression in Ovarian Carcinoma Cell Systems." *Cancer Research* 56 (3) (February 1): 556–562.

Perlikos, Fotis, Kevin J Harrington, and Konstantinos N Syrigos. 2013. "Key Molecular Mechanisms in Lung Cancer Invasion and Metastasis: A Comprehensive Review." *Critical Reviews in Oncology/hematology* (January 16). doi:10.1016/j.critrevonc.2012.12.007.

Rappa, G., J. Mercapide, F. Anzanello, L. Prasmickaite, Y. Xi, J. Ju, O. Fodstad, and A. Lorico. 2008. "Growth of Cancer Cell Lines Under Stem Cell-like Conditions Has the Potential to Unveil Therapeutic Targets." *Experimental Cell Research* 314 (10): 2110–2122.

Reya, T., S. J. Morrison, M. F. Clarke, and I. L. Weissman. 2001. "Stem Cells, Cancer, and Cancer Stem Cells." http://deepblue.lib.umich.edu/handle/2027.42/62862.

Ricci-Vitiani, Lucia, Roberto Pallini, Mauro Biffoni, Matilde Todaro, Gloria Invernici, Tonia Cenci, Giulio Maira, et al. 2010. "Tumour Vascularization via Endothelial Differentiation of Glioblastoma Stem-like Cells." *Nature* 468 (7325) (December 9): 824–828. doi:10.1038/nature09557.

Rivlin, Noa, Ran Brosh, Moshe Oren, and Varda Rotter. 2011. "Mutations in the P53 Tumor Suppressor Gene." *Genes & Cancer* 2 (4) (April): 466–474. doi:10.1177/1947601911408889.

Rodríguez-Rodríguez, L., I. Sancho-Torres, P. Leakey, D. G. Gibbon, J. T. Comerci, J. W. Ludlow, and C. Mesonero. 1998. "CD44 Splice Variant Expression in Clear Cell Carcinoma of the Ovary." *Gynecologic Oncology* 71 (2): 223–229.

Schneider, Verena, Michaela L Krieger, Gerd Bendas, Ulrich Jaehde, and Ganna V Kalayda. 2012. "Contribution of Intracellular ATP to Cisplatin Resistance of Tumor Cells." *Journal of Biological Inorganic Chemistry: JBIC: a Publication of the Society of Biological Inorganic Chemistry* (November 25). doi:10.1007/s00775-012-0960-6.

Shaw, Tanya J, Mary K Senterman, Kerri Dawson, Colleen A Crane, and Barbara C Vanderhyden. 2004. "Characterization of Intraperitoneal, Orthotopic, and Metastatic Xenograft Models of Human Ovarian Cancer." *Molecular Therapy: The Journal of the American Society of Gene Therapy* 10 (6) (December): 1032–1042. doi:10.1016/j.ymthe.2004.08.013.

Sherley, James L. 2002. "Asymmetric Cell Kinetics Genes: The Key to Expansion of Adult Stem Cells in Culture." *Stem Cells (Dayton, Ohio)* 20 (6): 561–572. doi:10.1634/stemcells.20-6-561.

Shiozawa, Yusuke, Elisabeth A Pedersen, Aaron M Havens, Younghun Jung, Anjali Mishra, Jeena Joseph, Jin Koo Kim, et al. 2011. "Human Prostate Cancer Metastases Target the Hematopoietic Stem Cell Niche to Establish Footholds in Mouse Bone Marrow." *The Journal of Clinical Investigation* 121 (4) (April): 1298–1312. doi:10.1172/JCI43414.

Silva, Ines A, Shoumei Bai, Karen McLean, Kun Yang, Kent Griffith, Dafydd Thomas, Christophe Ginestier, et al. 2011a. "Aldehyde Dehydrogenase in Combination with CD133 Defines Angiogenic Ovarian Cancer Stem Cells That Portend Poor Patient Survival." *Cancer Research* 71 (11) (June 1): 3991–4001. doi:10.1158/0008-5472.CAN-10-3175.

Singh, Sheila K, Ian D Clarke, Mizuhiko Terasaki, Victoria E Bonn, Cynthia Hawkins, Jeremy Squire, and Peter B Dirks. 2003. "Identification of a Cancer Stem Cell in Human Brain Tumors." *Cancer Research* 63 (18) (September 15): 5821–5828.

Section 1.0 – General Introduction

Soda, Yasushi, Tomotoshi Marumoto, Dinorah Friedmann-Morvinski, Mie Soda, Fei Liu, Hiroyuki Michiue, Sandra Pastorino, et al. 2011. "Transdifferentiation of Glioblastoma Cells into Vascular Endothelial Cells." *Proceedings of the National Academy of Sciences of the United States of America* 108 (11) (March 15): 4274–4280. doi:10.1073/pnas.1016030108.

Stordal, Britta, Marion Hamon, Victoria McEneaney, Sandra Roche, Jean-Pierre Gillet, John J O'Leary, Michael Gottesman, and Martin Clynes. 2012. "Resistance to Paclitaxel in a Cisplatin-resistant Ovarian Cancer Cell Line Is Mediated by P-glycoprotein." *PloS One* 7 (7): e40717. doi:10.1371/journal.pone.0040717.

Storms, Robert W., Aliana P. Trujillo, James B. Springer, Lisa Shah, O. Michael Colvin, Susan M. Ludeman, and Clay Smith. 1999. "Isolation of Primitive Human Hematopoietic Progenitors on the Basis of Aldehyde Dehydrogenase Activity." *Proceedings of the National Academy of Sciences* 96 (16) (August 3): 9118–9123. doi:10.1073/pnas.96.16.9118.

Sullivan, James P., John D. Minna, and Jerry W. Shay. 2010. "Evidence for Self-renewing Lung Cancer Stem Cells and Their Implications in Tumor Initiation, Progression, and Targeted Therapy." *Cancer and Metastasis Reviews* 29 (1) (January): 61–72. doi:10.1007/s10555-010-9216-5.

Svendsen, C N, M G ter Borg, R J Armstrong, A E Rosser, S Chandran, T Ostenfeld, and M A Caldwell. 1998. "A New Method for the Rapid and Long Term Growth of Human Neural Precursor Cells." *Journal of Neuroscience Methods* 85 (2) (December 1): 141–152.

Szotek, P. P. 2006. "Ovarian Cancer Side Population Defines Cells with Stem Cell-like Characteristics and Mullerian Inhibiting Substance Responsiveness." *Proceedings of the National Academy of Sciences* 103 (30) (July 25): 11154–11159. doi:10.1073/pnas.0603672103.

Szotek, P. P., R. Pieretti-Vanmarcke, P. T. Masiakos, D. M. Dinulescu, D. Connolly, R. Foster, D. Dombkowski, F. Preffer, D. T. MacLaughlin, and P. K. Donahoe. 2006. "Ovarian Cancer Side Population Defines Cells with Stem Cell-like Characteristics and Mullerian Inhibiting Substance Responsiveness." *Proceedings of the National Academy of Sciences* 103 (30): 11154–11159.

Takahashi, Kazutoshi, Koji Tanabe, Mari Ohnuki, Megumi Narita, Tomoko Ichisaka, Kiichiro Tomoda, and Shinya Yamanaka. 2007. "Induction of Pluripotent Stem Cells from Adult Human Fibroblasts by Defined Factors." *Cell* 131 (5) (November 30): 861–872. doi:10.1016/j.cell.2007.11.019.

Tan, Lei, Xin Sui, Hongkui Deng, and Mingxiao Ding. 2011. "Holoclone Forming Cells from Pancreatic Cancer Cells Enrich Tumor Initiating Cells and Represent a Novel Model for Study of Cancer Stem Cells." *PloS One* 6 (8): e23383. doi:10.1371/journal.pone.0023383.

Tavor, Sigal, Isabelle Petit, Svetlana Porozov, Abraham Avigdor, Ayelet Dar, Leonor Leider-Trejo, Noga Shemtov, et al. 2004. "CXCR4 Regulates Migration and Development of Human Acute Myelogenous Leukemia Stem Cells in Transplanted NOD/SCID Mice." *Cancer Research* 64 (8) (April 15): 2817–2824.

Thomson, J A, J Itskovitz-Eldor, S S Shapiro, M A Waknitz, J J Swiergiel, V S Marshall, and J M Jones. 1998. "Embryonic Stem Cell Lines Derived from Human Blastocysts." *Science (New York, N.Y.)* 282 (5391) (November 6): 1145–1147.

Trumpp, Andreas, Marieke Essers, and Anne Wilson. 2010. "Awakening Dormant Haematopoietic Stem Cells." *Nature Reviews Immunology* 10 (3) (March 1): 201–209. doi:10.1038/nri2726.

Van Jaarsveld, M T M, J Helleman, A W M Boersma, P F van Kuijk, W F van Ijcken, E Despierre, I Vergote, et al. 2012. "miR-141 Regulates KEAP1 and Modulates Cisplatin Sensitivity in Ovarian Cancer Cells." *Oncogene* (October 8). doi:10.1038/onc.2012.433.

Wang, Rong, Kalyani Chadalavada, Jennifer Wilshire, Urszula Kowalik, Koos E Hovinga, Adam Geber, Boris Fligelman, Margaret Leversha, Cameron Brennan, and Viviane Tabar. 2010. "Glioblastoma Stem-like Cells Give Rise to Tumour Endothelium." *Nature* 468 (7325) (December 9): 829–833. doi:10.1038/nature09624.

Watt, Fiona M. 2002. "Role of Integrins in Regulating Epidermal Adhesion, Growth and Differentiation." *The EMBO Journal* 21 (15) (August 1): 3919–3926. doi:10.1093/emboj/cdf399.

Wegner, S A, P K Ehrenberg, G Chang, D E Dayhoff, A L Sleeker, and N L Michael. 1998. "Genomic Organization and Functional Characterization of the Chemokine Receptor CXCR4, a Major Entry Co-receptor for Human Immunodeficiency Virus Type 1." *The Journal of Biological Chemistry* 273 (8) (February 20): 4754–4760.

Weinberg, R A. 1995. "The Retinoblastoma Protein and Cell Cycle Control." *Cell* 81 (3) (May 5): 323–330.

Section 1.0 – General Introduction

Woods, C M, J Zhu, P A McQueney, D Bollag, and E Lazarides. 1995. "Taxol-induced Mitotic Block Triggers Rapid Onset of a P53-independent Apoptotic Pathway." *Molecular Medicine (Cambridge, Mass.)* 1 (5) (July): 506–526.

Wu, Buchu, Shu Li, Lili Sheng, Jing Zhu, Liying Gu, Haoran Shen, Duanduan La, Brett D Hambly, Shisan Bao, and Wen Di. 2012. "Metformin Inhibits the Development and Metastasis of Ovarian Cancer." *Oncology Reports* 28 (3) (September): 903–908. doi:10.3892/or.2012.1890.

Xiang, Y, N Ma, D Wang, Y Zhang, J Zhou, G Wu, R Zhao, et al. 2013. "MiR-152 and miR-185 Co-contribute to Ovarian Cancer Cells Cisplatin Sensitivity by Targeting DNMT1 Directly: a Novel Epigenetic Therapy Independent of Decitabine." *Oncogene* (January 14). doi:10.1038/onc.2012.575.

Yancik, R. 1993. "Ovarian Cancer. Age Contrasts in Incidence, Histology, Disease Stage at Diagnosis, and Mortality." *Cancer* 71 (2 Suppl) (January 15): 517–523.

Yang, Wan-Lin, Andrew K. Godwin, and Xiang-Xi Xu. 2004. "Tumor Necrosis Factor-α-Induced Matrix Proteolytic Enzyme Production and Basement Membrane Remodeling by Human Ovarian Surface Epithelial Cells Molecular Basis Linking Ovulation and Cancer Risk." *Cancer Research* 64 (4) (February 15): 1534–1540. doi:10.1158/0008-5472.CAN-03-2928.

Yilmaz, Omer H, Riccardo Valdez, Brian K Theisen, Wei Guo, David O Ferguson, Hong Wu, and Sean J Morrison. 2006. "Pten Dependence Distinguishes Haematopoietic Stem Cells from Leukaemia-initiating Cells." *Nature* 441 (7092) (May 25): 475–482. doi:10.1038/nature04703.

Yin, Shengyong, Jinjun Li, Chen Hu, Xinhua Chen, Ming Yao, Mingxia Yan, Guoping Jiang, et al. 2007. "CD133 Positive Hepatocellular Carcinoma Cells Possess High Capacity for Tumorigenicity." *International Journal of Cancer. Journal International Du Cancer* 120 (7) (April 1): 1444–1450. doi:10.1002/ijc.22476.

Zhang, S., C. Balch, M.W. Chan, H.C. Lai, D. Matei, J.M. Schilder, P.S. Yan, T.H.M. Huang, and K.P. Nephew. 2008. "Identification and Characterization of Ovarian Cancer-initiating Cells from Primary Human Tumors." *Cancer Research* 68 (11): 4311.

Zhang, Shu, Curt Balch, Michael W Chan, Hung-Cheng Lai, Daniela Matei, Jeanne M Schilder, Pearlly S Yan, Tim H-M Huang, and Kenneth P Nephew. 2008. "Identification and Characterization of Ovarian Cancer-initiating Cells from Primary Human Tumors." *Cancer Research* 68 (11) (June 1): 4311–4320. doi:10.1158/0008-5472.CAN-08-0364.

Zheng, Wenxin, and Oluwole Fadare. 2012. "Fallopian Tube as Main Source for Ovarian and Pelvic (non-endometrial) Serous Carcinomas." *International Journal of Clinical and Experimental Pathology* 5 (3): 182–186.

Zhou, C H, S F Yang, and P Q Li. 2012. "Human Lung Cancer Cell Line SPC-A1 Contains Cells with Characteristics of Cancer Stem Cells." *Neoplasma* 59 (6): 685–692. doi:10.4149/neo_2012_087.

Materials and Methods

Section 2.0 – Materials and Methods:

2.1 Culture and Sub-Culture

Nine cell lines were utilised in this study (Table 2.1). All cell lines were cultured from departmental stocks, which were originally commercially acquired or gifted by other institutions (Table 2.1). For each cell line; 1 ml of stock cells was thawed from liquid nitrogen. Thawed cells were added to 14 ml of the appropriate culture media (Table 2.2), pre-warmed to 37 °C, in a T75 flask. Cells were incubated at 37 °C in a humidified incubator supplemented with 5 % CO_2.

Table 2.1: Origins of each cell line.

Cell Line	Origin
A2780	Originally purchased from the European collection of cell cultures (ECACC, Salisbury, UK).
A2780cis	Originally purchased from the ECACC.
IGROV-1	Originally gifted to the department by Prof. Jan Schellens (Netherlands Cancer Institute, Netherlands).
IGROV-CDDP	Originally gifted to the department by the cell line's founder; Prof. Jan Schellens (Netherlands Cancer Institute, Netherlands).
SK-OV-3	Originally purchased from the American Type Culture Collection (ATCC, Manassas, VA, USA).
59M	Originally purchased from the ECACC.
HIO-80	Originally gifted to the department by the cell line's founder; Prof. A. Godwin (Fox Chase Cancer Centre, Philadelphia, USA).
NTera2 (NT2)	Originally gifted to the department by the cell line's founder; Prof. P. Andrews (University of Sheffield, UK).
2102ep	Originally gifted to the department by the cell line's founder; Prof. P. Andrews.
Hela	Originally purchased from the ATCC.

Table 2.2: Cell Culture media used for each cell line.

Cell Line	Media
A2780	Roswell Park Memorial Institute media containing L-Glutamine (RPMI; Lonza Group Ltd, Switzerland) supplemented with 10 % (v/v) heat-inactivated Foetal Bovine Serum (FBS; Lonza) and 2 % (v/v) Penicillin-Streptomycin (P/S; Lonza).
A2780cis	RPMI supplemented with 10 % (v/v) FBS and 2 % (v/v) P/S.
IGROV-1	RPMI supplemented with 10 % (v/v) FBS (Lonza) and 2 % (v/v) P/S.
IGROV-CDDP	RPMI supplemented with 10 % (v/v) FBS (Lonza) and 2 % (v/v) P/S.
SK-OV-3	McCoys 5a media containing L-Glutamine (Lonza) supplemented with 15 % (v/v) FBS and 2 % (v/v) P/S.
59M	Dulbecco's Modified Eagle Medium (DMEM; Lonza) supplemented with 20 IU/l Bovine Insulin (Sigma-Aldrich Co. LLC, MO, USA), 10 % (v/v) FBS and 2 % (v/v) P/S.
HIO-80	1:1 mixture of medium 199 (Sigma) and MCDB-105 media* (Sigma) supplemented with 0.2 IU/ml recombinant human insulin, 10 % (v/v) FBS and 2 % (v/v) P/S.
NTera2	DMEM media supplemented with 10 % (v/v) FBS and 2 % (v/v) P/S.
2102ep	DMEM media supplemented with 10 % (v/v) FBS and 2 % (v/v) P/S.
Hela	Eagles Modified Essential Medium (Lonza) supplemented with 10 % FBS, 1x Non-Essential Amino Acids and 2 % (v/v) P/S.

* MCDB-105 was only available in a powder form. The entire bottle of powder was added to 960 ml of sterile water (Sigma), the bottle was then rinsed twice with 20 ml of sterile water and added to the 960 ml solution, bringing the total volume to 1000 ml. The pH was adjusted to 7.0 using 1M NaOH and 1 M HCl. This solution was then sterilised under vacuum pressure, using a Millipore Stericup vacuum filter unit (EMD Millipore Corporation, Billerica, MA, USA).

Two sub-culturing techniques and multiple split ratios were employed across the nine cell lines (Table 2.3). For both sub-culturing techniques, the old media was removed and the monolayer was gently rinsed with phosphate buffered saline (PBS; Lonza).

i) Trypsinisation: 0.25 % (v/v) trypsin/EDTA was then added, and the flask was returned to the 37 °C incubator for approximately 5 min. Once the cells had dissociated, the trypsin was neutralised by adding an equal volume of media.

ii) Scraping: PBS was added to reduce friction during scraping. A cell scraper was then used to remove the cells which were adhered to the flask. The flask was rinsed with PBS and cells are collected.

Cells were pelleted at 170 x g for 5 min. The supernatant was removed and cells were resuspended in complete media pre-warmed to 37 °C. An appropriate split was preformed and cells were replated in a culture flask and returned to the incubator.

Table 2.3: Passaging information for each cell line.

Cell Line	Sub-culturing	Passage rate	Split ratio
A2780	Trypsinisation	2-3 passages / week	1:3 – 1:6
A2780cis	Trypsinisation	2-3 passages / week	1:2 – 1:5
IGROV-1	Trypsinisation	2-3 passages / week	1:3 – 1:6
IGROV-CDDP	Trypsinisation	2-3 passages / week	1:2 – 1:5
SK-OV-3	Trypsinisation	2-3 passages / week	1:2 – 1:4
59M	Trypsinisation	2-3 passages / week	1:3 – 1:5
HIO-80	Trypsinisation	2 passages / week	1:2 – 1:4
NTera2	Scraping	2 passages / week	1:2 – 1:3
2102ep	Trypsinisation	2-3 passages / week	1:3 – 1:4
Hela	Trypsinisation	2-3 passages / week	1:3 – 1:5

Frozen stocks were made by dissociating and pelleting the cells, as described above. Cells were resuspended in Gibco's Recovery™ Cell Culture Freezing Medium (Life Technologies Corporation, CA, USA) and aliquoted into Nunc Cryotubes™ (Thermo Fisher Scientific Inc., MA USA). Each stock represented a 1:3 split of a T75 culture in 1ml of freezer media. Stocks were packaged in polystyrene and stored for 1 – 2 days a -80 °C, before being unpackaged and transferred to the liquid nitrogen storage tank.

2.2 All-Trans-Retinoic acid (RA) differentiation of NT2 cells

RA was used to terminally differentiate NT2 cells. Stock RA (Sigma) was prepared at 10 mM in dimethyl sulfoxide. Aliquots were stored in the dark at -20 °C. To differentiate the NT2, the cells were split 1:3 into a new culture flask, the media was supplemented with a 1:1000 dilution of RA stock, bring the final RA concentration to 10 μM. Cells were allowed to grow for 3-4 days, at which point they were split 1:2 into RA supplemented media. After 7 days total NT2 cells had terminally differentiated.

2.3 Cell Counting

A 50 µl sample of a cell suspension was transferred to a 1.5 ml Biosphere® tube (Sarstedt AG & Co., Nümbrecht, Germany). An appropriate dilution was made using PBS. The dilution was dependent on the estimated number of cells and allows for more efficient counting. The diluted sample was then mixed 1:1 (v/v) with 0.4 % Trypan Blue Solution (Life Technologies). Approximately 10 µl of this diluted and stained sample was loaded onto opposite sides of a hemocytometer, designated 'A' and 'B'. The hemocytometer divided the field of view into 9 large squares, each with many subdivisions Cells found within the four corner squares were counted on an inverted Carl Ziess Axiovert 35 microscope. The dead cells, which stained blue in the presence of Trypan Blue, were excluded from the count.

The cell/ml concentration was calculated as:

$$\mu(dilX)(2500) = cells/ml$$

where:
µ is the mean live cell count of the A and B sides of the hemocytometer.
dilX is the dilution factor by which the original 50 µl samples were diluted, including the Trypan Blue dilution.

2.4 Flow Cytometry based pCSC screen

The flow cytometry pCSC screen was composed of three independent assays; the ALDHFLUOR™ (ALDH) Assay, the Hoechst Side Population (HSP) Assay and the Cell Surface Protein (CSP) Assay. The materials and methods pertaining to each assay will be described individually, followed by materials and methods which were common to all assays.

2.4.1 ALDH Assay

Cells were dissociated and pelleted at 170 x g for 5 min. The ALDH Assay (STEMCELL Technologies Inc. Vancouver, Canada) is then conducted as per manufactures instructions. All reactions are carried out in 1.5 ml Biosphere® tubes and transferred to Flow Cytometry tubes at the final step. One adaptation was made to this protocol, the inclusion of a mixed population gating control (described in Section 3.3.2.1.2). This adaptation was implemented if the population being assayed had a high proportion of ALDH+ cells. Samples were analysed on a Cyan Advanced Digital Processor flow cytometer (Cyan ADP; Beckman Coulter Inc., CA, USA).

2.4.2 HSP Assay

Cells were dissociated and pelleted at 170 x g for 5 min. Cells were resuspended at a concentration of 1 x 10^6 cells/ml in DMEM+ pre-warmed to 37 °C. DMEM+ consists of DMEM supplemented with 2 % (v/v) FBS and 10 mM HEPES (Sigma). Hoechst 33342 dye (H342; Sigma) was added to a concentration of 5 µg/ml and allowed to incubate at 37 °C for 90 min in a shaking incubator at 100 rpm. After incubation, the cells were transferred to ice and immediately centrifuged at 170 x g for 5 min at 4 °C. This pellet was resuspended in ice cold HBSS+ and transferred to Flow Cytometry tubes. HBSS+ consists of Hanks Balanced Salt Solution (HBSS; Lonza) supplemented with 2 % (v/v) FBS and 10 mM HEPES. After samples were resuspended in HBSS+, they were placed on ice and analysed on a Cyan ADP flow cytometer.

Negative Verapamil controls were carried out by including Verapamil (Sigma) at a concentration of 50 µM to the reaction immediately prior to the addition of H342. A separate sample was used for Verapamil inhibited negative controls and uninhibited H342 staining.

Both H342 and Verapamil come in powdered form. Under sterile conditions H342 is dissolved in distilled water (dH_20) and brought to a concentration of 1 mg/ml. This bright yellow H342 solution is aliquoted and stored at -20 °C until needed.

Verapamil is weighed out and dissolved in pre-warmed DMEM+ at 37 °C at a concentration of 5 mM. Verapamil does not dissolve easily, and may require incubation at 37 °C for 10 min. Once dissolved, the Verapamil solution is filter sterilised using a 0.22 µm Millipore Filter (Millipore). Verapamil precipitates out of solution if stored overnight, so this solution is made up fresh for each experiment.

2.4.3 CSP Assay

Cells were dissociated and pelleted at 170 x g for 5 min. Cells were resuspended in PBS. 1 x 10^6 cells/sample were added to a 1.5 ml Biosphere® tube. The cells were pelleted at 2000 x g for 30 sec and resuspended in 80 µl PBS. The CSP Assay was composed of nine samples: one autofluorescence control, four antibody stained samples and four isotype controls

(Table 2.4), one for each antibody. 10 µl of each antibody/isotype control was added to the appropriate sample. Nothing was added to the autofluorescence control. All samples were then incubated at 4 °C for 30 min. After incubation 900 µl of PBS was added to each sample to dilute the antibody concentration. Cells were then pelleted and the supernatant was removed. Cells were resuspended in 1 ml of PBS and transferred to FC tubes. Samples were placed on ice and analysed on a Cyan ADP flow cytometer.

Isotype controls are used as negative staining and non-specific staining controls. They are antibodies of the same Immunoglobulin (IgG) class as the antibody used to detect the antigen of interest (experimental antibody). However, they are raised against an antigen which is not found on the target tissue/cells. They are also conjugated to the same fluorochrome as the experimental antibody.

Table 2.4: Samples included in the CSP Assay (The last four antibodies in this table are the Isotype Controls used in the CSP Assay).

Antigen	Antibody	Clone Identifier	Fluorescent Conjugate	Company
Autofluorescence	None	None	None	-
CD44	Mouse IgG_{2a} anti-CD44	F10-44-2	Fluorescein (FITC)	ABCAM[2]
CD117	Mouse IgG_1 anti-CD117	104D2	Phycoerythrin (PE)	ABCAM
CD133	Mouse IgG_{2b} anti-CD133	293C3	Allophycocyanin (APC)	Miltenyi[3]
CXCR4	Mouse IgG_{2a} anti-CXCR4	12G5	APC	R&D Systems[4]
A Synthetic Hapten[1]	Mouse IgG_{2a} Isotype	X5563	FITC	ABCAM
No Information[1]	Mouse IgG_1 Isotype	ICIG1	PE	ABCAM
Keyhole Limpet Hemocyanin (KLH)	Mouse IgG_{2b} Isotype	I56-11E5.11	APC	Miltenyi
KLH	Mouse IgG_{2a} Isotype	20102	APC	R&D Systems

[1] ABCAM considered this to be propriety knowledge and did not provide full details.
[2] ABCAM PLC., Cambridge, UK.
[3] Miltenyi Biotec GmbH, Bergisch Gladbach, Germany.
[4] Research & Diagnostics Systems, Inc., MN, USA.

2.4.4 Dead Cell Staining

All of the pCSC screening assays were compatible with the use of Propidium Iodide (PI) for dead cell staining. PI was added to each sample, to a final concentration of 0.5 μg/ml. Where necessary 1 mg/ml PI stock was diluted with PBS prior to adding to samples to a final concentration of 0.5 μg/ml.

2.4.5 Cyan ADP Flow Cytometric Analysis

The flow cytometer was initialised and samples were run as per manufactures instructions. When finished the machine was shut down as per manufactures instructions. With the exception of the HSP assay all detector channels covered the ranges stated in the Cyan ADP Analyser brochure (Table 2.Error: Reference source not found; page 2; https://www.beckmancoulter.com/wsrportal/bibliography?docname=BR-11390C.pdf).

Three technical controls were carried out for each sample of each assay. First, using a Forward Scatter versus Side Scatter plot, a gate was drawn around the events which represented cells (Figure 1.9A) and applied to a plot of Pulse Width versus Side Scatter. Second, the Pulse Width versus Side Scatter plot was used to put a gate around events which represented single cells (Figure 1.9B), and applied to a plot for discriminating dead cells. Third, a gate was drawn around the events which represented viable cells on the dead cell plot (Figure 1.9C) and applied to the assay specific experimental plots. This set of technical controls meant that the events that appeared in the experimental plots only represented single and viable cells. The format of the dead cell plots differed depending on the experimental parameters being examined. The x-axis was set at the experimental parameter (e.g. PE, FITC, APC), while the y-axis was set to PE/Cy5 for dead cell discrimination. Due to filter changes during the HSP assay the dead cell plot in the HSP assay was Side Scatter versus PE.

Table 2.5: CyAn™ ADP detector set-up for each of the pCSC screens.

Detector	ALDH assay	HSP Assay	CSP Assay
Side Scatter	483 nm – 493 nm	483 nm – 493 nm	483 nm – 493 nm
FITC (FL1)	510 nm – 550 nm	-	510 nm – 550 nm
PE (FL2)	-	562.5 nm – 587.5 nm	562.5 nm – 587.5 nm
PE/Cy5 (FL4)	665 nm – 695 nm	-	665 nm – 695 nm
PE/Cy7 (FL5)	>750 nm	-	-
Violet 1 (FL6)	-	425 nm – 475 nm	-
Violet 2 (FL7)	-	665 nm – 695 nm	-
APC (FL8)	-	-	655 nm – 675 nm

The experimental plot for the ALDH assay was FITC versus PE/Cy7. Thresholds set by the DEAB or Mixed Population controls allowed for the identification of pCSCs. The experimental plot for the HSP assay was Violet 2 versus Violet 1. Thresholds set by the Verapamil control allowed for the identification of pCSCs. There were 3 experimental plots used for the CSP assay. These were determined by the fluorochromes conjugated to the antibodies used to detect each marker in the CSP assay. FITC versus Side Scatter was used to detect anti-CD44 staining. PE versus Side Scatter was used to detect anti-CD117 staining. APC versus Side Scatter was used to detect both anti-CD133 and anti-CXCR4 staining. Thresholds set by the Autofluorescence control allowed for the identification of pCSCs in the CSP assay.

2.4.6 Multi-parametric Analysis

Multi-parametric analysis is defined as the co-staining of cells with multiple fluorochromes. With the exception of PI staining (dead cells), each sample was only stained with one fluorescent marker (single-parametric staining). This reduced the number of samples required, but limited the ability to detect overlaps between the various pCSC markers.

In some instances multi-parametric analysis was carried out to identify the overlaps between a reduced panel of pCSCs markers. Multi-parametric staining required; one unstained sample for an autofluorescence control, one single stained control and one fluorescence minus one (FMO) control for each of the stains used, along with one sample stained for all the parameters of interest. Single stained controls are defined as samples stained with only a single fluorochrome used in the multi-parametric analysis. Single stained controls were used to compensate for the similarities between the fluorescent profile of each of the fluorochromes used in the

multi-parametric analysis. FMO controls are defined as samples stained with all the fluorochromes used in the multi-parametric analysis bar one. FMO controls were used to set the background threshold for each of the fluorochromes being used. The final sample stained with all fluorescent parameters was the sample that produced the experimental data with respect to the controls

2.5 Fluorescence-activated Cell Sorting

Two generations of MoFlo cell sorters were used to isolate all the sub-populations described in this thesis; the MoFlo™ (Beckham Coulter) and MoFlo™ Xtreme Digital Processor (Moflo™ XDP; Beckham Coulter) cell sorters. Cell sorting was carried out using the same assays as in the pCSC screen. PI was used for dead cell staining as described in Section 2.4.4. The materials and methods pertaining to each assay will be described individually, followed by materials and methods which were common to all assays.

2.5.1 ALDH Assay

To sort cells based on the ALDH assay, cells were stained as described in Section 2.4.1. Two adaptations were made to this protocol;

i) The stained cells were resuspended in ALDH assay buffer supplemented with 2 % (v/v) P/S to reduce the risk of bacterial contamination while sorting.

ii) As described in Section 3.3.2.1.1, the cell concentration was scaled when cell sorting small sub-populations of ALDH+ cells.

Sorted cells were collected in ice cold ALDH assay buffer supplemented with 2 % (v/v) P/S. ALDH assay buffer was used above cell culture media as it prevents loss of fluorescent signal form the ALDH assay, allowing for post sort purity re-tests.

2.5.2 HSP Assay

To sort based on the HSP assay, cells were stained in as described in Section 2.4.2. The samples were scaled to provide adequate cell numbers post-sort. The stained cells were resuspended in HBSS+ supplemented with 2 % (v/v) P/S to reduce the risk of bacterial contamination while sorting. Sorted cells were collected into the appropriate ice cold complete culture medium (Table 2.2).

2.5.3 CSP Assay

To sorting cells based on the CSP assay, cells were stained in as described in Section 2.4.3. The samples were scaled to provide adequate cell numbers post-sort. The stained cells were resuspended in PBS supplemented with 2 % (v/v) P/S to reduce the risk of bacterial contamination while sorting. Sorted cells were collected into the appropriate ice cold complete culture medium (Table 2.2).

2.5.4 Post Cell Sorting

Post-sort a small sample of the sorted cells were transferred to a clean flow cytometry tube and re-analysed to measure sort purity. The rest of the cells were transferred to a 1.5 ml Biosphere® tube and pelleted at 2000 x g for 30 sec. Multiple rounds of removing supernatant and adding sorted cell suspension were required to collect all the cells in a single pellet. Biosphere® tubes were used over larger vessels as it was easier to visualise the pellet, which was generally very small, post cell sorting.

The pellet was resuspended in the appropriate cell culture media (Table 2.2), pre-warmed to 37 °C, transferred to a cell culture vessel of the appropriate surface are and returned to the incubator. The size of the culture vessel was estimated based on the cell yield predicted by the cell-sorter and the size of the pellet. Cells were generally returned to culture in a single well of a 6 -well plate or a T25.

2.6 Mouse Tumourgenicity Assay

The mouse tumourgenicity assay is used to validate pCSCs as CSCs which are able to efficiently generate tumours with a histology matching that of the tumour from which the cells were originally isolated.

For the reasons discussed in Section 6.1.1.1, 7-9 week old female NOD.CB17-Prkdc^{scid}/NCrHsd (NOD.SCID; Harlan Sprague Dawley Inc., IN, USA) mice were used for the tumourgenicity assay. Cells were administered via subcutaneous hindlimb injection in a matrigel supplemented, media based vehicle.

2.6.1 Ethics

Ethical approval was granted by the Trinity College Dublin ethics committee and the Irish Department of Health. The investigators who conducted the mouse tumourgenicity assay had past the Laboratory Animal Science and Training (LAST) exam and were qualified to work with laboratory animals. The Trinity College Dublin Bio-Resources staff provided the practical training required to handle the mice and conduct the procedures described in Sections 2.6.2 – 2.6.8. All experiments were designed to conform to the 3Rs principle (Replacement, Reduction and Refinement).

Reduction:

- Power study data was incorporated into experimental data.
- Multiple genders, weights and ages of animals were not required for this study.
- Initial power studies were conducted to establish the minimum number of animals and time required for our study.
- Experiments not meeting the *in vitro* criteria were not used in animal studies.

Refinement:

- Before commencement of animal studies, cell lines were assessed for and deemed free from any infection.
- Subcutaneous injection is least the invasive applicable procedure and leads to fewer complications than intraperitoneal injection.
- Normal animal behaviour was not restricted during the experiments, placing no additional negative effect on environmental enrichment.
- Routine post-mortem analysis of animals provided information for further refinement.
- Experiments were ended when scientific or human end-points were reached.

Replacement:

- Post-mortem examination provided information on multiple aspects of cancer from a single experiment, including; tumourigenic capacity, differentiation status, degree of malignancy, degree of vasculature and metastasis.
- Data from pilot studies were included in experimental data to enhance the power of the study.

2.6.2 Housing

NOD.SCID mice were housed in isolator cages. Corn Cob Bedding (Datesand Ltd.; Manchester, UK) was used. Half an iso-PAD™ (Omni BioResources Inc., NJ, USA) was included for nesting material. The bedding and iso-PAD™ were changed every 2 weeks to maintain a clean environment. Isolator cages came in two sizes, small cages were used to house a maximum of 4 mice, large cages were used to house a maximum of eight mice.

Mice were fed with 2018 Rodent Diet (Harlan) and water. Food and water was topped up as required.

2.6.3 Handling Mice

Mice were picked up by the base of the tail, to carrying mice for a short time period, for example; for moving mice between cages. To handle them for a longer duration, mice were scruffed. To scruff a mouse, the mouse was picked out of the cage by the tail and place on top of the cage. The thumb and index finger was used to apply gentle pressure to the back of the mouse, immobilising it. The fingers were moved up to the back of the head to pinch up the skin behind the neck, starting the pinch at the back of the jaw. The 3rd 4th and 5th fingers were used to grip and immobilise the tail and the hind-limb closest to the fingers. Mice can be handled for several minutes using this technique.

2.6.4 Ear Punching

The mice were ear punched to track individual mice within experiments. Mice were scruffed and ear punched using the marking system; no punch (NP), single left ear punch (LP), single right ear punch (RP), single punch to both ears (BP), two punches to the left ear (2LP), two punches to the right ear ear (2RP), two punches to both ears (2BP) and two punches to the right ear with a single punch to the left ear (2RP/LP).

2.6.5 Shaving

NOD.SCID mice have a full white coat. To aid with the injection process mice were shaved above their hindlimb on the day prior to injection. To achieve this, mice were scruffed and the region was shaved using a beard trimmer. Nude NOD.SCID mice (NOD.Cg-*Prkdc*^{scid}*Hr*^{hr}/NCrHsd) are now available from Harlan. However, these were not available at the time this study was started.

2.6.6 Injecting

The cells were dissociated and counted under tissue culture conditions. The cells were resuspended in a 4 is to 1 (v/v) mixture of Ham's F12 media (Lonza) is to 'high concentration matrigel' (BD Biosciences Inc., NJ, USA) at the required concentration. All work was kept on ice, and only removed to work in the tissue culture hood. The final cell suspension was kept on ice until injection to prevent the matrigel from solidifying.

The mouse was scruffed, a second individual extended the right hind-limb of the mouse with one hand and immobilised the right shoulder with the other. The injection was then administered using an ice cold Braun Omnifix® 1 ml syringe (B. Braun Medical Inc., Melsungen, Germany) and a 22 G JELCO® Peripheral I.V. Catheter (Smiths Medical International Ltd., Lancashire, UK). Cells were injected in a 100 µl volume above the right hindlimb. Not all injections of the 100 µl volume were equally successful. It was decided to classify, the injection administration success into four categories;

i) Perfect (P) – entire volume was administered successfully.

ii) Good (G) – small droplet came back out upon withdrawal of needle. (estimated 5-10 µl)

iii) Moderate (M) – large droplet came back out (estimated 10-40 µl).

iv) Failure (F) – very large volume not successfully injected. (estimated 40 -100 µl.).

The administration success was noted for every injection carried out on every mouse in this project.

2.6.7 Euthanasia

Mice were transferred to a 12 x 6 x 6 cm asphyxiation chamber. CO_2 was pumped into the bottom of the chamber at low pressure until mice activity was diminished (1-2 min). CO_2 pressure was then increased until mice were deceased (4-5 min). Mice were then removed from the chamber and a cervical dislocation was performed to confirm death

2.6.8 Post-mortem Inspection

The post-mortems were carried out via the following structure; the tumour was identified and recorded and samples were taken for histological analysis. The lungs were taken for histological analysis to identify the presence/absence of any distant metastases. The spleen was removed for histological analysis to identify the presence/absence of any distant metastases. The liver was removed for histological analysis for histological analysis to identify the presence/absence of any distant metastases. Specimens were fixed, embedded and stained for histological analysis

Examination of the lungs, spleen and liver were not central to the validation of pCSCs and non-pCSCs. As such, descriptions of these methods and be found in Appendix A.

2.6.8.1 i) Identifying and recording the tumour

The mouse was pinned to the dissection board through each limb. The skin was pinched and incised at the central posterior abdomen. An incision was made from the posterior abdomen to a point anterior of the thoracic cavity. The skin was peeled aside and pinned to the dissection board to reveal the sub-cutaneous regions along both flanks of the mouse. The mouse was photographed alongside a scale bar, to record the presence/absence and location of any sub-cutaneous tumours. The tumour was excised and photographed in the presence of a scale to record the size of the tumour, as sometimes the *in situ* photograph masked the size of the tumour. If no tumour was visible, the sub-cutaneous fat was excised from the injection site for histological analysis.

Excised tumours were bisected. One half was transferred to 10 % buffered formalin solution in a HistoPot® (Serosep Limited, Limerick, Ireland), the other was stored in ice cold PBS until it could be frozen.

ImageJ (http://rsb.info.nih.gov/ij/download.html) was used to measure the size of the tumour. The photograph of the excised tumour was loaded into ImageJ. The scale bar photographed alongside the mouse was used to determine the relationship between length in pixels and length in cm. The length in pixels of 7 cm along the scale bar was measured (let this be called 's'). The horizontal width of the tumour was measured in pixels (let this be called 'd1'). The vetrical width of the tumour was measured in pixels (let this be called 'd2'). The diameter of the tumour in cm (let this be called 'D') was then calculated as:

$$D = [(d1+d2)/2]/(s/7) \text{ cm}.$$

2.6.8.2 v) Fixing, embedding and staining

Histology samples could be stored for weeks in HistoPots before processing slides for histological analysis. Slides were prepared by staff of the Histology Lab, Coombe Women and Infants University Hospital. Samples were embedded in paraffin wax and sectioned on a microtome. Mounted sections were stained with hematoxylin and eosin, before being transferred to a pathologist for analysis.

2.7 Single Cell Self-renewal and Differentiation (SD) Assay

The SD assay was used to validate pCSCs as CSCs which have the potential to produce both CSCs and non-CSCs. To ensure the robustness of this assay self-renewal and differentiation had to be assessed via single cell clones.

2.7.1 Plating Single Cells

Cells were stained as per the cell sorting protocols described in Sections 2.5.1 – 2.5.3, and plated as single cells via the CyClone Automated Cloning Accessory with the MoFlo™ and MoFlo™ XDP cell sorters. Single cells were sorted into 100 µl of appropriate culture media (Table 2.2). Cells were plated into the 60 inner wells of a 96 well plate. The outer wells were filled with 150 µl PBS supplemented with 2 % (v/v) P/S. This helped to regulate the evaporation of media from the wells which contained the colonies.

2.7.2 Passaging the Colonies

After 1 week 100 µl of media was added to each well. It took 2.5 – 3.5 weeks for the single cells to grow into colonies that could be transferred out of to the 96 well plate and into a 24 well plate. To do this, the media was removed from all wells and 50 µl of PBS was added very gently to each well. The PBS was then removed from the wells and 40 µl of 0.25 % trypsin/EDTA mixed 1:1 with PBS was added to each well. The plate was returned to the incubator for 5 min. 60 µl of media was then added to each well and mixed thoroughly via pipetting. This 100 µl cell suspension, was then added directly to 1.1 ml of media in individual wells of a 24 well plate. The 24 well plate was then returned to the incubator.

To passage cells from 24 well plates to 6 well plates, the media was removed and the cell monolayer was rinsed with 500 µl of PBS. Cells were dissociated in 100 µl of 0.25 % trypsin/EDTA in the incubator for 5 min. 900 µl of media was then added to each well and mixed thoroughly via pipetting. This 1 ml cell suspension, was then added directly to 2 ml of media in individual wells of a 6 well plate. The 6 well plate was then returned to the incubator.

To passage cells from 6 well plates to T25 flasks, the media was removed and the cell monolayer was rinsed with 1 ml of PBS. Cells were dissociated in 500 µl of 0.25 % trypsin/EDTA in the incubator for 5 min. 1 ml of media was then added to each well and mixed thoroughly via pipetting. This 1.5 ml, from each well, was then transferred to individual 1.5 ml Biosphere® tubes and pelleted at 2000 x g for 30 sec. The supernatant was removed and cells were resuspended in 1 ml of appropriate culture media (Table 2.2) and added to a T25 containing 4 ml of media. Re-plated cells were returned to the cell culture incubator.

2.7.3 Retesting for Cancer Stemness Markers

Confluent 6 well colonies had sufficient cells to retest the ALDH assay pCSC marker. Confluent T25 colonies had sufficient cells to retest the HSP assay and CSP assay pCSC markers. The retesting was carried out as per the original screen as described in Section 2.4.

Established the
ALDH, HSP, CSP CSC Screening
Assays and the Mouse
Tumourgenicity and Single Cell
Self-renewal and Differentiation
CSC Validation Assays.

Section 3.0 – Establishing the CSC Assays

3.1 Introduction

As a whole, this project's experimental design is divided into three phases;

I) Identification of Putative Cancer Stem Cells (pCSCs)

II) Isolation of pCSCs

III) Validation of Cancer Stem Cells (CSCs)

This chapter will discuss optimisations applying to all phases of the project. In phase I, a flow cytometry based screen was used to identify pCSCs. In phase II, fluorescence-activated cell sorting (FACS) was used to isolate the pCSCs and non-pCSCs. In phase III, *in vivo* mouse tumourgenicity and *in vitro* single cell self-renewal and differentiation (SD) assays were used to validate pCSCs as CSCs. None of these techniques were established in the laboratory prior to the commencement of this project.

Several experiments were required to establish and optimise each of these techniques. This chapter will detail the technical considerations for each technique. It will then present the experimental data produced in the establishment and optimisation of the techniques. Finally it will describe how the final standard for each technique was decided upon, with respect to the experimental data produced. Through covering these technical topics up front, future results chapters can be presented in a more free flowing style.

3.1.1 Flow Cytometry Based Screening and Isolation:

Flow cytometry was described in detail in Section 1.11. Flow cytometry is widely used to identify pCSCs from heterogeneous populations (Hirschmann-Jax et al. 2004; Charafe-Jauffret et al. 2009; Curley et al. 2009). Prior to this current work there was no protocol established in the laboratory to identify pCSC via flow cytometry. A flow cytometry based screen was developed to identify pCSCs in ovarian cancer model systems. This screen involves fluorescently labelling cells based on the expression of various pCSC markers. The markers chosen divided the screening process into three independent assays;

i) The enzyme activity based – ALDEFLUOR™ (ALDH) assay.

ii) The dye efflux based – hoechst side population (HSP) assay.

iii) The antibody based – cell surface protein (CSP) assay.

Section 3.0 – Establishing the CSC Assays

This chapter will describe the optimisations required to establish each of these three flow cytometry assays. Further technical flow cytometric controls were also optimised. These optimisations were not assay specific and are described in Appendix A. The ALDH, HSP and CSP assays were selected as they cover all the published flow cytometry approaches to identifying and isolating pCSC, with one exception – quiescence based pCSC identification. Quiescence based identification may not be applicable to identifying pCSCs within cell lines, as tissue culture conditions select for the fastest dividing cells. Therefore quiescent cells should be eliminated.

FACS is discussed in detail in Section 1.11. It is a technique for purifying sub-populations of cells from a heterogeneous cell suspension. Prior to this current work there was no protocol established in the laboratory for the isolation of pCSCs via FACS. FACS is based on flow cytometry, so the optimisations carried out to establish the flow cytometry screen are also applicable to FACS.

The appropriate tissue culture media was used to collect sorted cells, until they could be returned to tissue culture conditions. The ALDH assay required cells to be collected in ALDH buffer to prevent loss of the fluorescent agent from the cell. This was required to preserve the fluorescence of the ALDH assay for post-sort purity testing. Cells sorted using the ALDH assay were sorted into ALDH buffer supplemented with 2 % penicillin/streptomycin, until they could be returned to tissue culture.

The CSP assay was able to transfer directly to FACS without further optimisations. The ALDH and HSP assays required further experiments to ensure that the results of the flow cytometry screen could be replicated on the cell sorter. The effects of scaling the staining process and the differing hardware had to be elucidated.

3.1.1.1 ALDH Assay Optimisations:

As the ALDH Assay was not an established technique in the laboratory, it was necessary to establish positive and negative staining controls to demonstrate that the assay was suitable for pCSC screening.

Furthermore, the ALDH positive (ALDH+) sub-population within some of the model systems was very small (0.15 %; detailed in Section 4.3.1.1). In such cases, samples of approximately 1×10^8 cells were required to obtain 1×10^5 ALDH+ cells post cell sorting. 1×10^5 cells were required to seed a single well of a 6-well plate. The ALDH kit is designed to stain 1×10^6 cells

in a 1 ml reaction. Staining 1 x 10^8 cells required scaling of the ALDH staining technique. Experiments were required to demonstrate that scaling the reaction did not alter the data obtained.

The internal negative control of the ALDH assay (diethylaminobenzaldehyde; DEAB), is useful for setting positive/negative thresholds when the positive sub-population is small. However, it is not able to properly inhibit the fluorescence of the ALDH+ cells to the same level as the ALDH- cells. As the ALDH+ fraction approached 70 % this presented a problem when setting the positive/negative threshold. A method of setting positive/negative thresholds was required when samples were sorted to high purity.

3.1.1.2 HSP Assay Optimisations:

As the HSP Assay was not an established technique in the laboratory, it was necessary to establish positive and negative staining controls to demonstrate that the assay was suitable for pCSC screening.

As described earlier (Section 1.12), the flow cytometers available for *en masse* screening were equipped with violet lasers (405 nm). The cell sorter was equipped with a UV laser (351 nm) but not a violet laser. This resulted in a slightly different fluorescent profile for the HSP assay when run for screening purposes on the standard flow cytometers (CyAn™ Advanced Digital Processing; CyAn™) and when run for sorting purposes on the cell sorter (MoFlo™ High Performance Cell Sorter; MoFlo™). The relationship between the two fluorescent profiles needed to be defined before cells identified in the flow cytometry screen could be brought forward to FACS.

3.1.1.3 CSP Assay Optimisations:

As the CSP Assay was not an established technique in the laboratory, it was necessary to establish positive and negative staining controls to demonstrate that the assay was suitable for pCSC screening.

3.1.1.3.1 Antibody and Fluorochrome Selection

There is often a range of unique, commercially available antibodies capable of detecting a given protein. Antibodies were selected that recognised epitopes common to the most isoforms, of the protein of interest. This broad spectrum approach was adopted as the literature had yet to make distinctions on which isoforms of proteins were marking ovarian CSCs (Zhang et al. 2008; Curley et al. 2009).

Only primary conjugated monoclonal antibodies were selected. The use of primary conjugated antibodies negates the need for staining with secondary antibodies. Secondary antibodies increase the complexity of an experiment, by increasing the number of control samples needed. The use of monoclonal antibodies over polyclonal antibodies, reduces the potential for non-specific binding.

In addition to the above considerations, fluorochrome conjugate options had to be compared and selected. Fluorochrome selection was balanced on inter-fluorochrome compatibility and the resolution between positive and negative populations. The former can be predicted based on documented excitation and emission properties. The latter cannot be determined until one has run a sample, therefore it requires optimisation. These experiments are described in Appendix A.

3.1.2 Validation

Isolated pCSCs needed to be validated as CSCs. The *in vivo* mouse tumourgenicity assay is the gold standard for validating CSCs (Qin et al. 2012; Dieter et al. 2011; Pang et al. 2010). A CSC can efficiently reproduce the original malignancy in an immunocompromised host while a non-CSC cannot. Prior to this current work, the laboratory had no experience working with live animals. Multiple factors had to be considered;

i) the strain of mouse

ii) the mode of injection

iii) the cell vehicle

iv) the cell number

v) specimen collection

vi) positive and negative controls

vii) histological assessment of tumours

Each of these considerations will be introduced momentarily (Section 3.1.2.1).

A second tier of validation, the SD assay, was also implemented. This assay queries a fundamental principle of stem cell biology. It interrogates a cells potential to produce two daughter cells of differing phenotype. This technique is very powerful but currently under utilised in the literature. Prior to this current work the laboratory had no protocol for probing the differentiation potential of cells. Multiple approaches were compared to determine how to

best implement this SD assay. These approaches will be introduced after the tumourgenicity assay (Section 3.1.2.2).

3.1.2.1 Tumourgenicity Assay

The tumourgenicity assay differentiates between CSCs and non-CSCs based on how efficiently they can form xenograft tumours in mice. The efficiency of tumour formation is measured by "days since innoculation" and tumour size. If "days since innoculation" or tumour size or indeed both are statistically significantly different between populations of cells the more efficient population is considered to be more cancer stem-like.

There were multiple considerations in the establishment of the mouse tumourgenicity assay. The primary one was the application for ethical approval and an animal licence. To make such an application one has to outline the experimental design and protocols. As the laboratory had no prior experience with *in vivo* tumourgenicity assays, several aspects of the tumourgenicity assay had to be designed using information from the literature.

This meant that prior to carrying out a single experiment, the strain of mouse, along with the mode and volume of injection were already finalised. It was decided to use the NOD.CB17-Prkdc^{scid}/NCrHsd (NOD.SCID) strain of mouse, injected subcutaneously at the hindlimb with cells in a 100 µl volume of vehicle. These decisions will be discussed in detail in Sections 6.1.1.1 and 6.1.1.2 respectively. Due to careful wording in the application, there was scope to optimise the cell vehicle and the cell number, as well as how specimens and tumourgenicity data was collected. This parameters will be optimised in this chapter (Section 3.3.2).

3.1.2.1.1 Cell Vehicle

The injection vehicle with the most precedence in the literature is media supplemented with matrigel. Matrigel is the solubilised extracellular component of Engelbreth-Holm-Swarm mouse sarcoma (Vukicevic et al. 1992). Matrigel contains many growth factors linked with the regulation of self-renewal and differentiation of CSCs. These growth factors include epidermal growth factor, insulin-like growth factor 1, fibroblast growth factor and transforming growth factor beta (Vukicevic et al. 1992). Experiments were carried out to examine how different vehicles effect the tumourgenicity assay.

PBS, Ham's F12 media supplemented with matrigel and Ham's F12 media only were all compared. Due to time constraints it was not possible to optimise the vehicle prior to commencing the validation of isolated pCSCs. It was decided to used the well published

matrigel supplemented vehicle approach for the validations in this project and to run optimisations concurrently to apply to future work. The comparison of these three vehicles is described Appendix A. Ham's F12 media and high concentration Matrigel were selected as they were demonstrated to support tumour growth with undifferentiated NTera2 (undiffNT2) cells (Watanabe et al. 2010). UndiffNT2 cells were used for proof of principle experiments (Section 3.3.2.1). The proof of principle conditions were applied to all validations in this project. Ham's F12 was used for the media only experiments so that the experiments would be specifically interrogating the effect of removing matrigel.

3.1.2.1.2 Proof of Principle

It was necessary to demonstrate that cancerous cells could be administered in a fashion conducive to tumour formation. The undiffNT2 model system was used as a positive tumour forming control, while 7 – 8 day retinoic acid terminally differentiated NTera2 (diffNT2) cells were used as a negative control (Andrews 1984). This experiment served as a proof of principle that CSCs could form tumours while differentiated cells could not. It also demonstrated that the CSC validation assay developed for this project was capable of discriminating between CSCs and non-CSCs.

3.1.2.2 SD Assay

To complement the mouse tumourgenicity assay, a SD assay was developed. This *in vitro* assay, probes the cells potential to self-renew and differentiate. To insure accurate interpretation of the results this assay must be carried out on a 100 % pure starting population. The best way to guarantee 100 % purity is to plate a single cell per well. Prior to this current work the laboratory had no protocols established for single cell plating. Multiple approaches were investigated when developing a single cell plating protocol;

i) serial dilution validated by microscope.

ii) FACS validated by high throughput imaging.

iii) FACS of pure populations – no visual validation, statistical approach to certainty.

The considerations, advantages and disadvantages of each approach are introduced below.

3.1.2.2.1 Serial Dilution

Performing cell counts on several samples of a single cell suspension provides a good estimate of its cell concentration. Through serially diluting the sample a measured number of times one can arrive at a concentration of 1 cell/100 µl media. By diluting to a 1 cell/100 µl concentration

it reduces the amount pipetting error will effect the delivery of a single when loading the 96-well plate.

Microscopy can validate which wells were actually seeded with single cells, which were empty and which seeded with two or more cells.

Serial dilution cannot take advantage of stains to sort cells. Therefore the starting population must be a pure population. Microscopy does not provide data on the marker status of the singly plated cells. Experiments were required to determine if this approach was suitable for large scale SD assays.

3.1.2.2.2 FACS Validated by High Throughput Imaging

FACS is based on selecting and sorting a single cell at a time. The MoFlo™ cell sorter is capable of sorting a single cell into a single well on a microtiter plate. Stained cells can be sorted as single cells across multiple plates. As staining is carried out, cells can be plated from an impure population and plated as they are sorted.

Post-sort validation can be carried out via high throughput imaging. The imaging machines have lasers and detectors which can detect fluorescence. This has the potential to identify a single cell in a well and to confirm it as 'marker positive' or 'negative'. Experiments were required to determine if this approach was suitable for large scale SD assays.

3.1.2.2.3 FACS of Pure Populations – No Visual Validation, Statistical Approach

Starting with a purified population decreases the probability of the cell sorter making an error while sorting. Reducing the chance of placing a negative cell where a positive cell is expected or vice versa. The probability of a doublet effecting the assay is reduced as the starting population becomes purer. As the risk of a doublet consisting of differing cell types is reduced.

With this approach a statistical model can work out the probabilities of doublets or impurities effecting the assay. This negates the need for post-sort validations. Experiments were required to determine if this approach was suitable for large scale SD assays.

3.1.3 Aims

There were three major aims driving the work presented in this chapter;

i) To develop a flow cytometry based screen for the identification of pCSCs

ii) To develop FACS protocols to allow for the isolation of pCSCs.

iii) To develop techniques for the validation of isolated pCSCs as CSCs

Each of these major aims had several sub-units as outlined below.

i) pCSC Screen:

- To identify the optimal approach for the implementation of the technical flow cytometry controls.
- To identify the optimal protocol for side-population discovery based on the accessible hardware.
- To identify a method of cell dissociation, which preserves the integrity of the CSPs.
- To identify the optimal combination of fluorochromes for the CSP assay.
- To demonstrate that all the screening assays established were capable of identifying both pCSCs and non-pCSCs.

ii) Isolation of pCSCs.

- To demonstrate the scalability of the ALDH assay.
- To develop a gating strategy to identify ALDH+ and ALDH negative (ALDH-) cells in high purity ALDH+ populations.
- To define the differences in HSP profile when screening compared to sorting pCSCs.

iii) Validation of pCSCs as CSCs:

- To establish an *in vivo* mouse tumourgenicity assay:
  - To define an optimal vehicle to inject cells with.
  - To establish a proof of principle experiment, to show that the tumourgenicity assay can discriminate between CSCs and non-CSCs
  - To develop protocols for specimen collection.
- To establish an *in vitro* SD assay:
  - To establish a method for single cell plating.
  - To establish a method for identifying cells with the potential to self renew and differentiate.

3.2 Materials and Methods

3.2.1 Cell Culture and Sub-Culture:

The A2780cis, IGROV-1, IGROV-1-CDDP, SK-OV-3, 59M, NTera2, 2102ep and Hela cell lines were used to perform optimisation experiments in this chapter. All cell lines were cultured and sub-cultured as described in Section 2.2.

3.2.2 Differentiation of NTera2 Cells

UndiffNT2 cells were differentiated using Retinoic Acid for a period of 7-9 days, as described in Section 2.3.

3.2.3 Cell Dissociation Techniques

Three dissociation techniques were used to perform the experiments in this chapter. These were 0.25 % Trypsin/EDTA, EDTA and Accutase™ mediated dissociations. 0.25 % trypsin/EDTA and EDTA dissociation was carried out as described in Section 2.2.

For Accutase™ dissociation, all media was removed from the T75 flask. The cell monolayer was then rinsed with 5 ml PBS. 2 ml of Accutase™ was added and the flask was returned to the incubator for 3-5 min. Accutase™ and dissociated cells were neutralised and collected with 5 ml of culture media. Cells were pelleted at 170 x g for 5 min. The supernatant was removed and the cells were re-suspended in 1 ml of PBS.

3.2.4 Flow cytometry

3.2.4.1 Technical Controls

Except where explicitly stated the three flow cytometric technical controls were carried out as described in Section 1.11.2.

3.2.4.2 ALDH Assay

Except where explicitly stated the ALDH Assay was carried out as described in Section 2.5.1.

3.2.4.3 HSP Assay

The HSP Assay was carried out as described in Section 2.5.2. DCV staining was carried out in the exact same fashion as the HSP Assay with one exception – instead of adding 5 μg/ml Hoechst 33342, DCV was added to a concentration of 10 μM.

3.2.4.4 CSP Assay

The CSP Assay was carried out as described in Section 2.5.3.

3.2.5 FACS

Cell sorting was carried out as described in Section 2.6.

3.2.6 *In Vivo* Mouse Tumourgenicity Assay

Except where explicitly stated the tumourgenicity assay was carried out as described in Section 2.7.

3.2.7 SD Assay

3.2.7.1 Serial dilution

4 samples were taken for cell counting using a hemocytometer. The cell concentration was then adjusted to 1 x 10^6 using appropriate culture media. 8 sequential 1:10 dilutions were performed to obtain a concentration of 1 cell/100 μl. 100 μl of this diluted cell suspension was added to each well of a 96-well plate.

3.2.7.2 InCELL Analyser

Cells were plated at a density of 1 cell per well of a 96 well plate via FACS. The cells were then returned to the incubator for 2 hours to allow cells to settle and adhere. The plate was then brought to the InCELL analyser for photographic analysis.

Multiple photos were taken at 100x magnification of each well and stitched together to form a picture of the well. Wells were imaged in bright field and fluorescent fields where appropriate.

3.3 Data

The following sections (Sections 3.3.1 – 3.3.3) describe the data from a series of experiments designed to identify the optimal approach to each of the techniques established in this project. The experiments divide into four major categories;

i) ALDH Assay Optimisations

ii) HSP Assay Optimisations

iii) CSP Assay Optimisations

iv) *In Vivo* Mouse Tumourgenicity Assay Optimisations

v) SD Assays Optimisations

This data section is designed to present the experiments behind each of these optimisations in a structured fashion. The experiments are laid out in a structure that respects the order in which they were discussed in the introduction (Section 3.1).

3.3.1 Flow Cytometry

3.3.1.1 Establishing the ALDH CSC Screening Assay:

To confirm the integrity of the down stream results, cell lines were identified to act as positively and negatively staining controls for the ALDH Assay. Further information on the positive and negative controls can be found in Appendix A.

The A2780cis cell line and the 59M cell line were stained using the ALDH assay. Cisplatin resistant models of the A2780 cell line have been shown to exhibit an ALDH+ sub-population (Deng et al. 2010). 59M was identified as a negatively staining model for the ALDH Assay from within the panel of ovarian cancer cell lines. An ALDH+ sub-population was identified within the A2780cis cell line (Figure 3.1). No ALDH+ sub-population was identified within the 59M cell line (Figure 3.2). This pair of observations demonstrates that the ALDH Assay is fit for the identification of novel sub-populations.

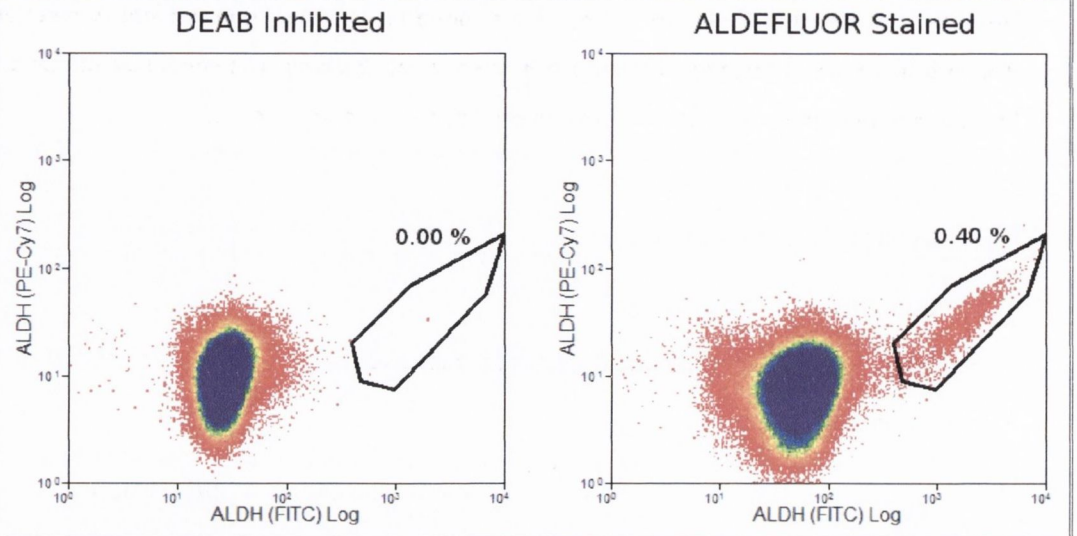

Figure 3.1: A2780cis is a positive control for the ALDH assay – The left panel shows the DEAB inhibited internal negative control. The right panel shows uninhibited ALDH staining. Subtracting the inhibited population from the uninhibited sample identifies a 0.4 % ALDH+ sub-population.

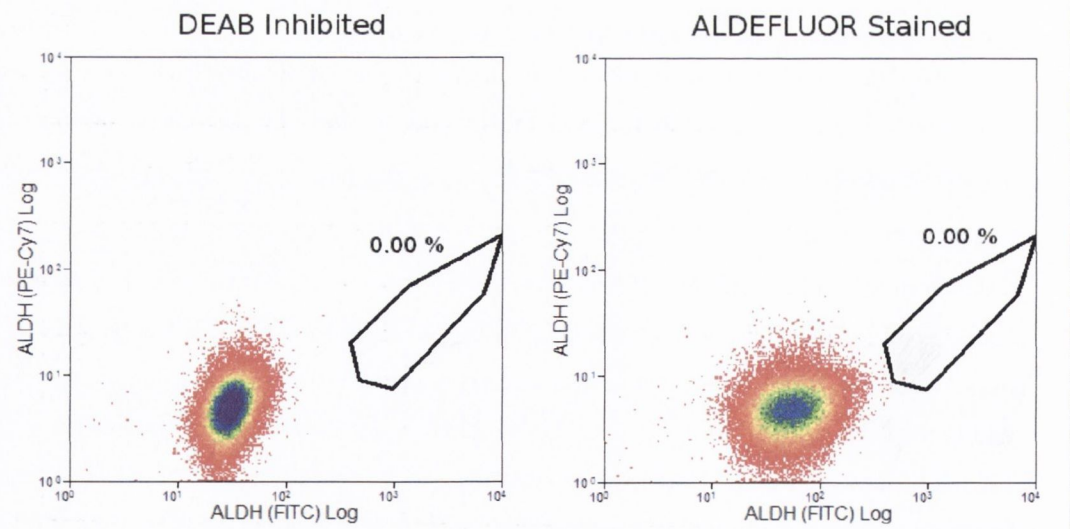

Figure 3.2: 59M is a negative control for the ALDH assay – The left panel shows the DEAB inhibited internal negative control. The right panel shows uninhibited ALDH staining. No ALDH+ sub-population is detected.

3.3.1.2 Establishing the ALDH CSC Isolation Procedure:

The ALDH assay required two optimisation experiments to transfer it to cell sorting: one to show it could scale to a level more appropriate for cell sorting and one to identify a better way of identifying the positive/negative threshold in enriched samples. The small size of some of the ALDH+ sub-populations required large numbers of cells for cell sorting.

3.3.1.2.1 Scaling the ALDH Assay

Two variations of the staining procedure were compared and contrasted. The ALDH manufacturer instructs to stain at 1 x 10^6 cells/ml. This was compared to the staining of cells at 5 x 10^6 cells/ml. This experiment showed that the ALDH assay was equally able to resolve the ALDH- and ALDH+ cells when stained at both 1 x 10^6 cells/ml and 5 x 10^6 cells/ml (Figure 3.3). The resolution between ALDH+ and ALDH- cells is very similar at both staining densities. The proportional size of each of theses sub-populations from both staining methods are with one standard deviation from the mean for this cell line (A2780cis; see Section 4.3.1.1).

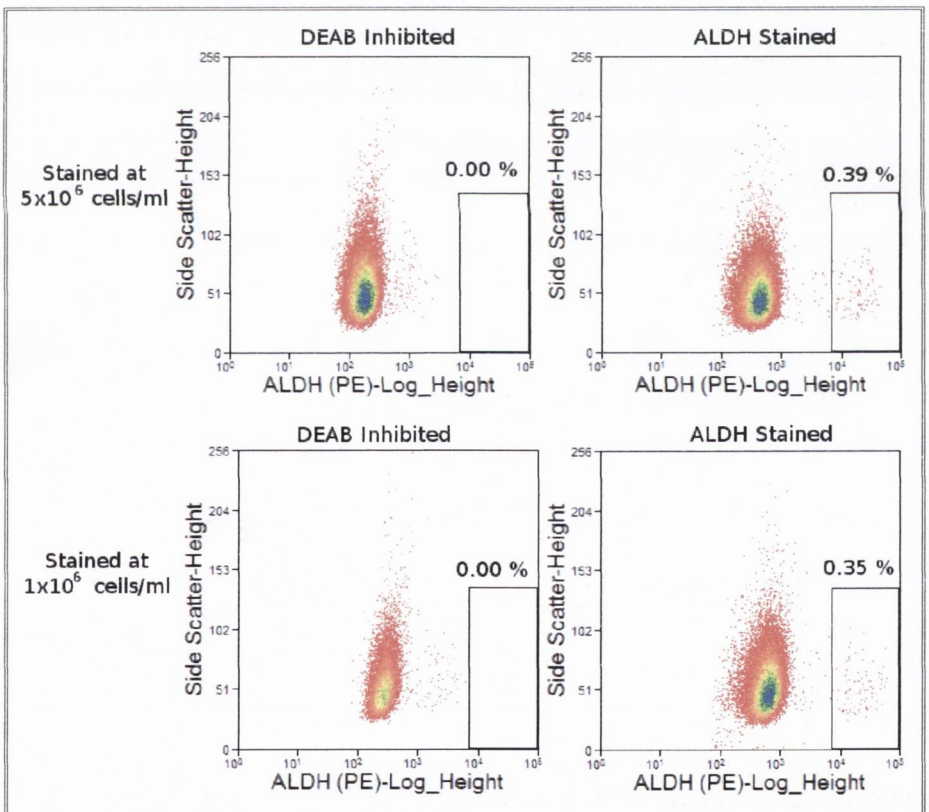

Figure 3.3: ALDH Assay Cell Densities – The diagrams show A2780cis cells stained at cell concentrations of 5 x 10^6 and 1 x 10^6 cells/ml.

3.3.1.2.2 Identifying the Positive/Negative Threshold

Two approaches were attempted to establish a protocol for accurate positive/negative gating in ALDH+ enriched populations. The first was to increase the concentration of the aldehyde dehydrogenase inhibitor, DEAB, in the inhibited sample. The second was to use a mixed population of positive and negative cells to set the gates.

The manufacturer instructs the addition of DEAB at 5 µl/500µl of reaction. This equates to 15 µM DEAB. A range of volumes of DEAB were tested: 5 µl/500µl – 100 µl/500µl (15 - 300 µM). It was found that the increasing concentrations of DEAB had a cytotoxic effect on the cells (Figure 3.4). This was probably due to the DEAB vehicle (95 % ethanol). Furthermore, increasing the concentration of DEAB did not decrease fluorescent intensity of the inhibited control (Figure 3.5). The reduction in cell numbers in the higher concentrations is due to increasing numbers of events being excluded by the live cell gate. These data show that increasing the volume of DEAB inhibitor per reaction is not a feasible approach to set the positive/negative threshold in ALDH+ enriched samples.

The other approach investigated was to establish an additional control reaction with a mixture (approximately 1:1) of ALDH- and ALDH + cells. Establishing a gate between the positively and negatively staining populations was more accurate than DEAB based gating for discriminating between ALDH+ and ALDH- cells within ALDH+ enriched populations (Figure 3.6).

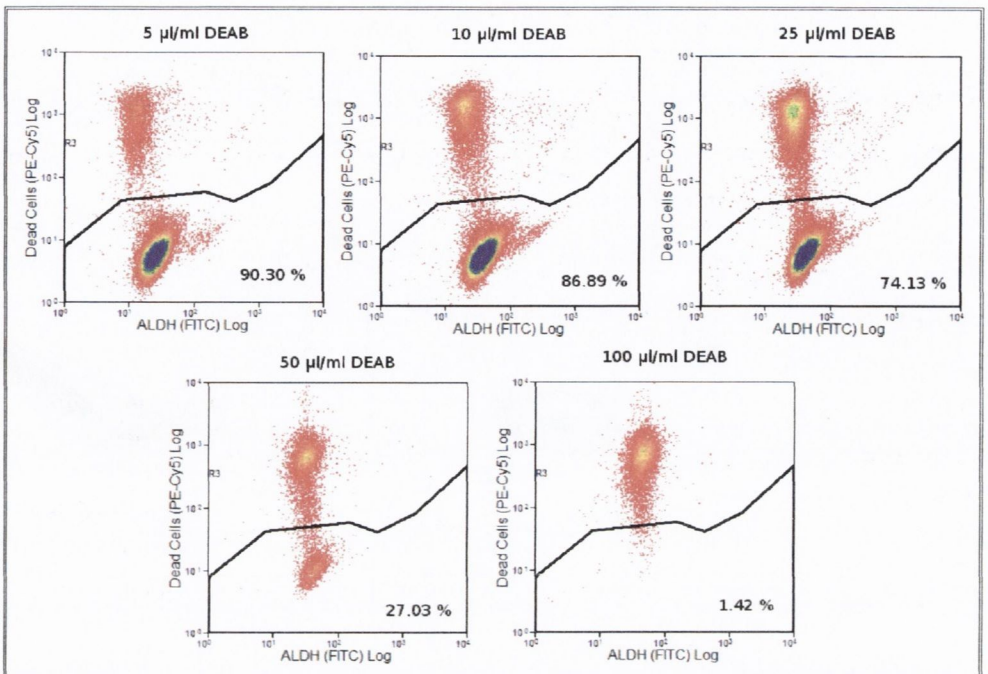

Figure 3.4: Increasing the DEAB inhibitor concentration increases cell death – Each panel shows a DEAB inhibited ALDH assay sample with increasing concentrations going from left to right. ALDH fluorescence is measured on the x-axis, cell viability is measured on the y-axis. The percentages shown represent the percentage viability of the sample.

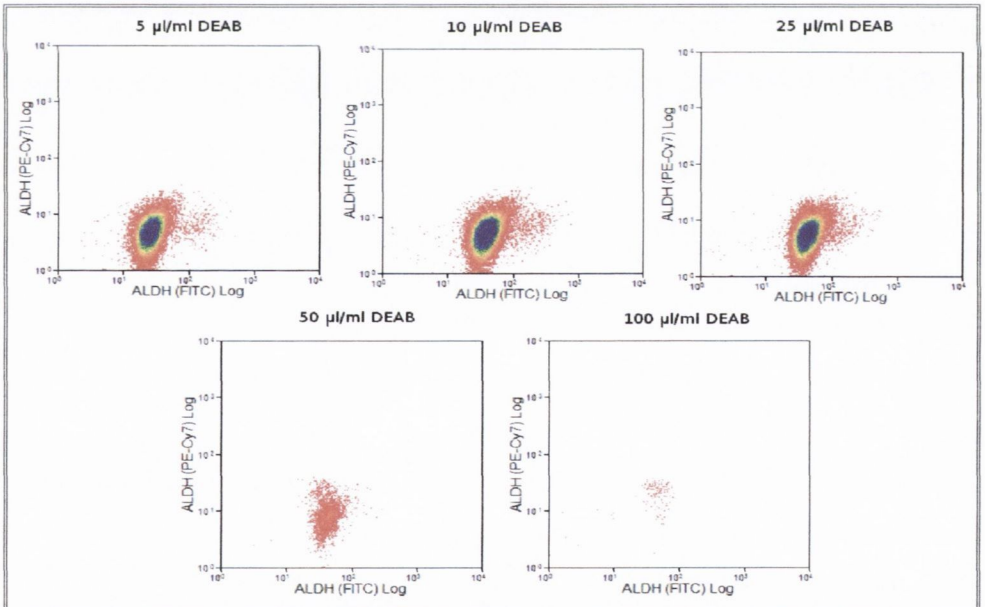

Figure 3.5: Increasing the DEAB inhibitor concentration did not decrease the fluorescence of the inhibited sample - Each panel shows a DEAB inhibited ALDH assay sample with increasing concentrations going from left to right. ALDH fluorescence is measured on both the x-axis, and with spill-over fluorescence on the y-axis. Increased DEAB inhibition would have presented itself as a left-shift on the x-axis.

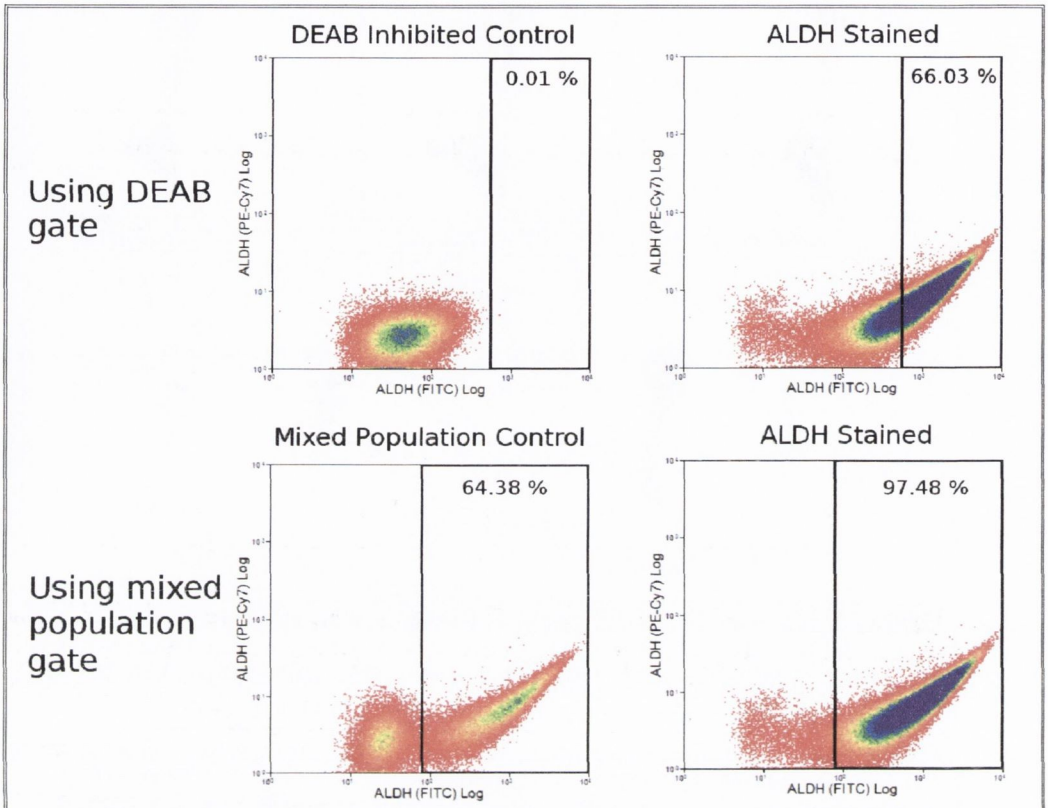

Figure 3.6: ALDH Mixed Populations Control – These diagrams compare the thresholds set using the DEAB control and the Mixed population control. The DEAB control underestimates the size of the ALDH+ population when compared to the mixed population control.

3.3.1.3 Establishing the HSP CSC Screening Assay:

To confirm the integrity of the down stream results, cell lines were identified to act as positively and negatively staining controls for the CSP Assay. Further information on the positive and negative controls can be found in Appendix A.

The IGROV-1-CDDP cell line and the A2780cis cell line were stained using the HSP assay. Data produced within the laboratory demonstrated that the IGROV-1-CDDP cell line expressed ABC transporters associated with hoechst dye efflux at very high levels. A2780cis was identified as a negatively staining model for the HSP Assay from within the panel of ovarian cancer cell lines. A side-population was identified within the IGROV-1-CDDP cell line (Figure 3.7). No side population was identified within the A2780cis cell line (Figure 3.8). This

pair of observations demonstrates that the HSP Assay is fit for the identification of novel sub-populations.

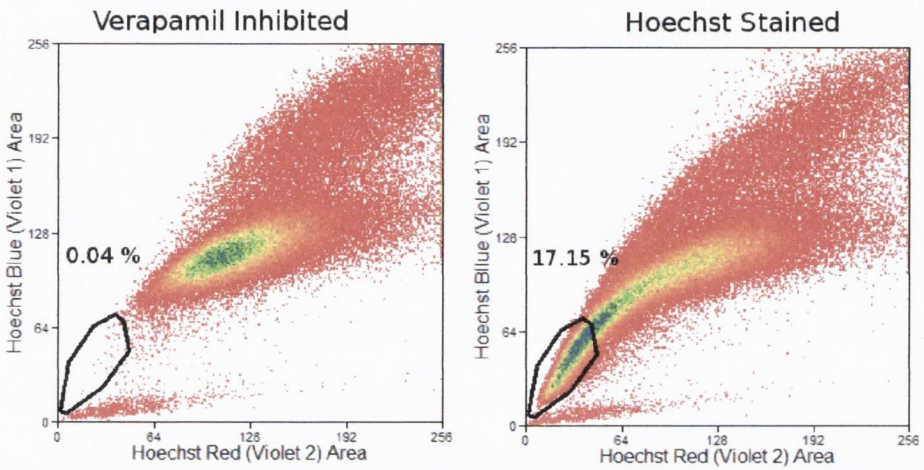

Figure 3.7: IGROV-1-CDDP is a positive control for the HSP assay – The left panel shows the Verapamil inhibited internal negative control. The right panel shows uninhibited Hoechst staining. Subtracting the inhibited population from the uninhibited sample identifies a 17.15 % Hoechst side-population.

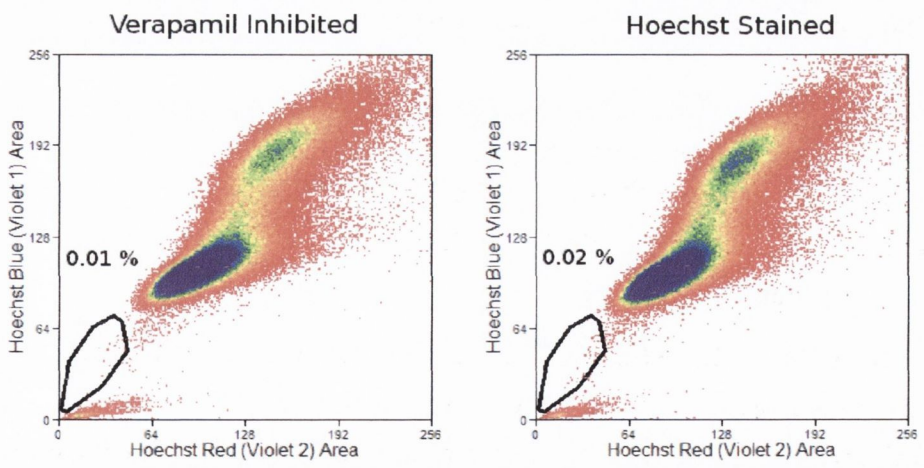

Figure 3.8: A2780cis is a negative control for the HSP assay - The left panel shows the Verapamil inhibited internal negative control. The right panel shows uninhibited Hoechst staining. No hoechst side-population is detected.

Section 3.0 – Establishing the CSC Assays

Due to differences in the hardware between the cell sorter (MoFlo™) and the screening flow cytometer (CyAn™) the HSP profile observed while screening was different to that observed when sorting. The relationship between the two HSP profiles were defined prior to sorting.

IGROV-1-CDDP cells were stained via the HSP assay and run on the Cyan (Figure 3.9A and 9B). The same set of samples were then run on the MoFlo™ (Figure 9C and 9D). The U.V. Laser on the MoFlo™ produced better resolution between SP and non-SP cells. To confirm the two populations observed on the MoFlo™ corresponded to those seen on the CyAn™ during screening. SP and non-SP cells were sorted on the MoFlo™ and re-analysed on the CyAn™. The resolution on the CyAn™ forces one to put the G_2 cells off scale, to give better resolution at the G_1 SP.

SP cells isolated on the MoFlo™ corresponded to SP cells identified on the CyAn™ (Figure 3.10). Non-SP cells isolated on the MoFlo™ corresponded to non-SP cells identified on the CyAn™ (Figure 3.10). This demonstrates that cells identified as being SP and non-SP during the screening phase, on the CyAn™, could be faithfully purified, on the MoFlo™, during the isolation phase.

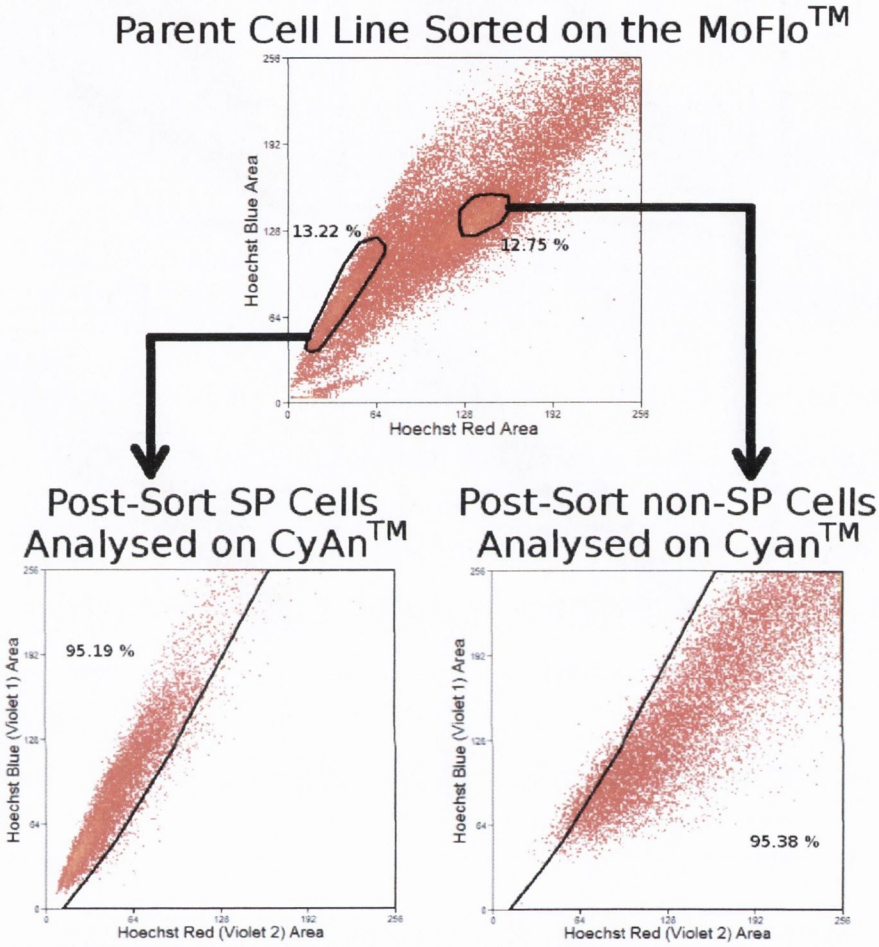

Figure 3.10: SP and non-SP cells sorted on the MoFlo™ correspond to SP and non-SP populations identified on the CyAn™ – This figure shows SP and non-SP cells sorted on the MoFlo™ (top graph) and re-analysed on the CyAn™ (bottom graphs). Verapamil controls were used to establish the gating strategies for SP and non-SP cells.

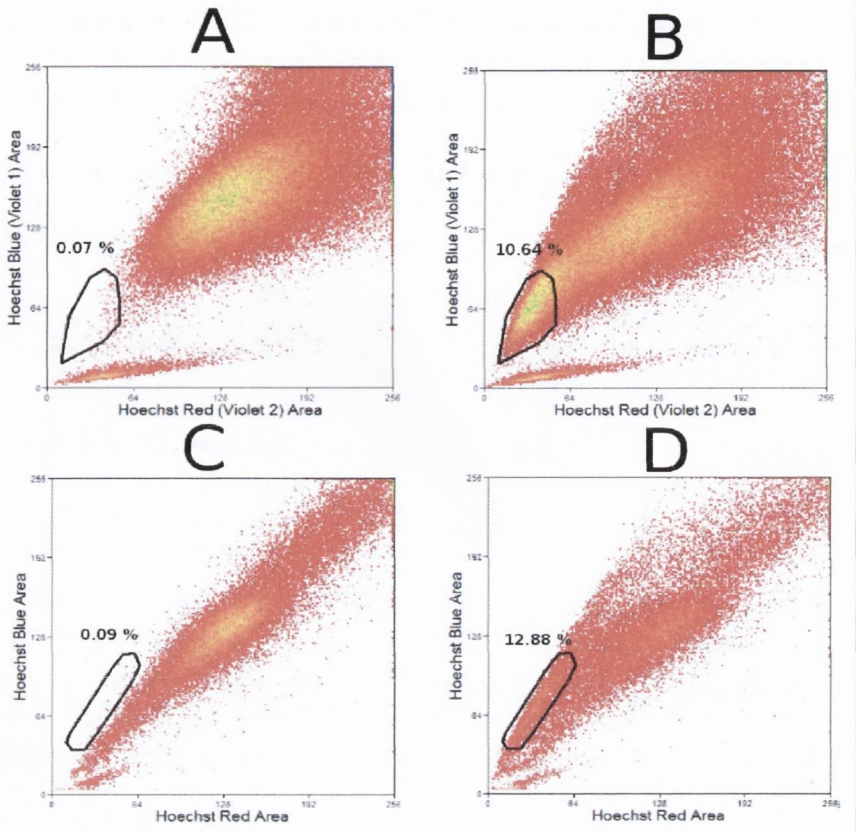

Figure 3.9: The CyAn™ and MoFlo™ produce slightly different profiles for the HSP assay – A) Shows the Verapamil inhibited control profile on the Cyan. B) Shows the uninhibited profile on the Cyan. C) Shows the Verapamil inhibited control profile on the MoFlo™. D) Shows the uninhibited profile on the MoFlo™.

3.3.1.4 CSP Assay Optimisations

To confirm the integrity of the down stream results, cell lines were identified to act as positively and negatively staining controls for the CSP Assay. Further information on the positive and negative controls can be found in Appendix A.

3.3.1.4.1 Establishing the CSP CSC Screening Assay – antiCD44 Staining

The SK-OV-3 cell line and the A2780cis cell line were stained with antiCD44-FITC using the CSP assay. Both of these cell lines were identified as staining controls from within the panel of ovarian cancer cell lines. A CD44+ population was identified within the SK-OV-3 cell line (Figure 3.11). No discrete CD44+ population was identified within the A2780cis cell line (Figure 3.12). There is a small CD44+ tail (1.16 %) in the negatively staining sample (A2780cis). The differences between tail populations and discrete populations will be discussed in section 6.4.5. This pair of observations demonstrates that the anti-CD44 antibody is fit for the identification of novel sub-populations.

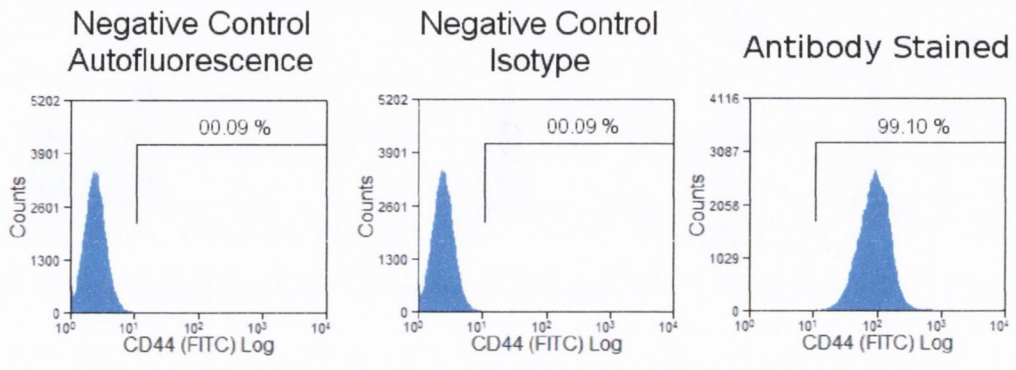

Figure 3.11: SK-OV-3 is a positive control for antiCD44 staining – The left panel shows the autofluorescence (background fluorescence) of the cells. The central panel shows the fluorescence when stained with an isotype control for antiCD44-FITC. The right panel shows the cells stained with antiCD44-FITC. The thresholds are set from the autofluorescence control. SK-OV-3 is a CD44+ cell line.

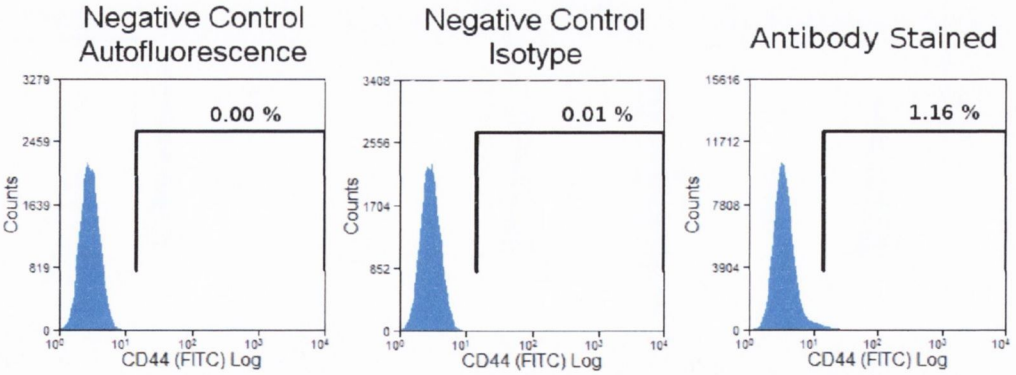

Figure 3.12: A2780cis is a negative control for anti CD44 staining - The left panel shows the autofluorescence of the cells. The central panel shows the fluorescence when stained with an isotype control for antiCD44-FITC. The right panel shows the cells stained with antiCD44-FITC. The thresholds are set from the autofluorescence control. A2780cis is a CD44- cell line.

3.3.1.4.2 Establishing the CSP CSC Screening Assay – antiCD117 Staining

The SK-OV-3 cell line and the A2780cis cell line were stained with antiCD117-PE using the CSP Assay. Both of these cell lines were identified as staining controls from within the panel of ovarian cancer cell lines. A CD117+ sub-population was identified within the SK-OV-3 cell line (Figure 3.13). No CD117+ sub-population was identified within the A2780cis cell line (Figure 3.14). This pair of observations demonstrates that the anti-CD117 antibody is fit for the identification of novel sub-populations.

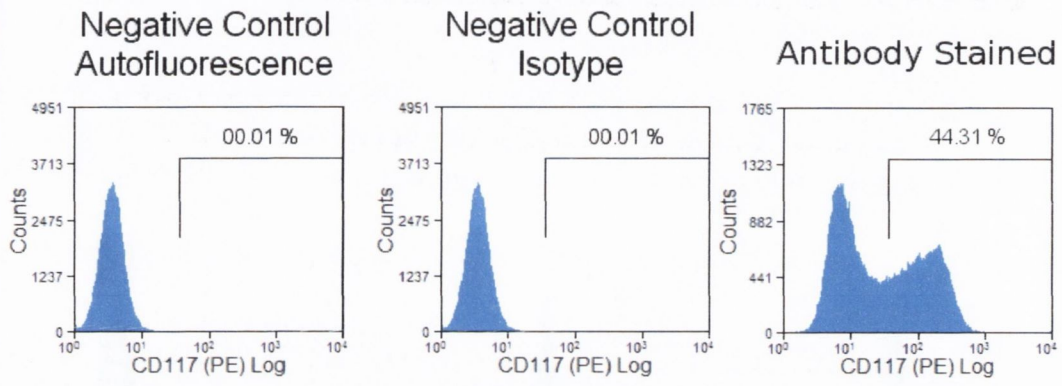

Figure 3.13: SK-OV-3 is a positive staining control for anti-CD117 staining - The left panel shows the autofluorescence of the cells. The central panel shows the fluorescence when stained with an isotype control for antiCD117-PE. The right panel shows the cells stained with antiCD117-PE. The thresholds are using the local minimum between the CD117- and CD117+ maxima. SK-OV-3 has a large CD117+ sub-population.

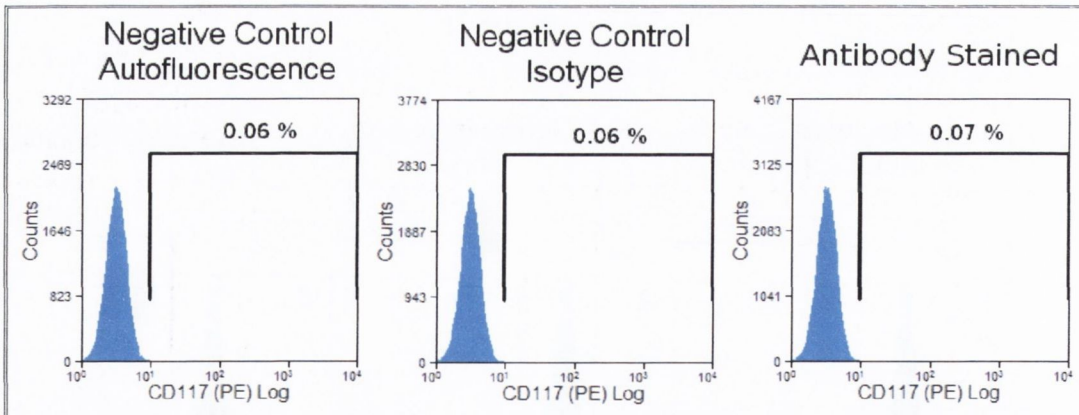

Figure 3.14: A2780cis is a negative control for anti-CD117 staining - The left panel shows the autofluorescence of the cells. The central panel shows the fluorescence when stained with an isotype control for antiCD117-PE. The right panel shows the cells stained with antiCD117-PE. The thresholds are set using the autofluorescence control. A2780cis is a CD117- cell line.

3.3.1.4.3 Establishing the CSP CSC Screening Assay – CD133

The UndiffNT2 cell line and the A2780cis cell line were stained with antiCD133-APC using the CSP Assay. The undiffNT2 cell line has been shown to exhibit CD133 expression (Dittfeld et al. 2009). A2780cis was identified as a negatively staining model for CD133 staining from within the panel of ovarian cancer cell lines. A CD133 positive population was identified within the undiffNT2 cell line (Figure 3.15). No CD133 positive population was identified within the A2780cis cell line (Figure 3.16). This pair of observations demonstrates that the anti-CD133 antibody is fit for the identification of novel sub-populations.

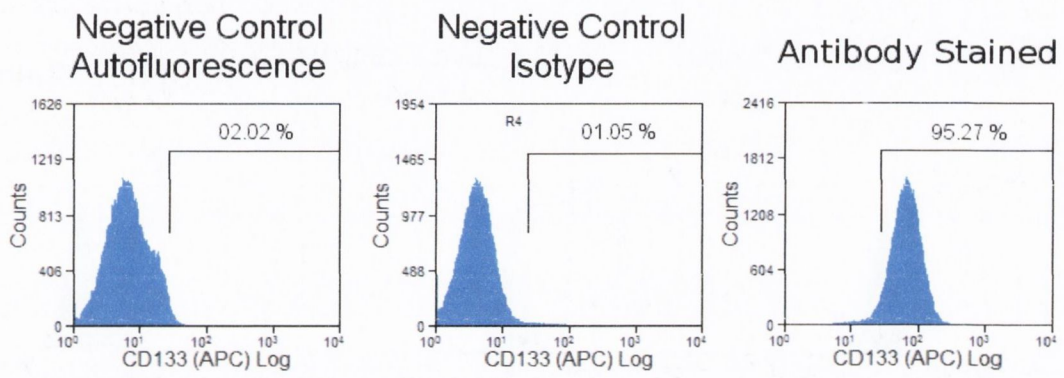

Figure 3.15: UndiffN2 is a positive staining control for anti-CD133 staining - The left panel shows the autofluorescence of the cells. The central panel shows the fluorescence when stained with an isotype control for antiCD133-APC. The right panel shows the cells stained with antiCD133-APC. The thresholds are set using the autofluorescence control. UndiffNT2 is a CD133+ cell line.

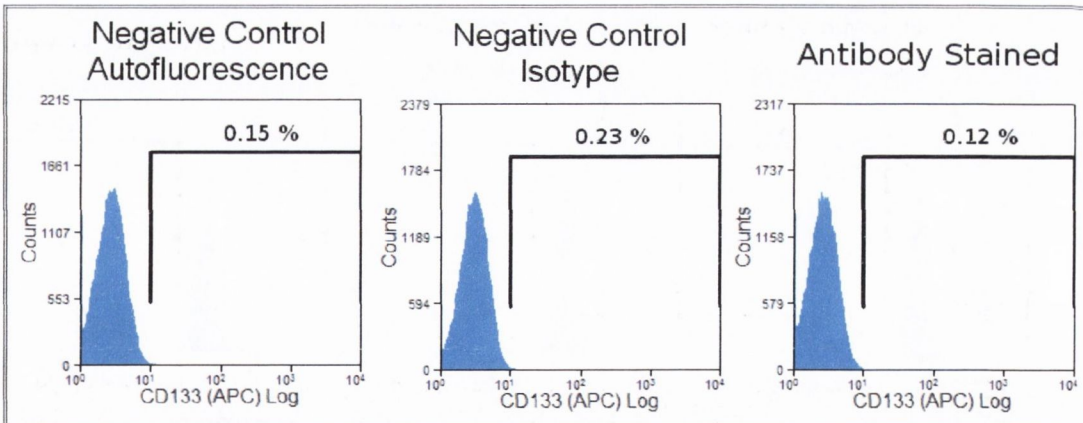

Figure 3.16: A2780cis is a negative staining control for anti-CD133 staining - The left panel shows the autofluorescence of the cells. The central panel shows the fluorescence when stained with an isotype control for antiCD133-APC. The right panel shows the cells stained with antiCD133-APC. The thresholds are set using the autofluorescence control. A2780cis is a CD133- cell line.

3.3.1.4.4 Establishing the CSP CSC Screening Assay – antiCXCR4 Staining

The Hela cell line and the A2780cis cell line were stained with antiCXCR4-APC using the CSP assay. The Hela cell line has been shown to exhibit CXCR4 expression (Yang et al. 2007). 59M was identified as a negatively staining model for CXCR4 staining from within the panel of ovarian cancer cell lines. A CXCR4 positive population was identified within the Hela cell line (Figure 3.17). No CXCR4 positive population was identified within the A2780cis cell line (Figure 3.18). This pair of observations demonstrates that the anti-CXCR4 antibody is fit for the identification of novel sub-populations.

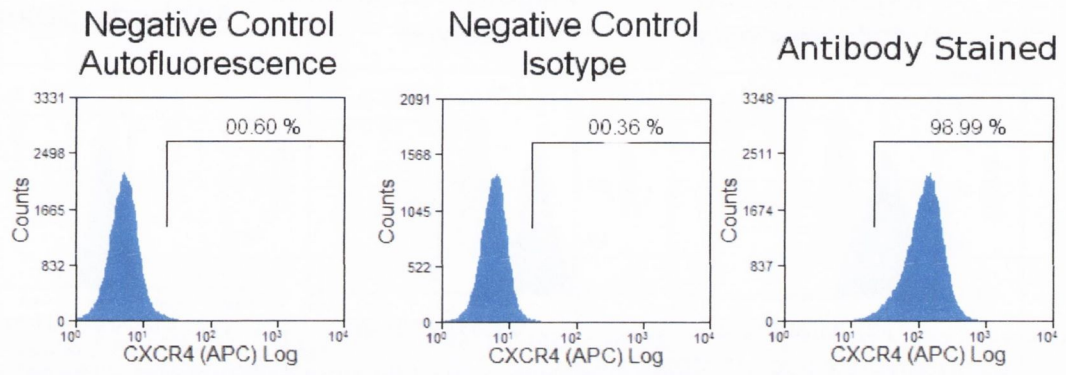

Figure 3.17: Hela is a positive staining control for anti-CXCR4 staining - The left panel shows the autofluorescence of the cells. The central panel shows the fluorescence when stained with an isotype control for antiCXCR4-APC. The right panel shows the cells stained with antiCXCR4-APC. The thresholds are set using the autofluorescence control. Hela is a CXCR4+ cell line.

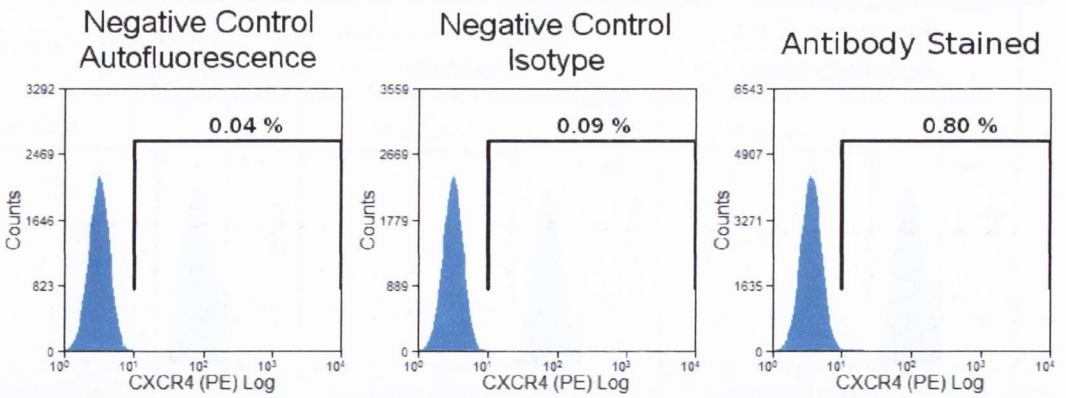

Figure 3.18: A2780cis is a negative staining control for anti-CXCR4 staining—The left panel shows the autofluorescence of the cells. The central panel shows the fluorescence when stained with an isotype control for antiCXCR4-PE. The right panel shows the cells stained with antiCXCR4-PE. The thresholds are set using the autofluorescence control. A2780cis is a CXCR4- cell line.

3.3.1.5 Summary of the Flow Cytometry Optimisations

The experiments described in this sub-section (Section 3.3.1), were carried out to optimise the techniques required to carry out the flow cytometry based pCSC screen for this project:

- ALDH Assay:
  - Positive and Negative staining controls were established.
  - It was found that the cell concentration used to stain for small sub-populations of cells could be scaled 5-fold, to 5×10^6 cells/ml adversely altering the results (Section 3.3.1.2.1). This was important as a large number of cells need to be stained to isolate the small ALDH+ sub-populations identified in the pCSC screen (Section 4.3.1).
  - It was found that a mixed population control was more efficient at setting a positive/negative threshold than the DEAB control, in samples containing a large fraction of ALDH+ cells (Section 3.3.1.2.2).
- HSP Assay:
  - Positive and Negative staining controls were established.
  - It was demonstrated that the cell sorter and the screening flow cytometers were declaring the same cells as SP and non-SP, despite the differing hardware (Section 3.1.1.2).
- CSP Assay:
  - Positive and Negative staining controls were established.

3.3.2 Establishing the In Vivo Mouse Tumourgenicity CSC Validation Assay:

Several experiments were carried out to establish the tumourgenicity assay. These experiments centred around identifying the optimal vehicle, establishing a proof of principle experiment, identifying the cell numbers at which the assay was effective and identifying the optimal method for processing the specimens collected.

As mentioned in section 3.1.2.1, it was decided to use NOD.SCID mice, injected subcutaneously at the hindlimb with cells in a 100 µl volume of vehicle. These decisions did not require experimental optimisations, therefore they will be detailed in validation chapter (Sections 6.1.1.1 and 6.1.1.2).

Section 3.0 – Establishing the CSC Assays

Cell number was a crucial factor that needed to be optimised for each set of pCSCs and non-pCSCs isolated. However, as the cell number optimisations also doubled as validations, this data will be presented in the validation chapter (Section 6.0). These established the correct cell number for each cell type. Many of the experiments in this section (Section 3.3.2) have dual purposes. The experiments were designed in such a fashion to reduce the numbers of animals used, which was a primary ethical consideration. As such, some data will be presented multiple times when addressing different questions.

All tumourgenicity data in this section (Section 3.3.2) will be presented in the following format. A graph will present the "days since innoculation" and tumour size. Photographs will illustrate the presence/absence, size and location of tumours. Welch's t-test will be used to determine statistically significant differences between to sets of experiments, with respect to "days since innoculation" and tumour size.

Tumourgenicity graphs are created using R (http://www.r-project.org/). "Days since innoculation" is shown in days on the y-axis. Tumour size is communicated through the size of the circular point, relative to a scale bar. Crosses are used to mark the "days since innoculation" at which point mice with no identifiable tumours were euthanised. Otherwise, mice were euthanised when tumours reached approximately 10 mm in diameter. Diameter of the tumour is defined here as the mean of two perpendicular measurements of the tumour width. These methods are detailed in Section 2.7.8.

Welch's t-test was performed using R. Welch's t-test is and adaptation of Student's t-test. It is used when the two datasets being compared do not have the same variance. Welch's t-test was used here, as there was no reason to expect the range of tumour latencies/sizes to be similar between cell-lines or sub-populations. Datasets were declared as significantly different if Welch's t-test identified the probability of the datasets being samples of the same population as p-value ≤ 0.05. In the stated instances, replicates which did not grow tumours were removed for the purpose of testing differences in latencies. Such replicates were removed as the "days since innoculation" value is arbitrary if no tumour formed, however this value still effects the resolution of the t-test. Such replicates were still included as a tumour of size 0 mm when testing the differences in sizes.

3.3.2.1 CSC Proof of Principle

Two validated CSC model systems are used within the laboratory – 2102ep and undiffNT2. 2102ep is a nullipotent embryonal carcinoma model (Andrews et al. 1982). UndiffNT2 is a pluripotent embryonal carcinoma model (Andrews et al. 1984). These models were compared to identify the best model to use to establish a proof of principle for mouse tumourgenicity CSC validation assays with (Appendix A). The undiffNT2 model produced more consistent results, with respect to tumour latencies. As such, it was selected as the optimal model for the CSC validation proof of principle experiments.

When establishing the mouse xenograft assay, it was found that 5 x 10^6 cells of both undiffNT2 and diffNT2 cells were capable of generating tumours (Figure 3.19). However, the diffNT2 cells had a significantly longer latency (p-value = 0.004; excluding the replicate which did not grow) than the undiffNT2 cells, to reach a non-significantly different size (p-value = 0.70). The different latency does identify the undiffNT2 cells as being more stem-like than the diffNT2 cells.

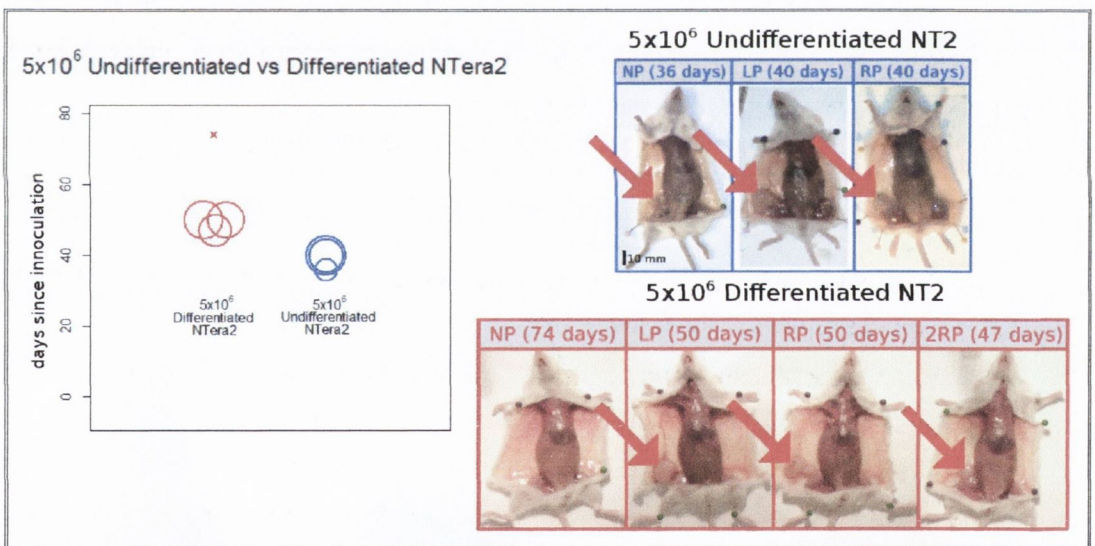

Figure 3.19: Comparison of the tumourgenicity of 5 x 10^6 undifferentiated and differentiated cells - Both undifferentiated and differentiated NT2 xenografts were capable of forming tumours. The diffNT2 cells were less efficient with a longer latency.

Experiments were conducted to establish a more qualitative negative control than the diffNT2 cells. Flow cytometric analysis of diffNT2 cells showed that it is possible for a small population of cells remain undifferentiated. This was observed via expression of the cell surface protein SSEA4 (Figure 3.20), which has high expression on undiffNT2 and reduced expression on diffNT2 (Draper et al. 2002).

One of the tumours produced by the diffNT2 xenografts was harvested and returned to tissue culture (Figure 3.21A). After 17 days, these cultured xenograft cells were assessed for SSEA4 expression via flow cytometry. It was observed that the tumours produced from the diffNT2 xenografts did contain undifferentiated cells (66.54 %; Figure 3.21B). The size of this population may not directly reflect proportion of undifferentiated cells in the tumour, as these proportions may have changed in tissue culture. However, it does indicate the presence of undiffNT2 cells in xenograft tumours formed by diffNT2 cells. DiffNT2 cells do not de-differentiate under tissue culture conditions when the RA morphogen is removed (Figure 3.22). This suggests that the growth seen in the 5 x 10^6 diffNT2 was due a small sub-population of undiffNT2 cells escaping differentiation by retinoic acid.

Two approaches were taken to investigate the unexpected finding tumour formation from diffNT2 cells. The first approach used a reduced cell inoculation number of diffNT2 and undiffNT2 cells. This was used to dilute the tumourigenic potential of the diffNT2 cells. The second approach ruled out contaminating undiffNT2 through using FACS to sort for diffNT2 cells using the SSEA4 differentiation marker. Both parameters had to be investigated concurrently, due to time constrains. It would not have been feasible to run each experiment sequentially, as the experimental run time is too long.

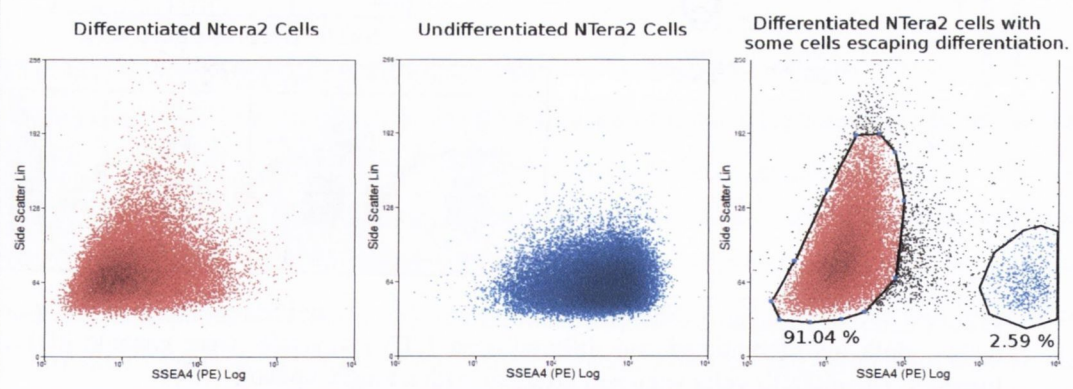

Figure 3.20: UndiffNT2 cells can escape differentiation - Undifferentiated NT2 cells express high levels of SSEA4 (middle panel). The majority of the time NT2 uniformly differentiate in the presence of RA (left panel). On occasion it has been observed that a small sub-population of cells escape differentiation (right panel).

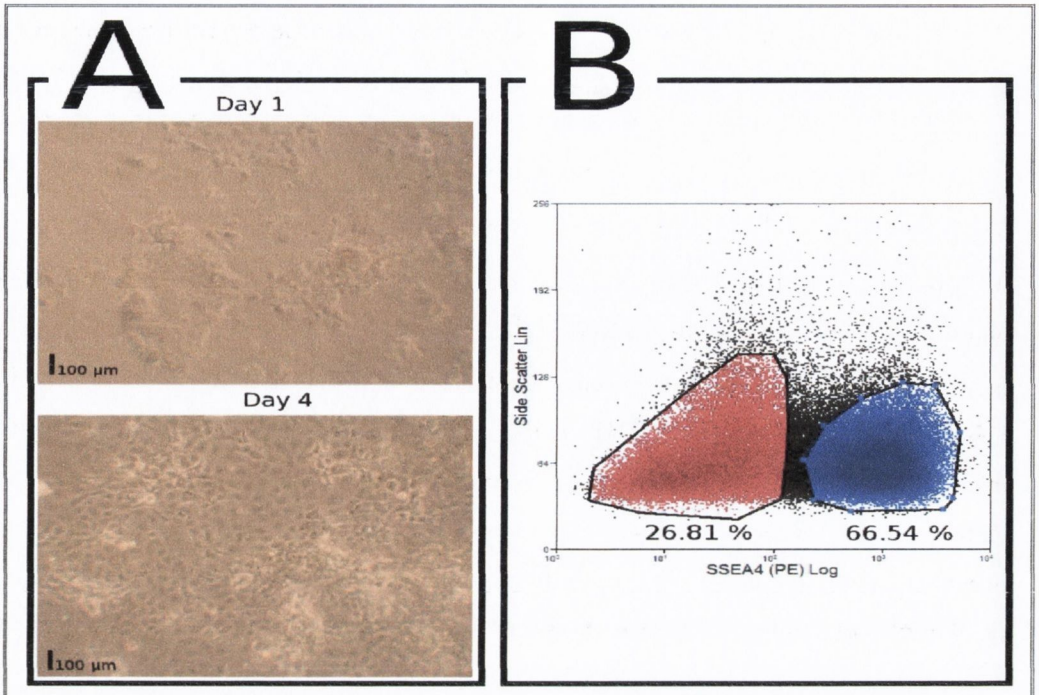

Figure 3.21: The diffNT2 tumour was made up of both diffNT2 and undiffNT2 cells – Xenograft tumour cells were returned to culture and tested for SSEA4 expression. A) Shows tissue culture photographs of the diffNT2 xenograft tumour cells after being returned to culture. B) Shows flow cytometric analysis of SSEA4 expression on the xenograft tumour cells. Blue events represent SSEA4+ undiffNT2 cells while red events represent SSEA4- diffNT2 cells.

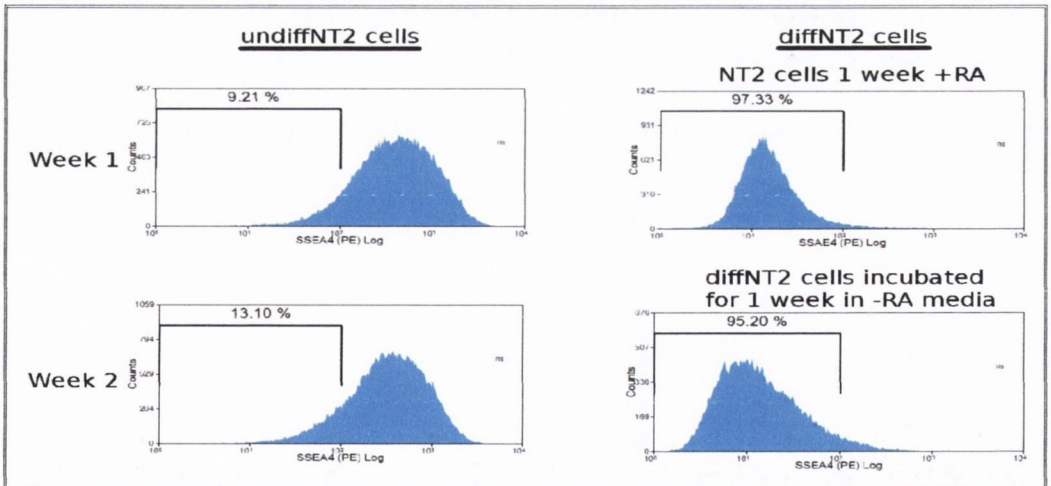

Figure 3.22: diffNT2 cells do not de-differentiate in the absence of RA - These flow cytometry graphs show that the diffNT2 cells do not loose their SSEA4- phenotype when cultured in the absence of RA for 1 week.

A quantitative difference was observed between diffNT2 and undiffNT2 when mice were injected with 5×10^6 cells. It was hypothesised that reducing the cell numbers would lead to a more qualitative difference between diffNT2 and undiffNT2 injected mice. To dilute the tumourigenic potential of the diffNT2 cells, 5×10^4 unsorted diffNT2 cells were injected into 4 mice. No tumour growth was observed within a 58 day period, at which point the mice were euthanised and a post-mortem was carried out. This is a significantly longer latency than the undiffNT2 cells (p-value = 0.02; excluding the undiffNT2 replicate which did not grow). 3 of the 4 mice had no observable sign of tumour growth. Samples of the s.c. region were taken for histological analysis. None of these samples had any signs of cancerous cells (Figure 3.24). 1 of 4 had a small growth which was attached to the peritoneal wall. The tumours produced by the undiffNT2 cells showed moderate invasion into the sub-cutaneous fat (Figure 25A) and exhibited a moderately differentiated histology, as exemplified the gland-like structures (Figure 25B). The size of the tumours produced by undiffNT2 and diffNT2 cells were not found to be significantly different (p-value = 0.07). This was due to the failure of one of the undiffNT2 replicates to form a tumour. When this replicate was excluded, the sizes were significantly different (p-value = 4.54×10^{-5}).

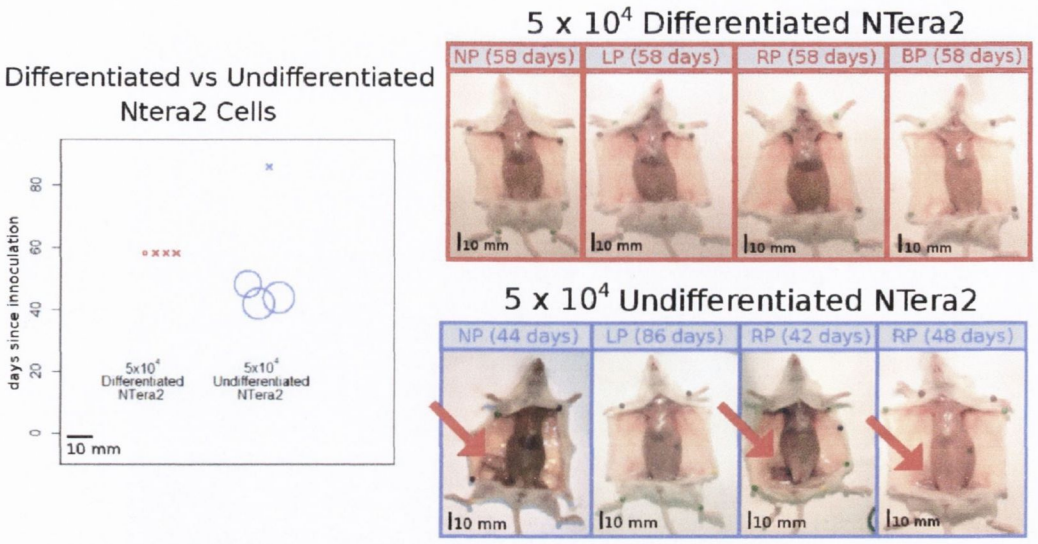

Figure 3.23: Comparison of the tumourgenicity of 5 x 10^4 undifferentiated and differentiated NT2 cells – 3 of 4 mice injected with undiffNT2 cells developed tumours at 42 – 48 days. None of the mice injected with diffNT2 had visual or tactile signs of tumours at 58 days and were euthanised. Post-mortem showed 1 of 4 had a small growth.

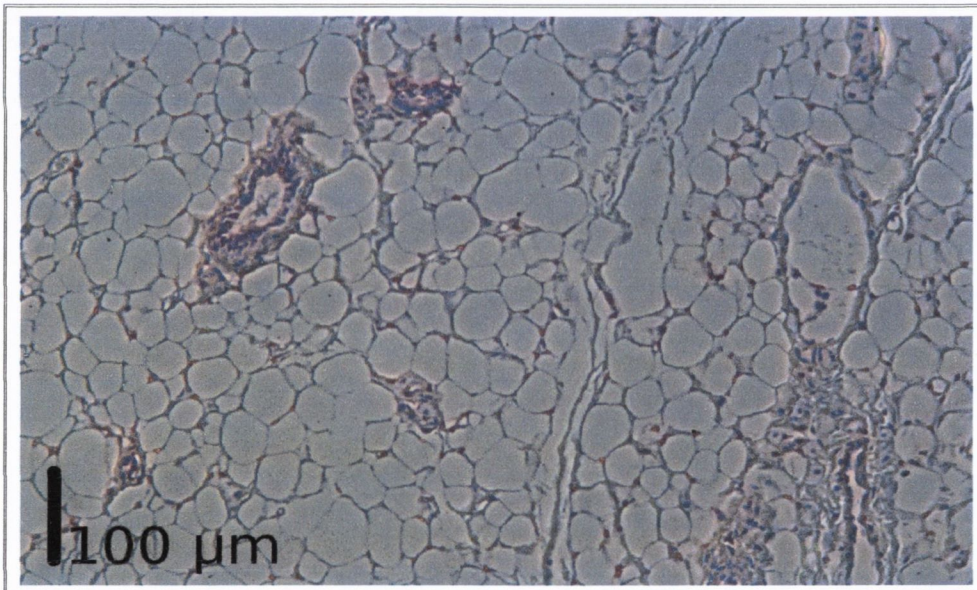

Figure 3.24: There were no sign of atypical cells in the 5 x 10^4 diffNT2 s.c. regions – This figure shows a photograph of the s.c. region of one of the one 5 x 10^4 differentiated NT2 that did not grow a tumour. The structures visible are mammary ducts. There were no atypical (cancerous) cells in this s.c. region.

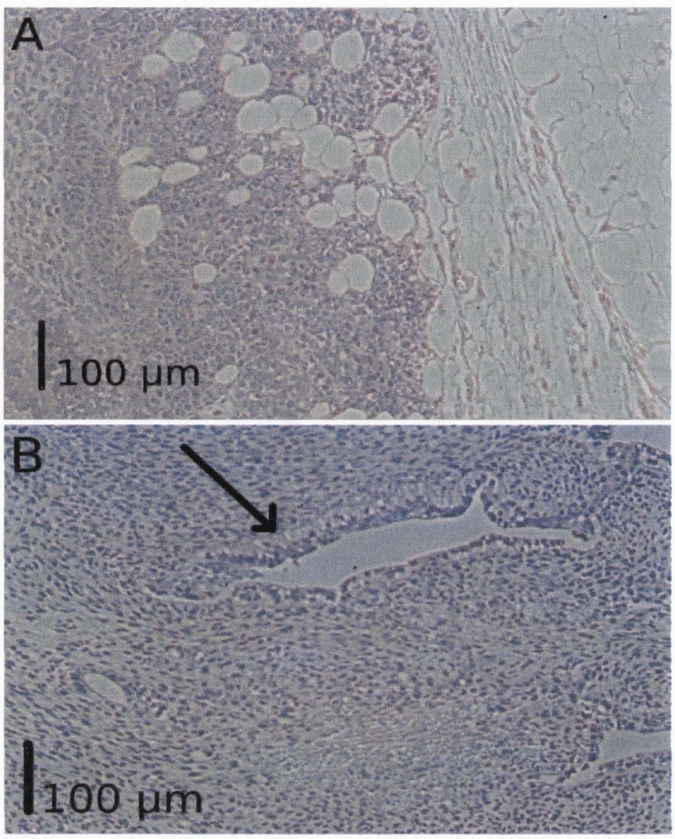

Figure 3.25: Hematoxylin and eosin stained undiffNT2 xenograft tumour – A) shows moderate invasion into the sub-cutaneous fat, with cells growing as sheets. B) shows some of the moderate differentiation seen in the undiffNT2 xenografts. The arrow points to a gland-like structure.

To rule out contaminating undiffNT2 cells within the diffNT2 xenografts. SSEA4-diffNT2 cells were isolated (diffNT2^{SSEA4-}) via FACS after RA induced differentiation and prior to s.c. injection into NOD.SCID mice (Figure 3.26). Both undiffNT2 and diffNT2^{SSEA4-} cells were injected at a range of cell densities from 5 x 10^2 to 5 x 10^4. At all cell densities, the undiffNT2 cells formed tumours (Figure 3.27). None of the diffNT2^{SSEA4-} xenografts at any of the cell densities developed tumours, even when allowed extra time to do so. UndiffNT2 cells did not have high uptake at 5 x 10^2 cells, with only 2 of 4 replicates forming tumours. UndiffNT2 did have high uptake at 5 x 10^3 and 5 x 10^4 cells, with 4of 4 and 3 of 4 replicates forming tumours

respectively. Excluding the diffNT2^{SSEA4-} replicate, which was euthanised early due to a spontaneous lymphoma, the 5 x 10^3 undiffNT2 cells generated tumours more efficiently that the diffNT2^{SSEA4-} cells. They grew in a significantly shorter time frame (p-value = 0.02) and grew to a significantly larger size (p-value= 0.002) within this shorter time frame. In a similar fashion the 5 x 10^4 undiffNT2 cells grew tumours more efficiently than the 5 x 10^4 diffNT2^{SSEA4-} cells. They grew to a significantly larger size (p-value = 0.02; excluding the undiffNT2 replicate which failed to grow) with a significantly shorter time frame (p-value = 0.002; excluding the undiffNT2 replicate which failed to grow).

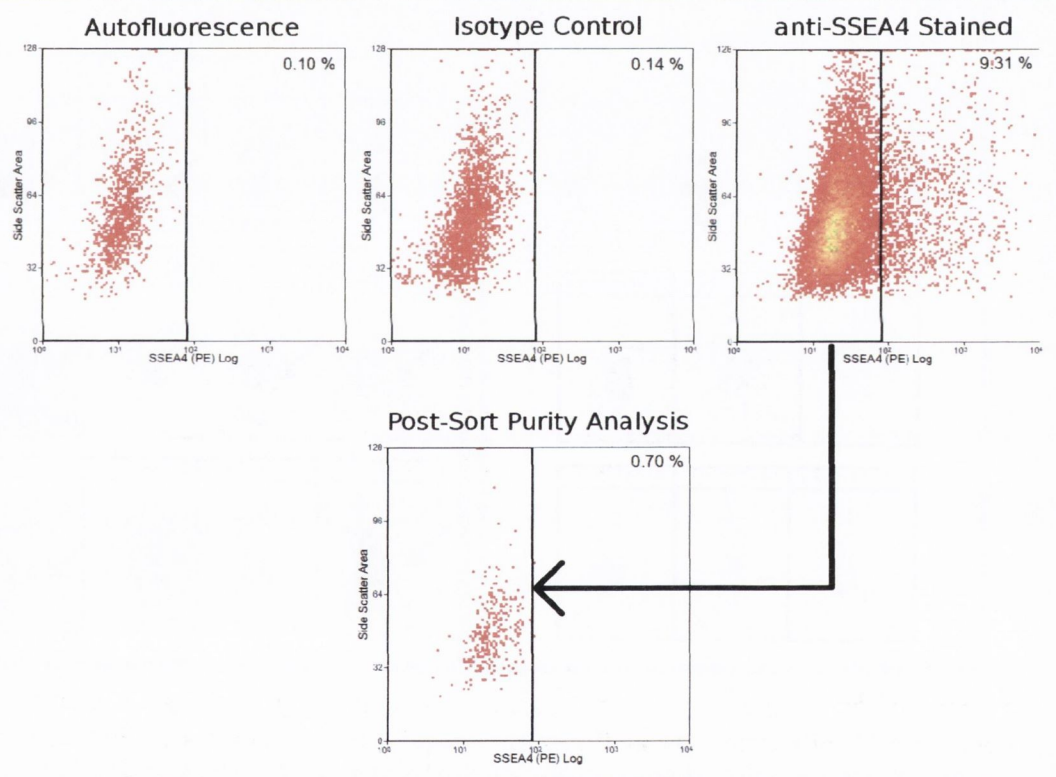

Figure 3.26: SSEA4- cells were purified from diffNT2 cells via FACS – diffNT2^{SSEA4-} cells were isolated from diffNT2 cells prior to injection into mice. DiffNT2^{SSEA4-} cells were purified to 99.30 % pure. Autofluorescence control was used to set the threshold between SSEA4+ and SSEA4- cells. Isotype control was used as an indicator of non-specific staining. The anti-SSEA4 stained sample shows the pre-sorting SSEA4 staining of diffNT2 cells. The Post-Sort Purity Analysis sample shows the post sort purity of the diffNT2^{SSEA4-} cells.

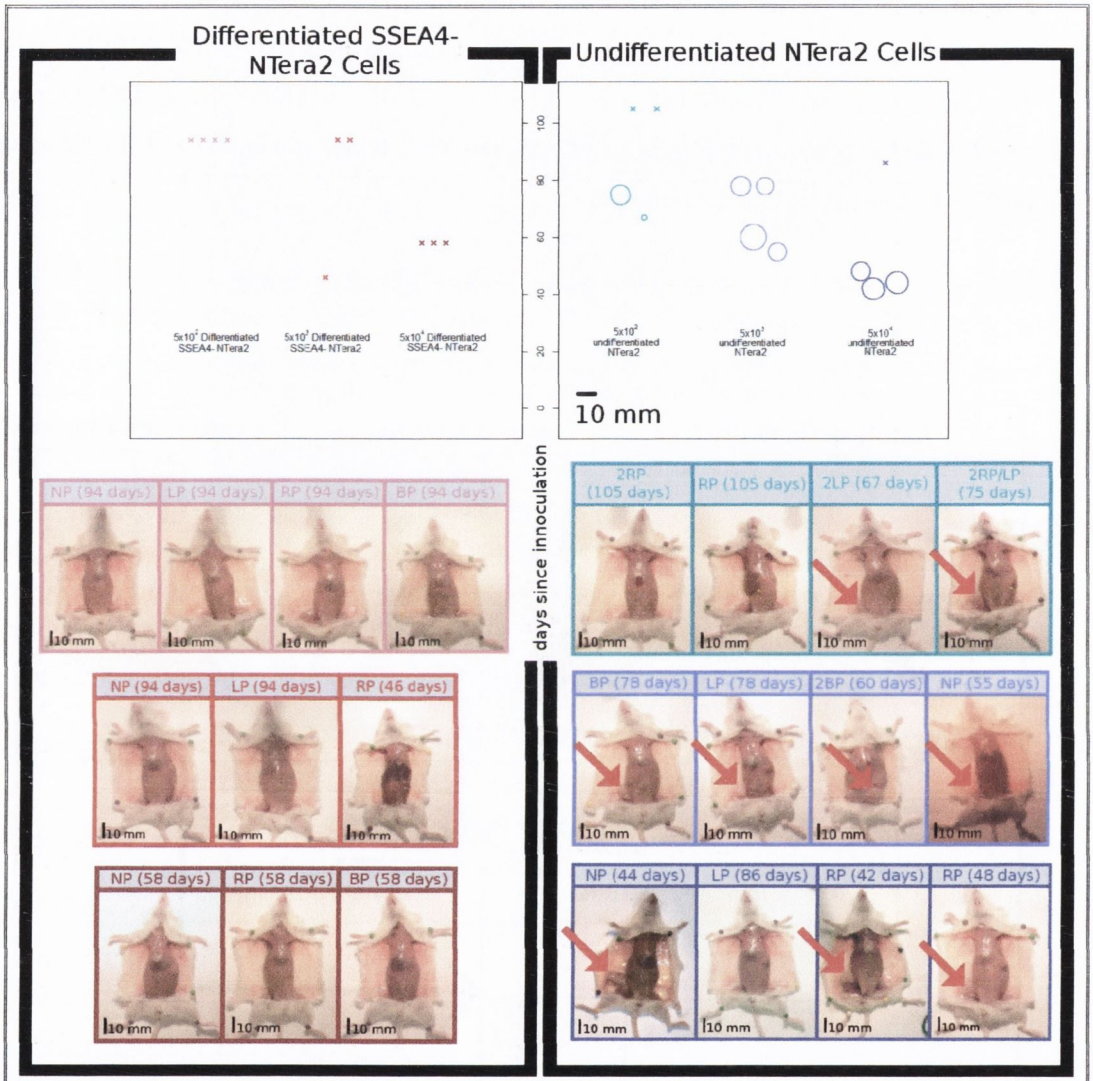

Figure 3.27: Tumourgenicity CSC Validation Assay, Proof of Principle – UndiffNT2 cells were capable of forming xenograft tumours using 5 x 10^2 – 5 x 10^4 cells. Diff$NT2^{SSEA4-}$ cells were not able to generate any tumours across this cell number range, even when given a longer time to do so.

3.3.3 Establishing the SD CSC Validation Assay:

A second tier of validation was established for this project. The SD assay probes a cells potential to self-renew and differentiate. The SD assay only stands up to scrutiny if the isolated samples are 100 % pure. It was decided the most efficient way to ensure that an isolated population was 100 % pure was to plate the cells at 1 cell/well.

3.3.3.1 Approaches to Single Cell plating

Prior to this current work the laboratory had no experience with single cell plating assays. Methods had to be established for the plating of single cells and validating the success of the single cell status. It was also necessary to determine whether a marker positive or marker negative cell had been plated. Three approaches were attempted to achieve this; pre-purified cells plated via serial dilution followed by light microscope validation, FACS followed by high content image analysis and pre-purified cells plated via FACS. The options were limited and determined by the availability of equipment.

3.3.3.1.1 Serial Dilution and Light Microscope

SK-OV-3 cells were dissociated into a cell suspension. The cell concentration was determined using four samples counted on a hemocytometer. This cell suspension was serially diluted using sequential 1:10 dilutions until the concentration was 1 cell/100 µl. 100 µl of this diluted cell suspension was added to every well of a 96 well plate.

The plate was then examined under a light microscope to confirm the single cell status of the wells. A sample of 18 wells were assessed. It was found that 10 of 18 wells had single cells. 8 of 18 wells had no cells. No wells were found to have had more than 1 cell (Figure 3.28).

This plate was allowed to grow for 18 days. The wells were then observed under light microscope again. It was found that of the wells visually confirmed as single cells 3 had developed into colonies. It was observed that of the wells marked as being devoid of cells 4 had colonies growing in them (Figure 3.29). This demonstrated that light microscope verification was not suitable for *en masse* single cell screening. The serial dilution and light microscopy validation was too labour intensive to be used for large scale SD assays.

Comparison of Figures 3.28 and 3.29, highlights the degree of error when using light microscope validation. 66.7 % of wells that were declared empty (red; Figures 3.28 and 3.29), were actually found to have colonies growing in them (green or orange; Figures 3.28 and 3.29). 14.3 % of wells that were declared as containing a single cell (green; Figures 3.28 and 3.29), showed evidence of more than one seeding cell (orange; Figures 3.28 and 3.29).

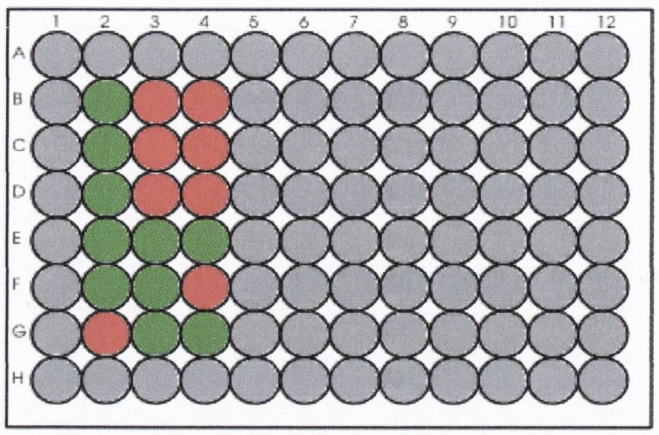

Figure 3.28: Initial analysis of Serial Dilution Single cell plating – Grey wells were not assessed post-plating. Green wells were identified as containing single cells. Red wells were Identified as containing no cells. No wells were identified as containing more than one cell.

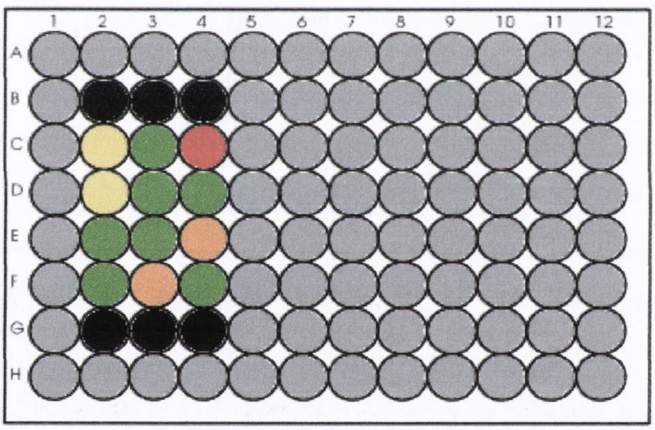

Figure 3.29: Analysis of Serial Dilution Single cell plating 18 days post-plating – Grey wells were not assessed post-plating. Black wells were not assessed as they was a large degree of evaporation from these wells. Green wells were identified as containing colonies which seemed to have a single focal point. Orange wells were identified as containing more than one discrete colonies – suggesting a multiple cells were present post-plating. Red wells were Identified as containing no cells. Yellow wells were found to contain less than 10 cells suggesting that these single cells had failed to divide normally.

3.3.3.1.2 FACS and High Content Analysis

The next approach was to plate single cells using FACS. Verification was attempted using high content image analysis via a GE INcell analyser. Cells were stained with antiCD44-PE/Cy7. 1000 cells/well were plated in the first row of a 96-well plate. Subsequent rows had 1 cell in each well. Cells were allowed to settle to the bottom of the plate for 2 h in a humidified incubator at 37 °C with 5 % CO_2. The plate was then analysed on the INcell analyser. There was a lot of background fluorescence. Cells were detected in the 1000 cells/well replicates however no cells could be observed in the singly plated wells (This data was not recorded as the approach was clearly not successful). This was probably due to the high levels of background fluorescence. There was too much noise in the images to use bright field images to detect the cells. Fluorescence mediated detection was necessary. Further to this the InCELL analyser was not capable of imaging the entire well. The round wells meant that the rectangular fields of view would always miss portions of the well. It was not possible to image fields of view that overlapped the edge of the well – as it interfered with the instruments ability to auto-focus. These limitations ruled out High Content Analysis as a method for assessing the single cell status of wells for the single cell SD assay.

3.3.3.1.3 Pre-purify and FACS

The final approach attempted was to remove the need for visual verification of single cell plating. Instead a statistical approach to verification was used. Cells were purified to greater than 99 % pure, prior to single cell plating. Cells were then plated as single cells via FACS. A statistical model was built to estimate the chance of purity contamination effecting the results of the SD assay.

This model incorporated the two sources of impurity that can lead to errors in single cell plating during cell sorting. The two sources of impurity are false recognition of markers by the cell sorter and false recognition of single cells by the cell sorter.

The following logic was used to model the false recognition of markers. Cells were purified as pCSCs and non-pCSCs prior to single cell plating. The purity of such samples are known. During single cell plating, the sample will be purified further, with the cell sorter recognising and discarding unwanted cells. If a sample of cells has been purified to > 99 % pure, for a given pCSC marker, there is a > 99 % chance that the desired cell type will be plated. This implies that the probability of a colony originating from a cell of a different pCSC marker type is < 0.01.

The following logic was used to model the false recognition of single cells. The cell sorter takes in a sample of cells containing both single cells and doublets. It then discards the doublets, retaining only the single cells. However, error in this process, results in a small amount of doublets being retained also. This is a quantifiable error. The percentage of doublets missed when sorting for single cells was quantified across 9 samples. This produced an estimate of the percentage doublets expected in the singly plated cells. It was found cell suspensions taken in by the cell sorter had 82.70 % +/- 9.83 % single cells. After single cell sorting cell there were 99.07 % +/- 1.07 % single cells in the sorted sample. With a post sort single cell purity of 99.07 % the chance of a colony arising from a doublet or cluster is 0.0093.

pCSCs and non-pCSCs were sorted to approximately 99 % purity, prior to single cell plating. Resulting in a probability of < 0.01 of false recognition of markers affection the single cell plating. Plating a doublet is only a problem if the doublet is a heterogeneous mix of a pCSC and a non-pCSC. Taking the probability of plating of a false positive/negative (< 0.01) and that of plating a doublet (0.0093) into account. The probability of plating a heterogeneous doublet can be calculated as being less than $0.0093(2 \times 0.01)$ which is < 0.000186.

The probability of an error in the single cell plating can there for be calculated as the cumulative probability of plating a false positive/negative and the probability of plating a heterogeneous doublet. This probability is calculated as being less than $0.01 + 0.000186$ which is < 0.010186. This is a probability of approximately 1 in 100.

With this approach of pre-purified cells being single cell plated via FACS, cells can be quickly and efficiently plated as single cells, with an approximately 1 in 100 risk of there being a false positive/negative cell plated.

3.3.3.2 Summary of SD Assay Optimisations

The experiments described in this sub-section (Section 3.3.3), were carried out to optimise the techniques required efficiently plate single cells for the purpose of carrying out the SD assay:

- It was found that FACS based single cell plating, supported by a statistical model was the optimal approach for the high-throughput single cell plating required to conduct the single cell SD assay (Section 3.3.3.1).

3.4 Discussion

There were four techniques needed for the completion of this project:

i) A flow cytometry based pCSC screen.
ii) FACS based isolation of pCSCs.
iii) An in vivo mouse tumourgenicity CSC validation assay.
iv) A SD CSC validation assay.

None of these techniques were established in the laboratory prior to the commencement of this current work. This chapter presented the experiments required to establish these techniques. The introduction (Section 3.1) described each of the techniques and focused on their unique considerations when establishing them in the laboratory. The data section (Section 3.3) presented the data obtained from each optimisation experiment. This discussion will focus on the final standards decided upon for each technique, with respect to the data presented in section 3.3 and the original considerations described in section 3.1. This discussion will follow the same structure as the introduction and the data sections.

3.4.1 Positive and negative controls were central to the establishment of flow cytometry based identification and isolation of pCSCs.

A series of experiments were carried out to establish and optimise the flow cytometry based identification and isolation of pCSCs from ovarian cancer sources. Three flow cytometry assays were implemented and optimised: ALDH assay, HSP assay and CSP assay. This involved standardisation of technical controls (See Appendix A), the establishment of positively and negatively staining controls for each assay, as well staining optimisations for all assays. The data produced by these experiments informed decisions made in the establishment of the pCSC screen. As a result of these optimisations there is now a flow cytometry based pCSC screen established in the laboratory. A similar screening system could be used to screen for CSC in any malignancy through adaptation of the pCSC markers utilised. It can also be applied directly to the screening of patient samples once a protocol for the generation of a single cell suspension from tumour samples has been established in the lab.

At a basic level the experiments demonstrated that flow cytometry was fit for purpose, with regard to screening for pCSCs. The hardware was suitable and the protocols were robust, demonstrating that a flow cytometry approach was capable of identifying pCSCs via fluorescent pCSC markers.

3.4.1.1 The scaling of the ALDH assay staining reaction and the inclusion of an additional gating control enables the use of the ALDH assay in the identification and isolation of pCSC regardless of the ALDH+ population size.

Deng et al (2010) showed that high ALDH1 expression is significantly associated with poor clinical outcome in ovarian cancer (n = 439, p = 0.0036). Due to the small size of ALDH+ sub-populations in some of the ovarian model systems it was necessary to scale the staining reactions. Experiments needed to be carried out to determine the effects of scaling the staining reaction. It was noted that staining at a 5x cell concentration did not effect the ability to detect ALDH+ cells from the parent population. This meant that cells could be stained using one fifth of the reagents which was useful when staining the approximately 1 x 10^8 cells required for cell sorting of the >0.5 % ALDH+ sub-populations identified within the A2780 and A2780cis cell lines. Using flow cytometry, Silva et al (2011) found that ovarian cancer patient samples had ALDH+ fractions as small as 0.25 %. Furthermore, using immunohistochenistry, Deng et al showed that over ¼ of ovarian cancers examined (n = 65) had ALDH+ sub-populations of less than 5 %. Many publications stain at 1 x 10^6 cells/ml when carrying out the ALDH assay. The experiments described in Section 3.3.1.2.1 allow for staining at 5 x 10^6 cells/ml allowing for more efficient identification and isolation of small populations of the clinically relevant ALDH CSC marker. These improvements allow isolation of small ALDH+ CSC sub-populations at reasonable economic cost.

As the ALDH+ sub-population was enriched it was observed that the internal DEAB negative control was not sufficiently able to inhibit the production of the fluorescent signal. This created a problem when establishing a positive/negative threshold in ALDH+ enriched samples. Experiments to optimise the inhibition of the enriched ALDH+ cells showed that it was not appropriate to increase the amount of DEAB used in the reaction. Increasing the volume/concentration of DEAB used resulted in increased cell death (from 9.7 % to 98.58 %; Figure 3.4). This was probably due to the DEAB vehicle which was 95 % ethanol. Experiments showed that using a mixed population of ALDH+ and ALDH- cells was a good method of determining where to set the ALDH+/- threshold in high purity ALDH+ samples. As shown in Figure 3.6, the DEAB control based gating the ALDH assay can under estimate the percentage of ALDH+ cells in a highly enriched ALDH+ population. This sort of limitation may account for some of the differences seen between Deng et al. and Silva et al.. Deng et al, via immunohistochemistry, found that greater than ¼ of ovarian cancer (n = 65) patients had ALDH+ sub-populations greater than 75 %, whereas, Silva et al, via flow cytometry, did not detect any ALDH+ sub-populations greater than 8 % in ovarian cancer patients (n = 13). Now

that these scaling optimisations have been established it is possible to accurately identify, measure and isolate ALDH+ sub-populations of all sizes.

These ALDH optimisations also informed the approach to the isolation of the small ALDH+ sub-populations identified within the A2780 and A2780cis models within this project (Section 4.0). It was decided that for the first enrichment step, model systems with a <1 % ALDH+ population would be stained at 5×10^6 cells/ml rather than 1×10^6 cells/ml. This first enrichment produced ALDH+ populations of >40 %. It was more economical to stain at 1×10^6 cells/ml with these enriched populations as less cells were required for sorting to get >99 % pure populations.

3.4.1.2 HSP Assay

The HSP assay is the most technically challenging of all flow cytometry based pCSC screens. As such, it is relatively under represented in the ovarian CSC literature compared to other CSC identification and isolation techniques.

In addition to experimental data generated in this project (Figure 3.9), other groups have reported reduced HSP resolution when using violet lasers or alternate non-UV excitable DNA dyes (Golebiewska et al. 2011). Experiments were carried out to define the relationship between these two profiles.

It was found that the cells identified and purified as SP cells by the MoFlo™ were also identified as SP cells by the on the CyAn™ (Figure 3.10). Similarly, it was found that the cells identified and sorted as non-SP cells by the MoFlo™ were also identified as non-SP cells by the on the CyAn™ (Figure 3.10). This demonstrated that cells identified as being SP and non-SP during the screening phase on the CyAn™ could be faithfully purified on the MoFlo™ during the isolation phase. While both the 405 nm and 351 nm excitation sources are capable of being used for the HSP assay, these experiments showed that the 351 nm excitation does produce a HSP profile with better resolution (Figures 3.9 and 3.10).

3.4.1.3 Positive and Negative Controls Established:

Experiments were carried out to identify positively and negatively staining controls for each of the pCSC screening assays (ALDH, HSP and CSP assays) used in this project. It was important to establish positive and negative controls as this was a newly established screen. Such controls proved that each screening assay was capable of identifying pCSCs.

Positive and negative controls were identified for all pCSC screening assays, including every antibody used in the CSP assay. Positive controls indicate that the assay is capable of identifying pCSCs. Negative controls allow for the quantification of false positives produced by a given assay.

3.4.2 UndiffNT2 and diffNT2^{SSEA4-} cells demonstrate that the *in vivo* tumourgenicity assay established in this project is fit for the purpose of CSC validation.

A series of experiments were carried out to establish and optimise the *in vivo* mouse tumourgenicity assay. This involved examining several vehicles in which cells could be injected (Appendix A) as well as the establishment of a proof of principle experiment. As a result of these optimisations there is now an *in vivo* mouse tumourgenicity assay established in the laboratory. This system could be used to validate CSCs isolated from any malignancy.

The study of vehicles was carried out to apply to future work and will be discussed in Appendix A. Media supplemented with matrigel was used for the validations within this project, as there was not enough time to wait for the outcomes of the vehicle optimisations prior to starting the validations. The Ham's F12/Matrigel vehicle was selected as it was shown to be sufficient for the growth of undiffNT2 cells in a high impact journal (Watanabe et al. 2010). They showed that 1000 undiffNT2 cells injected into nude mice with a Ham's F12/Matrigel formed tumours with a mean latency of ~40 days. Perhaps this particular vehicle was better suited to support the growth of undiffNT2 cells than 2012ep cells in the xenograft environment.

The undiffNT2 and diffNT2 cells used in the proof of principle experiment showed that CSCs are able to efficiently form tumours from low cell numbers. However, their differentiated counterparts were not, even at logarithmically undiffNT2higher cell numbers. This series of experiments demonstrates that the *in vivo* mouse tumourgenicity assay established for this project is able to discriminate between CSCs and their differentiated counterparts.

For the purpose of of investigating distant metastases, the lungs, liver and spleen were harvested from mice that developed s.c. tumours. The first round of pathology results indicated that none of the tumours, had led to distant metastasis in any of these organs (Appendix A). It was decided that the workload involved in harvesting the lungs, liver and spleen was not producing a sufficient amount of data to make it justifiable. It was decided, that for the actual validation experiments, specimen collection would be limited to the tumour itself or in the

absence of tumour growth the s.c. region where the cells were injected. Only on the suspicion of metastases or for the purpose of example cases would the other organs be harvested.

It takes 3 – 4 weeks to obtain the permit required to import the mice required to conduct the mouse tumourgenicity assay. In addition to this, the experiments run for approximately 4 weeks or more prior to tumour formation and harvesting. The mouse tumourgenicity assay, relies on previous work being carried out to identify the pCSCs which require validation. Due to this long experimental run time and the reliance on previous work, the mouse tumourgenicity assay can only be run a finite number of times and cannot be started on day one.

3.4.3 SD Assay is not only a Validation Assay but has the power to identify further sub-populations within purified samples:

Without single cell studies the self-renewal and differentiation potential of a given cell type cannot be accurately assessed. For example with respect to prostate cancer, (Yu et al. 2011) could not declare an ALDH+/CD44+ sub-population as CSCs because the ALDH-/CD44- sub-population could also produce ALDH+ and CD44+ during xenograft tumour formation. As will be presented in Section 7.0, single cell studies revealed a sub-set of ALDH- cells within our ovarian cancer models demonstrated a stem like potency while the rest of the ALDH- cells did not. If Yu et al. had established similar studies they may have identified further stem-like sub-populations within their pCSC marker negative fraction. Additionally, slight impurities (ALDH+/CD44+ cells) in the ALDH-/CD44- sub-population injected into mice may have contributed to the ALDH+ and CD44+ phenotypes seen upon re-analysis of the xenograft tumour.

A series of experiments were carried out to establish and optimise the SD assay. This involved developing a method to achieve single cell plating and a method of validating the purity/single cell status of the plated cells. As a result of these optimisations there is now a SD assay established in the laboratory. A similar system could be used to validate CSCs isolated from any malignancy.

Three approaches were investigated. Two were found to be unsuitable for a high throughput as SD assay. One approach was found to be suitable and was developed to validate isolated pCSC as CSCs in conjunction with the mouse tumourgenicity assay.

First it was attempted to use serial dilution to put a single cell in every well of a 96-well plate. Light microscopy was then used to assess the single well status of each well. It was found that

this approach to single cell plating was very slow at not very efficient at getting a single cell in every well. Further to this the light microscope validation was very slow. Once colonies started to grow it was noted that the light microscope validation was not very good at validating the presence or absence of single cells. This approach was dropped as it lacked the expediency and accuracy required to develop a high throughput assay. The experiment had highlighted the effect that evaporation had on long term (2.5 – 3.5 weeks) culture in 96 well plates. It was found that the rate of evaporation from the external wells was increasing the amount of maintenance required to culture the clones. To reduce the workload per plate it was decided to only plate cells in the inner wells and fill the external wells with PBS to buffer the colonies from the effects of evaporation.

The second approach was to used the CyClone™ accessory to the MoFlo™ to put a single cell in the 60 inner wells of a 96-well plate. The InCELL analyser was used to validate the single cell status and the cell marker status of the plated cells. It was found that the cell-sorter was able to expediently plate cells into 96-well plates. However, the background to signal ratio prevented the InCELL analyser from being able to detect the fluorescence signal of a single cell in a well. Furthermore, the InCELL analyser was not able to image 100 % of the circular wells, as it had a rectangular field of view. Overlapping the field of view with the edge of the well interfered with its ability to autofocus on the base of the well.

The third approach examined used the CyClone™ accessory on the MoFlo™ to put a single cell in the 60 inner wells of a 96-well plate. It took a statistical approach validating the single cell status of each well. This approach proved to be an expedient and accurate method to plating single cells. This approach was developed to validate isolated pCSC as CSCs in conjunction with the mouse tumourgenicity assay.

The SD assay takes 2.5 – 3.5 weeks to culture the colonies from a single cell to a point where enough cells are present to retest for the pCSC marker in question. After this it take approximately 1 week to synchronise and retest the cultures for the pCSC marker in question. The SD assay, relies on previous work being carried out to identify the pCSCs which require validation. Due to this long experimental run time and the reliance on previous work, the SD assay can only be run a finite number of times and cannot be started on day one.

3.4.4 Summary

Four assays were established to empower the identification, isolation, validation and characterisation of cancer stem cells. Many optimisations were required to establish and optimise each of these assays. The assays established can be applied to the identification, isolation and validation of CSC form any malignancy. The assays can also be used to study stem cells in normal tissues. This has major benefits when trying to identify therapeutically target-able pathways in CSCs. This techniques are also applicable to the study of stem cells for the purposes of regenerative medicine or understanding organogenesis.

Optimisations:- Primary Findings

Four new CSC techniques were established and optimised in the laboratory. Prior to this current work none of these techniques were being utilised in the laboratory.

i) Flow Cytometry pCSC screen established and optimised.
   - Positive and negative staining controls for each marker identified.

ii) FACS based pCSC/non-pCSC isolation established and optimised.

iii) Tumourgenicity CSC validation assay established and optimised.
   - Assay can distinguish between CSCs and differentiated (non-CSCs) cells.
   - PBS does not support CSC tumour growth
   - Assay is sensitive to tiny impurities of CSC within a non-CSC population.
   - Assay is not sensitive to moderate variations in s.c. Injection efficiency.

iv) Single cell SD CSC validation assay established and optimised.

3.5 References

Andrews. 1984. "Retinoic Acid Induces Neuronal Differentiation of a Cloned Human Embryonal Carcinoma Cell Line in Vitro." *Developmental Biology* 103 (2) (June): 285–293. doi:10.1016/0012-1606(84)90316-6.

Andrews, P W, I Damjanov, D Simon, G S Banting, C Carlin, N C Dracopoli, and J Føgh. 1984. "Pluripotent Embryonal Carcinoma Clones Derived from the Human Teratocarcinoma Cell Line Tera-2. Differentiation in Vivo and in Vitro." *Laboratory Investigation; a Journal of Technical Methods and Pathology* 50 (2) (February): 147–162.

Andrews, P W, P N Goodfellow, L H Shevinsky, D L Bronson, and B B Knowles. 1982. "Cell-surface Antigens of a Clonal Human Embryonal Carcinoma Cell Line: Morphological and Antigenic Differentiation in Culture." *International Journal of Cancer. Journal International Du Cancer* 29 (5) (May 15): 523–531.

Charafe-Jauffret, E., C. Ginestier, F. Iovino, J. Wicinski, N. Cervera, P. Finetti, M.H. Hur, et al. 2009. "Breast Cancer Cell Lines Contain Functional Cancer Stem Cells with Metastatic Capacity and a Distinct Molecular Signature." *Cancer Research* 69 (4): 1302.

Curley, M.D., V.A. Therrien, C.L. Cummings, P.A. Sergent, C.R. Koulouris, A.M. Friel, D.J. Roberts, et al. 2009. "CD133 Expression Defines a Tumor Initiating Cell Population in Primary Human Ovarian Cancer." *Stem Cells* 27 (12): 2875–2883.

Deng, S., X. Yang, H. Lassus, S. Liang, S. Kaur, Q. Ye, C. Li, et al. 2010. "Distinct Expression Levels and Patterns of Stem Cell Marker, Aldehyde Dehydrogenase Isoform 1 (ALDH1), in Human Epithelial Cancers." *PLoS One* 5 (4): e10277.

Dieter, Sebastian M., Claudia R. Ball, Christopher M. Hoffmann, Ali Nowrouzi, Friederike Herbst, Oksana Zavidij, Ulrich Abel, et al. 2011. "Distinct Types of Tumor-Initiating Cells Form Human Colon Cancer Tumors and Metastases." *Cell Stem Cell* 9 (4) (October 4): 357–365. doi:10.1016/j.stem.2011.08.010.

Dittfeld, Claudia, Antje Dietrich, Susann Peickert, Sandra Hering, Michael Baumann, Marian Grade, Thomas Ried, and Leoni A Kunz-Schughart. 2009. "CD133 Expression Is Not Selective for Tumor-initiating or Radioresistant Cell Populations in the CRC Cell Lines HCT-116." *Radiotherapy and Oncology: Journal of the European Society for Therapeutic Radiology and Oncology* 92 (3) (September): 353–361. doi:10.1016/j.radonc.2009.06.034.

Draper, Jonathan S, Christine Pigott, James A Thomson, and Peter W Andrews. 2002. "Surface Antigens of Human Embryonic Stem Cells: Changes Upon Differentiation in Culture." *Journal of Anatomy* 200 (3) (March): 249–258. doi:10.1046/j.1469-7580.2002.00030.x.

Golebiewska, A., N. H. C. Brons, R. Bjerkvig, and S. P. Niclou. 2011. "Critical Appraisal of the Side Population Assay in Stem Cell and Cancer Stem Cell Research." *Cell Stem Cell* 8 (2): 136–147.

Hirschmann-Jax, C., A. E. Foster, G. G. Wulf, J. G. Nuchtern, T. W. Jax, U. Gobel, M. A. Goodell, and M. K. Brenner. 2004. "A Distinct 'side Population' of Cells with High Drug Efflux Capacity in Human Tumor Cells." *Proceedings of the National Academy of Sciences of the United States of America* 101 (39): 14228.

Pang, Roberta, Wai Lun Law, Andrew C.Y. Chu, Jensen T. Poon, Colin S.C. Lam, Ariel K.M. Chow, Lui Ng, et al. 2010. "A Subpopulation of CD26+ Cancer Stem Cells with Metastatic Capacity in Human Colorectal Cancer." *Cell Stem Cell* 6 (6) (June 4): 603–615. doi:10.1016/j.stem.2010.04.001.

Qin, Jichao, Xin Liu, Brian Laffin, Xin Chen, Grace Choy, Collene R. Jeter, Tammy Calhoun-Davis, et al. 2012. "The PSA−/lo Prostate Cancer Cell Population Harbors Self-Renewing Long-Term Tumor-Propagating Cells That Resist Castration." *Cell Stem Cell* 10 (5) (May 4): 556–569. doi:10.1016/j.stem.2012.03.009.

Vukicevic, S, H K Kleinman, F P Luyten, A B Roberts, N S Roche, and A H Reddi. 1992. "Identification of Multiple Active Growth Factors in Basement Membrane Matrigel Suggests Caution in Interpretation of Cellular Activity Related to Extracellular Matrix Components." *Experimental Cell Research* 202 (1) (September): 1–8.

Watanabe, Kazuhide, Matthew J. Meyer, Luigi Strizzi, Joseph M. Lee, Monica Gonzales, Caterina Bianco, Tadahiro Nagaoka, et al. 2010. "Cripto-1 Is a Cell Surface Marker for a Tumorigenic, Undifferentiated Subpopulation in Human Embryonal Carcinoma Cells." *STEM CELLS* 28 (August): 1303–1314. doi:10.1002/stem.463.

Yang, Z-Y Lee, C-C Wu, T-C Chen, C-L Chang, and C-P Chen. 2007. "CXCR4 Expression Is Associated with Pelvic Lymph Node Metastasis in Cervical Adenocarcinoma." *International Journal of*

Gynecological Cancer: Official Journal of the International Gynecological Cancer Society 17 (3) (June): 676–686. doi:10.1111/j.1525-1438.2007.00841.x.

Yu, Chunyan, Zhi Yao, Jinlu Dai, Honglai Zhang, June Escara-Wilke, Xiaohua Zhang, and Evan T Keller. 2011. "ALDH Activity Indicates Increased Tumorigenic Cells, but Not Cancer Stem Cells, in Prostate Cancer Cell Lines." *In Vivo (Athens, Greece)* 25 (1) (February): 69–76.

Zhang, S., C. Balch, M.W. Chan, H.C. Lai, D. Matei, J.M. Schilder, P.S. Yan, T.H.M. Huang, and K.P. Nephew. 2008. "Identification and Characterization of Ovarian Cancer-initiating Cells from Primary Human Tumors." *Cancer Research* 68 (11): 4311.

Zheng, Wenxin, and Oluwole Fadare. 2012. "Fallopian Tube as Main Source for Ovarian and Pelvic (non-endometrial) Serous Carcinomas." *International Journal of Clinical and Experimental Pathology* 5 (3): 182.

Identification of Putative Cancer Stem Cells.

Section 4.0 – Identification of pCSCs

4.1 Introduction:

4.1.1 The Difference between Screening and Selection

The literature reports a variety of approaches for the identification and isolation of CSCs. These approaches can be classified into two categories, screening approaches and selection approaches. Screening uses protein markers or functions to identify pCSCs from a heterogeneous population of cells (Baba et al. 2008; Deng et al. 2010; Silva et al. 2011). Selection uses tissue culture techniques to exert selective pressures which enrich for CSCs. Such conditions include spheroid culture (Zhang et al. 2008) and holoclone culture (Tan et al. 2011).

As discussed in Section 1.11, selection based approaches limit the downstream analysis of CSCs: either through the lack of a comparable non-CSC sub-population or through possible phenotypic alterations due to the selective conditions used. These limitations reduce the power to identify therapeutically targetable pathways upon characterisation. A screening approach does not use selective pressures. It allows for the isolation of pCSCs and non-pCSCs. This enables direct comparison of pCSCs to non-pCSCs in the downstream analysis. All populations brought forward for downstream characterisation have been subjected to the same screening conditions allowing any screening affects on their molecular signatures to be normalised out. Screening is a faster technique than selection based techniques, for identifying CSCs. For these reasons screening approaches were adopted over selection approaches for the identification and isolation of pCSCs in this project.

4.1.2 pCSC Markers

pCSC markers are proteins that have been identified as having differential expression between CSCs and non-CSCs. This does not imply that a pCSC marker is necessary or sufficient to maintain the stem-like state in the CSC. It is based solely on a correlation between the protein expression and the differentiation status.

pCSC markers can be classified into categories, functional and non-functional. Functional pCSC markers are based on the metabolic-behaviour of CSC under certain staining conditions compared to non-CSC. Non-functional pCSC markers are based on the expression of antigens, with no functional interaction with the staining conditions. A given non-functional pCSC antigen is either present or absent on the pCSCs, allowing pCSCs to be detected via a fluorochrome conjugated antibody.

Section 4.0 – Identification of pCSCs

The consensus hypothesis (Vasiliou and Nebert 2005; Gottesman 2002) is that the proteins involved with the functional markers convey protection to long lived somatic stem cells (SSCs) against environmental insults. The ALDEFLUOR™ (ALDH) and Hoechst Side Population (HSP) Screens are both categorised as functional pCSC markers. While all the antigens screened in the CSP Screen (CD44, CD117, CD133 and CXCR4) are categorised as non-functional pCSC markers.

4.1.3 The pCSC marker panel

The pCSC markers selected for the pCSC screen in this project were discussed in Sections 1.9. With the exception of CXCR4 each of these markers have been used to isolate CSCs form Ovarian Cancers as well as other malignancies (ALDH: Silva et al. 2011; HSP: Szotek et al. 2006; CD44 Zhang et al. 2008; CD117 Zhang et al. 2008 CD133: Curley et al. 2009). CXCR4 has been used to discriminate between metastatic and non-metastatic CSCs (Hermann et al. 2007). Few of these publications place emphasis on investigating the overlap between all of the ovarian pCSC markers identified to date. In this project five pCSC markers and one marker of metastasis were used to screen each model system (Section 4.3). This approach allows statements to be made about the prevalence of the various pCSC markers and provides the opportunity to investigate overlaps of the various markers.

4.1.4 The Model Systems Screened

The model systems selected for the pCSC screen in this project were discussed in Sections 1.8. A diverse range of models were selected to allow for several comparisons to be made;

i) Chemosensitive versus Chemoresistant pCSCs – This question had not yet been addressed in Ovarian Cancer prior to the commencement of this project. A paper has subsequently been published by another group which directly supports some of the results presented in this chapter (Deng et al. 2010; Sections 4.0).

ii) Primary tumour versus Ascites (metastatic) pCSCs – This question has not yet been addressed in Ovarian Cancer. Some data has been produced through the diversity of patient sample sources used in studies (Alvero et al. 2009; Silva et al. 2011), however, there have been no definitive findings regarding similarities or differences between primary and metastatic pCSCs.

iii) Normal tissue versus Cancerous tissue putative stem cells – This question has not yet been addressed in Ovarian Cancer. Szotek et al. (2008) isolated pSSCs from the Ovarian

Surface Epithelium based on quiescence. However, they did not investigate the link to pCSC markers, with the exception of CD117, showing that the pSSCs were CD117-. Another group has started work isolating pSSCs from fallopian tube epithelium, as presented at the American Association for Cancer Research Annual Meeting 2012 (Kessler et al. 2012). However, no paper has yet been published on the subject.

All of the screening, isolation and validation techniques had to be established and optimised in our laboratory during this project. It was decided that cell lines should be used rather than patient samples. Several groups have demonstrated that CSCs can be isolated from cell lines (Patrawala et al. 2005; Pfeiffer and Schalken 2010; Silva et al. 2011). Although only cell lines were used in this project, these techniques were designed to ultimately allow screening, isolation and validation of CSCs from patient samples.

4.1.5 The Approach to Screening

Flow cytometry allows for the simultaneous detection of multiple fluorochromes. As such it provides a well proven method of defining co-expression of multiple proteins on a cell. Multi-parametric flow cytometry can be used to elucidate the overlaps between all the Ovarian Cancer pCSCs identified in the literature.

Multi-parametric flow cytometry requires more controls than single parametric flow cytometry. It is logistically more challenging. It was decided to screen the each model system for a single marker at a time. Any model systems which stained positive for more than one marker could then be brought forward for multi-parametric screening.

As described in the Data section (Section 4.3) there was poor overlap of the various pCSC markers across the model systems. As such, less emphasis was put on investigating overlaps between CSCs and more emphasis is put on investigating the different pCSC sub-populations identified by different pCSC markers across the model systems.

4.1.6 Ranking pCSCs

A large number of model systems and pCSC markers were utilised in this study. It was clear from the onset that it would not be possible to investigate every pCSC population identified. It was decided that a system would be developed to rank the pCSCs identified. The high ranking pCSC populations would be brought forward for isolation, validation and characterisation.

Section 4.0 – Identification of pCSCs

There were two ways to proceed once the pCSC populations were ranked;

i) The most interesting model system could be selected and all of its high and low ranking pCSC populations could be brought forward for further investigation.

ii) The highest ranking pCSC populations from each model system could be brought forward for further investigation.

The first approach has the power to map potential stem cell hierarchies. It has the potential to discriminate between CSCs, progenitors and differentiated cells. This could help identify which cells have true malignant potential. Such cells need to be targeted if we are to develop therapies which are not susceptible to relapse.

The second approach has the power to define the differences between chemosensitive CSCs and chemoresistant CSCs. It can describe the differences between ascites CSCs and solid tumour pCSCs. It can describe the differences between normal and cancerous stem cells.

Both approaches have strong scientific merit. It was decided to adopt the second approach. As discussed in Section 1.5, Ovarian Cancer is characterised by initial chemo-responsiveness and subsequent chemoresistant relapse and mortality. It was decided that the second approach had the greater potential for understanding the cause of chemoresistant relapse – the major cause of Ovarian Cancer mortality.

For the same reasons as discussed in Section 3.3.3, Welch's t-test with a significance cut-off of p-value < 0.05 was used to define significant/non-significant differences between sub-population sizes.

4.1.7 Aims

There were five aims driving the experiments presented in this chapter;

i) To screen six models of Ovarian Cancer and one model of Normal Ovarian Surface Epithelium for the presence of five pCSC markers and one metastatic cell marker.

ii) To identify any trends in marker expression between the different models of Ovarian Cancer.

iii) To identify overlaps between the various markers screened.

iv) To identify pCSC and corresponding somatic stem cell (SSC) sub-populations within these model systems.

v) To rank the pCSC sub-populations identified so that the highest ranking pCSC can be brought forward for downstream analysis.

4.1.8 Hypotheses

There were four hypotheses, which form the basis of the experiments, in this chapter;

i) The flow cytometry based pCSC screen would be able to identify pCSC/pSSC sub-populations within each model system based on a panel of protein markers.

- pCSCs identified within malignant models, should have non-malignant counterparts in the non-malignant model.

- Different pCSC signatures may correlate with the different models. For example cisplatin sensitive models and cisplatin resistant models may have different pCSC signatures.

ii) Identification of overlaps and hierarchies of pCSCs and pSSCs could lead to an understanding of stemness hierarchies and differentiation in Ovarian surface epithelium and Ovarian Cancer.

- This in turn could further the understanding of Ovarian tumourigenesis and post-therapy relapse.

iii) Fluorescence-Activated Cell Sorting (FACS) can be used to isolate these pCSC sub-populations to a high degree of purity.

iv) The study of pure pCSC and non-pCSC sub-populations will provide cues as to how they can be therapeutically targeted.

- Comparing and contrasting pCSCs form chemosensitive and chemoresistant pairs of parent and daughter models will elucidate the role of CSCs in the acquired chemoresistance of Ovarian Cancer.

4.2 Materials and Methods:

4.2.1 Cell Culture and Sub-Culture

The A2780, A2780cis, IGROV-1, IGROV-1-CDDP, SK-OV-3, 59M and HIO-80 cell lines were used to perform the screening experiments in this chapter. All cell lines were cultured and sub-cultured as described in Section 2.2.

4.2.2 Flow Cytometry

4.2.2.1 ALDH Assay

The ALDH assay was carried out as described in Section 2.5.1

4.2.2.2 HSP Assay

The HSP assay was carried out as described in Section 2.5.2.

4.2.2.3 CSP Assay

The CSP assay was carried out as described in Section 2.5.3.

4.2.2.4 Multi-parametric staining

Multi-parametric staining is the concurrent stain of cells with two pCSC markers.

4.2.2.4.1 Multi-marker CSP Assay Staining

Multi-marker CSP assay staining was carried out in a similar fashion to single-marker staining (described in Section 2.5.3). The only difference was that more than one antibody was included during the staining step. 1 x 10^6 cells were suspended in 80 µl PBS. 10 µl of each antibody was added to this cell suspension and cells were incubated at 4 °C for 30 min.

Extra controls were included to accurately interpret the results. In total multi-marker CSP staining has four types of controls.

i) Auto-fluorescence Control:- Consisting of an unstained sample of cells, to identify the threshold for background staining

ii) Isotype Control:- Consisting of cells stained with isotype control Antibodies for all of the antibodies used in the multi-marker staining. This indicates the level of non-specific staining expected from the pCSC-marker specific antibodies.

iii) Single-colour Staining Control:- Consisting of cells stained with one and only one of the antibodies used in the multi-marker staining. A single-colour staining control is required for each of the antibodies used in the multi-marker staining. This is to allow for compensation of fluorescence spillover between fluorescence detection channels on the flow cytometer.

iv) Fluorescence Minus One (FMO) Control:- Consist of cells stained with all but one of the antibodies used in the multi-marker staining. A FMO control is required for each of the antibodies used in the multi-marker staining. The control is used to set the background fluorescence thresholds for the marker which is excluded from the FMO control. Cells that appear above this threshold in the multi-marker stained sample are considered positive for this marker. In the case of dual-marker CSP staining the Single-colour Staining and FMO controls are the same control.

4.2.2.4.2 ALDH Assay and CSP Assay Staining

First, ALDH assay staining is carried out in a similar fashion to that described Section 2.5.1. The only exception is that cells are dissociated with EDTA rather than Trypsin as CSP assay staining is required. After ALDH staining has been completed, CSP assay staining is carried out in a similar fashion to that described in Section 2.5.3. The only exception is that ALDH assay buffer is used instead of PBS, to prevent the loss of ALDH fluorescence while carrying out CSP staining.

4.2.2.4.3 HSP Assay, ALDH Assay and CSP Assay Staining

First, HSP assay staining is carried out in a similar fashion to that described Section 2.5.2. The only exception is that cells are dissociated with EDTA rather than Trypsin as CSP assay staining is required. Second, HSP stained cells are stained via ALDH assay staining as described in Section 2.5.1. Finally, HSP/ALDH co-stained cells are stained via CSP assay. This CSP assay staining is carried out in a similar fashion to that described in Section 2.5.3. The only exception is that ALDH assay buffer is used instead of PBS, to prevent the loss of ALDH fluorescence while carrying out CSP staining.

Section 4.0 – Identification of pCSCs

4.3 Data:

Six models of ovarian cancer and one model normal ovarian surface epithelium were screened for the presence of ovarian CSCs and ovarian SSCs respectively. The screening process was comprised of three independent assays; ALDEFLUOR™ (ALDH), Hoechst Side-Population (HSP) and Cell Surface Protein (CSP) assays. Each of these assays identified a pCSC population within each of the ovarian cancer models: the populations identified are shown in Table 4.1. On no occasion did two independent assays identify the same pCSC population. However, ALDH and CD44 did identify the same pSSC population within the HIO-80 cell line. This will be discussed in further detail in Section 4.4.4.2.

Table 4.1: A Description of the Models Screened and the High Ranking pCSC Populations Identified.

Model	Description	Type of pCSC
A2780	Primary Ovarian Carcinoma	ALDH+/-; CD133+/-
A2780cis	Cisplatin Resistant Primary Ovarian Carcinoma	ALDH+/-
IGROV1	Primary Ovarian Carcinoma	ALDH+; HSP+/-; CD44+/-
IGROV-CDDP	Cisplatin Resistant Primary Ovarian Carcinoma	ALDH+/-; HSP+/-; CD44+/-; CD133+/-
SKOV3	Treated Ascites	CD44+; CD117+/-
59M	Untreated Ascites	CD44+; CD133+/-
HIO-80	Immortalised non-transformed Ovarian Surface Epithelium	ALDH+; CD44+

The standard flow cytometry gating strategies and controls, as described in Section 1.11.2, were applied to all data presented in this section. Positive controls for each of these screens have already been described in Section 3.3.1.5, and will not be included here. The screen specific negative controls included in this section (Section 4.3) are used to calibrate the flow cytometer and establish the gating strategy for each experiment within each screen. For this reason the negative control data for each screen will be presented along with the experimental data obtained.

4.3.1 ALDH Assay

As discussed in Section 1.10.1 the ALDH Assay identifies pCSCs based on their ability to metabolise a synthetic Aldehydrogenase 1 substrate, BODIPY-aminoacetaldehyde (BAAA), to produce a brightly fluorescing substance (BODIPY-aminoacetate). This reaction can be inhibited by an Aldehydrogenase inhibitor called Diethylaminobenzaldehyde (DEAB).

By adding BAAA to a sample of cells one can discriminate pCSCs and non-pCSCs based on fluorescent intensity. If DEAB is added to the reaction it prevents the production of the fluorescent by-product thus acting as a negative control. By subtracting the negative control data from the uninhibited sample data, pCSCs and non-pCSCs sub-populations can be discriminated and quantified.

All six of the ovarian cancer models and the normal ovarian surface epithelium (NOSE) model were screened in triplicate using the ALDH assay (See Appendix B). ALDH assay positive and negative staining controls were presented in Section 3.3.1.1. It was found that only the ascites models were devoid of ALDH+ cells (Table 4.2). Of the four ovarian cancer models identified to contain ALDH+ cells, three had ALDH+ sub-populations of less than 1 % (A2780, A2780cis and IGROV-CDDP). IGROV-1 was found to be 100 % ALDH +, with no consistent ALDH- sub-population (Section 4.3.5). This was the closest match to the NOSE model (HIO-80), which consisted entirely of ALDH+ cells. It was also noted that the size of the ALDH+ sub-population differed between chemosensitive parent cell lines and the chemoresistant daughter cell lines. In the case of the A2780 and A2780cis pair of models, this manifested as a 240.0 % increase in the size of the ALDH+ pCSC sub-population in the cisplatin resistant model compared to its cisplatin sensitive counterpart. In the case of the IGROV-1 and IGROV-CDDP pair of models, this manifested as a 99.6 % decrease in the size of the ALDH+ pCSC sub-population in the cisplatin resistant model compared to its cisplatin sensitive counterpart. Although the direction and size of the change from cisplatin sensitive parent models were different, they both arrived at a similar ALDH+ population size in both models.

Table 4.2: An Overview of the ALDH assay defined pCSCs within Malignant and Normal Ovarian Epithelial cell lines. Green rows identify cell lines in which both pCSCs and non-pCSCs were identified. Yellow rows identify cell lines in which a pCSC population was detected but no non-pCSC population was reliably detected. White rows identify cell lines in which non pCSC sub-population was reliably detected (described further in Section 4.3.5.1). This colour coding applies to all colour coded tables in this chapter.

Model	Percentage of ALDH+ pCSCs
A2780	0.15 % +/- 0.02 %
A2780cis	0.36 % +/- 0.03 %
IGROV1	95.01 % +/- 2.23 %
IGROV-CDDP	0.41 % +/- 0.08 %
SK-OV-3	0.08 % +/- 0.07 %
59M	0.00 % +/- 0.00 %
HIO-80	94.53 % +/- 4.00 %

4.3.2 The HSP Assay

As discussed in Section 1.10.2, the HSP assay discriminates pCSCs from non-pCSCs based on the expression and activity of dye efflux proteins. Hoechst 33342 (hoechst) is a plasma membrane permeable nuclear stain, which when bound to DNA produces a strong fluorescent profile. pCSCs can efflux hoechst resulting in a population of dimly staining cells. Hoechst dye efflux can be inhibited by an ABC transporter inhibitor called Verapamil.

Staining cells with hoechst for the discrimination of pCSCs from non-pCSCs is based on fluorescent intensity. If Verapamil is added to the reaction it prevents the efflux of hoechst from pCSCs, thus acting as a negative control. By subtracting the negative control data from the uninhibited sample data pCSCs and non-pCSCs sub-populations can be discriminated and quantified.

All six of the ovarian cancer models and the NOSE model were screened in triplicate using the HSP assay (See Appendix B). HSP assay positive and negative staining controls were presented in Section 3.3.1.2. It was found that only two of the seven models contained HSP+ pCSC sub-populations (Table 4.3). Only the parent and daughter pair of models – IGROV-1 and IGROV-CDDP exhibited HSP+ cells. It was also noted that the size of the HSP+ sub-population

was significantly different between cisplatin sensitive parent cell line (IGROV-1) and the cisplatin resistant daughter cell line (IGROV-CDDP; p-value = 0.04414). This manifested as a 375.2 % increase in the size of the HSP+ pCSC sub-population in the cisplatin resistant model compared to its cisplatin sensitive counterpart.

Table 4.3: An Overview of the HSP assay defined pCSCs within Malignant and Normal Ovarian Epithelial cell lines.

Model	Percentage of HSP+ pCSCs
A2780	0.01 % +/- 0.01 %
A2780cis	0.00 % +/- 0.01 %
IGROV-1	4.12 % +/- 0.86 %
IGROV-CDDP	15.46 % +/- 4.49 %
SK-OV-3	0.03 % +/- 0.01 %
59M	0.02 % +/- 0.02 %
HIO-80	0.02 % +/- 0.02 %

4.3.3 The CSP Assay

As discussed in Section 1.10.3, the CSP Assay identifies pCSCs based on the expression of pCSC cell surface protein markers. Monoclonal fluorescently conjugated primary antibodies are use to detect the expression pCSC cell surface protein markers. A corresponding fluorescently conjugated isotype control is used to estimate the level of non-specific binding in the sample. A sample devoid of fluorescently staining antibodies is used as an autofluorescence control. Events which fluoresce more brightly than the level set by the autofluorescence control are considered to be positive for the antigen being screened for.

By adding a pCSC-antigen directed, fluorescently conjugated antibody to a sample of cells one can discriminate pCSCs from non-pCSCs based on fluorescent intensity. By subtracting the autofluorescence control data from the fluorescently conjugated antibody sample data, while considering the level of non-specific staining produced by the Isotype control, pCSCs and non-pCSCs sub-populations can be discriminated and quantified.

All model systems were screened in triplicate for the presence of three pCSC (CD44, CD117, CD133) and one metastatic cell (CXCR4) cell surface protein markers using the CSP assay (See

Appendix B). Differing pCSC cell surface marker profiles were detected across the seven model systems screened (Table 4.4).

CD44+ pCSCs were identified within the IGROV-1, IGROV-CDDP, SK-OV-3, 59M and HIO-80 models. The other models (A2780 and A2780cis) had no CD44+ pCSCs (Table 4.4). The algorithm used to declare model systems as containing pCSCs is described in detail in Section 4.3.5.

This algorithm identified IGROV-1 and IGROV-CDDP as the only models containing both CD44+ and CD44- sub-populations. SK-OV-3, 59M and HIO-80 were deemed to have no consistent CD44- sub-population and were declared as 100 % CD44+ models. A2780 and A2780cis were deemed to have no consistent CD44+ sub-population and were declared as 100 % CD44- models. This will be discussed in further detail in Section 4.3.5.

CD117+ pCSCs were identified within the SK-OV-3 model. The other models (A2780, A2780cis, IGROV-1, IGROV-CDDP, 59M and HIO-80) had no CD117+ pCSCs (Table 4.4). The algorithm identified SK-OV-3 as the only model containing both CD117+ and CD117- sub-populations. A2780, A2780cis, IGROV-1, IGROV-CDDP, 59M and HIO-80 were deemed to have no consistent CD117+ sub-population and were declared as 100 % CD117- models. This will be discussed in further detail in Section 4.3.5.

CD133+ pCSCs were identified within the A2780, IGROV-CDDP and 59M models. The other models (A2780cis, IGROV-1, SK-OV-3 and HIO-80) had no CD133+ pCSCs (Table 4.4). The algorithm identified A2780, IGROV-CDDP and 59M as the only models containing both CD133+ and CD133- sub-populations. A2780cis, IGROV-1, SK-OV-3 and HIO-80 were deemed to have no consistent CD133+ sub-population and were declared as 100 % CD133- models. This will be discussed in further detail in Section 4.3.5.

No CXCR4+ putative metastatic cells were identified within any of the models investigated (Table 4.4). The algorithm identified deemed all models to have no consistent CXCR4+ sub-population and all were declared as 100 % CXCR4- models. This will be discussed in further detail in Section 4.3.5.

4.3.3.1 Summary of single parametric CSP Screen

All six of the ovarian cancer models and the normal ovarian surface epithelium (NOSE) model were screened using the CSP assay. Six of the seven models were found to be 100 % positive or to have a positive sub-population for one or more of the pCSC markers analysed. None of the models expressed CXCR4, the marker of putative metastatic cells (Table 4.4).

Compared to the ALDH and HSP assays the CSP produced more noise resembling pCSCs that were later deemed not to be true sub-populations (Section 4.3.5). CD133 was found to change expression between cisplatin sensitive parent cell lines (A2780 and IGROV-1) and their respective cisplatin resistant daughter cell lines (A2780cis and IGROV-CDDP). However, the direction of the change was different between both sets of models. Loss of CD133+ cells was associated with acquired cisplatin resistance in the A2780 models, while gain of CD133+ cells was associated with acquired cisplatin resistance in the IGROV models. One of the ascites derived models (59M) was also found to have a CD133+ sub-population while the other (SK-OV-3) was found to be CD133-.

Both of the ascites derived models (SK-OV-3 and 59M) are found to be 100 % CD44+, while the solid tumour derived models were either 100 % CD44- (A2780 and A2780cis) or consisted of a heterogeneous mixture of CD44+ and CD44- cells (IGROV-1 and IGROV CDDP).

It is apparent in these results (Table 4.4) that the sizes of the sub-populations marked by the various pCSC markers are inconsistent with good concordance between markers. This identifies the fact that all the putative ovarian CSC markers are not marking the same cell types. This will be discussed in further detail in Section 4.4.4.2.

Table 4.4: An Overview of the CSP assay defined pCSCs within Malignant and Normal Ovarian Epithelial cell lines.

Model	CD44+ pCSCs (%)	CD117+ pCSCs (%)	CD133+ pCSCs (%)	CXCR4+ pCSCs (%)
A2780	0.34 % +/- 0.14 %	0.02 % +/- 0.01 %	0.06 % +/- 0.02 %	0.05 % +/- 0.04 %
A2780cis	1.45 % +/- 1.09 %	0.02 % +/- 0.01 %	0.01 % +/- 0.01 %	0.12 % +/- 0.13 %
IGROV1	62.69 % +/- 9.64 %	0.17 % +/- 0.06 %	0.03 % +/- 0.03 %	0.06 % +/- 0.04 %
IGROV-CDDP	4.32 % +/- 0.88 %	0.22 % +/- 0.13 %	1.33 % +/- 0.16 %	0.52 % +/- 0.38 %
SK-OV-3	99.43 % +/- 0.34 %	39.96 % +/- 2.89 %	0.09 % +/- 0.04 %	0.23 % +/- 0.14 %
59M	99.51 % +/- 0.69 %	4.71 % +/- 1.58 %	0.19 % +/- 0.01 %	0.33 % +/- 0.20 %
HIO-80	94.81 % +/- 3.27 %	2.38 % +/- 1.19 %	0.10 % +/- 0.09 %	0.29 % +/- 0.32 %

4.3.4 pCSC Hierarchies

pCSC hierarchies are pCSC sub-populations which exist within pCSC sub-populations. When two or more pCSC sub-populations of differing sizes are observed within a cell line, it can be deduced that these pCSC sub-populations do not mark all of the same cells. Depending on the sizes of the sub-populations there could be many different possible relationships (overlaps) between each sub-population. There was insufficient time to fully characterise the overlaps of all pCSC populations. A few experiments were carried out to gauge the feasibility, before deciding whether or not to peruse the identification of hierarchical ovarian CSCs.

IGROV-1 (Section 4.3.4.1) and IGROV-CDDP (Section 4.3.4.2) were used to estimate the workload involved in characterising the hierarchies of pCSC populations. These experiments identified that considerable work was required to fully characterise the overlaps of all pCSC populations.

4.3.4.1 IGROV-1 Multi-Parametric Staining

Two experiments were performed to aid in the understanding of the CD44+/- sub-populations identified in the IGROV-1 cell line (Section 4.3.3), the logistics of carrying out CD44 and ALDH co-staining and the relationship between the 100 % ALDH+ population and CD44+/- sub-populations identified within the IGROV-1 cell line (Section 4.3.1 and 4.3.3).

As shown in Appendix B, via an antiCD44-FITC antibody, IGROV-1 has a CD44 population which spans from CD44- into CD44+. It was decided to try to use the more intensely fluorescent antiCD44-PE/Cy7 antibody to try to better resolve the CD44- and CD44+ sub-populations.

It was found that the antiCD44-PE/Cy7 antibody was over-staining the IGROV-1 cells, indicating that IGROV-1 was 89.64 % +/- 2.32 % CD44+ (Figure 4.1B). It was possible to determine that the antiCD44-PE/Cy7 was over-staining as opposed to antiCD44-FITC under-staining via multi-parametric staining. Co-staining the IGROV-1 cell line with both the antiCD44-PE/Cy7 and the antiCD44-FITC antibodies resulted in the disappearance of the CD44-FITC+ sub-population (Figure 4.1D). This indicates that the antiCD44-PE/Cy7 antibody is far more concentrated than the antiCD44-FITC antibody. It is competitively inhibiting the antiCD44-FITC antibody, thus preventing the antiCD44-FITC+ sub-population from being detected. Dilution of the antiCD44-PE/Cy7 or a new antiCD44 was required to better resolve the CD44+/- sub-population within the IGROV-1 cell line. Deduced hierarchical IGROV-1 pCSC sub-populations will be discussed further in Section 4.4.4.3.3.

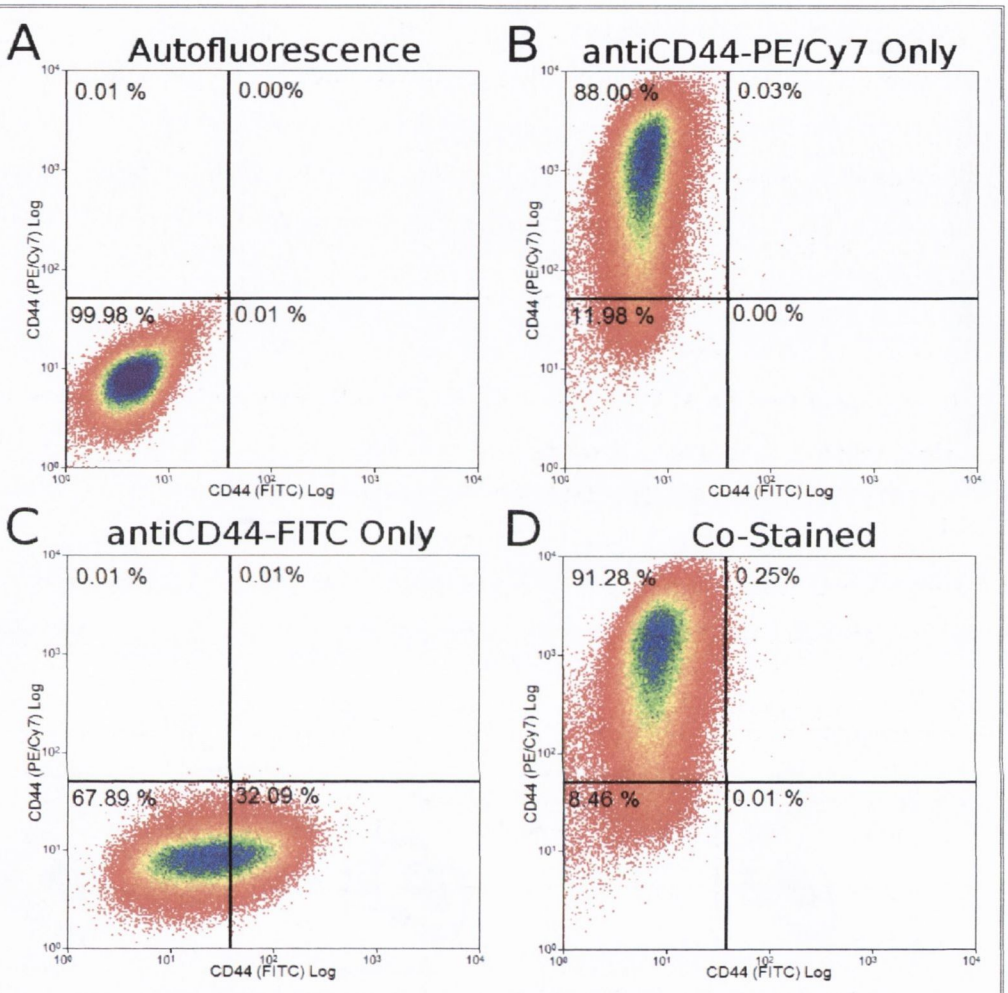

Figure 4.1: IGROV-1 multi-parametric CD44 staining - Multi-parametric CD44 staining indicates over-staining by antiCD44-PE/Cy7, resulting in a lack of correlation between antiCD44-FITC and antiCD44-PE/Cy7 staining. A) Shows unstained cells and was used to set the thresholds for the positively staining cells. B) Shows cells stained with with antiCD44-PE/Cy7 only and was used to control for spill-over fluorescence in the FITC channel caused by the antiCD44-PE/Cy7 antibody. C) Shows cells stained with with antiCD44-FITC only and was used to control for spill over fluorescence in the PE/Cy7 channel caused by the antiCD44-FITC antibody. D) Shows cells co-stained with antiCD44-PE/Cy7 and antiCD44-FITC.

4.3.4.2 IGROV-CDDP Multi-Parametric Staining

As shown in Sections 4.3.1 – 4.3.3, the IGROV-CDDP cell line contains four pairs of pCSC/non-pCSC sub-populations (ALDH+/-, HSP+/-, CD44+/- and CD133+/-). Due to the similarities of their fluorescent profiles, co-staining with ALDH and antiCD44-FITC was not possible. As described above (Section 4.3.4.1), the antiCD44-PE/Cy7 antibody was not optimised so could not be used instead of the anti-CD44-FITC antibody. Therefore, it was decided to focus on the hierarchical relationships between the ALDH+/-, HSP+/- and CD133+/- sub-populations.

It was found that the ALDH+ cells and CD133+ cells were mutually exclusive (Figure 4.2). This indicates that the IGROV-CDDP cell line can be divided into ALDH-/CD133-, ALDH+/CD133- and ALDH-/CD133+ sub-populations.

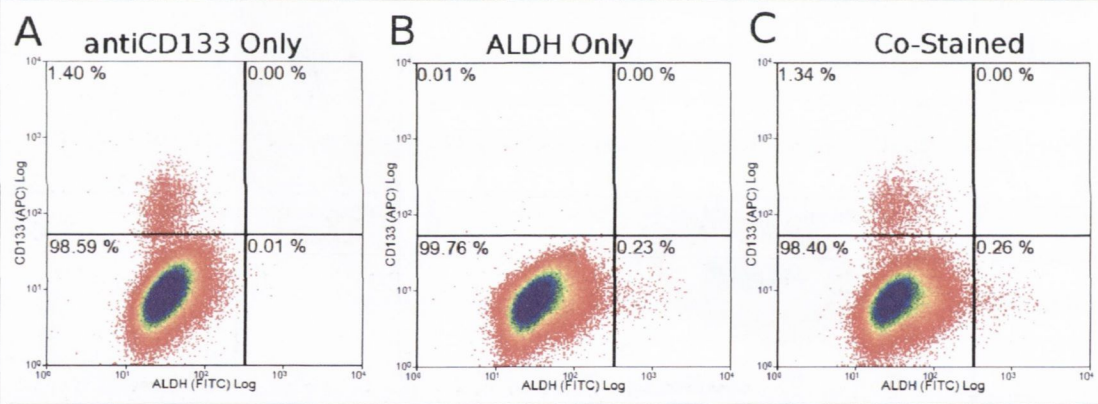

Figure 4.2: IGROV-CDDP multi-parametric CD133/ALDH Staining – The CD133+ and ALDH+ sub-populations in the IGROV-CDDP cell line are mutually exclusive. A) Shows cells stained with antiCD133-APC and DEAB inhibited ALDH assay. This was used to set the threshold for ALDH+ cells. B) shows cells stained with the ALDH assay only. This was used to set the threshold for CD133+ cells. C) Shows cells co-stained with both antiCD133-APC and the ALDH Assay. The absence of cells in the top right quadrant of panel C, shows that there are no CD133+/ALDH+ cells in the IGROV-CDDP cell line.

A separate experiment correlated each of these three sub-populations to the presence/absence of HSP+ cells. It was found that all three ALDH/CD133 based sub-populations contained both HSP+ and HSP- sub-populations. This indicates that the IGROV-CDDP cell line can be further divided into six sub-populations (Figure 4.3);

i) ALDH-/CD133-/HSP-

ii) ALDH-/CD133-/HSP+

iii) ALDH+/CD133-/HSP-

iv) ALDH+/CD133-/HSP-

v) ALDH-/CD133+/HSP-

vi) ALDH-/CD133+/HSP+

It was noted that ALDH-/CD133+ cells are HSP+ depleted. A HSP+ sub-population is still present but it is 55 % the size of the HSP+ sub-population identified in the entire IGROV-CDDP population (Figure 4.3D). The ALDH+/CD133- are HSP+ enriched. HSP- cells still represent the majority of ALDH+/CD133- cells, however, there is 541 % more HSP+ cells in the ALDH+/CD133- fraction than the entire IGROV-CDDP population (Figure 4.3F).

The HSP+ sub-population observed in this experiment (Figure 4.3B), is smaller than that normally observed in the IGROV-CDDP cell line (Section 4.3.2). The HSP profile was also different to that normally observed. This might be due to consecutive HSP and ALDH staining. Further work is required to investigate the optimal method to co-stain for ALDH and HSP.

Deduced hierarchical IGROV-CDDP pCSC sub-populations will be discussed further in Section 4.4.4.3.4.

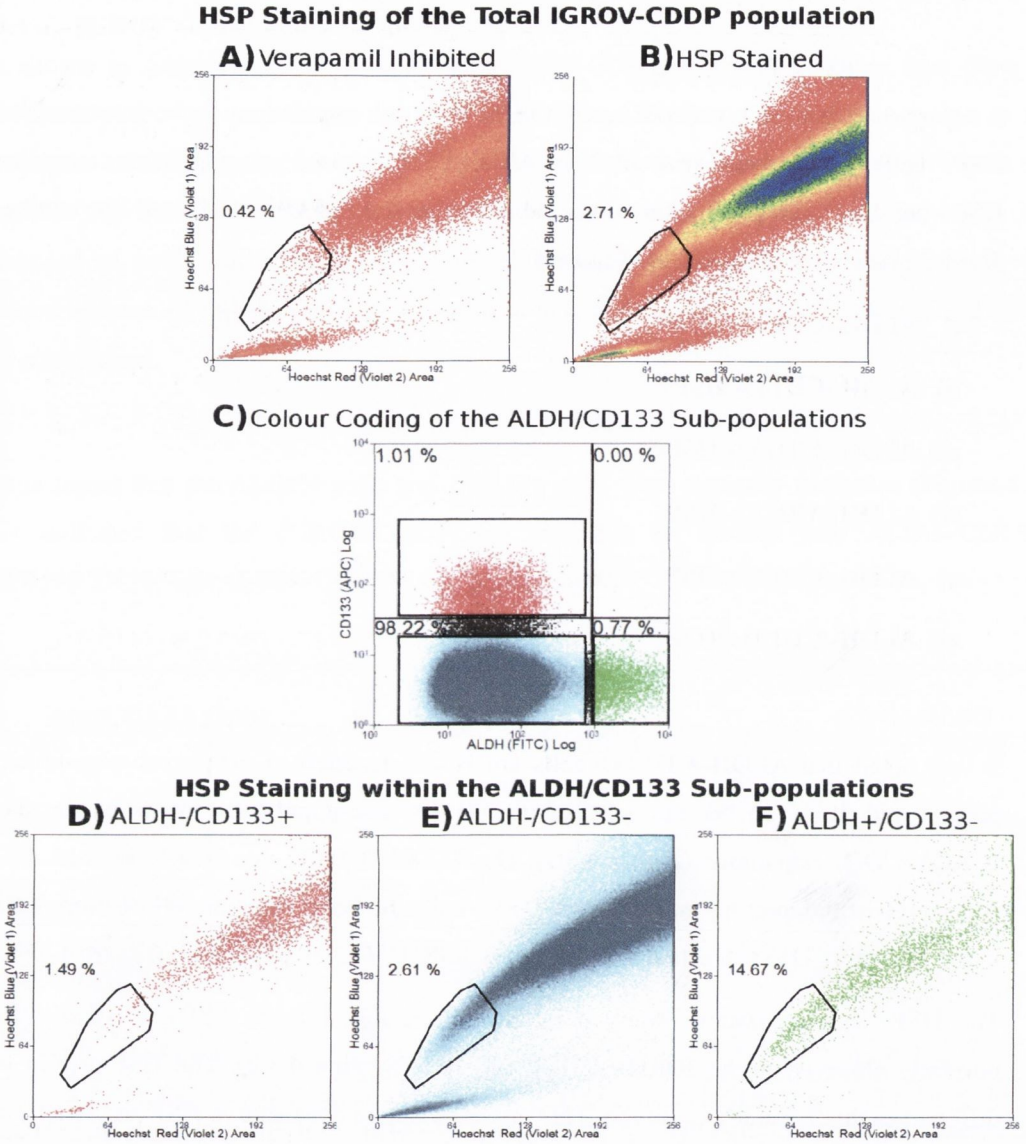

Figure 4.3: IGROV-CDDP multi-parametric ALDH/HSP/CD133 Staining – The ALDH+/CD133- sub-population is enriched for HSP+ cells within the IGROV-CDDP cell line. The ALDH-/CD133+ sub-population is depleted for HSP+ cells within the IGROV-CDDP cell line. The top pair of flow cytometry graphs, show (A) Verapamil Inhibited and (B) HSP Stained samples of the total IGROV-CDDP population. This is used to establish the HSP+ gate. The central panel (C) is used to distinguish the ALDH/CD133 sub-populations. The bottom three panels show HSP staining looking at only the cells with the colour coded gated regions of the central panel. D) Shows HSP staining of ALDH-/CD133+ cells. E) Shows HSP staining of ALDH-/CD133- cells. F) Shows HSP staining of ALDH+/CD133- cells.

4.3.5 Ranking the pCSC Populations Identified

Two compounding ranking systems were applied to the ranking of the pCSCs identified in the above screen (Section 4.3). First a statistical ranking system was applied to identify pCSC sub-populations which could be identified in a consistent fashion (Section 4.3.5.1). A second ranking system was applied to these statistically ranked pCSC in the form of hypothesis based ranking (Section 4.3.5.2). This simply meant selecting the pCSC sub-populations which could be used to address the most clinically relevant questions.

4.3.5.1 Statistical Ranking

It was decided to set a 99 % confidence threshold when ranking the pCSC identified in the above screen (Section 4.3). This is equivalent to setting a p-value cut-off of 0.01. The following algorithms were applied:

Lower Limit: (Mean Positive) – (Mean Autofluorescence) – (3 x (Positive Standard Deviation))

Upper Limit: (Mean Positive) + (Mean Autofluorescence) + (3 x (Positive Standard Deviation))

To qualify for the 99 % confidence threshold, the lower limit of a pCSC had to be > 0 % and the upper limit had to be < 100 %. In practical terms this means that pCSC sub-populations were within the 99 % confidence threshold if, statistically, there was a $\geq$ 99 % of detecting both marker positive and marker negative sub-populations every time the model was interrogated.

This algorithm was constructed using the following logic. The area under the curve of a normal distribution between the points ($\mu - 3\sigma$, $\mu + 3\sigma$) is equal to 99 % the total area. Where μ is the mean and σ is the standard deviation. Therefore, if $\mu - 3\sigma$ is > 0, then the marker positive sub-population with these dimensions should be detected greater than 99 % of the time it is investigated. If $\mu + 3\sigma$ is < 100, then the marker negative sub-population with these dimensions should be detected greater than 99 % of the time it is investigated. The Mean Positive size is measured with respect to false positives detected in the negative control (Autofluorescence). Therefore, the Mean Positive size is normalised against the mean false positives. This algorithm was applied to all the results of the pCSC screen (Tables 4.5 – 4.10). Only pCSC populations meeting the criteria of the upper and lower limits were considered for further analysis (Table 4.11).

Table 4.5: ALDH assay defined pCSCs within Malignant and Normal Ovarian Epithelial cells.

Model	Percentage of ALDH+ pCSCs	99 % Lower Limit	99 % Upper Limit
A2780	0.15 % +/- 0.02 %	0.101 %	0.192 %
A2780cis	0.36 % +/- 0.03 %	0.267 %	0.460 %
IGROV1	95.01 % +/- 2.23 %	88.326 %	101.694 %
IGROV-CDDP	0.41 % +/- 0.08 %	0.174 %	0.640 %
SK-OV-3	0.08 % +/- 0.07 %	-0.119 %	0.272 %
59M	0.00 % +/- 0.00 %	0.000 %	0.000 %
HIO-80	94.53 % +/- 4.00 %	82.519 %	106.541 %

Table 4.6: HSP assay defined pCSCs within Malignant and Normal Ovarian Epithelial cells.

Model	Percentage of HSP+ pCSCs	99 % Lower Limit	99 % Upper Limit
A2780	0.01 % +/- 0.01 %	-0.037 %	0.057 %
A2780cis	0.00 % +/- 0.01 %	-0.014 %	0.021 %
IGROV1	4.12 % +/- 0.86 %	1.019 %	7.227 %
IGROV-CDDP	15.46 % +/- 4.49 %	1.857 %	29.063 %
SK-OV-3	0.03 % +/- 0.01 %	-0.017 %	0.077 %
59M	0.02 % +/- 0.02 %	-0.056 %	0.102 %
HIO-80	0.02 % +/- 0.02 %	-0.075 %	0.115 %

Table 4.7: CD44 assay defined pCSCs within Malignant and Normal Ovarian Epithelial cells.

Model	Percentage of CD44+ pCSCs	99 % Lower Limit	99 % Upper Limit
A2780	0.34 % +/- 0.14 %	-0.091 %	0.778 %
A2780cis	1.45 % +/- 1.09 %	-1.851	4.744 %
IGROV1	62.69 % +/- 9.64 %	33.727 %	91.647 %
IGROV-CDDP	4.32 % +/- 0.88 %	1.638 %	6.996 %
SK-OV-3	99.43 % +/- 0.34 %	98.378 %	100.485 %
59M	99.51 % +/- 0.69 %	96.339 %	100.681 %
HIO-80	94.81 % +/- 3.27 %	84.527 %	105.086 %

Table 4.8: CD117 assay defined pCSCs within Malignant and Normal Ovarian Epithelial cells.

Model	Percentage of CD117+ pCSCs	99 % Lower Limit	99 % Upper Limit
A2780	0.02 % +/- 0.01 %	-0.011 %	0.044 %
A2780cis	0.02 % +/- 0.01 %	-0.028 %	0.061 %
IGROV1	0.17 % +/- 0.06 %	-0.091 %	0.424 %
IGROV-CDDP	0.22 % +/- 0.13 %	-0.180 %	0.620 %
SK-OV-3	39.96 % +/- 2.89 %	28.227 %	45.693 %
59M	4.71 % +/- 1.58 %	-0.202 %	9.622 %
HIO-80	2.38 % +/- 1.19 %	-1.365 %	6.119 %

Table 4.9: CD133 assay defined pCSCs within Malignant and Normal Ovarian Epithelial cells.

Model	Percentage of CD133+ pCSCs	99 % Lower Limit	99 % Upper Limit
A2780	0.06 % +/- 0.02 %	0.008 %	0.119 %
A2780cis	0.01 % +/- 0.01 %	-0.017 %	0.031 %
IGROV1	0.03 % +/- 0.03 %	-0.101 %	0.161 %
IGROV-CDDP	1.33 % +/- 0.16 %	0.782 %	1.878 %
SK-OV-3	0.09 % +/- 0.04 %	-0.085 %	0.258 %
59M	0.19 % +/- 0.01 %	0.023 %	0.357 %
HIO-80	0.10 % +/- 0.09 %	-0.266 %	0.466 %

Table 4.10: CXCR4 assay defined pCSCs within Malignant and Normal Ovarian Epithelial cells.

Model	Percentage of CXCR4+ pCSCs	99 % Lower Limit	99 % Upper Limit
A2780	0.05 % +/- 0.04 %	-0.068 %	0.168 %
A2780cis	0.12 % +/- 0.13 %	-0.279 %	0.519 %
IGROV1	0.06 % +/- 0.04 %	-0.085 %	0.198 %
IGROV-CDDP	0.52 % +/- 0.38 %	-0.651 %	1.698 %
SK-OV-3	0.23 % +/- 0.14 %	-0.203 %	0.663 %
59M	0.33 % +/- 0.20 %	-0.301 %	0.955 %
HIO-80	0.29 % +/- 0.32 %	-0.774 %	1.360 %

Table 4.11: pCSC sub-populations which passed the 99 % confidence test.

Model	pCSC sub-populations identified (99 % confidence)
A2780	**ALDH** (0.15 % +/- 0.02 %); **CD133** (0.06 % +/- 0.02 %)
A2780cis	**ALDH** (0.36 % +/- 0.03 %)
IGROV1	**HSP** (4.12 % +/- 0.86 %); **CD44** (62.69 % +/- 9.64 %)
IGROV-CDDP	**ALDH** (0.41 % +/- 0.08 %); **HSP** (15.46 % +/- 4.49 %); **CD44** (4.32 % +/- 0.88 %); **CD133** (1.33 % +/- 0.16 %)
SK-OV-3	**CD117** (39.96 % +/- 2.89 %)
59M	**CD133** (0.19 % +/- 0.01 %)
HIO-80	**N/A**

4.3.5.2 Hypothesis Based Ranking

After identifying the statistically sub-populations (Section 4.3.5.1; Table 4.11), it was found that there were too many pCSC sub-populations of interest, with too many possible overlaps and hierarchies to be able to investigate them all. Therefore, it was decided to take forward sets of pCSC sub-populations that could be used to address clinically relevant questions.

In the clinic, ovarian cancer is initially responsive to chemotherapy. However, relapse is common and is often associated with chemoresistance. The challenge of acquired chemoresistance is a major obstacle in the developing effective curative treatments for ovarian cancer. As initial therapy can frequently de-bulk ovarian tumours to undetectable levels but the residual cells can efficiently reform the tumour, CSC are suspected to play a role in acquired chemoresistance.

Having defined many putative ovarian CSCs across multiple cell lines. It was decided to investigate the difference between the pCSCs in cisplatin-sensitive cell lines and there daughter cell lines with acquired cisplatin-resistance. For this reason the principle comparisons we were interested in making were between A2780 and A2780cis and between IGROV-1 and IGROV-CDDP.

All of the pCSCs identified in a cisplatin sensitive parent cell line (A2780 or IGROV-1) were significantly altered in size in the cisplatin resistant daughter cell line (A2780cis or IGROV-CDDP respectively) as shown in Table 4.12.

Table 4.12: Acquired cisplatin resistance, significantly alters the size of all pCSC sub-populations identified.

pCSC Marker	A2780 to A2780cis	IGROV-1 to IGROV-CDDP
ALDH+	245 % increase in size (p-value < 0.0023)	99.6 % decrease in size (p-value < 0.0002)
HSP+	NA	375 % increase in size (p-value < 0.045)
CD44+	NA	93.1 % decrease in size (p-value < 0.0086)
CD133+	100 % decrease in size (p-value < 0.0039)	Appearance of a 1.33 % CD133+ sub-population. (p-value < 0.0039)

The principle comparison to make between the A2780 and A2780cis cell lines was the comparison of the ALDH+ and ALDH- sub-populations from each model. The A2780 cell line also had a CD133+ sub-population. However, isolation of this sub-population was more complicated due to its small size and proportion of false positives as indicated by the autofluorescence control (See Appendix B)

The smaller a sub-population is the more important false positives are when it comes to purifying the small sub-population. If one has a 10 % sub-population with 0.01 % false positive staining that means that only 0.1 % ((0.01/10*100) = 0.1 %) of the sub-population is attributable to false positives. However if the sub-population is only 0.06 % in size with 0.01 % false positive staining, that means that 16.67 % ((0.01/0.06)*100 = 16.7 %) of the population is attributable to false positive staining.

The A2780 CD133+ and CD133- sub-populations were not brought forward for isolation as the autofluorescence control had 0.01 % CD133+ cells (Appendix B), indicating that the 0.06 % CD133+ sub-population consisted of 0.01 % false positives and 0.05 % CD133+ cells. This meant that even if this A2780 CD133+ sub-population was isolated to 100 % purity, 16.7 % of the enriched population could be false positives. It is possible that such a population could be purified to 99 % pure CD133+ cells but this would be dependent on the degree of autofluorescence (false positives) in the sorted samples. False positive populations were not a problem for other small sub-populations, for example; A2780 ALDH+ and A2780cis ALDH+, as the resolution of these assays was so good that the negative controls had 0.00 % false positives.

For these reasons it was decided to isolate the ALDH+ and ALDH- sub-populations from the A2780 and A2780cis cell lines, with the intention of understanding the similarities and differences between cisplatin sensitive and cisplatin resistant pCSCs (Table 4.13).

The volume of work required to characterise the overlaps and hierarchies of all the sub-populations within the IGROV-1 and IGROV-CDDP cell lines, was not feasible under the time constraints of this project. Due to these limitations, it was decided to focus on one pCSC sub-populations from the IGROV-1 and IGROV-CDDP cell lines.

Only one pCSC sub-population in the IGROV-1/IGROV-CDDP models behaved in a similar fashion to the ALDH+/- sub-populations in the A2780/A2780cis models. ALDH+ cells were present in the parent cisplatin sensitive A2780 model and increased in proportion upon acquired cisplatin resistance in the A2780cis model. The HSP pCSC sub-populations of the IGROV-1/IGROV-CDDP models were the only sub-populations to behave in a similar fashion to that of the ALDH sub-populations in the A2780/A2780cis models. Other pCSC sub-populations (ALDH and CD44) present in the IGROV-1 cell line decreased in size with acquired cisplatin resistance in the IGROV-CDDP cell line. This suggests that these pCSC were not advantageous for cisplatin resistance.

CD133+ cells appeared in the IGROV-CDDP model, but there were no corresponding CD133+ pCSC in the cisplatin sensitive parent cell line (IGROV-1). This meant that there was no scope to compare cisplatin sensitive CD133+ pCSCs to cisplatin resistant CD133+ pCSCs.

For these reasons it was decided to isolate the HSP+ and HSP- sub-populations from the IGROV-1 and IGROV-CDDP cell lines, with the intention of understanding the similarities and differences between cisplatin sensitive and cisplatin resistant pCSCs (Table 4.13).

ALDH+/- and HSP+/- sub-populations were not identified within either of the ascites derived models (SK-OV-3 and 59M). Only CD117+/- and CD133+/- sub-populations were identified within these models. As ALDH and HSP assay based assays were planned in the cisplatin sensitive/resistant models, it was decided to use the ascites derived models to demonstrate the isolation of pCSC utilising the CSP assay. These CSP based isolations were of a lower priority than the ALDH and HSP based isolations as they were not central to the understanding of cisplatin sensitive and cisplatin resistant CSCs.

There was no common pCSC sub-population identified between the SK-OV-3 and 59M models. It was decided to reduce the confidence threshold to 95 % (equivalent to a p-value cut-off of 0.05). Under these conditions CD117+/- sub-populations were identified in both the SK-OV-3

and 59M models. The SK-OV-3 CD117+/- sub-populations were discrete sub-populations with a >99 % confidence. The 59M CD117+/- sub-populations were non-discrete sub-populations with a <99 % confidence. Comparison of these two sub-populations could give insight into the role of CD117+ pCSCs in metastatic Ovarian Cancer (ascites). It could also give insight into the appropriate confidence threshold cut-offs and the difference between discrete and non-discrete pCSC sub-populations.

For these reasons it was decided to isolate the CD117+ and CD117- sub-populations from the SK-OV-3 and 59M cell lines, with the intention of understanding the role of pCSCs in metastasis, and the technical considerations when identifying pCSC sub-populations (Table 4.13).

Table 4.13: pCSC and non-pCSC sub-populations which were selected to be brought forward for isolation and downstream analysis.

Model	pCSC Sub-populations	Non-pCSC Sub-populations
A2780	**ALDH+** (0.15 % +/- 0.02 %)	**ALDH-** (99.85 % +/- 0.02 %)
A2780cis	**ALDH+** (0.36 % +/- 0.03 %)	**ALDH-** (99.64 % +/- 0.03 %)
IGROV1	**HSP+** (4.12 % +/- 0.86 %)	**HSP-** (95.88 % +/- 0.86 %)
IGROV-CDDP	**HSP+** (15.46 % +/- 4.49 %);	**HSP-** (84.54 % +/- 4.49 %);
SK-OV-3	**CD117+** (39.96 % +/- 2.89 %)	**CD117-** (61.04 % +/- 2.89 %)
59M	**CD117+** (4.71 % +/- 1.58 %)	**CD117-** (95.29 % +/- 1.58 %)
HIO-80	N/A	N/A

4.3.6 pCSC screen Summary

Upon the completion of this screening phase of the project 16 pCSC/SSC populations had been identified across seven model systems (Tables 4.5 – 4.10). Eleven of these pCSC populations were sub-populations, dividing the model systems into 22 sub-populations of pCSCs and non-pCSCs (Table 4.11). Due to logistical constraints it was not possible to identify all of the possible overlaps of these sub-populations. Based on the size of the populations alone it can be deduced that more than 22 overlapping sub-populations exist. This is discussed in detail in Section 4.4.4.3.

Twelve positive/negative pCSC/non-pCSC sub-populations from across six model systems were brought forward for isolation and down stream analysis (Table 4.13). This selection was brought forward as they were good candidates for answering some of the questions most pertinent to the understanding of Ovarian Cancer.

4.4 Discussion:

The central aim of this Chapter was to identify pCSCs from Ovarian Cancer models and pSSCs from a Normal Ovarian Surface Epithelium (NOSE) model. The results shown (Section 4.3), identified the presence pCSCs or pSSCs in all of the models examined. Some models presented with multiple pCSC sub-populations while others presented with only a single pCSC population.

This discussion section will talk about the possible biological roles of the various pCSC sub-populations identified in Section 4.3. For the purpose of this study, strict thresholds were applied to the data obtained via the pCSC screen when declaring the detection of sub-populations above that of background signal. Only sub-populations that were statistically likely to be reproducible 99 % of the time were considered in this study and will be discussed here. As described in Section 4.3.5, a 99 % confidence interval was calculated for all pCSC sub-populations detected. Confidence intervals are calculated based on the mean and standard deviation of a population measurement. A 99 % confidence interval of a given pCSC sub-population, is the range of values in which one would expect 99 % of size measurements to fall for the given pCSC sub-population. This means that if the lower limit of the 99 % confidence interval is greater than 0: one would expect to detect the pCSC sub-population at least 99 % of the time one measured it. This means that the pCSC sub-populations detected in the pCSC screen and brought forward for downstream analysis were reliable and reproducible.

4.4.1 Screening for OvCSC:

As discussed in Section 1.5, Ovarian Cancer in usually responsive to first line therapy, but is prone to chemoresistant relapse. The CSC hypothesis suggests that the reason for such relapse, is due to CSCs evading first line therapy, adapting to the environmental conditions and regrowing the tumour, in a state that is refractory to therapy.

The long term aim is to develop novel therapies that directly target OvCSCs. Such approaches, should not be susceptible to CSC driven chemoresistant relapse. To develop such therapies, therapeutic targets expressed in CSCs need to identified. Currently it is very hard to study OvCSCs, as models of OvCSCs do not exist. Instead, OvCSCs must be identified and isolated from heterogeneous populations.

As discussed in Section 1.11, both screening and selection approaches can be used to identify and isolate pCSCs. For the reasons discussed in Section 1.11, a screening approach was adopted

in this project, utilising OvCSC markers published in the literature. To date there are no definitive OvCSC markers which identify OvCSC across all populations tested. There is no consensus as to how each of the validated OvCSC markers (ALDH: Silva et al. 2011; HSP: Szotek et al. 2006; CD44: Zhang et al. 2008; CD117: Zhang et al. 2008; CD133: Curley et al. 2009) relate to each other.

The pCSC screen carried out in this project (Section 4.3), utilised a wide range of OvCSC markers, in an attempt to develop the understanding of how each of the markers relate to one another. Additionally, the large screening panel increased the probability of detecting OvCSC within our model systems.

4.4.2 The OvCSC Field:

The current state of the OvCSC field was reviewed in detail in Section 1.6 and will only be summarised briefly here.

Bat et al. (2005) were the first to isolate stem-like clones from Ovarian Cancer patients ascites. Szotek et al. (2006) were the first to isolate OvCSC via marker based screening. Baba et al. (2008) were the first to isolate and validate OvCSCs from human derived Ovarian Cancer cell lines. They were also the first to utilise a single cell self-renewal and differentiation (SD) assay within an OvCSC context. Curley et al. (2009) showed that CD133+ cells, isolated from patient samples, demonstrated OvCSC characteristics. Kusumbe et al. (2009) called the CD133+ OvCSC marker into question, with findings that suggested that CD133+ cells were endothelial precursors cells rather than OvCSCs, suggesting that efficient xenograft uptake was due to augmented vasculature via CD133+ cells.

Prior to the commencement of this project in 2009, the work described above had made considerable findings regarding the presence of CSCs in Ovarian Cancer. However, little work had been done to relate the different types of OvCSC sub-populations to one another. Furthermore, a black and white picture of OvCSC biology was being painted. No studies were commenting on the possible presence of sub-populations within OvCSC sub-populations, despite many differing populations of OvCSC having been discovered. For example; Zhang et al. (2008) compared a CD44+/CD117+ population to a CD44-/CD117- population, showing that CD44+/CD117+ cells could form xenograft tumours at 100 cells while CD44-/CD117- could not form tumours at 10,000 cells. No data was presented on any CD44+/CD117- or CD44-/CD117+ populations. Alvero et al. (2009) identified CD44 as a marker of chemoresistance: they found that CD44+ ovarian cancer cells express TLR4 and MyD88 while

CD44- cells express TLR4 but not MyD88. They found that when CD44+ cells were treated with paclitaxel (a know ligand of TLR4) it resulted in increased NFκB activity. A similar response was not observed in CD44- cells: which instead underwent apoptosis. So with respect to the CD44+/CD117+ identified by Zhang et al. perhaps CD44-/CD117+ cells could be chemosensitive stem cells. CD44+/CD117+ cells could be chemoresistant stem cells and CD44+/CD117- cells could represent the differentiated cells in a reconstituted recurrent tumour.

As little work had be carried out on addressing overlaps of the differing pCSCs, it was decided to use a panel of six markers to screen seven models systems, with the intention of addressing the relationships between the various pCSC markers. The data produced identified several pCSC sub-populations within across all the model systems screened. Analysis of this data has identified that multiple pCSC populations and possible CSC hierarchies are pervasive in ovarian cancer. More recently, Silva et al. (2011) published work in an attempt to tackle this idea of overlapping pCSC sub-populations in Ovarian Cancer. They screened 18 patient samples and seven cell lines for the presence of six pCSC markers. They identified ALDH+ cells as CSCs: showing that 100 ALDH+ cells (from across three cell lines) formed tumours more efficiently than their ALDH- counterparts. Additionally, they defined CD133+/- sub-populations within this ALDH+ CSC population: finding that the CD133+ cells grew tumours with more microvascular (marked by CD31 and CD105) and of greater weight.

Studies with a similar format to the one in this project and that of Silva et al. are becoming increasingly important. As with every OvCSC paper published, the findings regarding OvCSCs appear to be diverging rather than converging. Larger screening studies will be able to shed light on the diversity of these findings and potentially elucidate the systems of cellular differentiation within Ovarian Cancer.

4.4.3 The Advantages and Disadvantages of Large Flow Cytometry Based pCSC Screens:

Through the screening of six ovarian cancer models and one normal ovarian surface epithelium model 14 pCSC marker positive populations and two pSSC marker positive populations were identified. Three classes of screen were implemented; ALDH, HSP and CSP. Each class of pCSC screen identified at least one putative stem-like population. Some models had pCSCs marked by more than one pCSC marker. A panel of OvCSC markers and a diverse range of Ovarian Cancer and Somatic models were used in preference to a more focused panel of pCSC

markers or model systems. The advantages and disadvantages of the broad versus focused screens will now be discussed.

The use of a broad panel of pCSC markers had the advantage of being able to elucidate the relationships between the different pCSC markers and their corresponding cell types. However, it presented a logistical disadvantage. Due to the time taken to screen for all pCSC markers, there was less time to investigate overlaps between sets of markers. As presented in the data section (Section 4.3), the pCSC screen identified numerous populations based on single marker expression. The differing sizes of each populations suggests that many different overlapping sub-populations exist within some of the models screened. However, due to time constraints it was not possible fully examine these overlaps. A more focused approach, with fewer model systems, could have allowed for more in depth analysis of such overlaps. However, without the results obtained from the more broad approach adopted in this project, the diversity in pCSC markers observed in Ovarian Cancer may have been overlooked.

Often publications show a broad flow cytometric based screen for several pCSC markers and identify several sub-populations but only select a sub-set of these when carrying out downstream analysis. For example, Curley et al (2009) screened for 5 pCSC markers: CD24, CD44, CD117, CD133 and EpCAM, but only carried out downstream analysis on the CD133+/- sub-populations. Similarly, Silva et al (2011) screened for 6 pCSC markers: CD24, CD44, CD80, CD117, CD133 and ALDH, but only carried out downstream analysis on the ALDH+/- CD133+/- sub-populations. This is as a result of the low throughput nature of the down stream analysis and CSC validation. As will be presented in Section 6.0 the single cell self-renewal and differentiation assay may represent a more high throughput method of validating larger sets of pCSCs. This type of downstream analysis may become invaluable in the understanding of the relationships between the different types of sub-populations identified within tumours.

In this project, the use of a broad panel of Ovarian Cancer and Somatic models had the advantage of being able to elucidate the roles of CSCs across the many aspects of Ovarian Malignancy. The use of the NOSE model offered extra power to identify healthy counterparts to any OvCSC identified. The use of a broad panel of models comes with the same disadvantages as using a broad panel of pCSC markers. It does present a better overview of the models being studied, however, due to time constraints it prevents the comprehensive analysis of any of the models. Cell line models of ovarian cancer were used in this project ahead of patient samples, as the screening, isolation and validation techniques had to be established and optimised in the laboratory during the course of this project and cell lines provided a more efficient source of

ovarian cancer material. With the completion of this project, this system for the identification, isolation and validation of OvCSCs has been established in the laboratory and can now be applied to the analysis of patient samples.

The pCSC markers used in this pCSC screen did not identify all the sub-populations present within the models examined. Further sub-populations were identified based on phenotypic behaviours in the downstream analysis (Section 6.3). Based on this information and the information obtained from the above screen, a better screening system could now be designed. It would be better to focus on 2 – 3 models, screened with a broad panel of markers. Two models should focus on one central question, for example; chemosensitive versus chemoresistant or solid tumour versus ascites. A third model should act as a healthy tissue comparison. Using more models than this limits the ability to gain a deep understanding of the parameters involved in the central question. Screening the model systems with 100s of markers would ensure a comprehensive understanding of the various sub-populations within each model. Using a more focused panel of pCSC markers could lead to an oversimplified picture of the sub-populations, which could be problematic in the downstream analysis. Current commercial technologies, which were not available the beginning of this project, allow for the screening of 100 CSP markers with a similar workload to screening for just four as shown above (Section 4.3.3). Other competing products allow for the screening of 242 CSP markers, which is considerably more work, but may still be an achievable target.

No large screens for OvCSCs, as presented in the data section (Section 4.3), were published prior to the commencement of this work. With the information available a broader panel of models appeared to be the best option. With the information gained from this work and some of the more recent publications, a more refined approach can now be developed.

4.4.4 Furthering the Understanding of OvCSC Biology:

As a result of the data presented in this chapter, the knowledge of OvCSC biology has been furthered. Within this sub-section (Section 4.4.4) the following advances in OvCSC biology will be discussed.

4.4.4.1 Novel pCSCs and pSSCs have been identified:

The pCSC screen identified 14 pCSC and 2 pSSC (marker positive) populations, which passed a 99 % confidence test (Section 4.3.5.1). The screen also identified 11 non-pCSC and 0 non-pSSC (marker negative) sub-populations, which passed a 99 % confidence test (Section 4.3.5.1).

The ALDH and CD44 pCSC markers were the most widely detected. This agrees with the findings of Silva et al. (2011), who screened 25 models, with 6 markers and found ALDH and CD44 most frequently detected on pCSCs (25/25 and 23/24 models respectively). They also found that CD24 detected sub-populations with high frequency (21/22 models). As shown in Section 4.3, ALDH and CD44 identified pCSC populations in 5 of the 7 models investigated (ALDH: A2780, A2780cis, IGROV-1, IGROV-CDDP and HIO-80; CD44: IGROV-1, IGROV-CDDP, SK-OV-3, 59M and HIO-80), with 99 % confidence. Two of the models consisted of 100 % ALDH+ cells (IGROV-1 and HIO-80), the other three models (A2780, A2780cis and IGROV-CDDP) consisted of ALDH+/- sub-populations. In these models the ALDH+ pCSC sub-population was found to represent less than 0.5 % of the cells. Three of the models consisted of 100 % CD44+ cells (SK-OV-3, 59M and HIO-80), the other two consisted of relatively large CD44+ pCSC sub-populations (IGROV-1: 63 %; IGROV-CDDP: 4 %), when compared to the ALDH+ sub-populations. Only the HIO-80 (NOSE) model was homogeneous for all the markers tested. This suggests that it consists entirely of pSSC cells. Such a finding requires downstream validations to confirm stemness characteristics. These findings correlate with those of (Flesken-Nikitin et al. 2013), who found SSCs of the mouse OSE were ALDH+. The validation systems are established as pairwise comparisons. Without a non-pSSC sub-population to compare it to, the validation of such a pSSC would be more difficult. All of the Ovarian Cancer models, including the models 100 % ALDH+ cells and 100 % CD44+ cells, contained pCSC marker positive and negative sub-populations. This finding suggests that there may be multiple types of pCSCs, even within a cell line model. This finding of hierarchical pCSC sub-populations is consistent with the findings of Silva et al. (2011), who put forward a hierarchical model of: 'stem cell' (ALDH+/CD133+) → 'intermediate transiently amplifying cell' (ALDH+) → 'late transiently amplifying cell' (ALDH-/CD133-) → 'differentiated cell' (unknown markers). This Silva et al. model was not based on direct evidence of a hierarchy but rather based on the indirect evidence of tumourgenicity and spheroid formation data.

After ALDH and CD44, CD133 was the most widely detected pCSC marker. CD133+/- sub-populations were identified in three models (A2780, IGROV-CDDP and 59M). While all other pCSC markers were either present or absent in both parent and daughter cell lines (A2780 and A2780cis; IGROV-1 and IGROV-CDDP), the CD133+ pCSC sub-populations did not conform to this trend. This will be discussed further in Section 4.4.4.4.3.

HSP+/- were identified in 2 models, the parent daughter pair of IGROV-1 and IGROV-CDDP. The HSP+ sub-populations (4.12 % – 15.46 %) were an order of magnitude bigger than the

ALDH+ and CD133+ sub-populations (0.06 % – 1.33 %) identified within the heterogeneous models. Szotek et al. (2006) also identified a HSP+ sub-population within the IGROV-1 cell line. However, the reported size (0.19 %) differs greatly to the findings presented here (4.12 % +/- 0.86 %; Section 4.3.2).

The CD117 pCSC marker also identified CD117+/- sub-populations within one model (SK-OV-3). This low frequency of CD117+ sub-populations across the various models correlates with observations of Curley et al (2009) and Silva et al. (2011) who only detected CD117+/- sub-populations in 0/5 and 8/21 models respectively.

The CXCR4 putative metastatic cell marker did not identify any putative metastatic cells in any of the models. CXCR4 has been linked to chemotaxis (Kucia et al. 2004) and has been demonstrated to mark a metastatic stem cell component in pancreatic cancer (Hermann et al. 2007). SK-OV-3 and 59M are Ovarian Cancer models derived from metastatic ascites (Hills et al. 1989). As such, they were considered to be good candidates for identifying a metastatic stem cell component. The data presented (Section 4.3.3) coincides with the findings of Scotton et al. (2001), who identified SK-OV-3 as a CXCR4- cell line via RNase protection assay. In isolation, these results suggest that CXCR4 does not play a central role in Ovarian Cancer metastasis. However, Scotton et al, did detect CXCR4 in 90 % (18/20) of ascites patient samples and 80 % (8/10) of tumour samples tested. Of the eight CXCR4+ tumour samples five had very weak banding patterns. Of the 18 CXCR4+ ascites samples 17 had very prominent banding patterns (Scotton et al. 2001). This suggests that perhaps the cell culturing of ascites derived cells, reverts the phenotype back to a CXCR4 low/negative phenotype. Supporting this idea, are the findings of Kusumbe et al. (2009). They generated 19 clones from patient ascites, and found that 8 of 19 of the clones had less than 5 % CXCR4+ cells. Only 5 clones had >40 % CXCR4+ cells.

4.4.4.2 Poor Correlation between OvCSC markers:

pCSCs/pSSCs were identified in all models examined. However, no single pCSC marker or set of markers identified pCSCs across all the models analysed. This correlates with what is also observed in the literature. Many papers have been published identifying OvCSCs. However, few have identified OvCSCs using the same pCSC markers. Silva et al. (2011) published the results of a large OvCSC screen, although they only focused on the validation of OvCSCs based on two of the markers (ALDH and CD133). This approach demonstrates a move away from attempting to classify cells as either CSCs or non-CSCs, to acknowledging that many

overlapping populations may exist within ovarian cancer. Older papers often focus on one or two pCSC markers when identifying OvCSCs and fail to comment on whether the OvCSC populations isolated express any of the other markers used to identify OvCSC across the literature. As discussed in Section 4.4.2, Zhang et al. (2008) identified CD44+/CD117+ cells as being OvCSCs while identifying CD44-/CD117- cells as non-OvCSCs population. No data was presented on any CD44+/CD117- or CD44-/CD117+ populations. Based on the Alvero et al. (2009) findings that CD44+ is a marker of chemoresistance perhaps CD44-/CD117+ cells could be chemosensitive stem cells and CD44+/CD117- cells could be differentiated cells with acquired chemoresistance.

Curley et al. (2009) identified CD133+ cells as OvCSCs and CD133- cells as non-OvCSCs. They were using tumour samples, and found that CD133 was the only population that identified sub-populations across all the samples. They also investigated the expression of CD44 and CD117, finding that CD44 was expressed across 5 of 5 primary tumours tested and CD117 was not expressed on any. The overlaps between CD44 and CD133 were not characterised. Kusumbe et al. (2009) found that clones isolated from the ascites of patient samples with a CD133+/- phenotype were non-tumourigenic, while clones with a 100 % CD133- phenotype were tumourigenic. They went on to show that although the CD133+/- clones could not form tumours, they could contribute to the vasculature of tumours. Kusumbe et al. (2009) stated that they assessed CD44 and CD117 expression in all clones, but only presented data from an unspecified clone, which indicates that the CD133+ cells were in fact CD133+/CD44+/CD117+. This suggests that this is at direct odds with the findings of Zhang et al. (2008) who identified CD44+/CD117+ cells as being tumourigenic.

There are many publications, which have identified OvCSC based on a variety of pCSC markers (ALDH, HSP, CD44, CD117, CD133). The poor correlation between markers and the apparently contradictory results may all stem from the negligible understanding of cellular differentiation in NOSE and Ovarian Cancer. There may be multiple different lineages, each with different patterns of differentiation marker expression. All of the assays implemented in CSC biology only give evidence for one population being more stem-like than another. Current techniques can never claim to have identified the one true stem cell population. Only that a more CSC-like population has been enriched form a more heterogeneous population. It is possible that cancerous tissues have stem-like, progenitor and differentiated cancer cells arranged in a hierarchical fashion. It is important to correlate all OvCSC populations to other

OvCSC markers identified across the literature. This will allow for a set of consensus hierarchies to be developed for OvCSC.

4.4.4.3 Hierarchical OvCSCs:

The pCSC screen results identified overlapping and non-overlapping pCSC populations in multiple models. Due to time constraints, it was not possible to experimentally define all of the overlaps. However, due to the differing sizes of the sub-populations many of the possible sub-sets can be deduced. These possible sub-sets will be described as they relate to each model (Sections 4.4.4.3.1 – 4.4.4.3.7). All populations discussed are only putative sub-populations, until validated in downstream analysis.

4.4.4.3.1 A2780 Hierarchies

As shown in Section 4.3.5.1, two pCSC sub-populations were identified within the A2780 cell line; ALDH (0.15 % +/- 0.02 %) and CD133 (0.06 % +/- 0.02 %). The ALDH+ sub-population is significantly bigger than the CD133+ sub-population (2.45 fold bigger; p-value < 0.003). This demonstrates that the ALDH and CD133 pCSC markers do not mark all of the same cells. It can be deduced that the A2780 cell line consists of mostly ALDH-/CD133- cells and definitely contains a ALDH+/CD133- sub-population. The A2780 cell line possibly contains ALDH+/CD133+ and/or ALDH-/CD133+ cells. Deng et al. (2010) also reported the presence of an ALDH+ sub-population (0.07 % +/- 0.06 %) in the A2780 cell line. They did not investigate the presence of CD133+ cells. Silva et al. (2011), Identified both ALDH+ and CD133+ cells within the A2780 cell line. The reported sizes of the sub-populations (ALDH+: 9.00 %; CD133+: 10.01 %) were considerably larger to what was identified in Section 4.3 (ALDH+: 0.15 % +/- 0.02 %; CD133+: 0.06 % +/- 0.02 %). Silva et al. went on to identify that 1.01% of the cells were ALDH+/CD133+, which by deduction, indicates the presence of a 9 % ALDH-/CD133+ sub-population.

Silva et al. also identified the A2780 cell line as being 78.43 % positive for CD117. Whereas the data presented above (Section 4.3.3) identifies it as 100 % CD117-. This result is most likely due to divergence between the two sets of A2780 models as the same antibody clone was used in each study (Clonal identifier: 104D2).

4.4.4.3.2 A2780cis Hierarchies

As shown in Section 4.3.5, only one sub-population was identified within the A2780cis cell line; ALDH (0.36 % +/- 0.03 %). This reduction in sub-population complexity, compared to the A2780 cells, is perhaps reflective of the selective pressures endured when the A2780cis cells were adapted to cisplatin treatment.

4.4.4.3.3 IGROV-1 Hierarchies

As shown in Section 4.3.5, three pCSC sub-populations were identified within the IGROV-1 cell line; ALDH (95.01 % +/- 2.23 %), HSP (4.12 % +/- 0.56 %) and CD44 (62.69 % +/- 9.64 %). No ALDH- sub-population was identified with 99 % confidence so the IGROV-1 cell line was considered 100 % ALDH+. Based on these findings, the IGROV-1 cell line could be considered a 100 % pCSC population. However, as sub-populations of HSP and CD44 are present, it can be said that not all of the pCSCs are the same. This suggests a pCSC hierarchy is present within the IGROV-1 cell line. The CD44+ sub-population is significantly bigger than the HSP+ sub-population (15.22 fold bigger; p-value < 0.0086). From these observations, it can be deduced that the IGROV-1 cell line definitely has a ALDH+/HSP-/CD44- and a ALDH+/HSP-/CD44+ sub-population. The IGROV-1 cell line also contains ALDH+/HSP+/CD44+ and/or ALDH+/HSP+/CD44- sub-populations.

4.4.4.3.4 IGROV-CDDP Hierarchies

As shown in Section 4.3.5, four pCSC sub-populations were identified within the IGROV-CDDP cell line; ALDH (0.41 % +/- 0.08 %), HSP (15.46 % +/- 4.49 %), CD44 (4.32 % +/- 0.88 %) and CD133 (1.33 % +/- 0.16 %). Preliminary experiments indicate that the ALDH+ and CD133+ sub-populations are mutually exclusive (Section 4.3.4). Further replicates would be required to ensure that this is a consistent observation. Further multi-parametric experiments indicated that both ALDH+/CD133- and ALDH-/CD133+ cells had both HSP+ and HSP- sub-populations. It was found that ALDH+/CD133- cells were HSP+ enriched and the ALDH-/CD133+ cells were HSP+ depleted when compared to the cell line as a whole. Further work is required to confirm that these observations can be made consistently. The single parametric pCSC screen found that the HSP+ sub-population is significantly bigger than the CD44+ sub-population (3.58 fold bigger; p-value < 0.046). Together, these observations indicate that of the 16 possible combinations of pCSC sub-populations, 4 can be excluded as ALDH+ and CD133+ cells appear to be mutually exclusive. Of the remaining 12 combinations, at least 4 sub-populations are likely to exist as they have either been directly or indirectly

observed (Table 4.14). A further 8 sub-populations may also exist with no supportive or dismissive evidence available (Table 4.14).

Table 4.14: Summary of the possible sub-populations present in the IGROV-CDDP cell line.

Status	Sub-population phenotype
Likely	ALDH+/HSP+/CD44-/CD133-
Likely	ALDH-/HSP+/CD44-/CD133+
Likely	ALDH-/HSP+/CD44-/CD133-
Likely	ALDH-/HSP-/CD44-/CD133-
Possible	ALDH-/HSP+/CD44+/CD133+
Possible	ALDH+/HSP+/CD44+/CD133-
Possible	ALDH+/HSP-/CD44+/CD133-
Possible	ALDH+/HSP-/CD44-/CD133-
Possible	ALDH+/HSP+/CD44+/CD133-
Possible	ALDH-/HSP+/CD44+/CD133-
Possible	ALDH-/HSP-/CD44+/CD133+
Possible	ALDH-/HSP-/CD44+/CD133-

4.4.4.3.5 SK-OV-3 Hierarchies

As shown in Section 4.3.5, two pCSC sub-populations were identified within the SK-OV-3 cell line; CD44 (99.43 % +/- 0.34 %) and CD117 (39.96 % +/- 2.89 %). No CD44- sub-population was identified with 99 % confidence, so the SK-OV-3 cell line was considered 100 % CD44+. Based on these findings, the SK-OV-3 cell line could be considered a 100 % pCSC population. However, as a sub-population of CD117 is present, it can be said that not all of the pCSCs are the same. SK-OV-3 consists of CD44+/CD117+ and CD44+/CD117- pCSC sub-populations.

Silva et al. (2011) also identified a large CD44+ sub-population (90.00 %) within the SK-OV-3 cell line. No standard deviation was presented for this measurement so it is possible to calculate the 99 % confidence interval. Silva et al. did not detect a CD117+ sub-population, within the SK-OV-3 cell line but did detect an ALDH+ (4.19 %) and CD133+ (0.33 %) sub-population. Baba et al. (2008) et al did not detect a CD133+ sub-population in the SK-OV-3 cell line.

4.4.4.3.6 59M Hierarchies

As shown in Section 4.3.5, two pCSC sub-populations were identified within the 59M cell line; CD44 (99.51 % +/- 0.69 %) and CD133 (0.19 % +/- 0.01 %). No CD44- sub-population was identified with 99 % confidence, so the 59M cell line was considered 100 % CD44+. Based on

these findings, the 59M cell line could be considered a 100 % pCSC population. However, as a sub-population of CD133 is present, it can be said that not all of the pCSCs are the same. 59M consists of CD44+/CD133+ and CD44+/CD133- pCSC sub-populations.

4.4.4.3.7 HIO-80 Hierarchies

As shown in Section 4.3.5, two pCSC sub-populations were identified within the HIO-80 cell line; ALDH (94.53 % +/- 4.00 %) and CD44 (94.81 % +/- 3.27 %). No ALDH- or CD44- sub-populations were identified with 99 % confidence, so the HIO-80 cell line was considered 100 % ALDH+/CD44+. Based on these findings, the HIO-80 cell line could be considered a 100 % pSSC population. The HIO-80 cell line was the only homogeneous model identified in the screen.

4.4.4.4 Comparison of pCSCs between models.

Multiple diverse models were utilised in this study, to allow observations to be made on the roles of OvCSCs in the many aspects of Ovarian malignancy. The similarities and contrasts of the pCSCs identified in all models will be discussed. First, the pCSCs identified within cisplatin sensitive and cisplatin resistant models will be compared and contrasted (Section 4.4.4.4.1). Second, the pCSCs identified within models derived from solid tissues and those derived from ascites will be compared and contrasted (Section 4.4.4.4.2). Finally, the possible role of CD133 pCSCs will be discussed (Section 4.4.4.4.3).

4.4.4.4.1 Cisplatin Sensitive and Cisplatin Resistant pCSCs

There were two pairs of parent/daughter cell lines analysed in the pCSC screen (A2780/A2780cis and IGROV-1/IGROV-CDDP). These parent/daughter pairs both modelled acquired cisplatin resistance within an Ovarian Cancer context. All of the pCSC populations identified in the parent cell lines had significantly changed size with acquired resistance (Table 4.11). A 2.4 fold increase in the size of the ALDH+ sub-population was observed in the A2780 models upon acquired cisplatin resistance. This suggests that ALDH+ pCSCs may play a role in acquired chemoresistance. However, a 231.7 fold decrease in the size was observed in the IGROV models upon acquired cisplatin resistance. This suggests that ALDH+ cells are not positively selected for with cisplatin resistance. Interestingly, although both the A2780 and the IGROV-1 models originally have significantly different ALDH+ population sizes (p-value < 0.0002). Upon acquired cisplatin resistance the A2780cis and IGROV-CDDP models do not demonstrate a significant difference between the size (p-value $= 0.4451$). Deng et al. (2010) also observed an increase in population size of ALDH+ cells from the A2780 parent cell

line to the acquired cisplatin resistant daughter cell lines (A2780/CP70, A2780/C200 and A2780/C30). They reported an increase from 0.07 % ALDH+ in the cisplatin sensitive A2780 cell line to 0.2 % – 2.1 % in the cisplatin resistant daughter cell lines. They also demonstrated a non-dose dependent cisplatin mediated expansion of the ALDH+ pCSC sub-population *in vivo* (0.09 % to 0.75 % and 0.42 % ALDH+), by treating mice inoculated with A2780 cells with cisplatin (2 mg/kg or 4 mg/kg every 7 days for 4 weeks) and assaying the percentage of ALDH+ cells in the residual tumours. It is possible a change in the cell types which make up the tumour may contribute to cisplatin resistance. This hypothesis will be discussed further in Section 6.4.3, with respect to data presented in Sections 6.3.1.1.1 and 6.3.2.1.1, as well as the published literature.

Within the IGROV models a 3.75-fold increase in the size of the HSP+ pCSC sub-population was associated with acquired cisplatin resistance. HSP+ cells express multi-drug efflux pumps, and have been associated with chemoresistance (Golebiewska et al. 2011). Both the ALDH+ and the CD44+ pCSC populations exhibited a decrease in size within the IGROV models upon acquired cisplatin resistance. These observations suggests that perhaps the best adapted pCSC sub-population gets selected for upon acquired chemoresistance to the detriment of all other pCSC populations. This could even apply if stemness itself does not convey a chemoresistant advantage. Within a CSC population there could be a range of genetic/epigenetic mutations, one of which could convey chemoresistance. Such a CSC sub-population could survive chemotherapy, divide and differentiate to produce a tumour, in which all cells are resistant to chemotherapy. CD133+ pCSCs also showed altered expression between the cisplatin sensitive and cisplatin resistant cell lines. These changes will be discussed separately in Section 4.4.4.4.3.

4.4.4.4.2 The Role of pCSCs in Metastasis

It was shown that all of the models which were originally derived from solid tissue sources (Cancerous and NOSE; A2780, A2780cis, IGROV-1, IGROV-CDDP and HIO-80) contained ALDH+ pCSC populations (Section 4.3.1). However, no ALDH+ sub-populations were identified within either of the metastatic ascites derived models (SK-OV-3 and 59M). This suggests that while ALDH+ cells may play an important role in the growth and development of solid tumours and the NOSE, they do not contribute to the growth and development of Ovarian metastatic ascites. Silva et al. (2011), screened 13 primary Ovarian tumour samples and 5 ascites samples with the ALDH assay. Their results indicate no significant difference (p-value = 0.2256) between primary tumours (ALDH+: 3.27 % +/- 2.15 %) and ascites (ALDH+: 4.72 %

+/- 2.07 %) with respect to the presence/absence of ALDH+ pCSCs. In a similar fashion to that discussed in Section 4.4.4.1, cultured cell lines derived from ascites may not fully reflect the diversity of sub-populations observed in patient samples. Having said this, Silva et al. did detect ALDH+ (4.19 %) cells within the SK-OV-3 cell line, which disagrees with the ALDH screen for the SK-OV-3 shown above (Section 4.3.1). This could be the result of divergence between models in different labs. Furthermore, no standard deviation was presented by Silva et al flow cytometry data: so it is hard to estimate how reproducible such measurements are.

It was also shown that both of the ascites models (SK-OV-3 and 59M) were 100 % CD44+ (Section 4.3.5.1). Of the other four Ovarian Cancer models, two had smaller CD44+ sub-populations (IGROV-1 and IGROV-CDDP) and two had no CD44+ sub-populations (A2780 and A2780cis). This suggests that CD44+ cells are central to the development of Ovarian ascites. Alvero et al. (2009), reported finding a higher percentage of CD44+ cells in patient ascites and metastatic tumours, compared to primary tumours, they only presented data from 1 representative replicate of 30 samples. Silva et al. (2011), screened 12 primary Ovarian tumour samples and 5 ascites samples for CD44. Their results indicate that primary tumours (CD44+: 65.95 % +/- 29.14 %) have a significantly higher proportion of CD44+ cells (p-value < 0.0072) than ascites (CD44+: 26.39 % +/- 16.74 %). The non-concordance of these results may be due to patient/cell line variation or the different antibody clones in the Silva et al study (antiCD44 antibody clone: G44-26) and this project (antiCD44 antibody clone: F10-44-2). Alvero did not report the antiCD44 antibody clone used. Interestingly, the HIO-80 cell line was also found to be 100 % CD44+ (Section 4.3.5.1). This suggests that CD44+ cells are central to the growth and development of NOSE.

4.4.4.4.3 The Role of the CD133+ pCSC

There were two pairs of parent/daughter cell lines analysed in the pCSC screen (A2780/A2780cis and IGROV-1/IGROV-CDDP). The parent cell lines were derived from human tumours. The daughter cell lines were derived, *in vitro*, from the parent cell lines. With the exception of CD133, all pCSC populations which were identified in a parent cell line were also present in its corresponding daughter cell line (Section 4.3.5). All pCSC populations were significantly altered between parent and daughter cell lines (Section 4.3.5.2). CD133+ cells were present in the A2780 cell line and absent in the A2780cis cell line (Section 4.3.5). While CD133+ cells were absent in the IGROV-1 cell line and present in the IGROV-CDDP cell line (Section 4.3.5). Baba et al. (2008) reported similar findings, A2780 had a CD133+ sub-population and A2780cis and IGROV-1 were CD133-. They did not analyse IGROV-CDDP. In

the case of A2780cis, the disappearance of CD133+ cells is associated with acquired cisplatin resistance, while in the case of IGROV-CDDP, the appearance of CD133+ cells is associated with acquired cisplatin resistance. These observations suggests that either these two cell lines contain unrelated populations of cells marked by CD133+ cells or that the CD133+ cells are an inducible cell type. Rather than being part of a central hierarchy of cell differentiation, CD133+ cells may be an inducible phenotype of one or more of the sub-populations of cells within an ovarian tumour. As discussed in Section 4.4.2, the findings of Kusumbe et al. (2009), suggested that CD133+ cells were not OvCSCs as Curley et al. (2009) had proposed. Instead Kusumbe et al. suggested that CD133+ cells were endothelial precursor cells, which aided in more rapid growth of xenograft tumours via enrichment of the tumour vasculature. They showed evidence to support this *in vitro* via a matrigel tube formation assay: demonstrating that 12 of 14 CD133+ clones (isolated from ovarian cancer derived ascites) exhibited the ability to undergo endothelial differentiation. The also presented *in vivo* data showing that CD133+ clones alone (0 of 14) could not form tumours but mixed population clones of what they called CSC+/CD133+ clones formed tumours with larger median weight and more vasculature than CSC+ clones alone. The A2780 cell line has a CD133+ sub-population, while the A2780cis cell line does not (Section 4.3.5.1). As presented in Section 6.3, it was found that the sub-populations isolated from the A2780 cell line, grew xenograft tumours faster than the sub-populations isolated from the A2780cis cell line. The A2780 cells formed tumours with a much richer blood supply than the A2780cis cells. This would appear to agree with the findings of Kusumbe et al. (2009). Kusumbe et al. used samples derived from patient sources, which means it is possible that the CD133+ cells identified may actually be tumour associated endothelial cells. However, the data presented in Section 4.3.3 show IGROV-CDDP cells acquired a CD133+ sub-population *in vitro*, after being derived from from a 100 % CD133- parent cell line (IGROV-1; Section 4.3.3). This suggests that while CD133+ cells may be endothelial precursor cells, they may in fact be malignant equivalents of endothelial precursor cells originating from an ovarian cancer source.

4.4.5 Future Directions:

There are three major future directions with respect to OvCSC screening:

In the short term a comprehensive multi-parametric screen should be completed on all of the sub-populations identified within the single parametric screen as presented in Section 4.3.

Preliminary experiments (Section 4.3.4) suggest the presence of multiple overlapping and non-overlapping sub-populations. Understanding the relationships between these sub-populations could lead to a greater understanding of the role of different cell populations in the growth and development of OvCSC.

In the medium term the screening techniques applied here should be applied to the screening of OvCSCs in patient samples. It would probably be prudent to focus on a small sample size, to allow for the comprehensive characterisation of any overlapping sub-population which may be identified. Over the longer term the data from several such focused studies could be combined to develop a better understanding of the cell biology of ovarian cancer.

In the long term a more generic system for identifying CSCs needs to be developed. Currently new CSC markers are discovered, by marker analysis of cells isolated via selection based CSC screens or using markers discovered SSCs. Lineage tracking experiments correlated to panels of CSPs, have the potential to identify complete cellular hierarchies within tumours, with no prior assumptions about CSC markers or selective conditions.

4.4.6 Summary:

Seven model systems were screened for the presence of pCSCs and pSSCs using a panel of six markers. The pCSC markers directly identified 14 pCSC populations and two pSSC populations across the seven models examined.

Three of the pCSC populations represented 100 % of the cell populations in their given models, with the remaining 11 pCSC populations having a marker negative non-pCSC sub-population in their given models. The pCSC screen also indirectly identified 12 hierarchical sub-populations and 12 theoretical hierarchical pCSC sub-populations.

Both of the pSSC populations, represented 100 % of the cell population in the NOSE model. Thus, they overlapped perfectly, forming one double positive population.

Section 4.0 – Identification of pCSCs

Until validated, all sub-populations can only be considered pCSCs. However, statistically significant differences in pCSC composition have been detected between the model systems screened. In both of the pair-matched cisplatin sensitive/adapted models tested, there was a statistically significant increase in the size of a pCSC sub-population. As discussed in Section 4.4.4.4.1, this is complicated by the presence of multiple pCSC populations within some models. However, the data suggests that CSCs do play a role in the chemo-adaptation of ovarian cancer. This reinforces the hypothesis that therapeutically targeting CSCs may yield a better prognosis for ovarian cancer patients.

Identification of pCSCs:- Primary Findings

Seven model systems were screened for the presence of pCSCs and pSSCs using a panel of six markers.

- 14 pCSC populations and 2 pSSC populations were identified across the 7 models examined.
- 11 of these directly observed pCSC populations had a statistically significant non-pCSC population present in the same model.
- 12 hierarchical pCSC sub-populations were deduced from the single-parametric data or were directly observed via preliminary multi-parametric experiments. A further 12 hierarchical pCSC sub-populations are possibly present within the models, based on the single and multi-parametric data.
- 6 pairs of high ranking pCSC/non-pCSC populations have been identified and brought forward for down stream analysis (**A2780**: ALDH+/-; **A2780cis**: ALDH+/-;**IGROV-1:** HSP+/-; **IGROV-CDDP:** HSP+/-; **SK-OV-3:** CD44+/CD117+/-; **59M:** CD44+/CD117+/-).

Section 4.0 – Identification of pCSCs

4.5 References:

Alvero, A.B., R. Chen, H.H. Fu, M. Montagna, P.E. Schwartz, T. Rutherford, D.A. Silasi, et al. 2009. "Molecular Phenotyping of Human Ovarian Cancer Stem Cells Unravel the Mechanisms for Repair and Chemo-resistance." *Cell Cycle (Georgetown, Tex.)* 8 (1): 158.

Baba, T., PA Convery, N. Matsumura, RS Whitaker, E. Kondoh, T. Perry, Z. Huang, et al. 2008. "Epigenetic Regulation of CD133 and Tumorigenicity of CD133+ Ovarian Cancer Cells." *Oncogene* 28 (2): 209–218.

Bapat, S.A., A.M. Mali, C.B. Koppikar, and N.K. Kurrey. 2005. "Stem and Progenitor-like Cells Contribute to the Aggressive Behavior of Human Epithelial Ovarian Cancer." *Cancer Research* 65 (8): 3025.

Curley, M.D., V.A. Therrien, C.L. Cummings, P.A. Sergent, C.R. Koulouris, A.M. Friel, D.J. Roberts, et al. 2009. "CD133 Expression Defines a Tumor Initiating Cell Population in Primary Human Ovarian Cancer." *Stem Cells* 27 (12): 2875–2883.

Deng, S., X. Yang, H. Lassus, S. Liang, S. Kaur, Q. Ye, C. Li, et al. 2010. "Distinct Expression Levels and Patterns of Stem Cell Marker, Aldehyde Dehydrogenase Isoform 1 (ALDH1), in Human Epithelial Cancers." *PLoS One* 5 (4): e10277.

Flesken-Nikitin, Andrea, Chang-Il Hwang, Chieh-Yang Cheng, Tatyana V. Michurina, Grigori Enikolopov, and Alexander Yu Nikitin. 2013. "Ovarian Surface Epithelium at the Junction Area Contains a Cancer-prone Stem Cell Niche." *Nature* 495 (7440): 241–245.

Golebiewska, Anna, Nicolaas H C Brons, Rolf Bjerkvig, and Simone P Niclou. 2011. "Critical Appraisal of the Side Population Assay in Stem Cell and Cancer Stem Cell Research." *Cell Stem Cell* 8 (2) (February 4): 136–147. doi:10.1016/j.stem.2011.01.007.

Gottesman, Michael M. 2002. "Mechanisms of Cancer Drug Resistance." *Annual Review of Medicine* 53: 615–627. doi:10.1146/annurev.med.53.082901.103929.

Hermann, Patrick C, Stephan L Huber, Tanja Herrler, Alexandra Aicher, Joachim W Ellwart, Markus Guba, Christiane J Bruns, and Christopher Heeschen. 2007. "Distinct Populations of Cancer Stem Cells Determine Tumor Growth and Metastatic Activity in Human Pancreatic Cancer." *Cell Stem Cell* 1 (3) (September 13): 313–323. doi:10.1016/j.stem.2007.06.002.

Hills, C. A., L. R. Kelland, G. Abel, J. Siracky, A. P. Wilson, and K. R. Harrap. 1989. "Biological Properties of Ten Human Ovarian Carcinoma Cell Lines: Calibration in Vitro Against Four Platinum Complexes." *British Journal of Cancer* 59 (4): 527.

Kessler, M., C. Fotopoulou, C. Winsauer, O. Thieck, and T. F. Meyer. 2012. "Abstract 3373: Identification of the Stem Cells in the Epithelium of Human Fallopian Tube." *Cancer Research* 72 (8 Supplement) (June 4): 3373–3373. doi:10.1158/1538-7445.AM2012-3373.

Kucia, Magda, Kacper Jankowski, Ryan Reca, Marcin Wysoczynski, Laura Bandura, Daniel J Allendorf, Jin Zhang, Janina Ratajczak, and Mariusz Z Ratajczak. 2004. "CXCR4-SDF-1 Signalling, Locomotion, Chemotaxis and Adhesion." *Journal of Molecular Histology* 35 (3) (March): 233–245.

Kusumbe, Anjali P., Avinash M. Mali, and Sharmila A. Bapat. 2009. "CD133-Expressing Stem Cells Associated with Ovarian Metastases Establish an Endothelial Hierarchy and Contribute to Tumor Vasculature." *STEM CELLS* 27 (3): 498–508. doi:10.1634/stemcells.2008-0868.

Patrawala, L., T. Calhoun, R. Schneider-Broussard, J. Zhou, K. Claypool, and D. G. Tang. 2005. "Side Population Is Enriched in Tumorigenic, Stem-like Cancer Cells, Whereas ABCG2+ and ABCG2- Cancer Cells Are Similarly Tumorigenic." *Cancer Research* 65 (14): 6207–6219.

Pfeiffer, Minja J., and Jack A. Schalken. 2010. "Stem Cell Characteristics in Prostate Cancer Cell Lines." *European Urology* 57 (2) (February): 246–255. doi:10.1016/j.eururo.2009.01.015.

Scotton, C J, J L Wilson, D Milliken, G Stamp, and F R Balkwill. 2001. "Epithelial Cancer Cell Migration: a Role for Chemokine Receptors?" *Cancer Research* 61 (13) (July 1): 4961–4965.

Silva, Ines A, Shoumei Bai, Karen McLean, Kun Yang, Kent Griffith, Dafydd Thomas, Christophe Ginestier, et al. 2011. "Aldehyde Dehydrogenase in Combination with CD133 Defines Angiogenic Ovarian Cancer Stem Cells That Portend Poor Patient Survival." *Cancer Research* 71 (11) (June 1): 3991–4001. doi:10.1158/0008-5472.CAN-10-3175.

Szotek, P. P., R. Pieretti-Vanmarcke, P. T. Masiakos, D. M. Dinulescu, D. Connolly, R. Foster, D. Dombkowski, F. Preffer, D. T. MacLaughlin, and P. K. Donahoe. 2006. "Ovarian Cancer Side

Population Defines Cells with Stem Cell-like Characteristics and Mullerian Inhibiting Substance Responsiveness." *Proceedings of the National Academy of Sciences* 103 (30): 11154–11159.

Szotek, Paul P, Henry L Chang, Kristen Brennand, Akihiro Fujino, Rafael Pieretti-Vanmarcke, Cristina Lo Celso, David Dombkowski, et al. 2008. "Normal Ovarian Surface Epithelial Label-retaining Cells Exhibit Stem/progenitor Cell Characteristics." *Proceedings of the National Academy of Sciences of the United States of America* 105 (34) (August 26): 12469–12473. doi:10.1073/pnas.0805012105.

Tan, Lei, Xin Sui, Hongkui Deng, and Mingxiao Ding. 2011. "Holoclone Forming Cells from Pancreatic Cancer Cells Enrich Tumor Initiating Cells and Represent a Novel Model for Study of Cancer Stem Cells." *PloS One* 6 (8): e23383. doi:10.1371/journal.pone.0023383.

Vasiliou, Vasilis, and Daniel W Nebert. 2005. "Analysis and Update of the Human Aldehyde Dehydrogenase (ALDH) Gene Family." *Human Genomics* 2 (2) (June): 138–143.

Zhang, S., C. Balch, M.W. Chan, H.C. Lai, D. Matei, J.M. Schilder, P.S. Yan, T.H.M. Huang, and K.P. Nephew. 2008. "Identification and Characterization of Ovarian Cancer-initiating Cells from Primary Human Tumors." *Cancer Research* 68 (11): 4311.

Isolation of Putative Cancer Stem Cells.

Section 5.0 – Isolation of pCSCs

5.1 Introduction:

5.1.1 The Role of Cell Sorting in Cancer Biology:

CSCs are hard to study as they only represent a small fraction of the tumour tissue. Very few models of CSCs exist and no models of Ovarian CSCs (OvCSCs) exist. Therefore, to study OvCSCs, they must first be identified within a heterogeneous source and purified.

Cancer research often focuses on the genetic mutations which correlate with oncogenesis or the molecular pathways associated with malignant growth, invasion and recurrence. This approach has greatly contributed to the understanding, screening and treatment of cancer. For example, genetic studies led to the identification of the BRCA1 and BRAC2 genes and their cancer associated mutations (Miki et al. 1994; Wooster et al. 1995). Genetic screening for BRCA1 and BRCA2 mutations are now used to inform the prophylactic treatment of women with family histories of breast and ovarian cancer (Kauff et al. 2008). In a similar fashion, the identification of the BCR-ABL fusion protein and its inhibitor Imantinib was a breakthrough in the treatment of chronic myelogenous leukemia (Deininger et al. 2000; Buchdunger, O'Reilly, and Wood 2002). Although such studies have revolutionised the understanding, screening and treatment of cancer, they do have limitations. Ovarian cancer may have its origins in genetic mutations and dysfunctional molecular pathways but it is not a disease of molecules, rather it is a disease of tissues. It is important to understand how the various genetic mutations and dysfunctional molecular pathways contribute to the functioning of the cells which make up the malignant tissue.

This project focuses on the study of CSCs, which are believed to be the root population from which all the other cell types in the malignancy are derived. Other studies focus on circulating tumour cells (Kallergi et al. 2008; Aktas et al. 2009), which are believed to be the cells responsible for establishing distant metastases. Treatments need to target these tumourigenic cells to prevent relapse and cure patients. Comparisons of the molecular biology of CSCs isolated from chemosensitive and chemo-adapted ovarian cancer should divulge some insight into how an initially chemosensitive ovarian tumour can go into remission and recur in a chemoresistant form. A better understanding of such mechanisms may lead to better treatments and better prognosis for patients.

Screening for, and cell sorting of different sub-populations of cells within cancerous tissues forms the foundation for investigating how different cell types contribute to the different

aspects of malignancy, such as proliferation, invasion and metastasis. Different cell types can be isolated from from malignant tissue and molecular, tissue culture and *in vivo* techniques can be used to probe the role of each cell type in the cancerous tissue. CSC biology and more recently circulating tumour cell biology are at the forefront of this cell biology based approach to studying cancer. Studying the molecular biology of individual cell types may provide information on why some cells manage to evade therapy and regenerate chemoresistant disease. A better understanding of such mechanisms may lead to better treatments and better prognosis for patients.

5.1.2 Approaches to CSC Isolation:

The different approaches to isolating pCSCs were discussed in detail in Section 1.10. In a similar fashion to identification of pCSCs, the approaches to the isolation of pCSCs can be categorised into selection and screening based approaches. Spheroid (Zhang et al. 2008) and Holoclone growth (Tan et al. 2011) are selection based approaches to the isolation of pCSCs. They utilise tissue culture techniques to exert selective pressures which enrich for pCSCs.

Such selection based approaches can not be used to isolate specific sub-populations based on pCSC marker expression. These selection based approaches were considered inferior to the screening based approach. As such, a screening based approach that can isolate both pCSC and non-pCSC sub-populations was utilised in this project. The two main techniques which fall under the category of screening based isolation are Fluorescence-Activated Cell Sorting (FACS) and Magnetic-Activated Cell Sorting (MACS).

FACS uses all the same staining techniques that were used in the Flow Cytometry based pCSC screen. The FACS hardware is essentially a flow cytometer with cell sorting hardware added on. FACS is based on deflecting charged droplets, which contain cells, in an electromagnetic field. MACS utilises magnetic micro-beads attached to antibodies, to isolate pCSCs and non-pCSCs. The magnetic micro-beads bind to the cells of interest via antibodies. These cells are then attracted towards a magnet and sorted into a collection tube. All of the cells, not attracted towards the magnet, are collected into a separate collection tube. MACS can not estimate the post-sort purity, so sorted samples need to be run on a flow cytometer to estimate this. MACS can only sort a cell suspension into two sub-populations. The MoFlo™ cell sorter can sort a cell suspension into four sub-populations. MACS is more scalable than FACS: MACS can sort larger numbers of cells without significantly increasing the sort time, whereas the FACS sort

time is directly proportional to the cell number being sorted. This makes MACS followed by FACS a powerful tool for sorting small sub-populations (< 2 %). However, MACS is not as favourable to FACS for larger sub-populations.

As MACS is antibody mediated it is only compatible with one of the pCSC screens used in this project – the CSP assay. Both the ALDH and HSP assay are not compatible with MACS, as they are not antibody based assays. Therefore the sub-populations identified by theses assays had to be sorted via FACS. As the sub-populations identified via the CSP assay were relatively large, it was decided that a FACS only approach was the best approach to cell sorting.

5.1.3 Prioritisation of pCSC for Isolation:

The pCSC screen identified multiple pCSC and non-pCSC sub-populations. Ultimately, each of these sub-populations need to be isolated and studied to understand the role they play in ovarian cancer.

There were too many sub-populations identified to be able to isolate and study them all within this project. For this reason a selection of pCSCs and non-pCSCs were brought forward for isolation (Table 4.13). These sub-populations were selected ahead of the others, as they were considered to be the best selection to elucidate the role CSCs play in acquired chemoresistance in Ovarian Cancer. The logic behind these decisions was discussed in Section 4.3.5.

5.1.4 Summary:

A FACS based approach was adopted to isolate pCSC and non-pCSC populations, enabling their downstream analysis. The main considerations when isolation pCSCs have been discussed above (Sections 5.1.2 – 5.1.3).

The aim driving the work carried out in this chapter was to isolate pure populations of pCSCs and non-pCSCs, to facilitate the downstream analysis of these populations. There were two hypotheses central to the work presented in this chapter. First, FACS can be used to isolate the pCSC and non-pCSC sub-populations identified in the pCSC screen (Section 4.0) to a high degree of purity. Second, the study of CSCs and non-CSCs in isolation will allow for the development of novel therapeutic to kill or differentiate CSCs. Such therapies should not be susceptible to CSC driven chemoresistant relapse and metastases.

5.2 Materials and Methods:

5.2.1 Cell Culture and Sub-Culture

The A2780, A2780cis, IGROV-1, IGROV-1-CDDP, SK-OV-3, 59M cell lines were used to perform the isolation experiments in this chapter. All cell lines were cultured and sub-cultured as described in Section 2.2.

5.2.2 Flow Cytometry

The following staining protocols were used to label pCSCs and non-pCSCs for cell sorting.

5.2.2.1 ALDH Assay

The ALDH assay was carried out as described in Section 2.5.1.

5.2.2.2 HSP Assay

The HSP assay was carried out as described in Section 2.5.2.

5.2.2.3 CSP Assay

The CSP assay was carried out as described in Section 2.5.1.

5.2.3 FACS

FACS was used to isolate pCSCs and non-pCSCs to a high degree of purity. This cell sorting protocol was carried out as described in Section 2.6. The ALDH Assay was scaled for the first round of cell sorting of the A2780 and A2780cis ALDH+/- sub-populations, as described in Section 3.3.2.1.1. Sorted cells were returned to tissue culture at a high seeding density (70 % – 80 % confluency).

5.3 Data:

The data presented in this section will demonstrate that pCSCs and non-pCSCs were successfully isolated to a high degree of purity (Table 5.1). Four of twelve sub-populations, were not purified sufficiently after one round of cell sorting. Therefore, two rounds of cell sorting were carried out on these sub-populations to obtain the desired purity (> 99 %). One of four of these sub-populations did not sufficiently maintain its marker positive phenotype to obtain a post-sort purity of > 99 % (59M CD117+; Section 5.3.6).

Table 5.1: pCSC and non-pCSCs sub-populations were successfully isolated to a high degree of purity:

Model	pCSC Purity	Non-pCSC Purity
A2780	**ALDH+** (100.00 %)	**ALDH-** (100.00 %)
A2780cis	**ALDH+** (99.35 %)	**ALDH-** (100.00 %)
IGROV1	**HSP+** (99.81 %)	**HSP-** (99.52 %)
IGROV-CDDP	**HSP+** (99.38 %);	**HSP-** (100.00 %);
SK-OV-3	**CD117+** (99.47 %)	**CD117-** (99.08 %)
59M	**CD117+** (90.89 %)	**CD117-** (99.95 %)

The data in this section (Section 5.3) will be presented in the following format. The sub-population sizes measured on the day will be presented using the internal negative controls of each respective assay to establish the positive/negative gating thresholds. The sizes of these sub-populations measured over several replicates were presented and recorded with the pCSC screen data (Section 4.3).

All of the flow cytometry technical controls (as described in Section 1.11.2) were applied to these experiments. Positive controls for each of these assays were presented in Section 3.3.1.5 and will not be presented here. The internal negative controls were used to establish the flow cytometry gates and will be presented here.

5.3.1 A2780

ALDH+ pCSCs and ALDH- non-pCSCs were isolated from the cisplatin sensitive A2780 model. Both sub-populations were isolated to a purity of 100.00 % (Figures 5.1 and 5.2). As the ALDH+ sub-population was very small (0.17 %), the sort was carried out in two phases. First, the ALDH+/- sub-populations were sorted on Enrich mode. Then the ALDH+ enriched sub-population was taken for a second round of cell sorting and was sorted on Single Cell mode. Enrich mode purified the ALDH- non-pCSCs from 99.83 % pure to 100.00 % pure after one round of cell sorting. The ALDH- sub-population had met the > 99 % pure criteria. These ALDH- non-pCSCs were returned to tissue culture and stocks were made. Enrich mode bulked up the proportion of the ALDH+ pCSCs from 0.17 % pure to 52.03 % pure after one round of cell sorting (Figure 5.1). This ALDH+ enriched population was returned to tissue culture to allow for amplification of the cell number. The ALDH+ enriched cells were then further purified via a second round of FACS on Single Cell mode. This purified the ALDH+ cells from from 38.68 % pure to 100.00 % pure (Figure 5.2). The ALDH+ sub-population had met the > 99 % pure criteria. These ALDH+ pCSCs were returned to tissue culture and stocks were made. Now that these pCSCs and non-pCSCs have been isolated they are available for validation assays and downstream analysis.

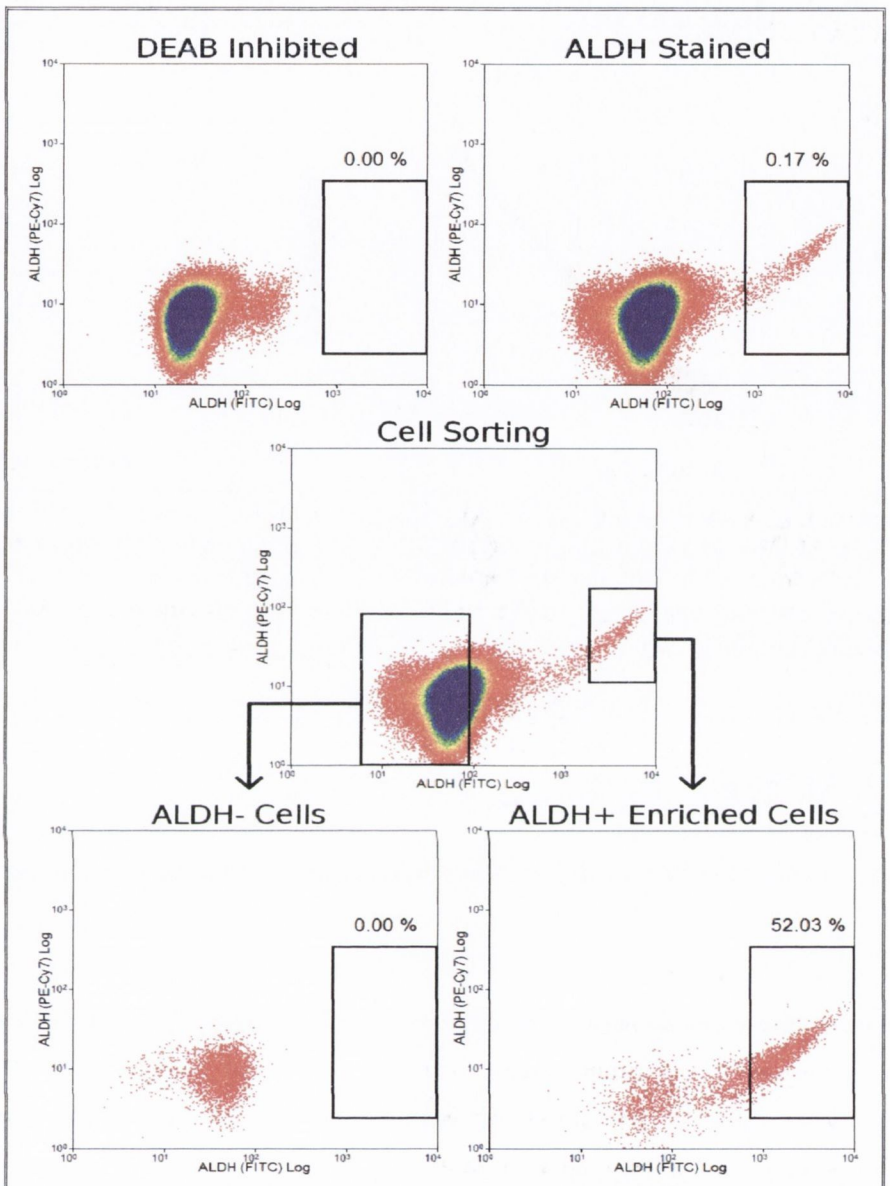

Figure 5.1: ALDH+/- Cell Sorting of the A2780 Cell Line – The A2780 ALDH- non-pCSCs were isolated via FACS, to a purity of 100.00 %. The A2780 ALDH+ pCSCs were isolated via FACS, to a purity of 52.03 %. The top pair of graphs show the ALDH+/- profile of the A2780 cell line prior to cell sorting. The gates are established based on the subtraction of the negative control data (DEAB Inhibited) from the experimental sample (ALDH Stained). The middle graph shows the gates used to sort the A2780 cell line into its ALDH+/- sub-populations. The bottom two graphs show the post-sort purity of the ALDH- and ALDH+ sub-populations.

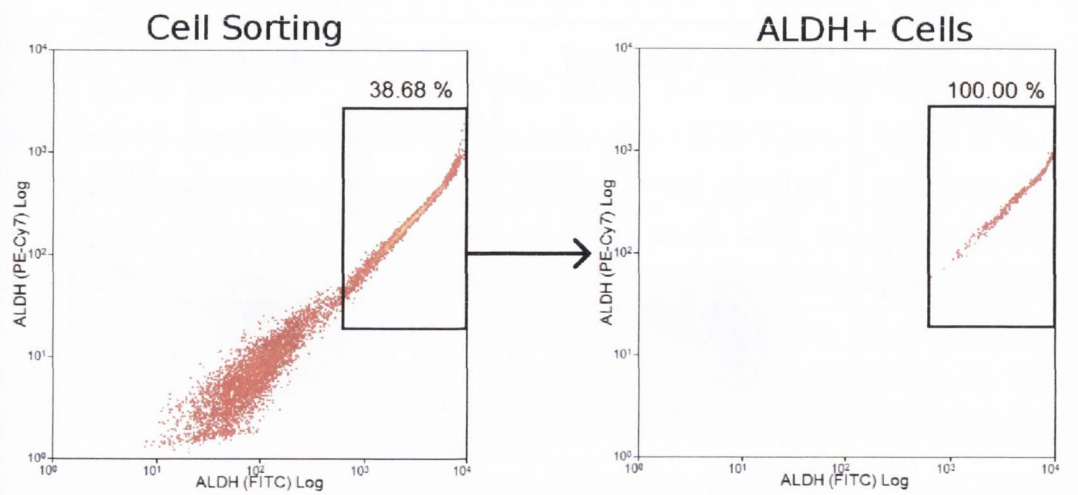

Figure 5.2: Second round A2780 ALDH+ purification - Second round FACS purified A2780 ALDH+ pCSCs to a purity of 100.00 %. The graph on the left shows the gate used to sort cells from the A2780 ALDH+ Enriched Cells obtained from first round cell sorting of the A2780 cell line. The graph on the right shows the second round post sort purity of the ALDH+ sub-population.

5.3.2 A2780cis

ALDH+ pCSCs and ALDH- non-pCSCs were isolated from the cisplatin resistant A2780cis model. As the ALDH+ sub-population was very small (0.79 %), the sort was carried out in two phases. First, the ALDH+/- sub-populations were sorted on Enrich mode. Then the ALDH+ enriched sub-population was taken for a second round of cell sorting and was sorted on Single Cell mode. Enrich mode purified the ALDH- non-pCSCs from 99.21 % pure to 100.00 % pure after one round of cell sorting (Figure 5.3). The ALDH- sub-population had met the > 99 % pure criteria. These ALDH- non-pCSCs were returned to tissue culture and stocks were made. Enrich mode bulked up the proportion of the ALDH+ pCSCs from 0.79 % pure to 61.90 % pure after one round of cell sorting (Figure 5.3). This ALDH+ enriched population was returned to tissue culture to allow for amplification of the cell number. The ALDH+ enriched cells were then further purified via a second round of FACS on Single Cell mode. This purified the ALDH+ cells from 61.39 % pure to 99.35 % pure (Figure 5.4). The ALDH+ sub-population had met the > 99 % pure criteria. These ALDH+ pCSCs were returned to tissue culture and stocks were made. Now that these pCSCs and non-pCSCs have been isolated they are available for validation assays and downstream analysis.

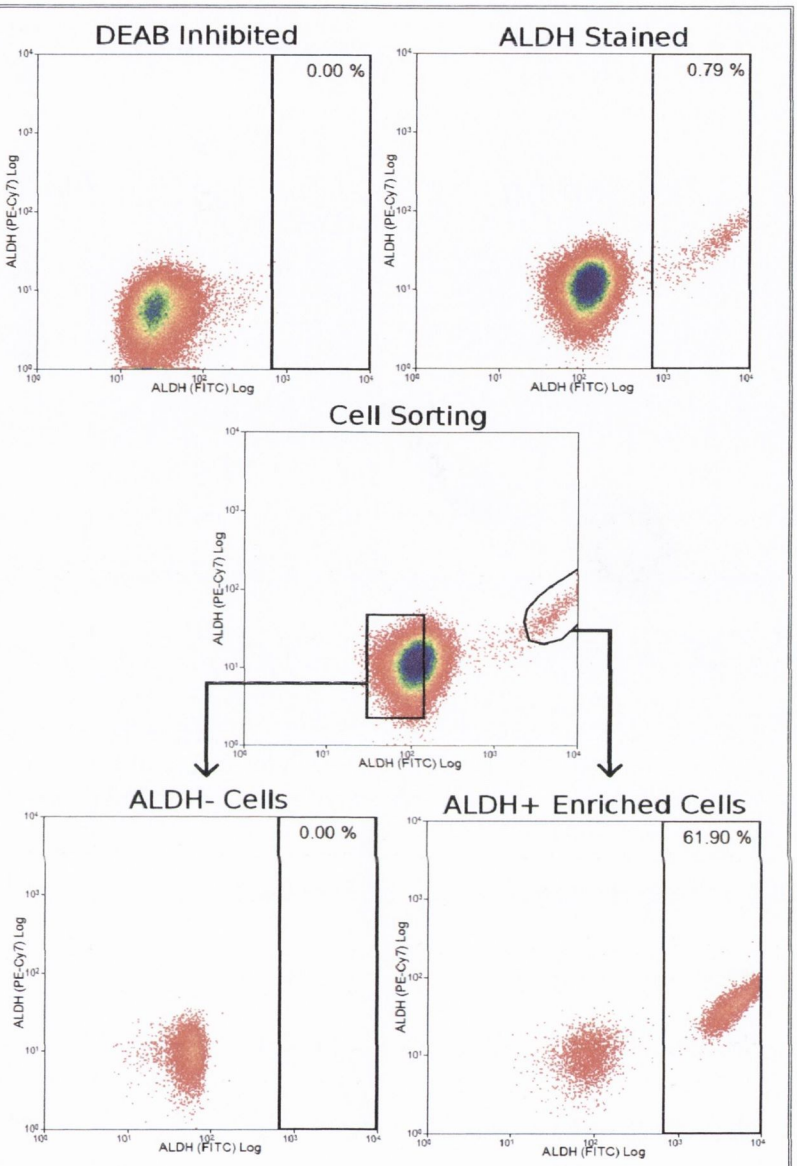

Figure 5.3: ALDH+/- Cell Sorting of the A2780cis Cell Line – The A2780cis ALDH- non-pCSCs were isolated via FACS, to a purity of 100.00 %. The A2780 ALDH+ pCSCs were isolated via FACS, to a purity of 61.90 %. The top pair of graphs show the ALDH+/- profile of the A2780cis cell line prior to cell sorting. The gates are established based on the subtraction of the negative control data (DEAB Inhibited) from the experimental sample (ALDH Stained). The middle graph shows the gates used to sort the A2780cis cell line into its ALDH+/- sub-populations. The bottom two graphs show the post-sort purity of the ALDH- and ALDH+ sub-populations.

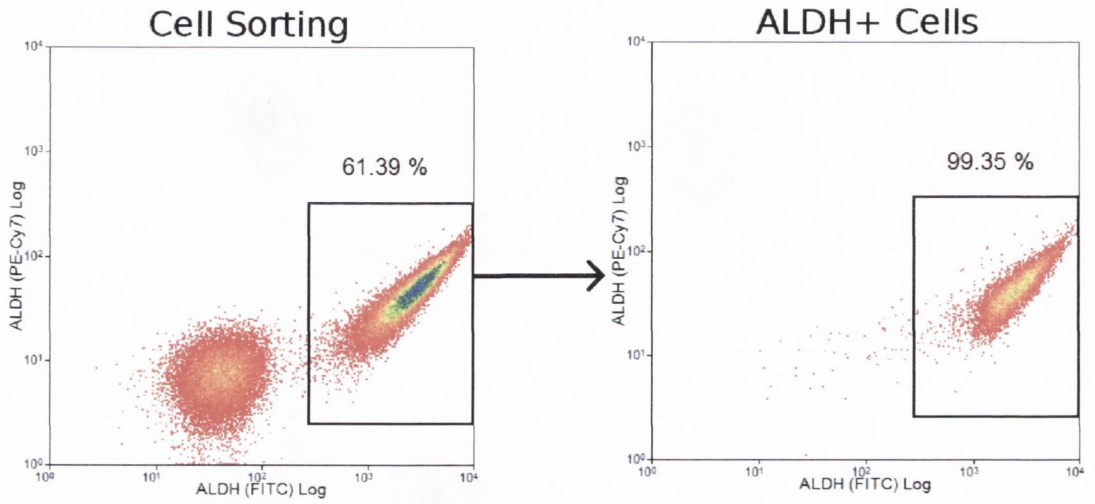

Figure 5.4: Second round A2780cis ALDH+ purification - Second round FACS purified A2780cis ALDH+ pCSCs to a purity of 99.35 %. The graph on the left shows the gate used to sort cells from the A2780 ALDH+ Enriched Cells obtained from first round cell sorting of the A2780cis cell line. The graph on the right shows the second round post sort purity of the ALDH+ sub-population.

5.3.3 IGROV-1

HSP+ pCSCs and HSP- non-pCSCs were isolated from the cisplatin sensitive IGROV-1 model. These sub-populations were sufficiently big to only require one round of FACS to purify them to > 99 % pure. The HSP+/- sub-populations were sorted using Single Cell mode. The HSP+ pCSCs were enriched from 8.28 % pure to 99.81 % pure after one round of cell sorting (Figure 5.5). HSP- non-pCSCs were enriched from 91.72 % pure to 99.52 % pure after one round of cell sorting (Figure 5.5). These isolated sub-populations were returned to tissue culture ahead of their downstream analysis. Now that these pCSCs and non-pCSCs have been isolated the are available for validation assays and downstream analysis.

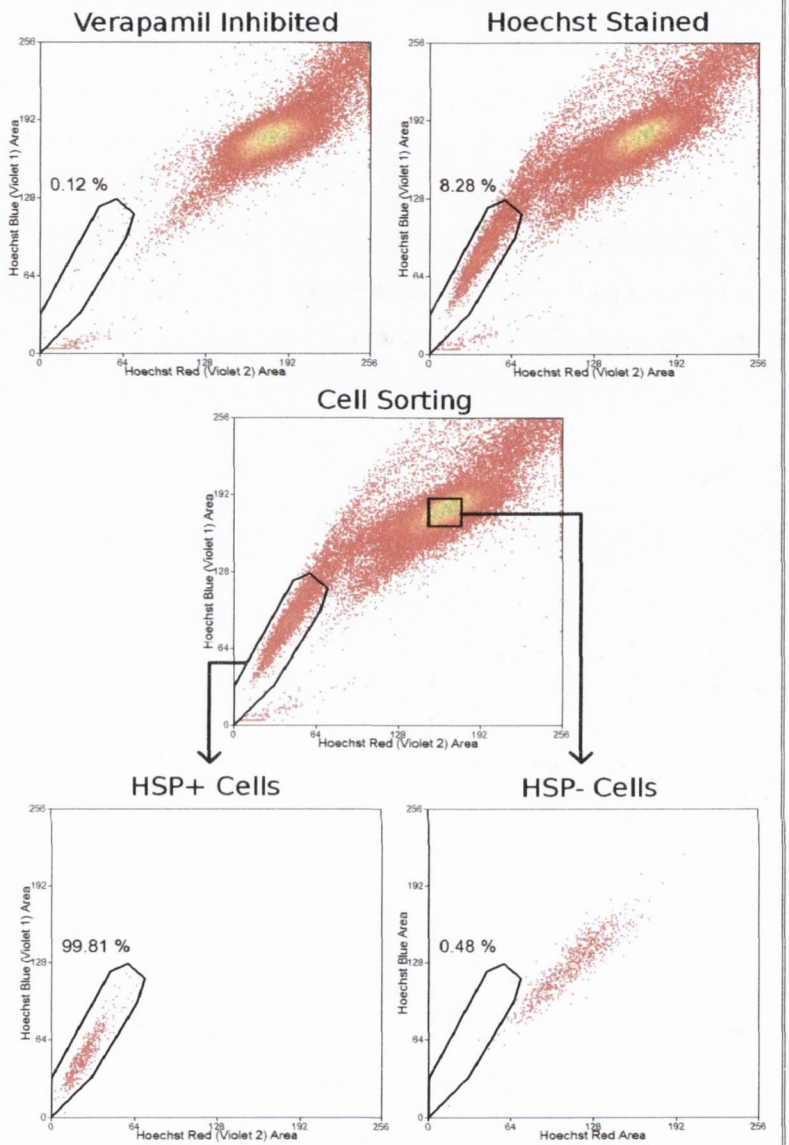

Figure 5.5: HSP+/- Cell Sorting of the IGROV-1 Cell Line – The IGROV-1 HSP+ pCSCs were isolated via FACS, to a purity of 99.81 %. The IGROV-1 HSP- non-pCSCs were isolated via FACS, to a purity of 99.52 %. The top pair of graphs show the HSP+/- profile of the IGROV-1 cell line prior to cell sorting. The gates are established based on the subtraction of the negative control data (Verapamil Inhibited) from the experimental sample (Hoechst Stained). The middle graph shows the gates used to sort the IGROV-1 cell line into its HSP+/- sub-populations. The bottom two graphs show the post-sort purity of the HSP- and HSP+ sub-populations.

5.3.4 IGROV-CDDP

HSP+ pCSCs and HSP- non-pCSCs were isolated from the cisplatin sensitive IGROV-1 model. These sub-populations were sufficiently big to only require one round of FACS to purify them to > 99 % pure. The HSP+/- sub-populations were sorted using Single Cell mode. The HSP+ pCSCs were enriched from 26.13 % pure to 99.38 % pure after one round of cell sorting (Figure 5.6). HSP- non-pCSCs were enriched from 73.87 % pure to 100.00 % pure after one round of cell sorting (Figure 5.6). These isolated sub-populations were returned to tissue culture ahead of their downstream analysis. Now that these pCSCs and non-pCSCs have been isolated the are available for validation assays and downstream analysis.

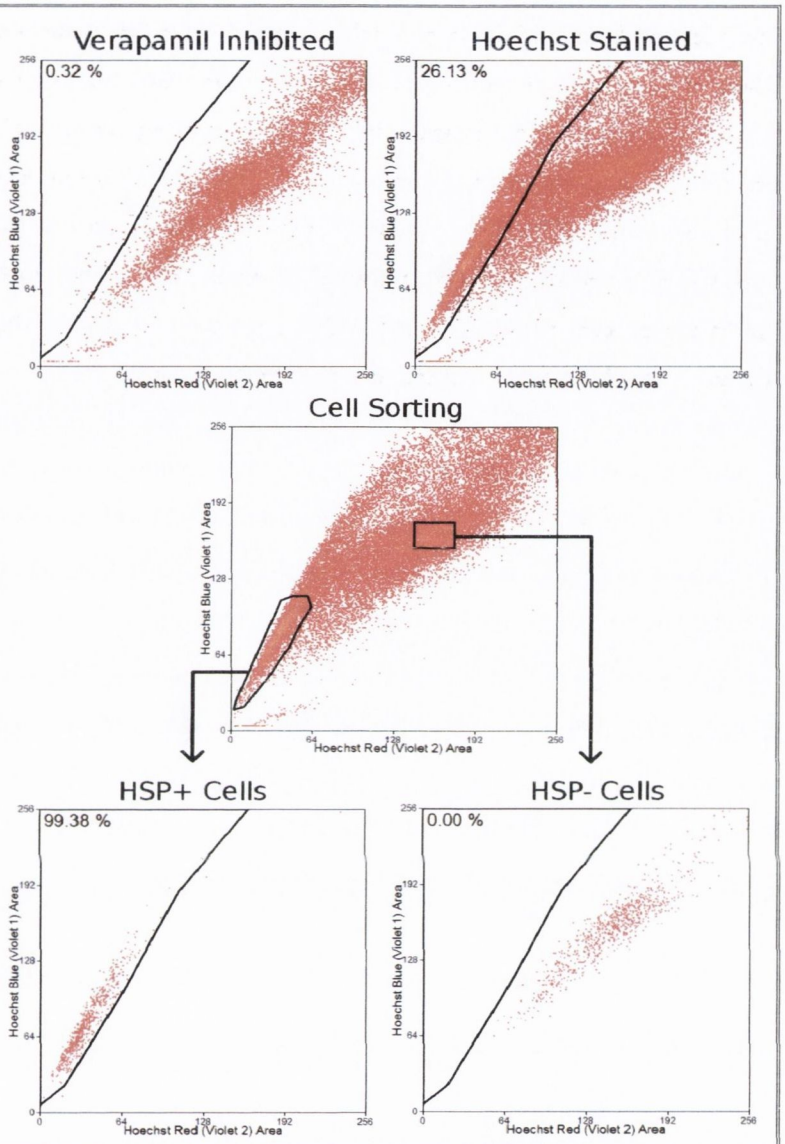

Figure 5.6: HSP+/- Cell Sorting of the IGROV-CDDP Cell Line – The IGROV-CDDP HSP+ pCSCs were isolated via FACS, to a purity of 99.38 %. The IGROV-CDDP HSP- non-pCSCs were isolated via FACS, to a purity of 100.00 %. The top pair of graphs show the HSP+/- profile of the IGROV-CDDP cell line prior to cell sorting. The gates are established based on the subtraction of the negative control data (Verapamil Inhibited) from the experimental sample (Hoechst Stained). The middle graph shows the gates used to sort the IGROV-CDDP cell line into its HSP+/- sub-populations. The bottom two graphs show the post-sort purity of the HSP- and HSP+ sub-populations.

5.3.5 SK-OV-3

CD117+ pCSCs and CD117- non-pCSCs were isolated from the metastatic ascites SK-OV-3 model. These sub-populations were considered to be sufficiently big to only require one round of FACS to purify them to > 99 % pure. The CD117+/- sub-populations were sorted on Single Cell mode. The CD117- non-pCSCs were enriched from 67.97 % pure to 99.08 % pure after one round of cell sorting (Figure 5.7). This CD117- sub-population had met the > 99 % pure criteria. The CD117- non-pCSCs were returned to tissue culture and stocks were made. The CD117+ pCSCs were only enriched from 32.03 % pure to 83.50 % pure after one round of cell sorting (Figure 5.7). This CD117+ pCSC sub-population required further cell sorting to obtain the desired purity of > 99 %. The CD117+ enriched population was returned to tissue culture, to allow for amplification of the cell number. The CD117+ cells were then further purified via a second round of FACS, on Single Cell mode. Second round FACS purified the CD117+ cells from 73.33 % pure to 99.47 % pure (Figure 5.8). This CD117+ sub-population had met the > 99 % pure criteria. The CD117+ pCSCs were returned to tissue culture and stocks were made.

Upon returning the CD117- and CD117+ cells to tissue culture it was noted that the two sub-populations had different morphologies. The CD117- cells formed a tightly packed monolayer and had a more compact cytoplasm, while the CD117+ cells were flatter cells resulting in a less tightly packed monolayer (Figure 5.9). Now that these pCSCs and non-pCSCs have been isolated the are available for validation assays and downstream analysis

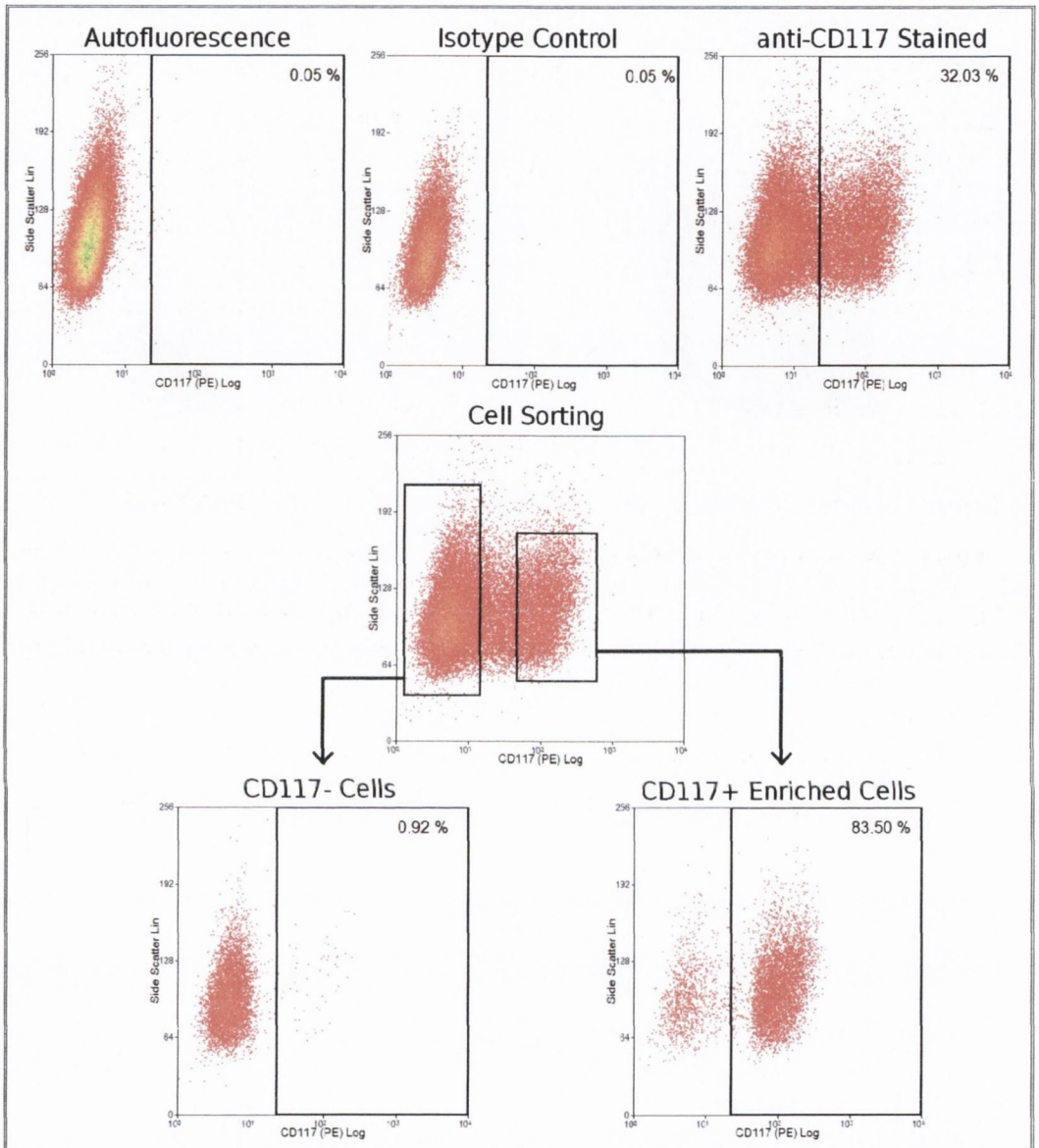

Figure 5.7: CD117+/- Cell Sorting of the SK-OV-3 Cell Line – The SK-OV-3 CD117- non-pCSCs were isolated via FACS, to a purity of 99.08 %. The SK-OV-3 CD117+ pCSCs were isolated via FACS, to a purity of 83.50 %. The top pair of graphs show the CD117+/- profile of the SK-OV-3 cell line prior to cell sorting. The gates are established based on the subtraction of the negative control data (Autofluorescence) from the experimental sample (anti-CD117 Stained). The middle graph shows the gates used to sort the SK-OV-3 cell line into its CD117+/- sub-populations. The bottom two graphs show the post-sort purity of the CD117- and CD117+ sub-populations.

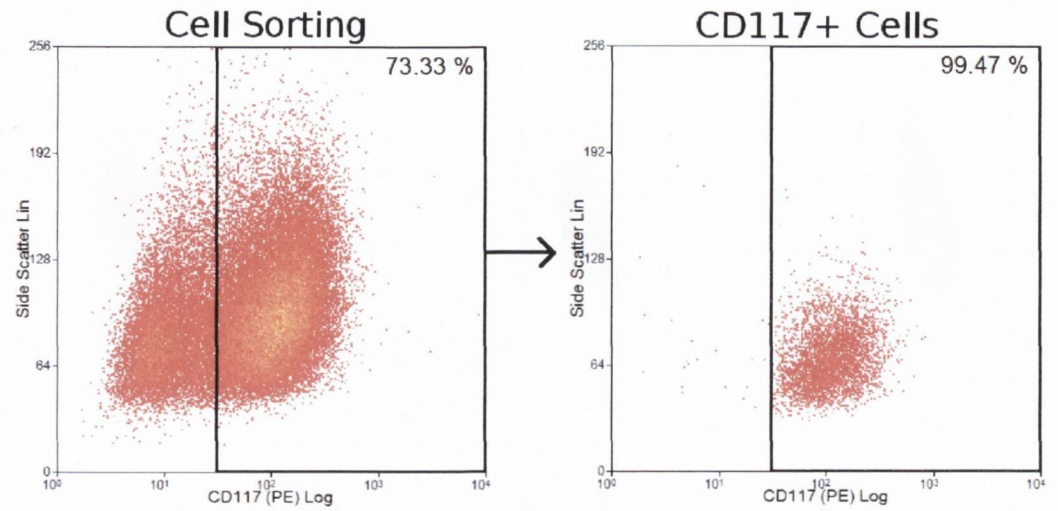

Figure 5.8: Second round SK-OV-3 CD117+ purification - Second round FACS purified SK-OV-3 CD117+ pCSCs to a purity of 99.47 %. The graph on the left shows the gate used to sort cells from the SK-OV-3 CD117+ Enriched Cells obtained from first round cell sorting of the SK-OV-3 cell line. The graph on the right shows the second round post sort purity of the CD117+ sub-population.

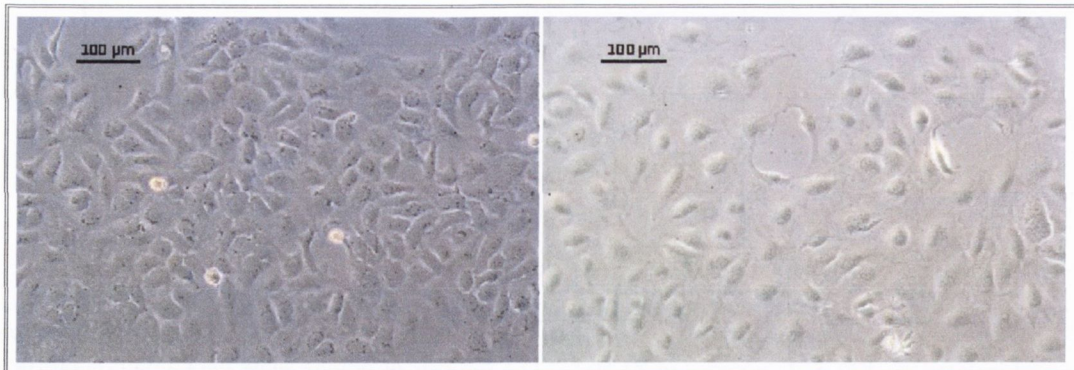

Figure 5.9: The CD117- and CD117+ sub-populations of SK-OV-3 have a different morphology in tissue culture – The photograph on the left shows SK-OV-3 CD117- cells, purified via FACS. The photograph on the right shows SK-OV-3 CD117+ cell, purified via FACS.

5.3.6 59M

CD117+ pCSCs and CD117- non-pCSCs were isolated from the metastatic ascites 59M model. These sub-populations were considered to be sufficiently big to only require one round of FACS to purify them to > 99 % pure. The CD117+/- sub-populations were sorted on Single Cell mode. The CD117- non-pCSCs were enriched from 84.48 % pure to 99.95 % pure after one round of cell sorting (Figure 5.10). This CD117- sub-population had met the > 99 % pure criteria. The CD117- non-pCSCs were returned to tissue culture and stocks were made. The CD117+ pCSCs were only enriched from 15.52 % pure to 90.89 % pure after one round of cell sorting (Figure 5.10). This CD117+ pCSC sub-population required further cell sorting to obtain the desired purity of > 99 %. The CD117+ enriched population was returned to tissue culture, to allow for amplification of the cell number. The CD117+ cells were then re-stained in preparation for further purification via a second round of FACS. Upon running the samples it was noted that the CD117+ enriched sample had lost its CD117+ enriched phenotype (Figure 5.11). This suggested that it was not going to be possible to purify the 59M CD117+ cells over multiple rounds of FACS. The loss of enriched phenotypes will be discussed in Section 5.4.2.

The 59M CD117+/- sub-populations were the lowest ranking of all the sub-populations to be isolated (Section 4.3.5). Therefore, it was not considered justifiable to dedicate the considerable time it would have required to tackle this unexpected result. It was decided that 59M CD117+ cells would be isolated immediately prior to the downstream assays, and any impurities would be incorporated into the interpretation of the results.

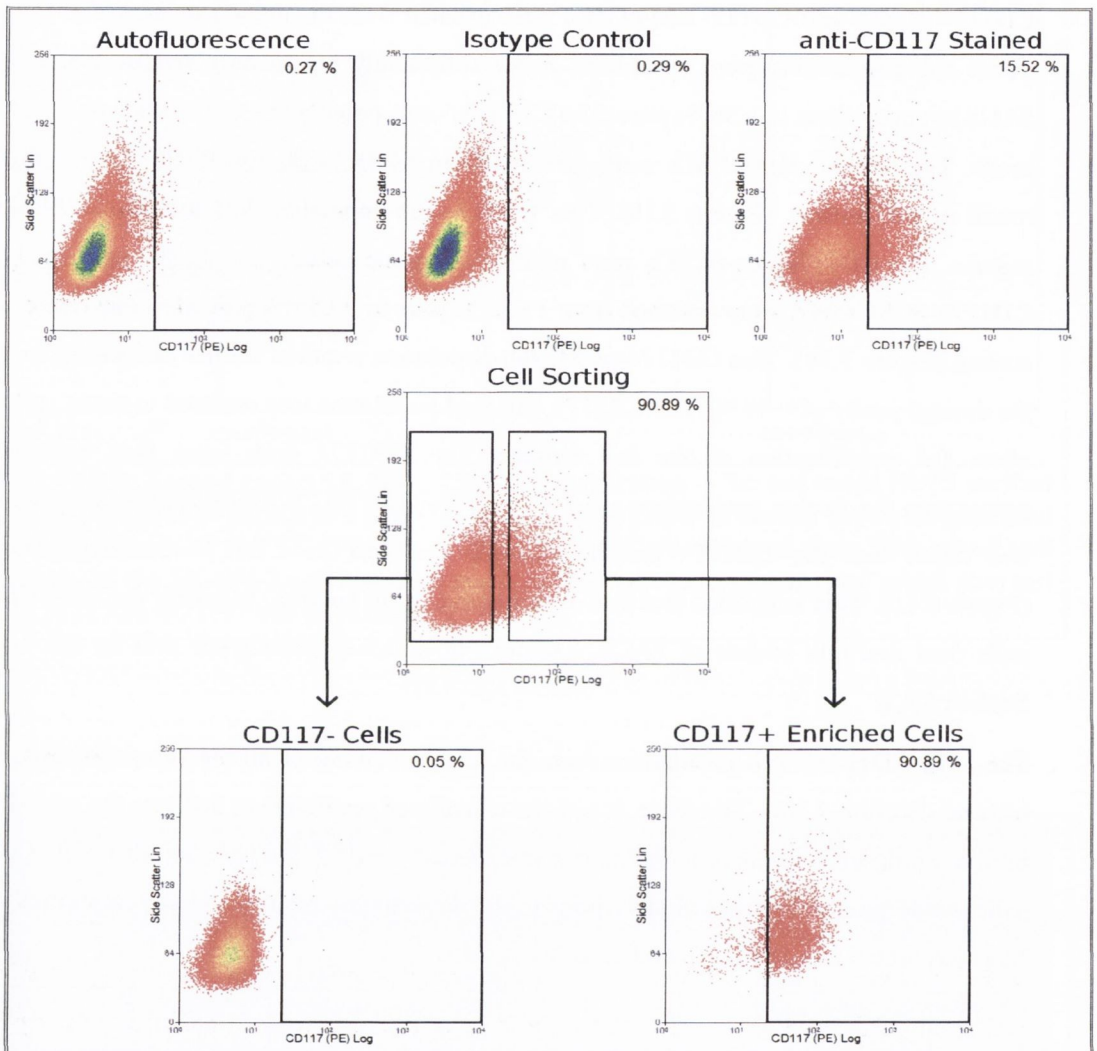

Figure 5.10: CD117+/- Cell Sorting of the 59M Cell Line – The 59M CD117- non-pCSCs were isolated via FACS, to a purity of 99.95 %. The 59M CD117+ pCSCs were isolated via FACS, to a purity of 90.89 %. The top pair of graphs show the CD117+/- profile of the 59M cell line prior to cell sorting. The gates are established based on the subtraction of the negative control data (Autofluorescence) from the experimental sample (anti-CD117 Stained). The middle graph shows the gates used to sort the 59M cell line into its CD117+/- sub-populations. The bottom two graphs show the post-sort purity of the CD117- and CD117+ sub-populations.

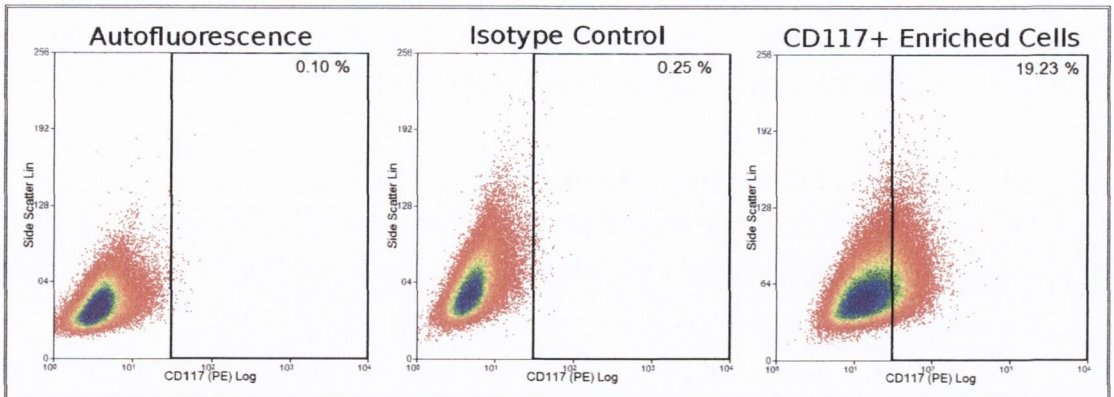

Figure 5.11: The 59M CD117+ Enriched Cells lost the CD117+ Phenotype – These three panels illustrate the proportion of CD117+ cells present in the 59M CD117+ Enriched Cells, when they were returned for a second phase of cell sorting. Due to the loss of the CD117+ phenotype, no second round cell sorting was attempted.

5.4 Discussion

To facilitate the study of OvCSCs, pure populations of CSCs and non-CSCs are required for the testing and establishment of OvCSC models. Pure populations and models are needed as CSCs and SSCs often only represent a small percentage of tumours and tissues (Goodell et al. 1996 [Haematopoietic SSCs: 0.1 %]; Bonnet and Dick 1997 [CD34+/CD38- acute myeloid leukemia CSCs: 0.2 % - 2.0 %]) and no models of OvCSCs currently exist. Pure populations of pCSCs and non-pCSCs were successfully isolated to a high degree of purity (Section 5.3). These sub-populations were successfully isolated using a variety of CSC staining assays.

To isolate CSCs, first, CSCs must be identified from within a heterogeneous source (as described in Section 4.0). Then, the cells of interest must be isolated to a high degree of purity, to facilitate their downstream analysis. In this project it was decided to isolate six pairs of pCSC and non-pCSC sub-populations. Four of these pairs were selected to facilitate the study of the role of CSCs in acquired chemoresistance. The other two pairs were selected to facilitate the study of the role of CSCs in the development of metastatic ascites. All of the three pCSC screening assays are represented within each of the six selected pCSC/non-pCSC sub-populations.

FACS was used to successfully isolate pCSCs and non-pCSCs of interest based on all three of the assays (ALDH, HSP and CSP) used to screen for OvCSCs. It was attempted to isolate six pairs of pCSCs/non-pCSCs from across six ovarian cancer models. 11 of 12 of these sub-populations were isolated to a purity of greater than 99 % pure. This will be discussed in

Section 5.4.1. One of the sub-populations, 59M CD117+ pCSCs did not stably maintain its CD117+ phenotype for long enough to allow it to be purified to greater than 99 %. The stability of the isolated sub-populations will be discussed in Section 5.4.2.

5.4.1 Isolation of Sub-populations:

The pCSC and non-pCSC sub-populations selected for isolation in this project were selected to address two separate questions. First, what are the roles of CSCs/non-CSCs in the evasion of therapeutics and acquired chemoresistance in ovarian cancer? This will be discussed in Section 5.4.1.1. Second, what is the role of CSCs/non-CSCs in the development of metastatic ascites in ovarian cancer? This will be discussed in Section 5.4.1.2.

5.4.1.1 The CSCs' Role in Therapeutic Evasion and Acquired Chemoresistance:

Recurrent chemoresistance in ovarian cancer is currently the major obstacle in the treatment of ovarian cancer. The underlying hypothesis of this project is that recurrent chemoresistant ovarian cancer is driven by a small residual population of OvCSCs, which have adapted to chemotherapy. The isolations described in this chapter (Section 5.0), facilitate the study of pCSCs and non-pCSCs from chemosensitive and chemoresistant models.

Two phase purification was successfully utilised to purify ALDH+ pCSCs from < 1 % to > 99 % pure, from both the A2780 and A2780cis cell lines (Sections 5.3.1 and 5.3.2). The corresponding ALDH- non-pCSCs were also isolated to > 99 % pure (Sections 5.3.1 and 5.3.2). Isolation of these sub-populations facilitates the comparison of CSC to non-CSCs within cisplatin sensitive and cisplatin resistant ovarian cancer models (A2780 and A2780cis respectively). There are several experiments which could be carried out on these isolated populations to probe the roles of CSC in acquired chemoresistance.

5.4.1.1.1 Probing the intrinsic resistance of CSCs:

Comparison of the dose response of chemosensitive CSCs to the chemosensitive non-CSCs could indicate if CSCs are intrinsically resistant to some or all chemotherapeutic agents. If the CSCs showed a reduced response to a chemotherapeutic agent compared to the non-CSCs, this would support the hypothesis that the CSC population is intrinsically resistant. However, if the CSCs showed a similar response to a chemotherapeutic agent compared to the non-CSCs, this would support the hypothesis that chemoresistance is acquired upon exposure to the agent.

Silva et al. (2011) showed that the ALDH+ CSC fraction within an ovarian cancer cell line had a selective advantage when the cell line was treated with cisplatin. They described a dose-

dependent decrease in the total number of viable cells, with a concurrent significant increase ($p < 0.01$) in the presence of ALDH+ cells. In the untreated state the ALDH+ fraction represented ~4 % of the total population. When treated with 3.0 μg/ml cisplatin for 72 h the ALDH+ fraction represented ~30 % of the total population. They went on to show that ALDH+ cells were more chemoresistant than ALDH- cells: observing ~80 % and ~91 % cell death respectively after a 72 h treatment of 1.5 μg/ml cisplatin. However, the most obvious difference between the ALDH+ and ALDH- cells with respect to chemoresistance was their ability to recover after withdrawal of chemotherapeutics. At 11 days after removal of cisplatin the ALDH+ cells had recovered to ~70 % the starting cell concentration, while the ALDH- cells had only recovered to ~20 % the starting cell concentration. These reported findings suggest that CSCs not only have intrinsic chemoresistance but are also better able to adapt and regrow tumours post-chemotherapy. The A2780cis ALDH+ sub-population isolated (Section 5.3.2), was substantially smaller than the A2780 ALDH+ sub-population identified by Silva et al. However, there was a statistically significant increase in the size of the ALDH+ sub-population in our A2780 model compared to our A2780cis model. This suggests that the change in the size of a CSC sub-population between a chemosensitive and chemoresistant ovarian cancer is more important that the absolute size of the CSC sub-population.

Comparison of the dose response to other chemotherapeutic agents, of cisplatin-sensitive CSCs to the -resistant CSCs and -sensitive non-CSC to -resistant non-CSCs could indicate if acquired resistance to one chemotherapeutic agent correlates positively or negatively with resistance to other agents. Platinum and taxol agents are commonly used to treat ovarian cancer (McGuire et al. 1996). These both act through different mechanisms, platinum based agents cause direct DNA damage and apoptosis via a p53-dependent pathway (Perego et al. 1996). Taxol based agents bind and stabilise tubulin, predominantly causing mitotic arrest and apoptosis at the G_2/M checkpoint via a p53-independent pathway (Woods et al. 1995). Even though these two agents are administered together and act via different mechanisms, a residual population of cells (presumably CSCs), can evade and adapt to the combination therapy and produce a recurrent tumour which is resistant to both agents. Understanding the tumour/CSCs ability to adapt to multiple synergistic chemotherapeutics is essential to the successful treatment of ovarian cancer. The successful isolation of CSCs and non-CSCs from chemosensitive and chemo-adapted models described in Section 5.3, may facilitate the investigation of how the different sub-populations can evade chemotherapy and lead to recurrence.

To carry out such comparisons, a serial dilution of chemotherapeutic agents such as cisplatin, carboplatin and paclitaxel, used in conjunction with a cell proliferation assay such as the dimethylthiazol-diphenyltetrazolium bromide (MTT) assay could be used to map chemotherapeutic dose response curves for each of the chemosensitive and chemoresistant CSC and non-CSC sub-populations. While Silva et al. have done similar experiments with chemosensitive CSCs they lack the comparison with CSCs isolated from chemo-adapted models.

5.4.1.1.2 Identifying the molecular pathways behind intrinsic and/or acquired chemoresistance:
Depending on the outcome of the above experiments, microarray based comparisons of different sets of populations could be used to investigate different aspects of intrinsic and/or acquired chemoresistance.

In the case of intrinsic chemoresistance being identified in CSCs it would be most interesting to compare the chemosensitive CSCs to the chemosensitive non-CSCs. Such a comparison could elucidate the molecular mechanisms behind intrinsic chemoresistance. Furthermore, it would be interesting to compare the difference in gene expression observed between the sensitive CSCs and sensitive non-CSCs to the gene expression observed between the resistant CSCs and resistant non-CSCs. Such a comparison could elucidate the molecular mechanisms behind the initial responsiveness of ovarian tumours to chemotherapy followed by the often unresponsive malignancy observed upon relapse.

In the case of non-intrinsic, acquired chemoresistance being identified in CSCs it would be interesting to compare the sensitive CSCs to the resistant CSCs. Such a comparison could elucidate the molecular mechanisms behind the acquired chemoresistance. Such a comparison should be made in both chemotherapy exposed sensitive CSCs and resistant CSCs, as well as comparing the populations when in their untreated states. This would facilitate the detection of mechanisms of resistance that are dynamically activated upon chemotherapy exposure, as opposed to constitutively expressed mechanisms of resistance.

Such analysis could be carried out using single channel Affymetrix™ microarrays would allow for multiple pairwise comparisons of different sub-populations using one set of data for each sub-population. Dual channel Agilent™ microarrays would require the sub-population comparisons to be made on the array, preventing the re-use of data for different comparisons, unless each sub-population was compared to one standardised sample on each array.

5.4.1.1.3 Investigating the hereditary changes associated with acquired chemoresistance in ovarian cancer:

For residual CSCs, which have evaded first-line therapy, to be able to generate a tumour which is refractory to further therapy, requires a heritable difference present in the residual CSCs which was not widespread in the primary tumour. Gene sequencing and chromosome methylation studies on target genes/loci identified by microarray analysis could provide information on heritable changes associated with acquired chemoresistance in ovarian cancer.

The above comparisons could elucidate the mechanisms CSCs may be using to evade therapeutics and mediate post-therapeutic relapse. Comparisons of the differentiation of cisplatin sensitive and cisplatin resistant CSCs could elucidate how CSCs, which have evaded therapeutics, confer chemoresistance to the entire tumour upon relapse.

Single phase purification was successfully utilised to purify HSP+ pCSCs and HSP- non-pCSCs to > 99 % pure from both cisplatin sensitive and cisplatin resistant ovarian cancer models (IGROV-1 and IGROV-CDDP respectively; Sections 5.3.3 and 5.3.4). In a similar fashion to the A2780 and A2780cis models, now that these sub-populations have been isolated, they can be studied via the experiments described above, to help elucidate the role of CSCs in therapeutic evasion and acquired chemoresistance. Furthermore, all four models (A2780, A2780cis, IGROV-1 and IGROV-CDDP) and their pCSC/non-pCSC sub-populations can be used together to examine if the different types of CSCs (ALDH+ and HSP+), have convergent or divergent mechanisms in their roles in therapeutic evasion and acquired chemoresistance. This type of analysis has yet to be done in the ovarian cancer field. Most studies focus on the chemoresistant properties of chemo-naïve CSCs rather than compare CSCs isolated from chemosensitive and pair matched chemoresistant sources (Szotek 2006; Silva et al. 2011).

The experiments described above can be used to address questions regarding chemoresistance, such as:

- Do ALDH+ and HSP+ CSCs contribute to acquired chemoresistance in a similar fashion?
- Are CSCs intrinsically more resistant to therapeutics?
    - Is a change in the cellular composition or differentiation status responsible for acquired chemoresistance?
- Are genetic/epigenetic mutations responsible for the evasion of therapeutics by CSCs?

- Is a simple hereditary model responsible for the acquired chemoresistance?

5.4.1.2 The CSCs' Role in Metastatic Ascites:

In a similar fashion to the hypothesis that recurrent chemoresistant ovarian cancer is driven by a small residual population of OvCSCs, which have adapted to chemotherapy, it is hypothesised that metastatic tumours are seeded by metastatic ovarian cancer stem cells. The isolations described in this chapter (Section 5.0), facilitates the study of pCSCs and non-pCSCs from models derived from metastatic ascites and solid tumour sources.

Single phase purification was successfully utilised to purify CD117- non-pCSC cells to > 99 % pure from the metastatic ascites derived SK-OV-3 model (Figure 5.7). However, a second phase was required to purify CD117+ pCSCs to > 99 % pure (Figure 5.8). As the CD117+ sub-population was comparatively large it was not expected to require two phases of purification.

Interestingly, the SK-OV-3 CD117+ and CD117- cells exhibited a noticeably different morphology when returned to tissue culture (Figure 5.9). These were the only sub-populations to exhibit differences in morphology of all the sub-populations isolated. Other cell lines were composed of cells with heterogeneous morphologies. However, the isolated sub-populations did not refine this heterogeneity. To investigate the difference morphologies within a cell line, cells could be plated as single cells in individual wells of a microtitre plate and allowed to grow into clones. If the heterogeneous morphologies are related to differentiation, then some of the clones will have a reduced differentiation potential with respect to the production of the various morphologies. Antibody based surface marker panels can then be used to assess the clones, to see which surface marker based populations appear or disappear, with respect to the presence or absence of the various morphologies.

Single phase purification was also successfully utilised to purify CD117- non-pCSC cells to > 99 % pure from the metastatic ascites derived 59M model (Figure 5.10). However, the CD117+ pCSCs did not purify to > 99 %. A second phase purification was attempted to purify CD117+ pCSCs to > 99 % pure. However, it was noted that the 59M CD117+ pCSCs did not maintain their CD117+ enriched phenotype (Figure 5.11). However, CSCs have been previously isolated from metastatic ascites sources. Zhang et al. (2008) were the first to isolate CSCs from ovarian metastatic ascites. They used spheroid growth to enrich for a CSC phenotype and then demonstrated that these CSC enriched spheroids had an increased proportion of CD44+ and CD117+ cells. Interestingly, in this study CD117+ pCSCs were only identified in (Section 4.3)

and isolated from (Section 5.3) the ascites derived models. These pCSCs may represent a CSC population central to the metastasis of ovarian cancer.

Isolation of these sub-populations facilitates the comparison of CSC to non-CSCs within the metastatic ovarian cancer models (SK-OV-3 and 59M). Ovarian cancer, predominately metastasises throughout the peritoneal cavity (Lengyel 2010). Ascites are considered to be central to this dissemination. Understanding the role of CSCs in tumour dissemination, could lead to novel therapies which protect against metastatic spread. Furthermore, comparison of the metastatic sub-populations to those derived from solid tumours may elucidate, the roles of the different cell types involved in the spread of the malignancy.

5.4.2 Stability of the isolated sub-populations:

The CSC hypothesis suggests that differentiation of CSCs into non-CSCs is partially responsible for tumour heterogeneity. This suggests that the isolated pCSC sub-populations are expected to be capable of generating the non-pCSCs.

As the sizes of pCSC sub-populations identified in the pCSC screen are relatively stable between the replicates, it is possible that there is a homoeostasis between the 'undifferentiated' pCSC and the 'differentiated' non-pCSC populations. Therefore, it is not unexpected that when the pCSC population is isolated to a high degree of purity, they will differentiate to produce a heterogeneous population of pCSCs and non-pCSCs. This concept of intrinsic rather than induced differentiation is central to the premise of the single cell self-renewal and differentiation (SD) assay. One could also hypothesise that under the correct growth conditions, isolated CSCs could be maintained in their 'undifferentiated' state. Such growth conditions, would facilitate the generation of CSC model systems.

When mouse embryonic stem (ES) cells were first isolated a similar problem of stem cell stability was faced. The isolated ES cells would spontaneously differentiate when plated in plastic culture dishes. To overcome this, ES cells were plated on a monolayer of mitomycin C-treated embryonic fibroblasts (feeder cells), which provided the chemokines and cytokines required to maintain the undifferentiated state of the ES cells (Smith and Hooper 1987). Later, feeder cells were replaced by 'Buffalo rat liver cells' conditioned media, allowing for a less complicated model of undifferentiated ES cells (Smith and Hooper 1987). Further progress allowed the conditioned media to be replaced by the addition of purified polypeptides (Leukemia Inhibitory Factor: LIF), to unconditioned media (Smith et al. 1988). LIF was identified as a self-renewal maintaining agent almost serendipitously. Smith et al. noted that the

Section 5.0 – Isolation of pCSCs

'Buffalo rat liver cells' conditioned media was not only capable of maintaining the undifferentiated state of ES cells but also capable of the prolonged culture of induced murine leukemia cells (DA-1a). Another paper had identified a LIF DNA clone capable of similar prolonged culture DA-1a cells (Moreau et al. 1988). Through the creation of a LIF plasmid Smith et al. (1988) were able to generate a fibroblast cell line which secreted LIF into the conditioned media. They showed that even a 1:200 dilution of this LIF conditioned media could maintain the undifferentiated state of the ES cells.

With the wide availability of fluorescent-activated cell sorting and microarray analysis more methodical systems can be employed to identify the conditions required to maintain the stemness state of a stem cell population. The pure pCSCs isolated in this chapter can now be validated as CSCs and compared, via microarray analysis, to a population of CSCs which have been allowed to differentiate. Such a comparison should identify the self-renewal/differentiation pathways, which turn off/on to facilitate differentiation. In a similar fashion to use of LIF for ES cultures, stimulation and inhibition of these respective pathways, should facilitate the generation of a stable model of CSCs. As such, cell culture conditions that allow maintenance of the undifferentiated state and manipulations such as transfections and drug treatments should be achievable for each cell type.

As seen in the case of the 59M CD117+ pCSC sub-population, the intrinsic differentiation/loss of pCSC phenotype, can effect the downstream analysis carried out on these isolated sub-populations. Therefore, it is desirable to assess the purity of the sub-populations immediately prior to carrying out the downstream analysis. However, carrying out staining and flow cytometry protocols required to assess the purity and then starting an experiment can be logistically challenging and is often to the detrimental to the quality of the work being carried out. Additionally, carrying out downstream experiments directly after FACS, may lead to unexpected results, as the cells can be stressed by the sorting protocol. This is often exemplified the next day after returning cells to tissue culture after cell sorting, when an elevated level of floating/dead cells can be seen in the culture.

Every effort was made to quantify the purity of the isolated populations before carrying out the downstream experiments. However, it was not always possible to do this immediately before the experiment was carried out. Most isolated populations were relatively stable, only varying 5 – 10 % after multiple passages.

5.4.3 Summary:

This chapter described the FACS based isolation of pCSC and non-pCSC to a high degree of purity. pCSCs and non-pCSCs were isolated from six models of ovarian cancer models: four pairs of pCSC/non-pCSC sub-populations were isolated across two pairs of cisplatin and cisplatin adapted ovarian cancer models. Two pairs of pCSC/non-pCSC sub-populations were isolated across two models of ovarian cancer originally derived from ascites. Three independent pCSC screening assays were used during the pCSC screen (ALDH, HSP and CSP; Section 4.0). The work described in this chapter demonstrated the isolation of pCSC and non-pCSCs based on each of these independent pCSC screening assays.

Now that these pCSC and non-pCSC sub-populations had been isolated, they could be validated as CSCs and non-CSCs via xenograft mouse tumourgenicity assays and SD assays. Validated CSCs and non-CSCs can then be utilised to address the comparisons discussed in Sections 5.4.1.1 and 5.4.1.2.

Isolation of pCSCs:- Primary Findings

12 sub-populations of interest were isolated from 6 models of Ovarian Cancer. It was possible to isolate sub-populations to high degree of purity, via all of the techniques used to identify pCSCs (ALDH, HSP and CSP Assays):

- A2780 ALDH+ pCSCs were isolated to a purity of 100.00 %. A2780 ALDH- non-pCSCs were isolated to a purity of 100.00 %.
- A2780cis ALDH+ pCSCs were isolated to a purity of 99.35 %. A2780cis ALDH- cells were isolated to a purity of 100.00 %.
- IGROV-1 HSP+ pCSCs were isolated to a purity of 99.81 %. IGROV-1 HSP- non-pCSCs were isolated to a purity of 99.52 %
- IGROV-CDDP HSP+ pCSCs were isolated to a purity of 99.38 %. IGROV-CDDP HSP- non-pCSCs were isolated to a purity of 100.00 %
- SK-OV-3 CD117+ pCSCs were isolated to a purity of 99.47 %. SK-OV-3 CD117- non-pCSCs were isolated to a purity of 99.08 %
- 59M CD117+ pCSCs were isolated to a purity of 90.89 %. 59M CD117- non-pCSCs were isolated to a purity of 99.95 %

5.5 References

Aktas, Bahriye, Mitra Tewes, Tanja Fehm, Siegfried Hauch, Rainer Kimmig, and Sabine Kasimir-Bauer. 2009. "Stem Cell and Epithelial-mesenchymal Transition Markers Are Frequently Overexpressed in Circulating Tumor Cells of Metastatic Breast Cancer Patients." *Breast Cancer Research: BCR* 11 (4): R46. doi:10.1186/bcr2333.

Bonnet, D, and J E Dick. 1997. "Human Acute Myeloid Leukemia Is Organized as a Hierarchy That Originates from a Primitive Hematopoietic Cell." *Nature Medicine* 3 (7) (July): 730–737.

Buchdunger, Elisabeth, Terence O'Reilly, and Jeanette Wood. 2002. "Pharmacology of Imatinib (STI571)." *European Journal of Cancer (Oxford, England: 1990)* 38 Suppl 5 (September): S28–36.

Deininger, M W, S Vieira, R Mendiola, B Schultheis, J M Goldman, and J V Melo. 2000. "BCR-ABL Tyrosine Kinase Activity Regulates the Expression of Multiple Genes Implicated in the Pathogenesis of Chronic Myeloid Leukemia." *Cancer Research* 60 (7) (April 1): 2049–2055.

Goodell, M A, K Brose, G Paradis, A S Conner, and R C Mulligan. 1996. "Isolation and Functional Properties of Murine Hematopoietic Stem Cells That Are Replicating in Vivo." *The Journal of Experimental Medicine* 183 (4) (April 1): 1797–1806.

Kallergi, Galatea, Sofia Agelaki, Antonia Kalykaki, Christos Stournaras, Dimitris Mavroudis, and Vassilis Georgoulias. 2008. "Phosphorylated EGFR and PI3K/Akt Signaling Kinases Are Expressed in Circulating Tumor Cells of Breast Cancer Patients." *Breast Cancer Research: BCR* 10 (5): R80. doi:10.1186/bcr2149.

Kauff, Noah D, Susan M Domchek, Tara M Friebel, Mark E Robson, Johanna Lee, Judy E Garber, Claudine Isaacs, et al. 2008. "Risk-reducing Salpingo-oophorectomy for the Prevention of BRCA1- and BRCA2-associated Breast and Gynecologic Cancer: a Multicenter, Prospective Study." *Journal of Clinical Oncology: Official Journal of the American Society of Clinical Oncology* 26 (8) (March 10): 1331–1337. doi:10.1200/JCO.2007.13.9626.

Lengyel, Ernst. 2010. "Ovarian Cancer Development and Metastasis." *The American Journal of Pathology* 177 (3) (September): 1053–1064. doi:10.2353/ajpath.2010.100105.

McGuire, W P, W J Hoskins, M F Brady, P R Kucera, E E Partridge, K Y Look, D L Clarke-Pearson, and M Davidson. 1996. "Cyclophosphamide and Cisplatin Compared with Paclitaxel and Cisplatin in Patients with Stage III and Stage IV Ovarian Cancer." *The New England Journal of Medicine* 334 (1) (January 4): 1–6. doi:10.1056/NEJM199601043340101.

Miki, Y, J Swensen, D Shattuck-Eidens, P A Futreal, K Harshman, S Tavtigian, Q Liu, C Cochran, L M Bennett, and W Ding. 1994. "A Strong Candidate for the Breast and Ovarian Cancer Susceptibility Gene BRCA1." *Science (New York, N.Y.)* 266 (5182) (October 7): 66–71.

Moreau, J F, D D Donaldson, F Bennett, J Witek-Giannotti, S C Clark, and G G Wong. 1988. "Leukaemia Inhibitory Factor Is Identical to the Myeloid Growth Factor Human Interleukin for DA Cells." *Nature* 336 (6200) (December 15): 690–692. doi:10.1038/336690a0.

Perego, P, M Giarola, S C Righetti, R Supino, C Caserini, D Delia, M A Pierotti, T Miyashita, J C Reed, and F Zunino. 1996. "Association Between Cisplatin Resistance and Mutation of P53 Gene and Reduced Bax Expression in Ovarian Carcinoma Cell Systems." *Cancer Research* 56 (3) (February 1): 556–562.

Silva, Ines A, Shoumei Bai, Karen McLean, Kun Yang, Kent Griffith, Dafydd Thomas, Christophe Ginestier, et al. 2011. "Aldehyde Dehydrogenase in Combination with

CD133 Defines Angiogenic Ovarian Cancer Stem Cells That Portend Poor Patient Survival." *Cancer Research* 71 (11) (June 1): 3991–4001. doi:10.1158/0008-5472.CAN-10-3175.

Singh, Sheila K, Cynthia Hawkins, Ian D Clarke, Jeremy A Squire, Jane Bayani, Takuichiro Hide, R Mark Henkelman, Michael D Cusimano, and Peter B Dirks. 2004. "Identification of Human Brain Tumour Initiating Cells." *Nature* 432 (7015) (November 18): 396–401. doi:10.1038/nature03128.

Smith, A G, J K Heath, D D Donaldson, G G Wong, J Moreau, M Stahl, and D Rogers. 1988. "Inhibition of Pluripotential Embryonic Stem Cell Differentiation by Purified Polypeptides." *Nature* 336 (6200) (December 15): 688–690. doi:10.1038/336688a0.

Smith, A G, and M L Hooper. 1987. "Buffalo Rat Liver Cells Produce a Diffusible Activity Which Inhibits the Differentiation of Murine Embryonal Carcinoma and Embryonic Stem Cells." *Developmental Biology* 121 (1) (May): 1–9.

Szotek, P. P. 2006. "Ovarian Cancer Side Population Defines Cells with Stem Cell-like Characteristics and Mullerian Inhibiting Substance Responsiveness." *Proceedings of the National Academy of Sciences* 103 (30) (July 25): 11154–11159. doi:10.1073/pnas.0603672103.

Tan, Lei, Xin Sui, Hongkui Deng, and Mingxiao Ding. 2011. "Holoclone Forming Cells from Pancreatic Cancer Cells Enrich Tumor Initiating Cells and Represent a Novel Model for Study of Cancer Stem Cells." *PloS One* 6 (8): e23383. doi:10.1371/journal.pone.0023383.

Woods, C M, J Zhu, P A McQueney, D Bollag, and E Lazarides. 1995. "Taxol-induced Mitotic Block Triggers Rapid Onset of a P53-independent Apoptotic Pathway." *Molecular Medicine (Cambridge, Mass.)* 1 (5) (July): 506–526.

Wooster, R, G Bignell, J Lancaster, S Swift, S Seal, J Mangion, N Collins, S Gregory, C Gumbs, and G Micklem. 1995. "Identification of the Breast Cancer Susceptibility Gene BRCA2." *Nature* 378 (6559) (December 21): 789–792. doi:10.1038/378789a0.

Zhang, S., C. Balch, M.W. Chan, H.C. Lai, D. Matei, J.M. Schilder, P.S. Yan, T.H.M. Huang, and K.P. Nephew. 2008. "Identification and Characterization of Ovarian Cancer-initiating Cells from Primary Human Tumors." *Cancer Research* 68 (11): 4311.

Validation of Cancer Stem Cells

Section6.0 – Validation of CSC

6.1 Introduction:

"Stem cells are defined as cells that have the ability to perpetuate themselves through self-renewal and to generate mature cells of a particular tissue through differentiation"

– Reya et al. 2001

The cancer stem cell hypothesis suggests that there is a sub-population of self-sustaining cells within tumours, which drive the growth and development of the tumour. Such a sub-population is called the CSC sub-population. The 2006 American Association for Cancer Research (AACR) workshop on CSCs arrived at a consensus definition for CSCs:

"The consensus definition of a cancer stem cell that was arrived at in this Workshop is a cell within a tumor that possess the capacity to self-renew and to cause the heterogeneous lineages of cancer cells that comprise the tumor."

– Clarke et al. 2006

Multiple populations of pCSCs and non-pCSCs were identified and isolated in the previous chapters (Section 4.0 and 5.0). These pCSC and non-pCSC populations were identified based on pCSC marker phenotypes that have been shown to correlate with cancer stemness (ALDH: Silva et al. 2011; HSP: Szotek et al. 2006; CD117: Zhang et al. 2008). These markers do not have any implied causative role in the stemness characteristics of CSCs. CSCs, like stem cells, are defined solely by functional characteristics (Clarke et al. 2006). Therefore, the pCSCs and non-pCSCs identified via protein expression characteristics, must be functionally validated before they can be considered CSC and non-CSC populations. This chapter will describe the functional validation of the pCSC and non-pCSC sub-populations, via an *in vivo* xenograft mouse tumourgenicity assay and a single cell self-renewal and differentiation (SD) assay.

The *in vivo* xenograft mouse tumourgenicity assay queries the potential of a pCSC population to develop a tumour, which represents that of the malignancy from which it was isolated. This assay was used to validate the pCSCs identified and isolated in this project. As described in Section 3.1.3.1, some of the parameters of the mice experiments had to be decided upon before any experiments were carried out. These predefined parameters were required for the ethical review process, which precedes the commencement of animal based experiments.

6.1.1 Predefined Xenograft Mouse Assay Parameters:

6.1.1.1.1 Strain of Mouse

Selection of the mouse model in which to establish the tumourgenicity assay required careful consideration. A variety of mice are used in the literature, each with their own advantages and disadvantages (Table 6.1).

The main considerations when selecting a mouse model for tumourgenicity assays were;

i) Precedence – had this model been used in such assays previously?

ii) Immune status – what was its level of immunodeficiency?

iii) Hairlessness – injection and observation of tumour growth is easier in nude mice.

All mice considered for this study had previously been successfully used in CSC tumourgenicity assays found in the literature (BALB/c: Zhang et al. 2008; NOD.SCID: Curley et al. 2009; Athymic: Pan et al. 2010).

There are multiple aspects to immunodeficiency including deficiencies in Bursa of Fabricius (B) cells, Thymus (T) cells and Natural Killer (NK) cells. The different strains of mice have different combinations of immunodeficiency (Table 6.1). NOD.SCID mice have the most immune cell deficient phenotype.

Table 6.1: A comparison of immune cell deficiencies across three common mouse strains.*

Strain	Nomenclature	T cell	B cell	NK cell
NOD.SCID	NOD.CB17-Prkdc^{scid}/NCrHsd	Non-functional	Non-functional	Impaired
BALB/c nude	BALB/c OlaHsd-Foxn1^{nu}	Non-functional	Functional	Functional
Athymic nude	Hsd: Athymic Nude-Foxn1^{nu}	Non-functional	Functional	Functional

* Adapted from Harlan Oncology Brochure page 4 of 12;
http://www.harlan.com/products_and_services/research_models_and_services/research_models_by_research_use/oncology/oncology_rodent_models

NOD.SCID mice have hair while BALB/c nude and Athymic nude mice are hairless. Having hair was not considered to be a major disadvantage as it was possible to shave the region of interest. The decision on the strain of mice was therefore based mainly on precedence and immunodeficiency.

The NOD.SCID strain was selected for the experiments in this project. It had strong precedence in CSC tumourgenicity assays, across many malignancies (Ovarian: Curley et al. 2009; Breast: (Londoño-Joshi et al. 2011); Prostate: Salvatori et al. 2012). It also had the most immunodeficient phenotype.

6.1.1.1.2 Mode of Injection

Multiple modes of injection are used throughout the literature for the study of tumour growth. Tail vein injection is used to study lung metastases (Elkin and Vlodavsky 2001). Intraperitoneal (i.p.) injection is used to study peritoneal dissemination of tumour cells. The i.p. mode is considered to better mimic the clinical behaviour of human ovarian cancer (Ward et al. 1987). Injection into the mammary fat pad is used for the study of breast cancer (Price 1996). Sub-cutaneous (s.c.) injection is the most common mode of injection for tumour xenografts.

There were three ethical principles ('the three Rs') to consider in the establishment of the tumourgenicity assay; replacement, reduction and refinement. Refinement required the experiment to cause the minimum amount of distress to the animal as possible. There was evidence that i.p. injection may be appropriate for the study of ovarian cancer (Ward et al. 1987). However the i.p. mode was also associated with more aggressive disease progression. Measurement of the efficiency of tumour growth was the primary purpose of the experiment. This could be achieved by s.c. injection, which results in less aggressive disease. The principle of refinement ruled out the i.p. mode on ethical grounds alone. In addition to this, the s.c mode had the advantage of producing tumours that were easy to observe and measure compared to i.p. injection.

It was decided to used the s.c. mode of injection. There was an option of the dorsal s.c. (Szotek et al. 2006) or hind limb s.c. (Zhang et al. 2008) route. The hind limb s.c. route was selected as it had greater representation in the literature with regards to CSC validation.

With the hind limb s.c. mode of injection there was the option of injecting cells on one or both flanks of the animal. Injection of both flanks had the potential to reduce the number of animals required. However, it had disadvantages, it meant that both tumours had to be harvested when the fastest growing one was ready. It increased the tumour burden on the animal. Each animal required two injections, this doubled the risk of loosing a replicate to a bad injection. It was decided to use a hind limb s.c mode of injection to a single flank, for the mouse tumourgenicity assay.

6.1.2 Principles of the Xenograft Mouse Assay:

During the AACR workshop on CSCs, Clarke et al. (2006) concluded that CSCs can only be defined upon the verification of their ability to form a 'continuously growing tumour'. A 'continuously growing tumour' is a tumour which is formed from a population of pCSCs, which generates a tumour, while maintaining a pCSC sub-population. This concept of a continuously growing tumour demonstrates that CSCs are a population of cells with unlimited proliferative potential, which can self-renew and differentiate to drive the malignant potential of a tumour.

The current gold standard for CSC validation is the serial transplantation mouse xenograft assay. This assays demonstrates the self-renewal, differentiation and malignant potential of a CSC population. Xenografting isolated CSCs into an immunocompromised mouse and shows that it has the malignant potential to generate a tumour with the same histology (differentiation) of that from which the CSCs were originally isolated. Furthermore, self-renewal is demonstrated, by identifying the CSCs population in the xenograft tumour, isolating the CSCs and re-xenografting them back into an immunodeficient mouse.

Time did not permit the use of the serial transplantation mouse xenograft assay in this study. However, it was possible to meet the strictest criteria for the validation of CSCs by combining the *in vivo* xenograft mouse assay with the SD assay. Through the combination of these assays it was possible to assess the self-renewal, differentiation and malignant potential of the isolated pCSC and non-pCSC sub-populations.

Tumourgenicity assays are intended to be a qualitative assay. CSCs should be able to generate tumours while non-CSCs should not. Some studies even show that while CSCs can form tumours at low cell seeding densities, non-CSCs can not form tumours with logarithmically higher cell seeding densities (Zhang et al. 2008; Curley et al. 2009; Silva et al. 2011).

The SD assay can be used to assess the self-renewal and differentiation potential of isolated sub-populations. Implemented together with the xenograft mouse assay it was possible to assess the self-renewal, differentiation and malignant potential of the isolated pCSC and non-pCSC populations. The principles of the SD assay will be described in Section 6.1.3.

6.1.3 Principles of the SD Assay:

Stem cell potency refers to the cells ability to differentiate into more mature cell types, while also being able to self-renew and maintain the stem cell pool (Inaba and Yamashita 2012). CSCs are also considered to have stem-like potency (Clarke et al. 2006).

The pCSCs and non-pCSCs identified in this project, were stably maintained in tissue culture across several passages in their respective culture media (Section 4.3). This suggests that these culture conditions support a homoeostasis between CSCs and non-CSCs, as opposed to inducing forced differentiation or self-renewal of CSCs. This principle, of a homoeostasis between CSCs and non-CSCs, is the principle behind the SD assay. If a pure CSC population is plated in such culture conditions, it should produce both CSC and non-CSC populations. On the other hand, a pure non-CSC population should not have the differentiation potential to produce both a CSC and a non-CSC population. Therefore, a pure non-CSC population should remain as a pure non-CSCs population whereas a CSC population should return to a mixture of CSCs and non-CSCs.

The single cell aspect was introduced due to concerns over the purity of the population. Plating a single cell was the most efficient way of ensuring that a cell population was 100 % pure, as opposed to > 99 % pure. If there is only a single cell in a well then it is guaranteed to be a pure population. If a single cell produces two different populations of cells, one faithful to the phenotype of the original cell and one of a different cell type, this is a demonstration of self-renewal and differentiation.

Stem cells exhibit three classes of cell division:

1. symmetrical self-renewal:- the production of two 'undifferentiated' daughter cells.
2. symmetrical differentiation:- the production of two 'differentiated' daughter cells
3. asymmetric division:- the production of one 'undifferentiated' and one 'differentiated' daughter cell.

For a single cell to produce a heterogeneous population, it could be argued that it has either undergone at least one asymmetric division, or it has undergone symmetrical self-renewal followed by symmetrical differentiation. In the latter case, if it was truly symmetrical self-renewal followed by symmetrical differentiation. One would expect the entire population to consist of 'differentiated' cells. For a heterogeneous population to arise via this pattern of cell division requires some cells to undergo symmetrical self-renewal and others to undergo

symmetrical differentiation. Such a situation suggests an asymmetry in the self-renewing population, prior to the onset of symmetrical differentiation cell division in the colony.

Using the SD assay in combination with the *in vivo* xenograft mouse tumourgenicity assay allows for the assessment of the self-renewal, differentiation and malignant potential of the pCSC and non-pCSC sub-populations identified and isolated in Sections 4.0 and 5.0 respectively.

6.1.4 Tumourgenicity based versus SD based validation:

CSCs are the focus of study as they are believed to be the malignant driving force in tumours. They are believed to be the cell population which must be killed if therapies are to be successful, without the risk of relapse (Visvader and Lindeman 2012). The tumourgenicity based validation assay is the only assay that directly demonstrates the malignant potential of a pCSC population, a characteristic that is fundamental to the validation of pCSCs as CSCs. Tumourgenicity based validation also provides information on the differentiation potential of CSCs via the formation of a tumour with a similar histology (differentiation) as that of the tumour from which the CSCs were originally isolated. Serial tumourgenicity based validation can demonstrate the self-renewal capacity of CSCs. These measures of differentiation and self-renewal are qualitative measures. The SD assay gives a more detailed analysis of the differentiation and self-renewal potential of CSCs, which can be quantified via flow cytometry.

Xenograft tumours could be dissociated and analysed via flow cytometry to produce quantitative data. However, tumours would have to be seeded from single cells, to ensure 100 % purity of the original population. This is technically improbable and would result in tumour growth times that were outside of the scope of this project. The SD assay has a higher throughput than a single cell tumourgenicity assay, as the quantification of self-renewal and differentiation potential achieved by a single mouse experiment, can be achieved by a single well of a 96-well plate.

Section6.0 – Validation of CSC

6.1.5 Aims:

To validate the pCSCs identified in Section 4.0 and isolated in Section 5.0, as being more stem-like than their non-pCSC counterparts identified in Section 4.0 and isolated in Section 5.0. This aim has two major components:

i. To demonstrate that a single pCSC, but not a single non-pCSC, is capable of generating both the pCSC and non-pCSC phenotype. Thus, demonstrating that the pCSCs but not the non-pCSCs are capable of both self-renewal and differentiation.

Together these studies can validate the pCSC population as CSCs: by validating their augmented malignant potential, ability to self-renew and augmented differentiation potential when compared to the non-pCSCs.

ii. To demonstrate that the pCSCs can generate xenograft tumours more efficiently than their non-pCSC counterparts. Thus, demonstrating the augmented malignant potential of the pCSCs over the non-pCSC counterparts.

6.1.6 Hypothesis

The validations in the chapter are based upon two hypotheses:

i. CSCs harbour the malignant potential of the tumour. Therefore, they should be more efficient at regenerating the tumour. This more efficient tumourgenicity should be observable via the *in vivo* mouse xenograft tumourgenicity assay. It is possible for non-CSCs to form tumours if sufficient cell numbers are transplanted. This is why an approach of logarithmic dilutions of cells are used.

ii. CSCs have a greater self-renewal and differentiation potential than non-CSCs. Therefore, CSCs should be able to produce both CSCs and non-CSCs, while non-CSCs should only be able to produce more non-CSCs.

6.2 Materials and Methods:

6.2.1 Cell Culture and Sub-Culture:

Two sub-populations from each of the A2780, A2780cis, IGROV-1, IGROV-CDDP, SK-OV-3 and 59M cell lines were used for the experiments presented in this chapter (Table 6.2). These sub-populations were cultured in an identical fashion to that of their parent cell line (as described in Section 2.2).

Table 6.2: A summary of the sub-populations used in this chapter.

Parent Cell Line	pCSC Sub-population	non-pCSC Sub-population
A2780	ALDH+	ALDH-
A2780cis	ALDH+	ALDH-
IGROV-1	HSP+	HSP-
IGROV-CDDP	HSP+	HSP-
SK-OV-3	CD117+	CD117-
59M	CD117+	CD117-

6.2.2 Mouse Tumourgenicity Assay:

pCSCs and non-pCSCs were validated via the mouse tumourgenicity assay. Ethical approval was granted, for these animal studies by the Trinity College Dublin ethics committee and the Irish Department of Health. The investigators who conducted the mouse tumourgenicity assay had past the Laboratory Animal Science and Training (LAST) exam and were qualified to work with laboratory animals. The Trinity College Dublin Bio-Resources staff provided the practical training required to handle the mice and conduct the procedures described in Sections 6.2.2.1 – 6.2.2.7. All experiments were designed to conform to the 3Rs principle (Replacement, Reduction and Refinement).

6.2.2.1 Housing

Mice were housed as described in Section 2.7.2.

6.2.2.2 Handling

Mice were handled as described in Section 2.7.3.

6.2.2.3 Ear-punching

For the purposes of identifying individual mice within each isolator, mice were ear-punched as described in Section 2.7.4.

6.2.2.4 Shaving

To aid with the injection of cells, mice were shaved at the injection site as described in Section 2.7.5.

6.2.2.5 Injecting

Mice were injected with cells as described in Section 2.7.6.

6.2.2.6 Euthanasia

When scientific or humane experimental end-points were reached, mice were euthanised as described in Section 2.7.7.

6.2.2.7 Post-mortem Inspection

Post-mortems were carried out as described in Section 2.7.8

6.2.3 Single Cell Self-renewal and Differentiation Assay

pCSCs and non-pCSCs were validated via the SD assay. Single cells were plated as described in Section 2.8.1. The resulting colonies were passaged as described in Section 2.8.2. Clones were retested for cancer stemness markers via flow cytometry.

6.2.4 Flow Cytometry:

6.2.4.1 ALDH Assay

The ALDH assay was carried out as described in Section 2.5.1.

6.2.4.2 HSP Assay

The HSP assay was carried out as described in Section 2.5.2.

6.2.4.3 CSP Assay

The CSP assay was carried out as described in Section 2.5.3.

6.3 Data:

A pCSC and a non-pCSC sub-population from each of the A2780, A2780cis, IGROV-1, IGROV-CDDP, SK-OV-3 and 59M cell lines (Table 4.13), were brought forward from the pCSCs screen (Section 4.3.5) for validation. The validation of these pCSC and non-pCSC sub-populations will now be described in this Data Section (Section 6.3).

The A2780, A2780cis, IGROV-1 and IGROV-CDDP pCSC and non-pCSC sub-populations were all assessed via both the mouse tumourgenicity and SD CSC validation assays (Sections 6.3.1 – 6.3.4). Due to time constraints, it was not possible to assess the SK-OV-3 and 59M pCSC and non-pCSC sub-populations via the mouse tumourgenicity assay. However, their self-renewal and differentiation potential were assessed via the SD assay (Sections 6.3.5 – 6.3.6).

The data in this section is divided into sub-sections based on the parent cell line from which the pCSC and non-pCSCs were isolated. The order of these sub-sections will respect that of Table 4.13. Within each sub-section the data will be presented in the following structure;

1. **Mouse Tumourgenicity:** where applicable, the mouse tumourgenicity data will be described. All replicates will be shown in the tumourgenicity graphs. Only a subset of the post-mortem images will be displayed. The rest of the post-mortem images are presented in Appendix C.
    i. Size and Latency: First, the data relating to tumour size and latency will be described.
    ii. Histopathology: Then the histopathology of the resulting tumours will be described.
2. **Single Cell Self-renewal and Differentiation:** After the mouse tumourgenicity data, the SD data will be described. Only a representative sample of the data from the SD assay will be presented. The rest of the of the SD assay replicates are presented in Appendix C.
    i. Non-pCSC clones: First, the data from the analysis of the non-pCSC clones will described.
    ii. pCSC clones: Then, the data from the analysis of the pCSC clones will described.

iii. Morphology: Multiple different types of colony morphologies were observed via the SD assay, these morphologies are described in Appendix C.

For the purposes of these mouse tumourgenicity experiments, 'tumour latency' is defined as the numbers of days, post injection of the cells, until the mouse was euthanised. Mice were euthanised when the tumour reached approximately 1 cm in size. While the mouse was alive, tumour size was calculated as the mean of two perpendicular measurements of the tumour diameter, made by callipers. Upon post-mortem it was noted that a dissected image of the mouse was a more accurate method to measure tumour size. Callipers based measurement was a good guide for determining the end-points but tended to under-estimate the size of the tumour, as determined post-dissection. The mean of two perpendicular diameters of the tumour, measured digitally from a photograph, are the source of the tumour sizes presented in this Data Section. Section 3.2.6 describes in detail the measurement of tumour size.

To reduce repetition, the format in which the tumourgenicity figures will be presented will be explained here. The graphs show the tumour latency on the y-axis expressed in days compared to tumour size, expressed as the size of the circle points relative to the scale bar. Circle points mark the latency and size of tumours. Crosses mark the time at which animals, which did not develop tumours were euthanised. The photographs show a dissected view of each of the tumours/mice represented on the graphs and are colour coded to their respective points.

6.3.1 Primary Ovarian Cancer A2780 CSC Assay Data:

6.3.1.1 Mouse Tumourgenicity Assay:

6.3.1.1.1 Size and Latency:

To assess the differentiation and malignant potential of the A2780 pCSC and non-pCSC sub-populations, A2780 ALDH+ pCSC and ALDH- non-pCSC cells were injected sub-cutaneously into NOD.SCID mice.

Eight mice were injected with ALDH+ pCSCs (Figure **6.1**). Initially, a pilot study assessed the optimal cell concentration at which to carry out the comparison between pCSC and non-pCSC sub-populations. Two mice were injected with 5×10^4 ALDH+ pCSCs, two with 5×10^3 ALDH+ pCSCs and two with 5×10^2 ALDH+ pCSCs. All xenografts produced tumours (Figure **6.1**). One of the 5×10^4 mice developed an i.p. tumour without a s.c. tumour. This was probably due to an error while injecting. As such, this replicate was not included in the results. Having demonstrated that ALDH+ pCSCs can efficiently form tumours at 5×10^2 cells it was decided to make 5×10^2 cells the base-line to which the non-pCSCs would be compared. The lowest cell concentration was selected to maximally exploit the different malignant potentials of the CSC and non-CSC cells. To increase the power of the tumourgenicity findings at 5×10^2 cells, a further two replicates of ALDH+ pCSCs were injected into two mice at concentration of 5×10^2 cells. Both of these replicates also produced tumours with a similar size and latency (Figure 6.1).

Eleven mice were injected with ALDH- non-pCSCs (Figure 6.1). Initially, a pilot study assessed the optimal cell concentration at which to carry out the comparison between the non-pCSCs and the pCSCs, which successfully formed tumours at 5×10^2 cells. Two mice were injected with 5×10^4 ALDH- non-pCSCs, two with 5×10^3 ALDH- non-pCSCs and two with 5×10^2 ALDH- non-pCSCs. Unexpectedly, five of the six injected mice generated tumours (Figure **6.1**). One of the 5×10^3 mice did not develop a tumour. To clarify whether this was a function of reduced malignant potential or an outlying replicate, a further 1 replicate of 5×10^4 and 2 replicates of 5×10^3 were carried out using the ALDH- non-pCSCs. All of these non-pCSCs formed tumours, indicating that the one replicate which did not grow was probably not due to reduced malignant potential.

As the pilot study indicated no qualitative difference between the A2780 pCSCs and non-pCSCs at a concentration of 5×10^2 cells, a further two replicates of ALDH- 5×10^2 non-pCSCs were conducted. This was done to increase the power of a quantitative comparison of

tumour latency and tumour size between the 5 x 10^2 ALDH+ pCSCs and the 5 x 10^2 ALDH- non-pCSCs. It was found that there was no significant difference in the latencies of the pCSCs and non-pCSCs (p-value = 0.7052). Nor was there any significant difference in the tumour size of the pCSCs and non-pCSC (p-value = 0.3048).

These findings demonstrate that there is no significance difference in the malignant potential of the pCSCs and non-pCSCs isolated from the A2780 cell line. Interestingly, both the pCSCs and the non-pCSCs were able to produce tumours at 5 x 10^2 cells: a cell number at which non-CSCs do not usually form tumours at in xenograft models (Zhang et al. 2008; Curley et al. 2009; Silva et al. 2011). This will be discussed further in Section 6.4.2.1. Due to time limitations and other related findings (Section 6.3.1.2.1), it was decided not to scale these mice experiments to 50 cells. These other findings were investigated further in additional experiments presented the next chapter (Section 7.0).

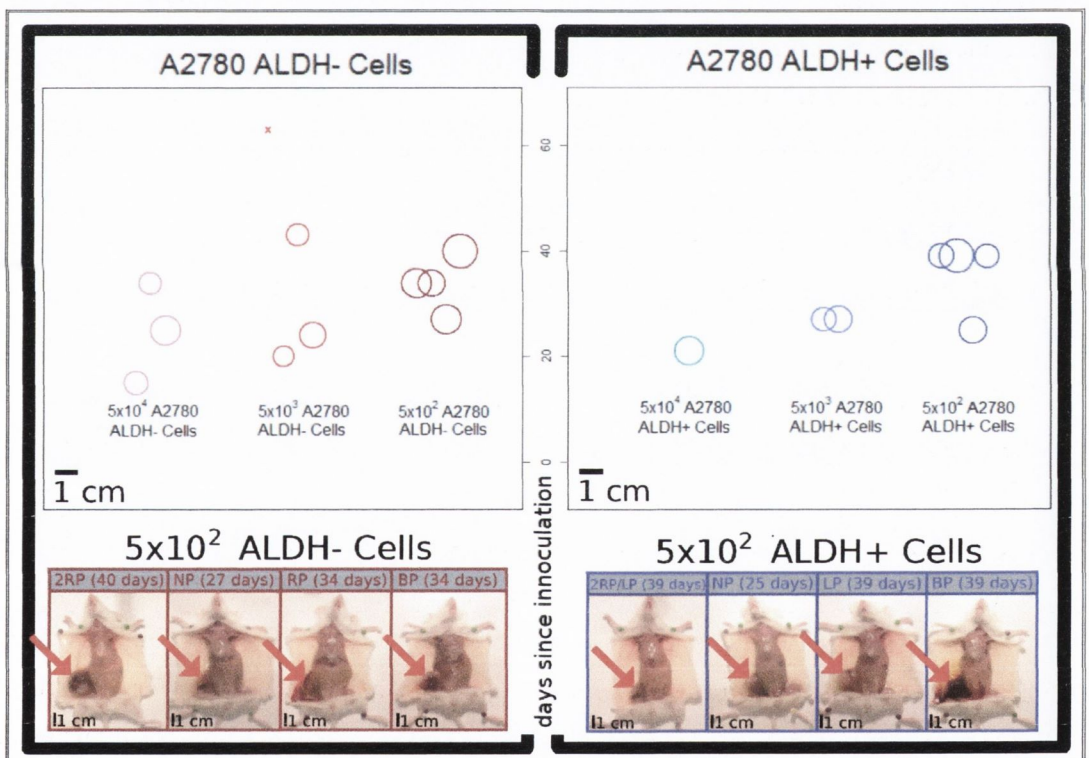

Figure 6.1: A2780 ALDH+ versus ALDH- Mouse Tumourgenicity Experiments – There is no significant difference in the latency (p-value = 0.7052) or size (p-value = 0.3048) of the tumours produced by the A2780 ALDH+ pCSCs compared to the A2780 ALDH- non-pCSCs. Neither sub-population can be declared more stem-like than the other based on these results. However, both the pCSC and non-pCSC demonstrated a stem-like malignant potential by generating tumours at 5 x 10^2.

6.3.1.1.2 Histopathology:

Hematoxylin and eosin stained sections of the tumours produced by the A2780 ALDH+ pCSC and A2780 ALDH- non-pCSC tumours were assessed for histopathology. It was found that both the A2780 ALDH+ pCSCs (Figure 6.2A) and A2780 ALDH- non-pCSCs (Figure **6.2**B) produced poorly differentiated, high grade tumours. Both the pCSC and non-pCSC tumours grew as sheets of cells with high mitotic activity and necrosis.

The histology of the original tumour from which the A2780 cell line was derived is not known (Molthoff et al. 1991). However, the A2780 cells have been shown to produce poorly differentiated high grade tumours (Molthoff et al. 1991; Shaw et al. 2004). Therefore, it can be stated that both the pCSC and non-pCSC sub-populations have the malignant potential to regenerate a tumour of similar histology to that of the parent cell line from which they were isolated.

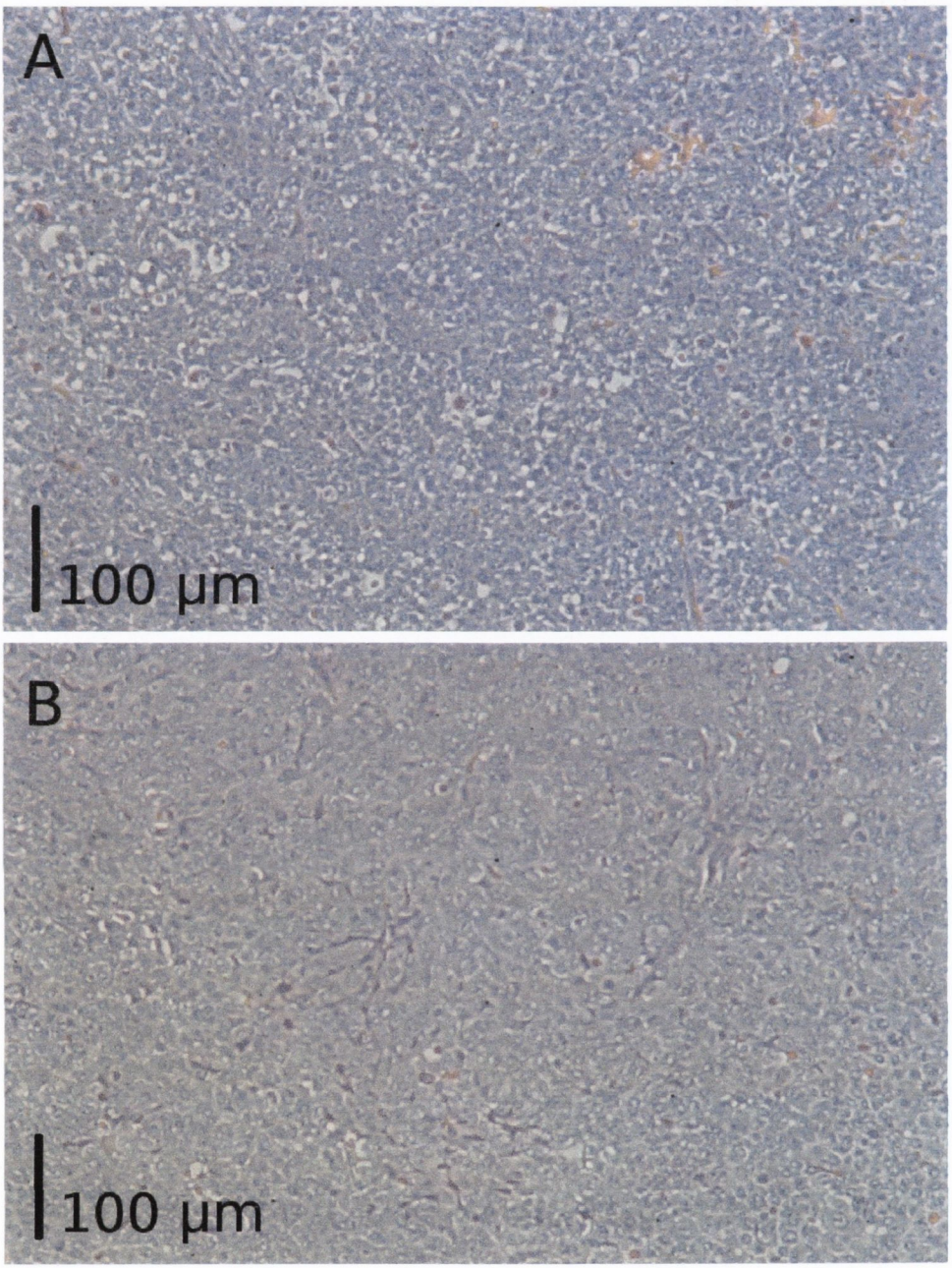

Figure 6.2: Hematoxylin and eosin stained of the A2780 ALDH+ and ALDH- derived tumours – A) shows a photograph of an ALDH+ derived tumour taken at 100x magnification. B) shows a photograph of an ALDH- derived tumour taken at 100x magnification.

6.3.1.2 Single Cell Self-renewal and Differentiation Assay:

Two sets of 60 wells, across two 96-well plates, were seeded with a single cell. One plate was seeded with single A2780 ALDH- non-pCSCs, sorted from a pre-purified population. The other plate was seeded with single A2780 ALDH+ pCSCs, sorted from a pre-purified population. 31 of the 60 single non-pCSCs formed colonies. 23 of the 60 single pCSCs formed colonies. These clonal colonies were allowed to expand (96-well plate to 6-well plate) until sufficient numbers of cells were present to facilitate retesting for the ALDH pCSC marker expression based upon which they were originally sorted.

6.3.1.2.1 A2780 ALDH- non-pCSC clones:

A set of 13 A2780 ALDH- non-pCSC clones were randomly selected for retesting. Originally only 4 clones were selected, but due to unexpected results (described below) a further 9 clones were included to add further power to the experiment. Upon flow cytometry analysis of these clones, it was observed that the clones segregated into three distinct classes: 'ALDH_NegA', 'ALDH_NegB' and 'ALDH- (unclassified)'. This nomenclature was coined to help describe the three phenotypes observed in the ALDH- SD assay:

- ALDH_NegA clones:- were ALDH- clones which were found to contain ALDH+ and ALDH- cells upon flow cytometry analysis. This was an unexpected result as ALDH- cells were predicted to be non-CSCs. As such, the were predicted to have a limited differentiation potential and were not thought to be capable of differentiating to produce ALDH+ cells. These ALDH- clones have demonstrated the ability to differentiate and self-renew. This classifies these ALDH_NegA cells as CSCs.
- ALDH_NegB clones:- were ALDH- clones which were found to contain only ALDH- cells upon flow cytometry analysis. This was the expected result for the ALDH- SD assay. These ALDH- clones have demonstrated a limited differentiation potential. This classifies these ALDH_NegB clones as non-CSCs, pending confirmation of reduced malignant potential.
- ALDH- (unclassified) clones:- were ALDH- clones which could not be confidently categorised into either the ALDH_NegA or ALDH_NegB phenotypes. This uncertainty spawned from the nature of their fluorescent ALDH profile. It was not as well defined as the clones of the ALDH_NegA and ALDH_NegB phenotypes. As such, it was not clear whether the ALDH+ pCSCs observed in these clones were true ALDH+ cells or artefacts of the 'noisier' ALDH profile.

46.15 % (6/13) of the ALDH- non-pCSC clones exhibited the expected non-CSC phenotype (Figure 6.3). These clones were classified as ALDH_NegB clones. These clones consisted entirely of ALDH- cells. This demonstration of limited differentiation potential means that these ALDH_NegB clones can be classified as non-CSCs, pending confirmation of reduced malignant potential.

Unexpectedly, 30.77 % (4/13) of the ALDH- non-pCSC clones exhibited an unexpected CSC phenotype (Figure 6.4). These clones were classified as ALDH_NegA clones. These clones consisted of both ALDH- and ALDH+ cells. This demonstration of differentiation and self-renewal potential means that these ALDH_NegA clones can be classified as CSCs.

The remaining 23.08 % (3/13) of the ALDH- non-pCSC clones could not be confidently classified into either the ALDH_NegA or ALDH_NegB phenotypes (Figure 6.5), due to their 'noisier' ALDH profile. The flow cytometry analysis of these clones did reveal some possible ALDH+ cells. However, these 'ALDH+ cells' may have been artefacts of the noisier ALDH profile. It can be said that these ALDH- (unclassified) clones did not clearly reconstitute the parent phenotype. As such, these clones probably represent non-CSCs. However, further experiments are required to confirm this. These experiments are discussed in Section 6.4.5.

The identification of different classes of ALDH- cells within the A2780 ALDH- non-pCSC sub-population allows for a different interpretation of the unexpected malignant potential of the non-pCSCs observed in Section 6.3.1.1. These interpretations will be discussed further in Section 6.4.2.

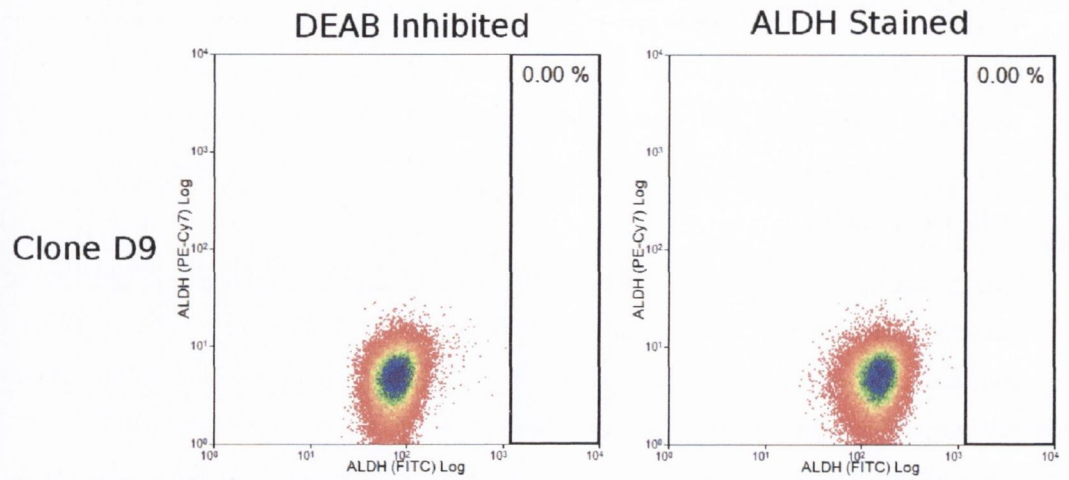

Figure 6.3: A2780 ALDH_NegB SD Assay – The group of ALDH- clones classified as ALDH_NegB exhibited a reduced differentiation potential and did not produce any ALDH+ pCSC progeny. This sub-set of A2780 ALDH- non-pCSC clones exhibit the functional characteristics of true non-CSCs. A 'DEAB inhibited' and an 'ALDH stained' sample is shown for each clone. The positive/negative threshold is set using the DEAB inhibited negative control. The percentage of cells declared as ALDH+ is shown on each graph.

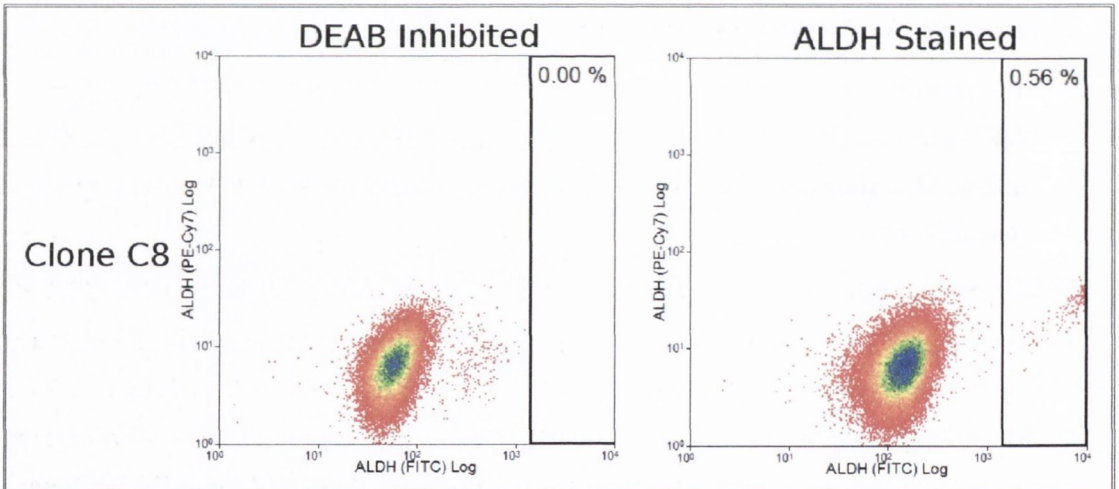

Figure 6.4: A2780 ALDH_NegA SD Assay – The group of ALDH- clones classified as ALDH_NegA exhibited a differentiation and self-renewal potential, through the formation of ALDH+ pCSC and ALDH- non-pCSC progeny. This sub-set of A2780 ALDH- non-pCSC clones exhibit the functional characteristics of CSCs. A DEAB inhibited and an ALDH stained sample is shown for each clone. The positive/negative threshold is set using the DEAB inhibited negative control. The percentage of cells declared as ALDH+ is shown on each graph.

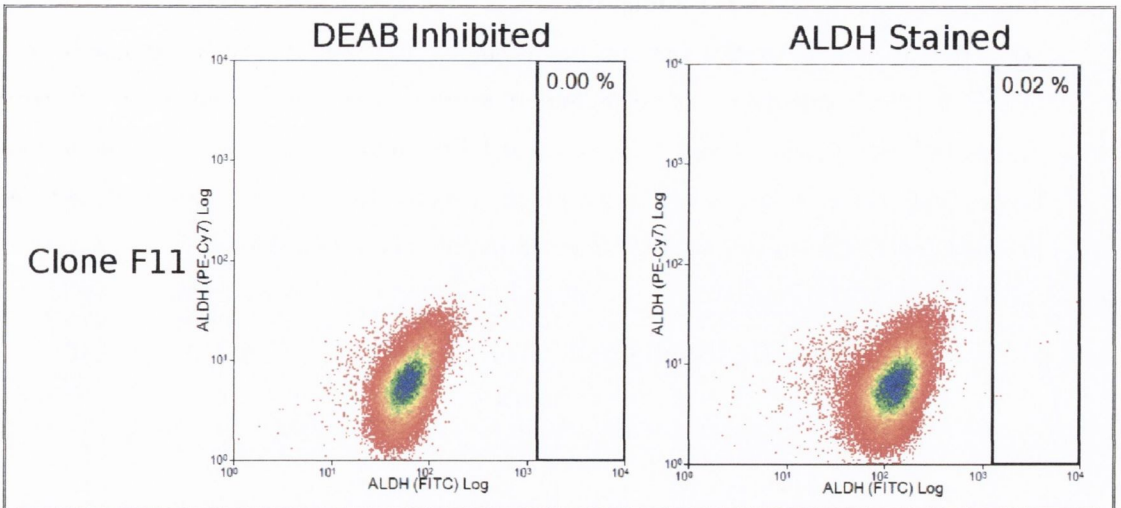

Figure 6.5: A2780 ALDH- (Unclassified) SD Assay – Three of the thirteen ALDH- clones retested after the SD assay could not be classified as either ALDH_NegA or ALDH_NegB clones, as the flow cytometry profile produce was not as well defined as those of the other clones. No statement of the stem-like behaviour of these clones can be made. A DEAB inhibited and an ALDH stained sample is shown for each clone. The positive/negative threshold is set using the DEAB inhibited negative control. The percentage of cells declared as ALDH+ is shown on each graph.

6.3.1.2.2 A2780 ALDH+pCSC clones:

A set of 4 A2780 ALDH+ pCSC clones were randomly selected for retesting. Upon flow cytometry analysis of these clones it was observed that 100 % (4/4) of the pCSC clones exhibited a CSC phenotype. As expected all of the ALDH+ pCSC clones had produced both ALDH+ pCSCs and ALDH- non-pCSCs, demonstrating an ability to self-renew and differentiate (Figure 6.6). These findings, taken together with the malignant potential of the ALDH+ pCSCs observed in Section 6.3.1.1, suggests that the A2780 ALDH+ pCSCs do have the functional characteristics of a CSC population. Interestingly, the size of the ALDH+ pCSC sub-population generated by the pCSC clones (52.61 % +/- 26.38 ; Section 6.3.1.2.2) is significantly different (p-value = 0.02844) to that of the parent A2780 population (0.15 % +/- 0.02 %; Section 4.3.1). Whereas, the size of the ALDH+ pCSC sub-population generated by the ALDH_NegA clones (0.18 % +/- 0.25 %; Section 6.3.1.2.1) is not significantly different (p-value = 0.7955) to that of the parent A2780 population (0.15 % +/- 0.02 %; Section 4.3.1). The interpretations of these findings will be discussed further in Section 6.4.2.

These data from the SD assay demonstrated that the A2780 ALDH+ cells possess self-renewal and differentiation properties and can be declared CSCs. The A2780 ALDH- cells are now observed to be a heterogeneous population of at least ALDH_NegA and ALDH_NegB cells. The ALDH_NegA cells possess self-renewal and differentiation properties and can be declared CSCs. The ALDH_NegB cells demonstrated reduced differentiation potential and can be declared non-CSCs, pending confirmation of reduced malignant potential.

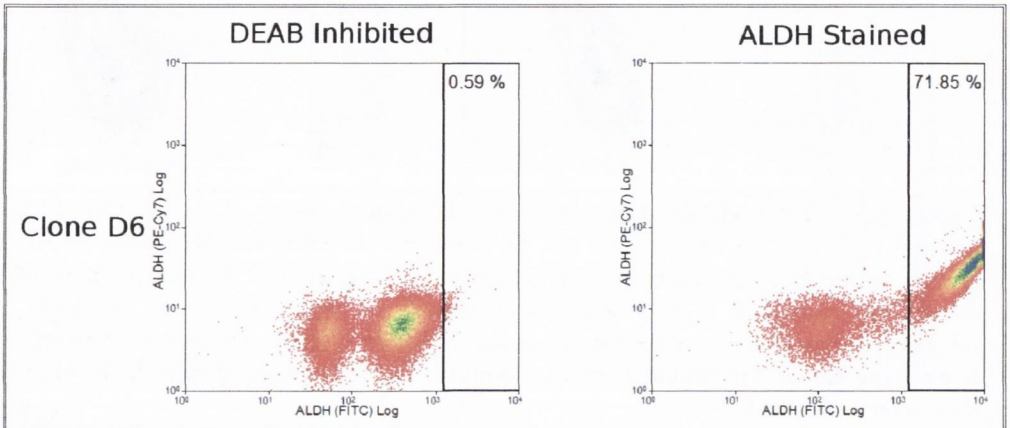

Figure 6.6: A2780 ALDH+ SD Assay – All of the ALDH+ pCSC clones exhibited a differentiation and self renewal potential, through the production of both ALDH- non-pCSC and ALDH+ pCSC populations. The A2780 ALDH+ pCSC clones exhibited the functional characteristics of CSCs. A DEAB inhibited and an ALDH stained sample is shown for each clone. The positive/negative threshold is set at the gap between the bright and dim populations in the ALDH stained sample. The percentage of cells declared as ALDH+ is shown on each graph.

6.3.2 Cisplatin-Adapted Primary Ovarian Cancer A2780cis CSC Assay Data:

6.3.2.1 Mouse Tumourgenicity Assay:

6.3.2.1.1 Size and Latency:

To assess the differentiation and malignant potential of the A2780cis pCSC and non-pCSC sub-populations, A2780cis ALDH+ pCSC and ALDH- non-pCSC cells were injected sub-cutaneously into NOD.SCID mice.

Nine mice were injected with ALDH+ pCSCs (Figure **6.7**). Initially, a pilot study assessed the optimal cell concentration at which to carry out the comparison between pCSC and non-pCSC sub-populations. Two mice were injected with 5×10^4 ALDH+ pCSCs, two with 5×10^3 ALDH+ pCSCs and two with 5×10^2 ALDH+ pCSCs. All xenografts produced tumours (Figure **6.7**). One of the 5×10^3 mice developed an i.p. tumour without a s.c. tumour. This was probably due to an error while injection. As such, this replicate was not included in the results. Having demonstrated that ALDH+ pCSCs can efficiently form tumours at 5×10^2 cells it was decided to make 5×10^2 the base-line to which the non-pCSCs would be compared. To increase the power of the tumourgenicity findings at 5×10^2 cells, a further three replicates of ALDH+ pCSCs were injected into three mice at concentration of 5×10^2 cells. All additional replicates also produced tumours with a similar size and latency (Figure **6.7**).

Eight mice were injected with ALDH- non-pCSCs (Figure **6.7**). Initially a pilot study assessed the optimal cell concentration at which to carry out the comparison between the non-pCSCs and the pCSCs, which successfully formed tumours at 5×10^2 cells. Two mice were injected with 5×10^4 ALDH- non-pCSCs, two with 5×10^3 ALDH- non-pCSCs and two with 5×10^2 ALDH- non-pCSCs. Unexpectedly, all of the ALDH- non-pCSC inoculated mice developed s.c. tumours. The pilot study indicated no qualitative difference between the pCSCs and non-pCSCs. A further two replicates ALDH- 5×10^2 non-pCSCs were conducted to increase the power of a quantitative comparison of tumour latency and tumour size between the 5×10^2 ALDH+ pCSCs and the 5×10^2 ALDH- non-pCSCs. It was found that there was no significant difference in the latencies of the pCSCs and non-pCSC (p-value = 0.1973). Nor was there any significant difference in the tumour size of the pCSCs and non-pCSC (p-value = 0.8069).

These findings demonstrate that there is no difference in the malignant potential of the ALDH+ pCSCs and ALDH- non-pCSCs isolated from the A2780cis cell line. Interestingly, both the pCSCs and the non-pCSCs were able to generate tumours at 5×10^2 cells: a cell number which non-CSCs can not usually form tumours (Zhang et al. 2008; Curley et al. 2009; Silva et al.

2011). This will be discussed further in Section 6.4.2. Similar to the A2780 tumourgenicity experiments, due to time limitations and other related findings (Section 6.3.2.2.1), it was decided not to scale these mice experiments to 50 cells. These other findings were investigated further in additional experiments presented in the next chapter (Section 7.0).

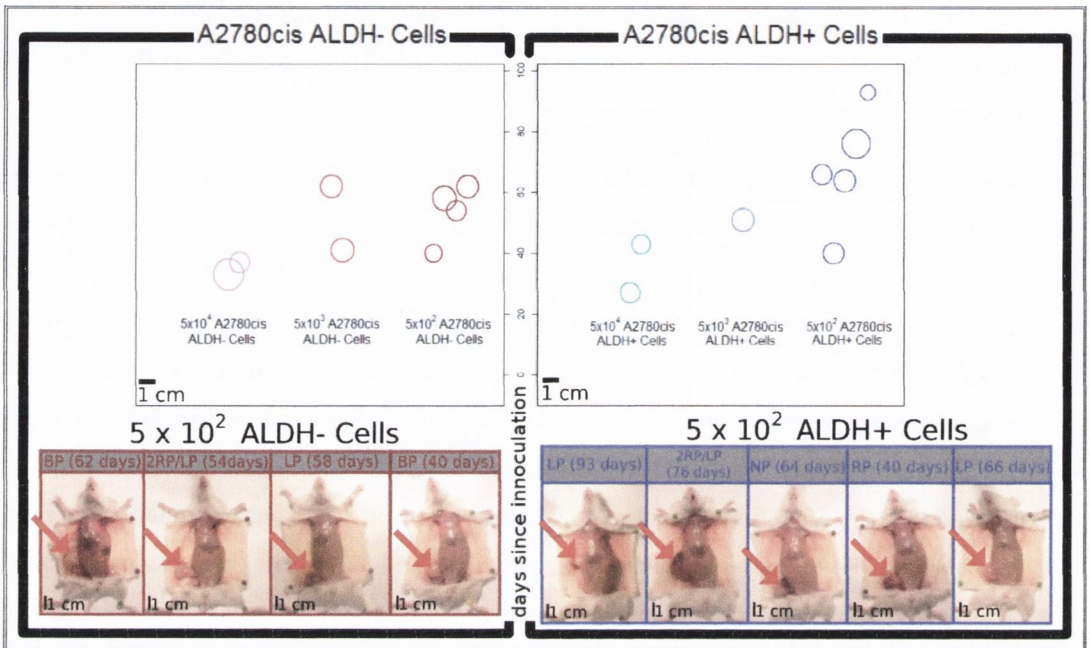

Figure 6.7: A2780cis ALDH+ versus ALDH- Mouse Tumourgenicity Experiments – There is no significant difference in the latency (p-value = 0.1973) or size (p-value = 0.8069) of the tumours produced by the A2780cis ALDH+ pCSCs compared to the A2780cis ALDH- non-pCSCs. Neither sub-population can be declared more stem-like than the other based on these results. However, both the pCSC and non-pCSC demonstrated a stem-like malignant potential by generating tumours at 5 x 10^2.

6.3.2.1.2 Histopathology:

Hematoxylin and eosin stained sections of the tumours produced by both the A2780cis ALDH+ pCSCs and A2780cis ALDH- non-pCSCs was assessed for histopathology. It was found that both sub-populations produced poorly differentiated high grade tumours, both the pCSC and non-pCSC tumours grew as sheets of cells with high mitotic activity and necrosis.

As the A2780cis cell line was derived from the A2780 cell line. It can be said that both the A2780cis ALDH+ pCSCs (Figure 6.8A) and ALDH- non-pCSCs (Figure 6.8B) had the malignant potential to reproduce a tumour of similar histology to that of the parent cell line (Molthoff et al. 1991; Shaw et al. 2004).

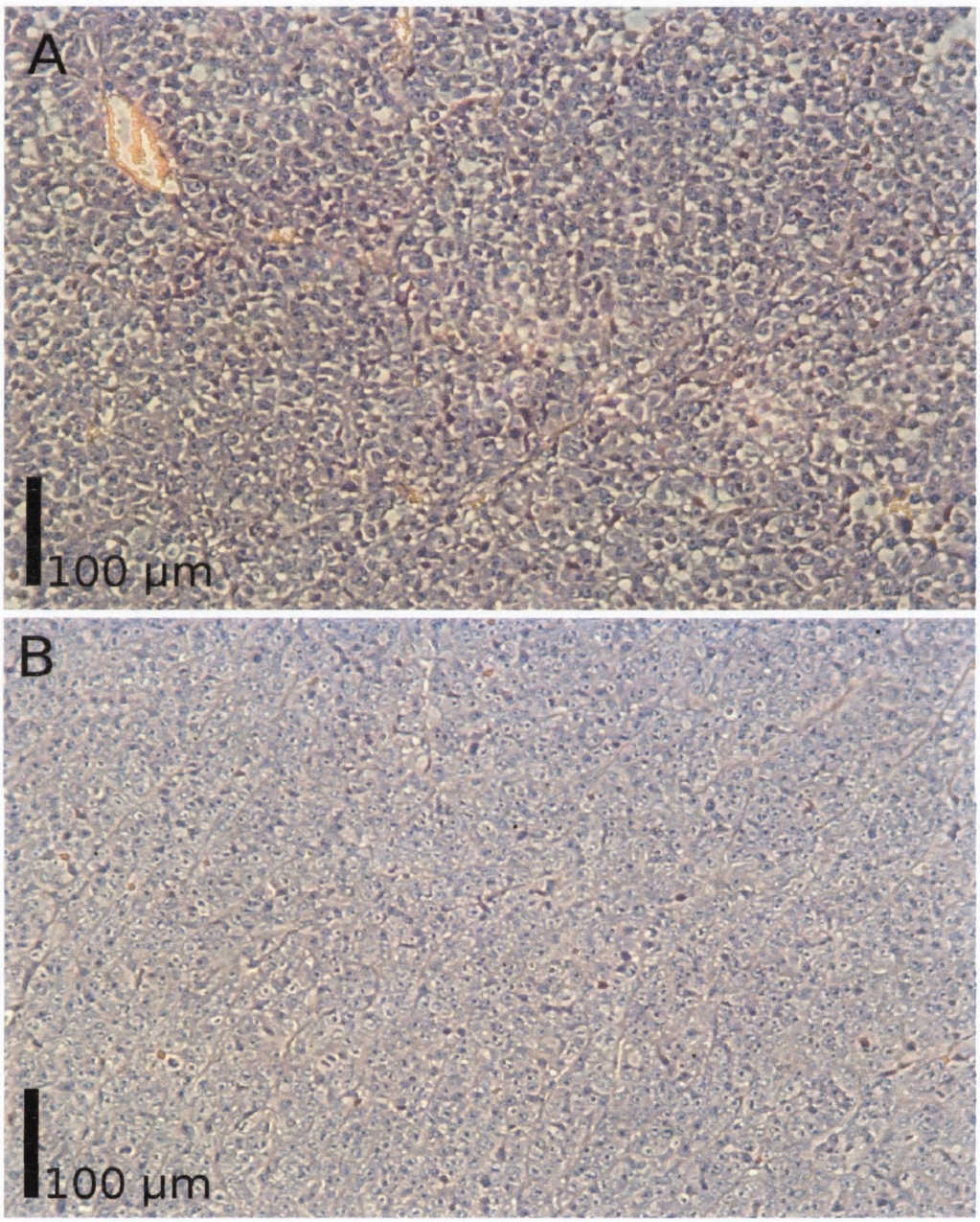

Figure 6.8: Hematoxylin and eosin stained of the A2780cis ALDH+ and ALDH- derived tumours – A) shows a photograph of an ALDH+ derived tumour taken at 100x magnification. B) shows a photograph of an ALDH- derived tumour taken at 100x magnification.

6.3.2.2 Single Cell Self-renewal and Differentiation Assay:

Two sets of 60 wells across two 96-well plates were seeded with a single cell. One plate was seeded with single A2780cis ALDH- non-pCSCs, sorted from a pre-purified population. The other plate was seeded with single A2780cis ALDH+ pCSCs, sorted from a pre-purified population. 45 of the 60 single non-pCSCs formed colonies. 31 of the 60 single pCSCs formed colonies. These clonal colonies were allowed to expand (96-well plate to 6-well plate) until sufficient numbers of cells were present to facilitate retesting for the ALDH pCSC marker expression based upon which they were originally sorted.

6.3.2.2.1 A2780cis ALDH- non-pCSC clones:

A set of 7 A2780cis ALDH- non-pCSC clones were randomly selected for retesting. Upon flow cytometry analysis of these clones, it was observed that the clones segregated into two distinct classes: 'ALDH_NegA' and 'ALDH- (unclassified)'. These classes are the same as described in Section 6.3.1.2.1.

None of the ALDH- non-pCSC clones exhibited a non-CSC phenotype consistent with the ALDH_NegB clones identified in the A2780 ALDH- sub-population (6.3.1.2.1). Unexpectedly, 71.43 % (5/7) of the ALDH- non-pCSC clones exhibited a CSC phenotype (Figure 6.9). These clones were classified as ALDH_NegA clones. These clones consisted of both ALDH- and ALDH+ cells. This demonstration of differentiation and self-renewal potential means that these ALDH_NegA clones can be classified as CSCs.

The remaining 28.57 % (2/7) of the ALDH- non-pCSC clones could not be confidently classified into either the ALDH_NegA or ALDH_NegB phenotypes (Figure 6.10), due to their 'noisier' ALDH profile. The flow cytometry analysis of these clones did reveal some possible ALDH+ cells. However, these 'ALDH+ cells' may have been artefacts of the noisier ALDH profile. It can be said that these ALDH- (unclassified) clones did not clearly reconstitute the parent phenotype. As such, these clones probably represent non-CSCs. However, further experiments are required to confirm this.

The identification of different classes of ALDH- cells within the A2780 ALDH- non-pCSC sub-population allows for a different interpretation of the unexpected malignant potential of the non-pCSCs observed in Section 6.3.2.1. These interpretations will be discussed further in Section 6.4.2.

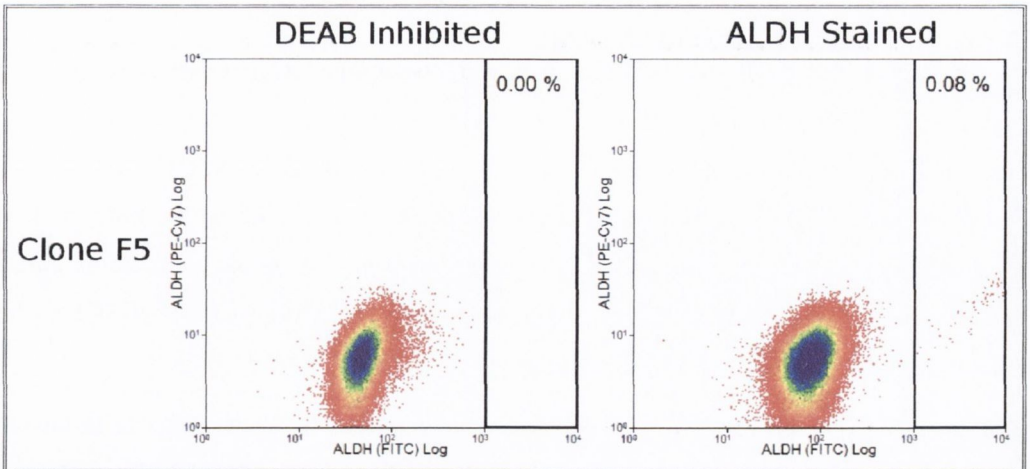

Figure 6.9: A2780cis ALDH- ALDH_NegA SD Assay - The group of ALDH- clones classified as ALDH_NegA exhibited a differentiation and self-renewal potential, through the production of ALDH+ pCSCs and ALDH- non-pCSCs. This sub-set of A2780 ALDH- non-pCSC clones exhibited the functional characteristics of CSCs. A 'DEAB inhibited' and an 'ALDH stained' sample is shown for each clone. The positive/negative threshold is set using the DEAB inhibited negative control. The percentage of cells declared as ALDH+ is shown on each graph.

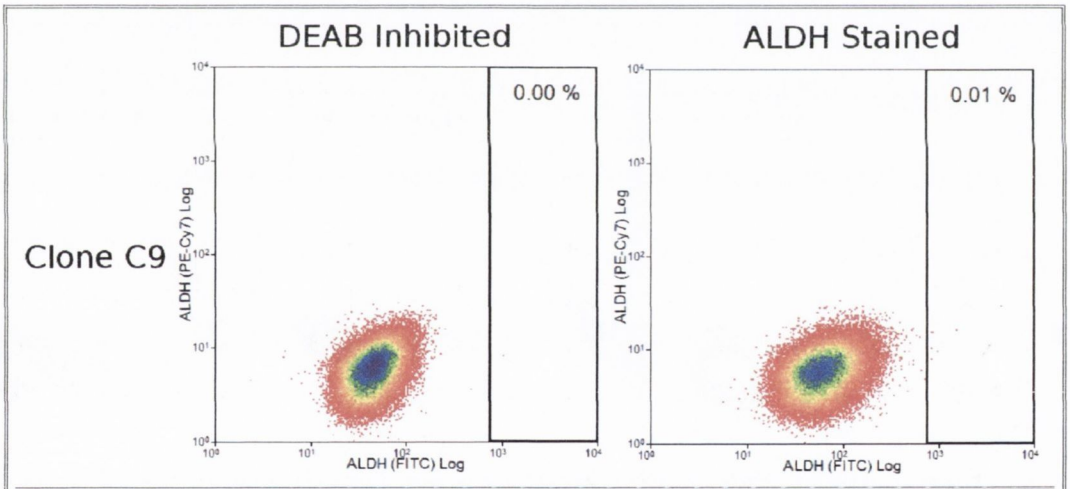

Figure 6.10: A2780cis ALDH- (Unclassified) SD Assay – Two of the seven ALDH- clones retested after the SD assay could not be classified as either ALDH_NegA or ALDH_NegB clones, as the flow cytometry profile produce was not as well defined as those of the other clones. No statement of the stem-like behaviour of these clones can be made. A DEAB inhibited and an ALDH stained sample is shown for each clone. The positive/negative threshold is set using the DEAB inhibited negative control. The percentage of cells declared as ALDH+ is shown on each graph.

6.3.2.2.2 A2780cis ALDH+ pCSC clones:

A set of 5 A2780cis ALDH+ pCSC clones were randomly selected for retesting. Upon flow cytometry analysis of these clones it was observed that 100 % (5/5) of the pCSC clones exhibited a CSC phenotype (Figure 6.11). As expected, all of the ALDH+ pCSC clones had produced both ALDH+ pCSCs and ALDH- non-pCSCs, demonstrating an ability to self-renew and differentiate. These findings taken together with the malignant potential of the ALDH+ pCSCs observed in Section 6.3.2.1, suggests that the A2780cis ALDH+ pCSCs do have the functional characteristics of a CSC population.

These data from the SD assay demonstrated that the A2780cis ALDH+ cells possess self-renewal and differentiation properties and can be declared CSCs. The A2780 ALDH- cells are now observed to be a heterogeneous population of at least ALDH_NegA and ALDH- (unclassified) cells. The ALDH_NegA cells possess self-renewal and differentiation properties and can be declared CSCs. The ALDH- (unclassified) cells are suspected to be non-CSCs. However, further experiments are required to confirm this (discussed in Section 6.4.5).

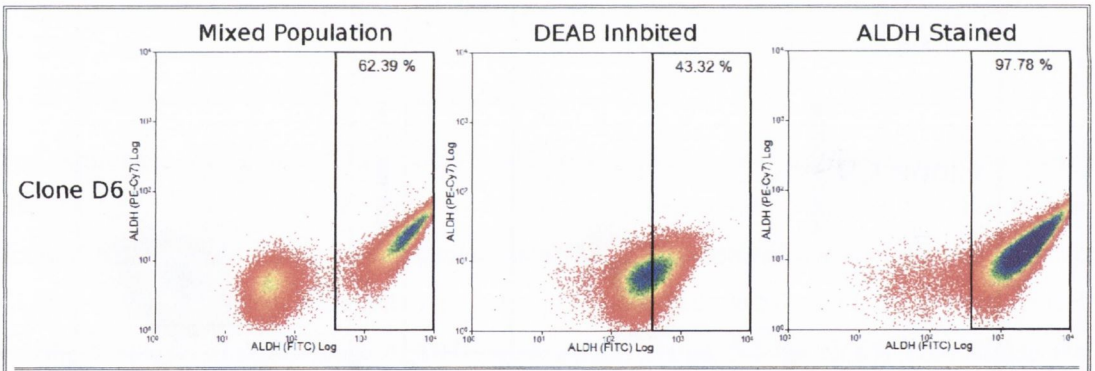

Figure 6.11: A2780cis ALDH+ SD Assay – All of the ALDH+ pCSC clones exhibited a differentiation and self renewal potential, through the production of both ALDH- non-pCSC and ALDH+ pCSC populations. The A2780cis ALDH+ pCSC clones exhibited the functional characteristics of CSCs. A mixed population, a DEAB inhibited and an ALDH stained sample is shown for each clone. The positive/negative threshold is set at the gap between the bright and dim populations in the mixed population sample. The percentage of cells declared as ALDH+ is shown on each graph.

6.3.3 Primary Ovarian Cancer IGROV-1 CSC Assay Data:

6.3.3.1 Mouse Tumourgenicity Assay:

To assess the differentiation and malignant potential of the IGROV-1 pCSC and the IGROV-1 non-pCSC sub-populations, IGROV-1 HSP+ pCSC and HSP- non-pCSC cells were injected sub-cutaneously into NOD.SCID mice.

Due to time constraints, it was not possible to conduct a pilot study to determine the optimal cell concentration at which to perform the comparisons between pCSC and non-pCSC sub-populations. It was decided to carry out the comparison of pCSCs to non-pCSCs at a concentration of 5 x 10^2 cells, as both sub-populations from both the A2780 and the A2780cis cells lines demonstrated efficient generation of tumours at 5 x 10^2 cells.

Four mice were injected with HSP+ pCSCs (Figure 6.12). Only two of four mice developed SC tumours. Four mice were injected with HSP- pCSCs (Figure 6.12). All of these mice developed tumours. These results indicate, in a semi-quantitative fashion, that the non-pCSCs may be more efficient at generating tumours than the pCSCs. 4/4 non-pCSC mice generated tumours before 111 days, while only 2/4 pCSC mice generated tumours in the same time. However, due to the wide spectrum of tumour sizes produced by the non-pCSCs (0.25 cm – 0.72 cm) and the pCSCs (0 cm – 1.00 cm), this semi-quantitative difference does not translate into a significant result, based on the size of the tumour produced (p-value = 0.6868). Nor was their any significant difference in the tumour latency (p-value = 0.391). However, this observation comes with the caveat that the latencies of the tumour produced are at the limit of what this xenograft model can analyse (described below). Increasing the cell number or using a different injection vehicle may confirm these findings at a lower tumour latency.

The tumour latencies in the IGROV-1 HSP+ and HSP- tumourigenicity assay were at the limit of analysis of the xenograft model established in this project. The latency of these tumours was very long at 111 days. The HSP+ pCSC mouse that was euthanised at 88 days, was euthanised for humane reasons rather than the scientific end-point. It had developed a spontaneous lymphoma. These mice were 160 – 174 days old when tumour latency was 111 days. The incidence of spontaneous thymic lymphoma is very high in NOD.SCID mice. 83 % of female mice were shown to have developed thymic lymphomas at 280 days of age (Prochazka et al. 1992). Therefore these experiments were stopped at 111 days post-injection (160 – 174 days old mice), to ensure compliance with the 'three Rs' and not to cause/allow unnecessary suffering to the animals by allowing the incidence of spontaneous lymphoma to increase.

These results also indicate that the NOD.SCID xenograft model is not conducive to running tumourgenicity experiments in which the tumour latency exceeds 90-100 days. Possible solutions to this challenge are discussed in Section 6.4.4.

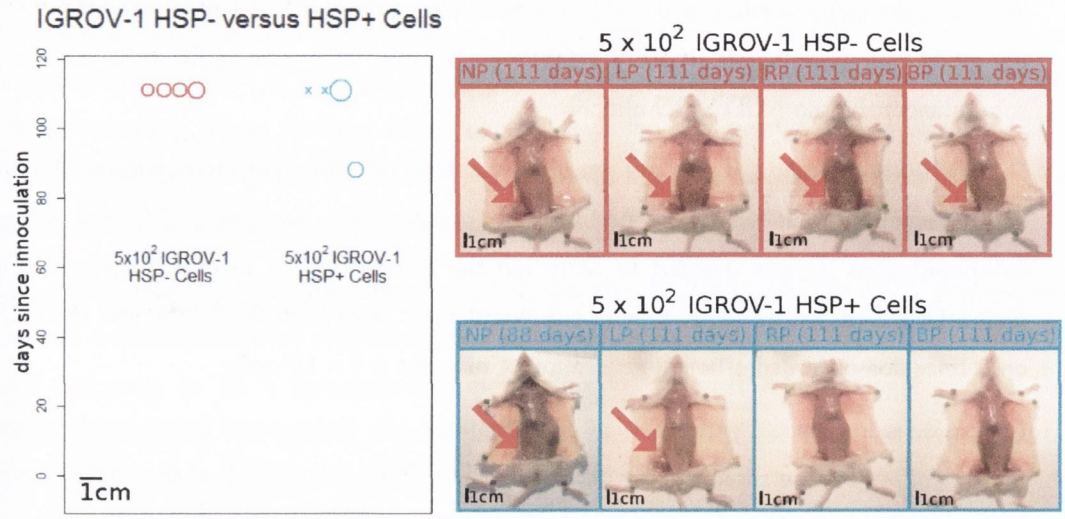

Figure 6.12: IGROV-1 HSP+ versus HSP- Mouse Tumourgenicity Experiments – There is no significant difference in the latency (p-value = 0.391) or size (p-value = 0.6868) of the tumours produced by the IGROV-1 HSP+ pCSCs compared to the IGROV-1 HSP- non-pCSCs. Neither sub-population can be declared more stem-like than the other based on these results.

Hematoxylin and eosin stained sections of the tumours produced by both the IGROV-1 HSP+ pCSCs and IGROV-1 HSP- non-pCSCs were assessed for histopathology. It was found that both sub-populations produced poorly differentiated, high grade tumours, with an insular/packeted growth pattern, high mitotic activity and little necrosis. Some of the HSP+ tumours had clear cell and serous foci. Some of the HSP- had clear cell foci, no serous differentiation was detected in these tumours. This could indicate a restriction of serous differentiation to the IGROV-1 HSP+ sub-population. Immunohistochemistry could be used to investigate this further. Staining for expression of the following proteins could be used to identify the different lineages of differentiation:

- High grade serous: p53+ WT-1+ CA125+ CD15-
- Endometrioid: p53- WT-1- CA125+ CD15-
- Clear cell: p53-/+ WT-1- CA125- CD15+

6.3.3.2 Single Cell Self-renewal and Differentiation Assay:

Two sets of 60 wells, across two 96-well plates were seeded with a single cell. One plate was seeded with single IGROV-1 HSP- non-pCSCs, sorted from a pre-purified population. The other plate was seeded with single IGROV-1 HSP+ pCSCs, sorted from a pre-purified population. 38 of the 60 single non-pCSCs formed colonies. 51 of the 60 single pCSCs formed colonies. These clonal colonies were allowed to expand (96-well plate to T25 flask) until sufficient numbers of cells were present to facilitate retesting for the HSP pCSC marker expression upon which they were originally sorted.

A set of 4 IGROV-1 HSP- non-pCSC clones were randomly selected for retesting. Unexpectedly, 100 % (4/4) of the non-pCSC clones exhibited a CSC phenotype. The IGROV-1 HSP- non-pCSCs exhibited the stem like ability to differentiate and self-renew by producing both HSP- and HSP+ progeny (Figure 6.13).

A set of 5 IGROV-1 HSP+ pCSC clones were randomly selected for retesting. Upon flow cytometry analysis of these clones, it was observed that 100 % (5/5) of the pCSC clones exhibited a CSC phenotype. As expected, all of the HSP+ pCSC clones produced both HSP+ pCSCs and HSP- non-pCSCs, demonstrating an ability to differentiate and self-renew (Figure 6.14).

From the findings described in Section 4.3 and discussed in Section 4.4.4.3.3, it is known that the HSP+ and HSP- sub-populations of the IGROV-1 cell line themselves have further pCSC and non-pCSC sub-populations. These additional (hierarchical) sub-populations are defined by the expression of the pCSC markers; ALDH and CD44. One possible explanation of the CSC-like activity in the HSP- and HSP+ sub-populations of the IGROV-1 cell line is that HSP+ does not define the most stem-like population of CSCs in the IGROV-1 cell line.

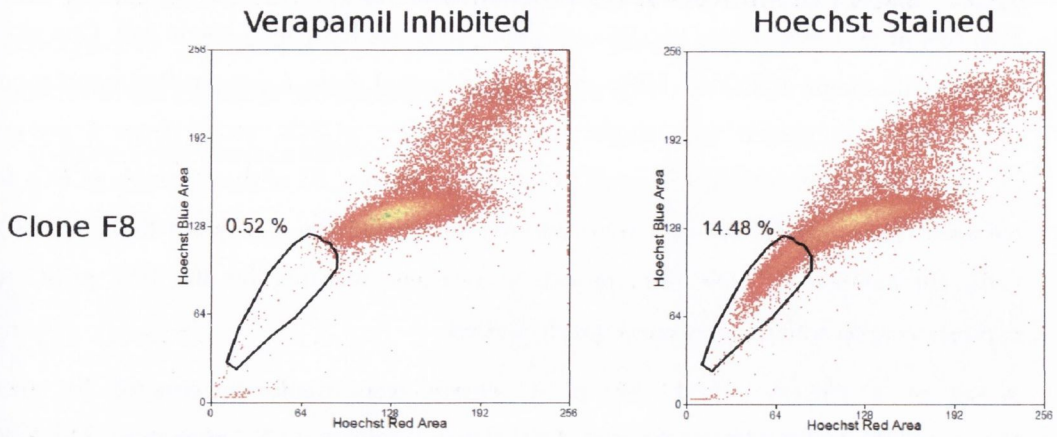

Figure 6.13: IGROV-1 HSP- SD Assay – None of the IGROV-1 HSP- clones exhibited a non-CSC phenotype. All HSP- non-pCSC clones produced both HSP- and HSP+ progeny, exhibiting the functional CSC characteristics of differentiation and self-renewal. A 'Verapamil inhibited' and a 'hoechst stained' sample is shown for each clone. The positive/negative threshold is set using the Verapamil inhibited negative control. The percentage of cells declared as HSP+ is shown on each graph.

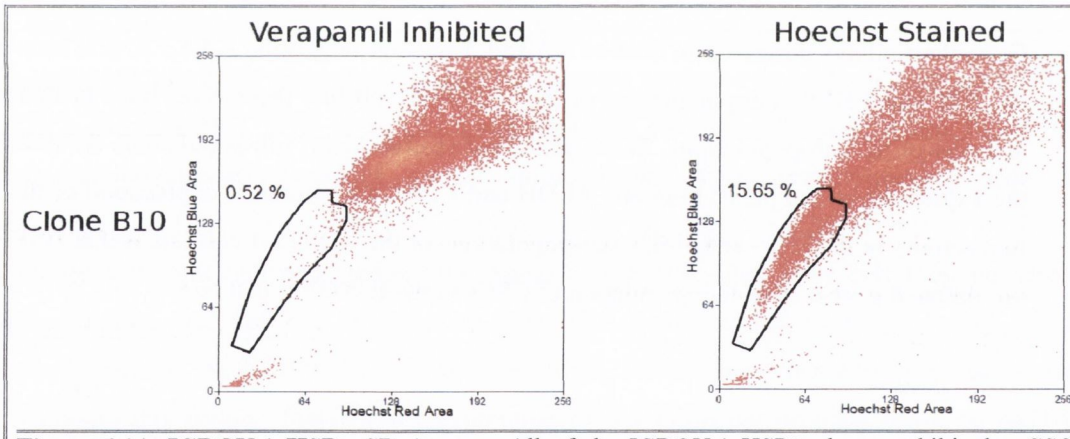

Figure 6.14: IGROV-1 HSP+ SD Assay – All of the IGROV-1 HSP+ clones exhibited a CSC phenotype. All HSP+ pCSC clones produced both HSP- and HSP+ progeny, exhibiting the functional CSC characteristics of differentiation and self-renewal. A 'Verapamil inhibited' and a 'hoechst stained' sample is shown for each clone. The positive/negative threshold is set using the Verapamil inhibited negative control. The percentage of cells declared as HSP+ is shown on each graph.

6.3.4 Cisplatin-adapted Primary Ovarian Cancer IGROV-CDDP CSC Assay Data:

6.3.4.1 Mouse Tumourgenicity Assay:

To assess the differentiation and malignant potential of the IGROV-CDDP pCSC and the IGROV-CDDP non-pCSC sub-populations, IGROV-CDDP HSP+ pCSC and HSP- non-pCSC cells were injected sub-cutaneously into NOD.SCID mice.

Due, to time constraints it was not possible to conduct a pilot study to determine the optimal cell concentration at which to perform the comparisons between pCSC and non-pCSC sub-populations. It was decided to carry out the comparison of pCSCs to non-pCSCs at a concentration of 5×10^2 cells, as both the sub-populations from both the A2780 and the A2780cis cells lines demonstrated efficient generation of tumours at 5×10^2 cells.

Four mice were injected with HSP+ pCSCs and four mice were injected with HSP- pCSCs. No mice developed SC tumours, before 111 days (Figure 6.15), at which point the experiments were stopped for humane reasons and the mice were euthanised. The HSP- non-pCSC and the HSP+ pCSC mice that were euthanised at 88, 71 and 81 days, were euthanised then for humane reasons rather than the scientific end-point. They had developed spontaneous lymphomas. As described in Section 6.3.3.1, these mice were quite old for NOD.SCID mice and the risk of spontaneous lymphoma was increasing. To ensure compliance with the 'three Rs' and not to cause/allow unnecessary suffering to the animals, the experiments were stopped at 111 days and the mice were euthanised.

These results indicate that the NOD.SCID xenograft model is not conducive to running tumourgenicity experiments in which the tumour latency exceeds 90-100 days. The use of a higher concentration of cells may reduce the tumour latency and allow for better interpretation of the results.

As no tumours formed in either the pCSC or non-pCSC populations, these cells have not demonstrated any malignant potential and are declared non-CSCs. However, the SD assay produced data identifying both populations as CSCs (Section 6.3.4.2). As such, further xenograft studies may alter this non-CSC classification (discussed in Section 6.4.4)

None of the mice injected with IGROV-CDDP HSP+ or HSP- cells developed tumours. However, hematoxylin and eosin stained sections of the subcutaneous fat tissue from the injection site were assessed for histopathology. It was noted that these regions contained very rare atypical cells most likely representing the injected cells.

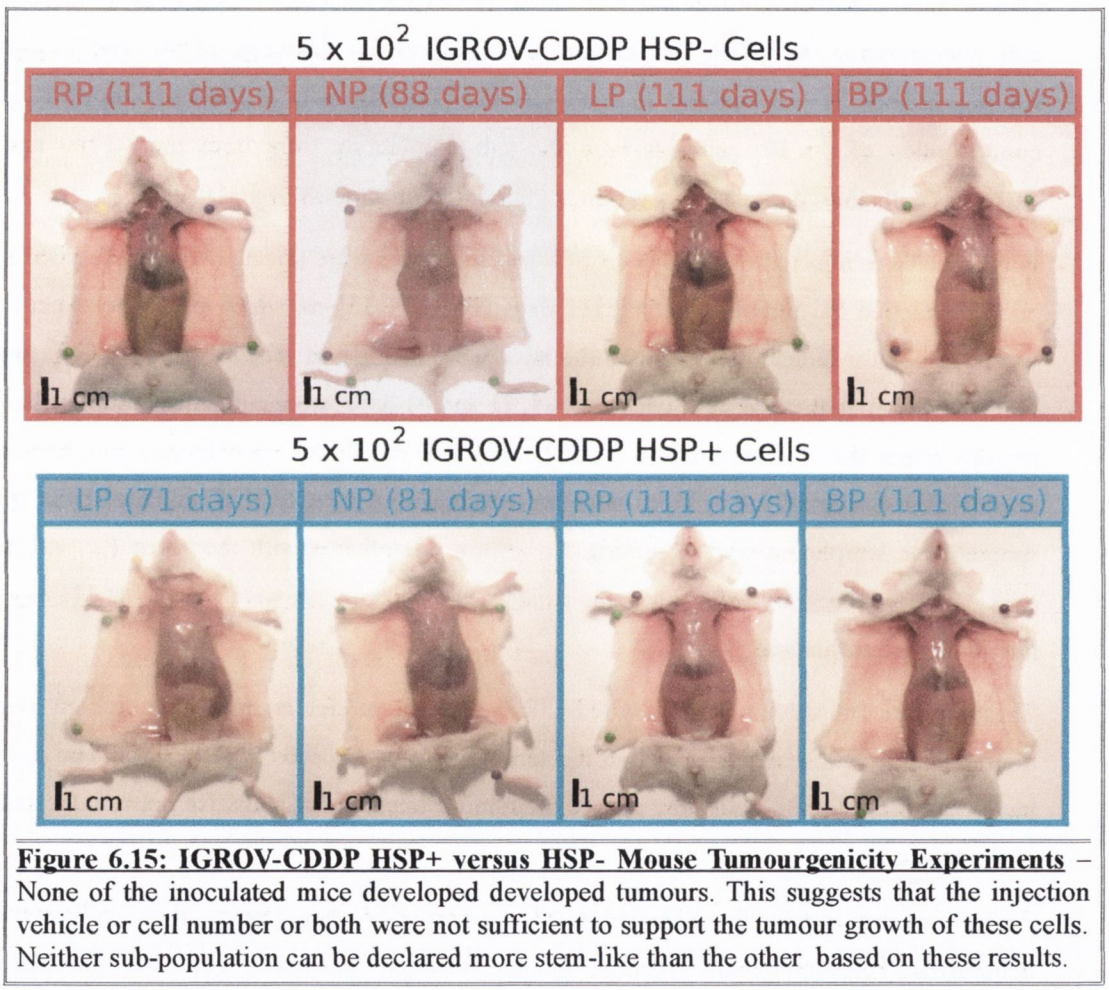

Figure 6.15: IGROV-CDDP HSP+ versus HSP- Mouse Tumourgenicity Experiments – None of the inoculated mice developed developed tumours. This suggests that the injection vehicle or cell number or both were not sufficient to support the tumour growth of these cells. Neither sub-population can be declared more stem-like than the other based on these results.

6.3.4.2 Single Cell Self-renewal and Differentiation Assay:

Two sets of 60 wells, across two 96-well plates were seeded with a single cell. One plate was seeded with single IGROV-CDDP HSP- non-pCSCs, sorted from a pre-purified population. The other plate was seeded with single IGROV-CDDP HSP+ pCSCs, sorted from a pre-purified population. 28 of the 60 single non-pCSCs formed colonies. 41 of the 60 single pCSCs formed colonies. These clonal colonies were allowed to expand (96-well plate to T25 flask) until sufficient numbers of cells were present to facilitate the retesting of HSP pCSC marker expression based upon which they were originally sorted.

A set of 5 IGROV-CDDP HSP- non-pCSC clones were randomly selected for retesting. Unexpectedly, 80 % (4/5) of the non-pCSC clones exhibited the CSC-like functional characteristics of differentiation and self-renewal by producing both HSP- and HSP+ progeny (Figure 6.16). 20 % (1/5; Clone F5) of the non-pCSC clones did not exhibited differentiation potential and only produced HSP- non-pCSC progeny. (Figure 6.17). There was insufficient time to increase the number of replicates to determine if the IGROV-CDDP HSP- non-pCSC clustered into HSP_NegA and HSP_NegB groupings, similar to the NegA and NegB groupings observed in the A2780 ALDH- non-pCSCs (Section 6.3.1.2.1). It can be stated that 80 % of the HSP- non-pCSC clones exhibited the CSC-like functional characteristics of differentiation and self-renewal, while 20 % of the clones exhibited the clones exhibited functional characteristics of non-CSCs, by demonstrating a limited differentiation potential.

A set of 5 IGROV-CDDP HSP+ pCSC clones were randomly selected for retesting. Upon flow cytometry analysis of these clones, it was observed that 100 % (5/5) of the pCSC clones exhibited a CSC phenotype. As expected, all of the HSP+ pCSC clones produced both HSP+ pCSCs and HSP- non-pCSCs, demonstrating an ability to differentiate and self-renew.

From the findings described in Section 4.3 and discussed in Section 4.4.4.3.4, it is known that the HSP+ and HSP- sub-populations of the IGROV-CDDP cell line, themselves have further pCSC and non-pCSC sub-populations. These additional (hierarchical) sub-populations are defined by the expression of the pCSC markers ALDH, CD44 and CD133. One possible explanation of the CSC-like activity in the HSP- and HSP+ sub-populations of the IGROV-CDDP cell line is that HSP+ does not define the most stem-like population of CSCs in the IGROV-CDDP cell line.

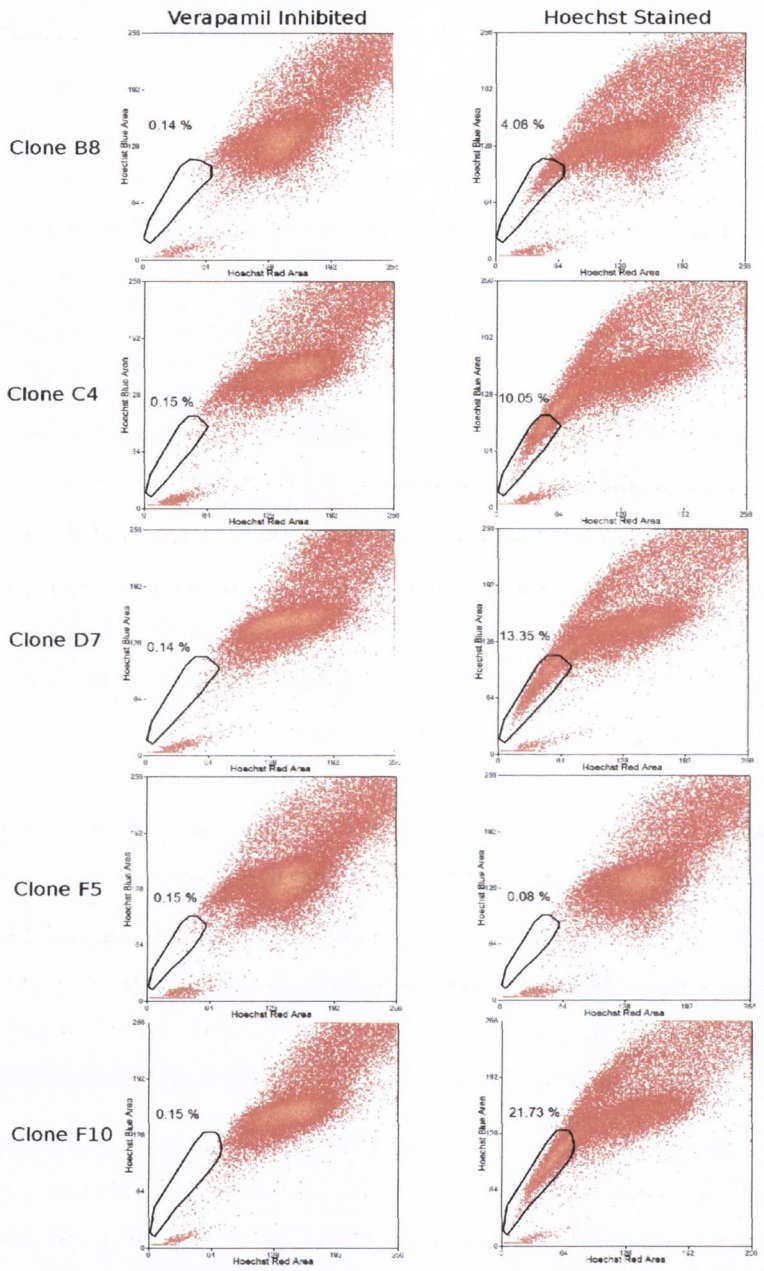

Figure 6.16: IGROV-CDDP HSP- SD Assay – 1 of 5 IGROV-CDDP HSP- clones exhibited a non-CSC phenotype (Clone F5). All the other HSP- non-pCSC clones produced both HSP- and HSP+ progeny, exhibiting the functional CSC characteristics of differentiation and self-renewal. A 'Verapamil inhibited' and a 'hoechst stained' sample is shown for each clone. The positive/negative threshold is set using the Verapamil inhibited negative control. The percentage of cells declared as HSP+ is shown on each graph.

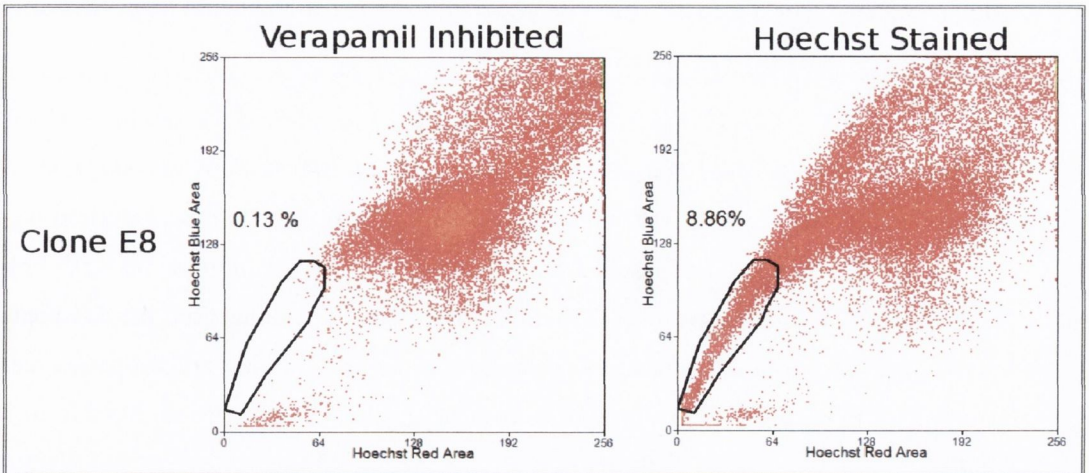

Figure 6.17: IGROV-CDDP HSP+ SD Assay – All of the IGROV-CDDP HSP+ clones exhibited a CSC phenotype. All HSP+ pCSC clones produced both HSP- and HSP+ progeny, exhibiting the functional CSC characteristics of differentiation and self-renewal. A 'Verapamil inhibited' and a 'hoechst stained' sample is shown for each clone. The positive/negative threshold is set using the Verapamil inhibited negative control. The percentage of cells declared as HSP+ is shown on each graph.

6.3.5 SK-OV-3:

6.3.5.1 Single Cell Self-renewal and Differentiation Assay:

Two sets of 60 wells, across two 96-well plates were seeded with a single cell. One plate was seeded with single SK-OV-3 CD117- non-pCSCs, sorted from a pre-purified population. The other plate was seeded with single SK-OV-3 CD117+ pCSCs, sorted from a pre-purified population. 34 of the 60 single non-pCSCs formed colonies. 31 of the 60 single pCSCs formed colonies. These clonal colonies were allowed to expand (96-well plate to T25 flask) until sufficient numbers of cells were present to facilitate the retesting of CD117 pCSC marker expression based upon which they were originally sorted.

A set of 5 SK-OV-3 CD117- non-pCSC clones were randomly selected for retesting. Unexpectedly, all of the non-pCSC clones expressed a small population of CD117+ pCSCs (Figure 6.18). However, the rate of false positives contributing to these small populations of CD117+ pCSCs could be as high as 45 % (0.05/0.11: Clone B5; Figure 6.18). This makes it hard to interpret these results. It is possible that these clones are exhibiting a CSC-like potential to differentiate and self-renew. It is also possible that the CSP assay used to retest these clones is not robust enough to resolve such small sub-populations. One of the SK-OV-3 CD177- non-pCSC clones (Clone G2), does exhibit a true CD117+ pCSC sub-population. However, this

CD117+ progeny does not form a discrete population similar to the CD117+ pCSCs originally observed in the SK-OV-3 cell line (Section 4.3.3.5.2).

A set of 5 SK-OV-3 CD117+ pCSC clones were randomly selected for retesting. Upon flow cytometry analysis of these clones, it was observed that 100 % (5/5) of the pCSC clones exhibited both CD117- and CD117+ sub-populations (Figure 6.19). However, these were not the discrete CD117- and CD117+ sub-populations originally observed in the SK-OV-3 cell line (Section 4.3.3.5.2). These were CD117+ and CD117+ 'tails' extending from the one population of cells. Therefore, it is not possible to determine if this is CSC-like differentiation and self-renewal or if it is drift in the expression level of the CD117 protein attributable to clonal selection.

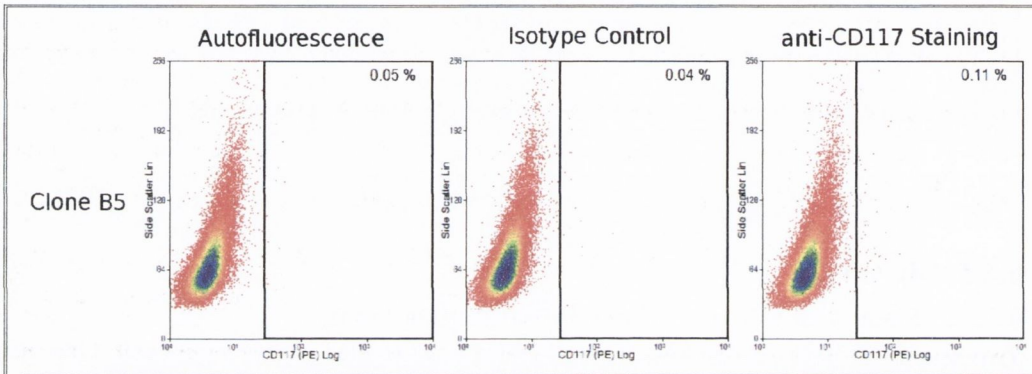

Figure 6.18: SK-OV-3 CD117- SD Assay - None of the SK-OV-3 CD117- non-pCSC reproduced the discrete CD117+/- sub-populations of the parent cell line. However, all clones did produce non-discrete CD117+/- sub-populations. It is not possible to determine if these non-discrete sub-populations represent a true differentiation potential. An 'autofluorescence', an 'isotype control' and an 'anti-CD117 stained' sample is shown for each clone. The positive/negative threshold is set using the autofluorescence negative control. The percentage of cells declared as CD117+ is shown on each graph.

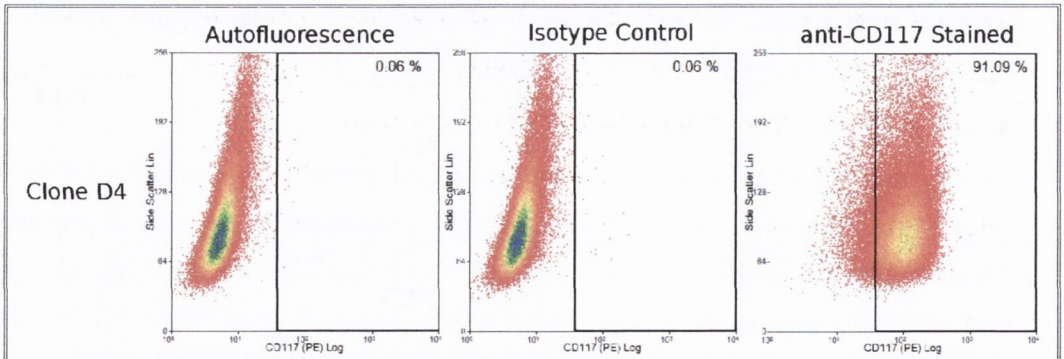

Figure 6.19: SK-OV-3 CD117+ SD Assay - None of the SK-OV-3 CD117+ pCSC reproduced the discrete CD117+/- sub-populations of the parent cell line. However, all clones did produce non-discrete CD117+/- sub-populations. It is not possible to determine if these non-discrete sub-populations represent a true differentiation potential. An 'autofluorescence', an 'isotype control' and an 'anti-CD117 stained' sample is shown for each clone. The positive/negative threshold is set using the autofluorescence negative control. The percentage of cells declared as CD117+ is shown on each graph.

6.3.6 59M:

6.3.6.1 Single Cell Self-renewal and Differentiation Assay:

Two sets of 60 wells, across two 96-well plates were seeded with a single cell. One plate was seeded with single 59M CD117- non-pCSCs, sorted from a pre-purified population. The other plate was seeded with single 59M CD117+ pCSCs, sorted from a pre-purified population. 37 of the 60 single non-pCSCs formed colonies. 29 of the 60 single pCSCs formed colonies. These clonal colonies were allowed to expand (96-well plate to T25 flask) until sufficient numbers of cells were present to facilitate the retesting of CD117 pCSC marker expression based upon which they were originally sorted.

A set of five 59M CD117- non-pCSC clones were randomly selected for retesting. Unexpectedly, all of the non-pCSC clones expressed a small population of CD117+ pCSCs (Figure 6.20). However, the rate of false positives contributing to these small populations of CD117+ pCSCs could be as high as 86 % (0.19/0.22: Clone F7; Figure 6.20). This makes it hard to interpret these results (Clones E6, G6 and F7). It is possible that these clones are exhibiting a CSC-like potential to differentiate and self-renew. It is also possible that the CSP assay used to retest these clones is not robust enough to resolve such small sub-populations. Two of the 59M CD177- non-pCSC clones (Clone G3 and C11), do exhibit a true CD117+ pCSC sub-population, similar to that observed in the parent cell line (Section 4.3.3.6.2). These CD117- non-pCSC clones do exhibit the CSC-like functional characteristics of differentiation and self-renewal.

A set of five 59M CD117+ pCSC clones were randomly selected for retesting. Upon flow cytometry analysis of these clones, it was observed that 100 % (5/5) of the pCSC clones exhibited both CD117- and CD117+ sub-populations, similar to those observed in the parent cell line (Figure 6.21; Section 4.3.3.6.2). These CD117+ pCSC clones do exhibit the CSC-like functional characteristics of differentiation and self-renewal.

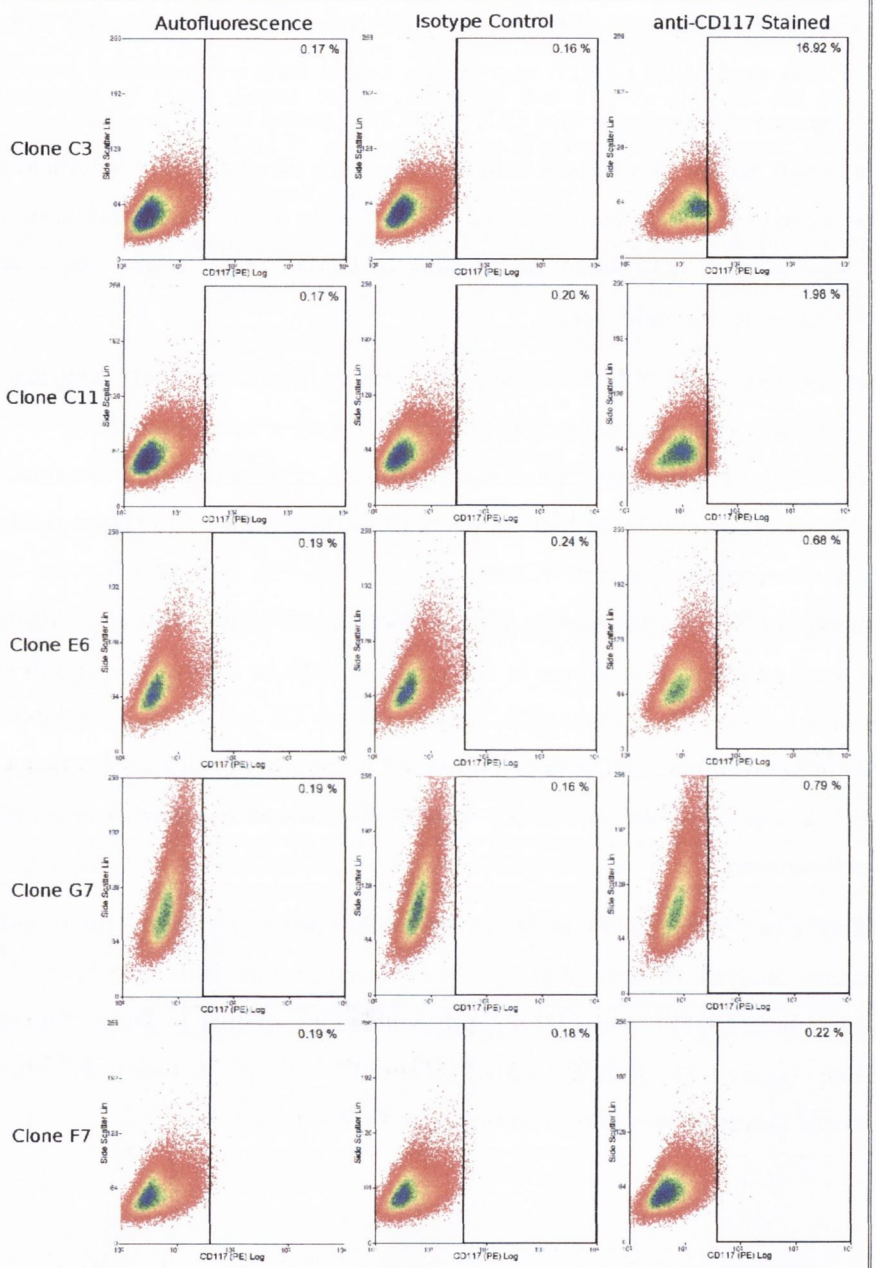

Figure 6.20: 59M CD117- SD Assay - Two of five 59M CD117- non-CSC clones exhibited a CSC phenotype (Clones C3 and C11). The other CD117- non-pCSC clones produced both HSP- and HSP+ progeny. However, due to the high proportion of CD117+ cells attributable to false positives, it was not possible to determine if these CD117+ cells represented true differentiation potential. An 'autofluorescence', an 'isotype control' and an 'anti-CD117 stained' sample is shown for each clone. The positive/negative threshold is set using the autofluorescence negative control. The percentage of cells declared as CD117+ is shown on each graph.

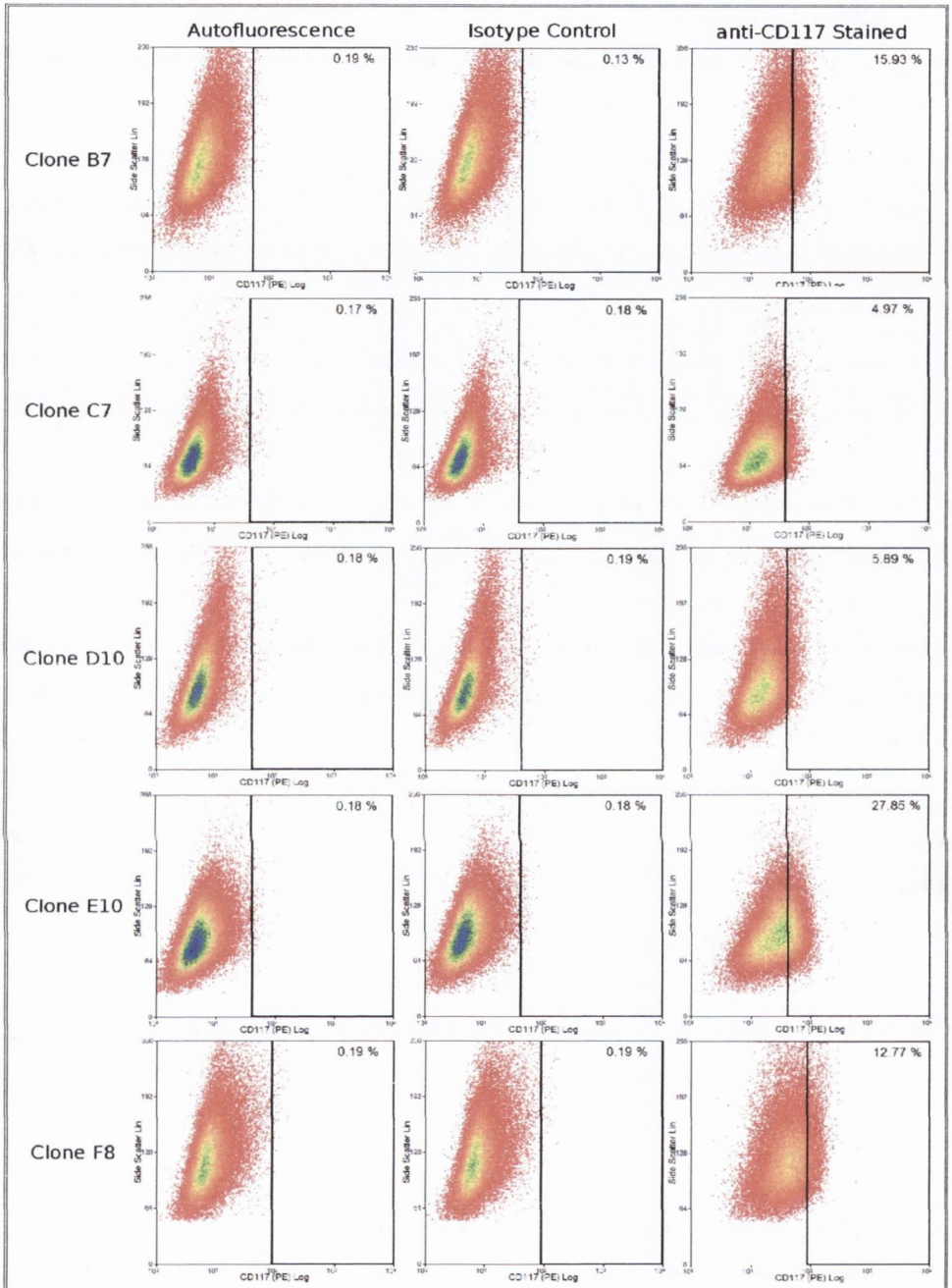

Figure 6.21: 59M CD117+ SD Assay - All of the 59M CD117+ pCSC clones exhibited a CSC phenotype. All CD117+ pCSC clones produced both CD117- and CD117+ progeny, exhibiting the functional CSC characteristics of differentiation and self-renewal. An 'autofluorescence', an 'isotype control' and an 'anti-CD117 stained' sample is shown for each clone. The positive/negative threshold is set using the autofluorescence negative control. The percentage of cells declared as CD117+ is shown on each graph.

6.4 Discussion:

Multiple pCSC and non-pCSC sub-populations were identified in the pCSC screen (Section 4.3.1 – 4.3.2). Six pairs of pCSC and non-pCSC sub-populations were selected from across six model systems for downstream analysis (Table 6.2). These sub-populations were isolated (Section 5.0) and brought forward for validation. The validation experiments described in this chapter (Section 6.3) have elucidated the functional CSC-like characteristics of many of these sub-populations.

The functional validation of the differentiation, self-renewal and malignant potential of each pCSC and non-pCSC sub-population will be discussed with respect to the literature in Section 6.4.1. After this, the most comprehensive validated CSC populations of the A2780 and A2780cis models will be discussed in further detail, with respect to a revised hypothesis regarding their CSC biology (Section 6.4.2). Some of the validation assays indicate a contrast in CSC differentiation patterns between the cisplatin sensitive A2780 model and the cisplatin resistant A2780cis model. The differing roles of CSCs upon acquired chemoresistance will be discussed in Section 6.4.3, with respect to the literature. Observations from the A2780 and A2780cis tumourgenicity validation experiments, in conjunction with information in the literature, will be used to put forward an additional hypothesis for the role of cellular sub-populations in the acquired chemoresistance of ovarian cancer. This will also be discussed in Section 6.4.3. Finally, some of the functional validations presented challenges to the confident interpretation of the results. Possible ways to overcome these challenges will be discussed across two sections. The challenges encountered while validating the IGROV-1 and IGROV-CDDP pCSC and non-pCSC sub-populations will be discussed in Section 6.4.4. The challenges encountered while validating the SK-OV-3 and 59M pCSC and non-pCSC sub-populations will be discussed in Section 6.4.5.

6.4.1 Outcomes of the Functional Validations

The pCSC screen identified several pCSC, non-pCSC and pSSC populations across the seven ovarian cancer and ovarian surface epithelium cell line model systems tested (Section 4.0). Pairs of pCSC/non-pCSC sub-populations from six ovarian cancer cell line models were brought forward for functional CSC validation via the mouse tumourgenicity and SD assays (Section 4.3.5). Section 6.3 presented the data from these validations. Sections 6.4.1.1 – 6.4.1.3 will discuss which populations can be declared CSCs and non-CSCs based on these validations.

6.4.1.1 The A2780 and A2780cis cell lines contains more than one CSC sub-population:

Based on the evidence in the literature (Breast: Charafe-Jauffret et al. 2009; Colon: Huang et al. 2009; Brain: Corti et al. 2006; Liver: Ma et al. 2008; Ovary: Silva et al. 2011), the ALDH+ cells identified in the A2780 and A2780cis cell lines were predicted to be pCSCs, while the ALDH- cells were predicted to be non-pCSCs. As expected, the ALDH+ pCSCs in both cell lines exhibited malignant, differentiation and self-renewal potential via the mouse tumourgenicity assay (Section 6.3.1.1) and the SD assay (Section 6.3.1.2). Having met the three functional characteristics of CSCs (Section 1.4), the A2780 ALDH+ cells and the A2780cis ALDH+ cells can be declared CSCs.

Unexpectedly, the ALDH- cells identified in the A2780 and A2780cis cell lines also exhibited malignant, differentiation and self-renewal potential via the mouse tumourgenicity assay (Section 6.3.1.1) and the SD assay (Section 6.3.1.2). Furthermore, the SD assay identified the ALDH- sub-population within the A2780 cell line could be further sub-divided into ALDH_NegA and ALDH_NegB cells. The ALDH_NegA cells exhibit differentiation and self-renewal potential while the ALDH_NegB cells do not (Section 6.3.1.2.1). In a similar fashion to the A2780 ALDH- cells, the SD assay showed that the A2780cis ALDH- sub-population could self-renew and differentiate, classifying them as ALDH_NegA cells.

These findings mean that the A2780 ALDH- sub-population can be declared as containing a CSC population (ALDH_NegA). The SD experiment identifies the ALDH_NegB sub-population as being non-CSCs, pending the validation of their reduced malignant potential. This will be discussed further in Section 6.4.5. These findings mean that the A2780cis ALDH- sub-population can be declared as a CSC population (ALDH_NegA). These results indicate a change to the stem cell hierarchy induced by cisplatin adaptation. Understanding and regulating such a change to stem cell hierarchies could be of therapeutic value to ovarian cancer patients.

The power of the SD assay to resolve the self-renewal and differentiation potential of sub-populations is of great scientific value to the CSC field. The ability to detect 'unmarked' CSC sub-populations as demonstrated via the identification of A2780 ALDH_NegA CSCs and the ability to reliably assess the self-renewal and differentiation potential of sub-populations are currently limitations for CSC research. For example, Yu et al. (2011) identified an ALDH+/CD44+ pCSC sub-population in the prostate cancer cell line PC3 and showed that this population was more clonogenic than the ALDH+/CD44-, ALDH-/CD44+, ALDH-/CD44- and parent populations. They also showed that the ALDH+/CD44+ cells had a greater metastatic potential via transwell matrigel invasion assays. Additionally, they showed that the

ALDH+/CD44+ sub-population could form tumours more efficiently in NOD.SCID mice inoculated subcutaneously with 100 and 1000 cells. However, they failed to declare this ALDH+/CD44+ sub-population as CSCs because all sub-populations demonstrated the ability to reconstitute the parent phenotype (ALDH+: 18 %; CD44+ 55 %; Overlap ALDH+/CD44+: 7.2 %) after xenograft formation. Yu et al failed to consider/mention the purity of the cells which went into the mice. The reconstitution ability of all sub-populations may be attributable to small numbers of CSCs present in all populations due to the limitations of cell sorting. The SD assay overcomes such limitations by plating only single cells. As such it may serve as a major tool in overcoming the current limitations of CSC research.

6.4.1.2 The HSP+ sub-populations of IGROV-1 and IGROV-CDDP cell lines are non-apical CSCs/progenitors in a stem cell hierarchy:

Based on the evidence in the literature (Brain: Bleau et al. 2009 Colon: Haraguchi et al. 2006; Lung: Ho et al. 2007; Liver: Chiba et al. 2006; Ovary: Szotek et al. 2006), the HSP+ cells identified in the IGROV-1 and IGROV-CDDP cell lines were predicted to be pCSCs, while the HSP- cells were predicted to be non-pCSCs. As expected, the HSP+ pCSCs from both cell lines exhibited differentiation and self-renewal potential via the SD assay (Section 6.3.3.2). Unexpectedly, the HSP- cells identified in both cell lines also exhibited differentiation and self-renewal potential via the SD assay (Section 6.3.3.2). There was insufficient time to add extra replicates to investigate if these HSP- clones sub-divided into HSP_NegA and HSP_NegB clones similar to that observed in the A2780 cell line (Section 6.3.1.2.1).

The unexpectedly long tumour latency of both the IGROV-1 and IGROV-CDDP HSP+/- sub-populations identified an upper limit to tumour latency which can be analysed by the xenograft model established for this project (Section 6.3.3.1). None of the mice inoculated with IGROV-CDDP HSP+ or HSP- cells developed tumours prior to being euthanised (Section 6.3.4.1). Therefore, neither population demonstrated a malignant potential so both are declared non-CSCs based on this result. However, further experiments with higher cell numbers or a more optimal vehicle may result in a re-classification of the malignant potential of the IGROV-CDDP HSP+ and HSP- sub-populations (discussed further in section 6.4.4). The demonstrated differentiation and self-renewal potential of both the IGROV-CDDP HSP+ and HSP- sub-populations via the SD assay means both sub-populations can be declared as CSC populations, pending further investigations in relation to their malignant potential. Szotek et al. (2006) demonstrated that HSP+ isolated from a murine model (MOVCAR7) of ovarian cancer were

more efficient at generating tumours than HSP- cells when 5 x 10^5 cells were injected into female Swiss nude mice.

Four of four mice injected with IGROV-1 HSP- cells formed tumours, while only two of four mice injected with IGROV-1 HSP+ cells formed tumours. This suggests that while both HSP+ and HSP- cells have the malignant potential to form tumours from 5 x 10^2 cells, HSP- negative cells are more tumourigenic. However, as described in Section 6.3.3.1 this did not translate into a statistically significant result. Additionally, these tumour latencies were at the limit of detection of the tumourgenicity assay (> 100 days). Further experiments with higher cell numbers or a more optimal vehicle may better quantify these findings (discussed further in section 6.4.4). Based on the SD and limited tumourgenicity data, it can be stated that both HSP+ and HSP- cells demonstrated malignant, differentiation and self-renewal potential. Both the IGROV-1 HSP+ and HSP- cells can be declared as CSCs, pending further investigations to confirm their malignant potential.

The demonstrated presence of multiple pCSC populations within the IGROV-1 model (Section 4.4.4.3.3) may have contributed to this unexpected observation. It is most probable that both the HSP+ and HSP- cells contain a more stem-like sub-population. The possible CSC hierarchies require further investigation. Hierarchical stemness refers to stepwise differentiation of stem cells and was described in Section 1.2. It is also possible that multiple CSCs pools exist that are not arranged in a hierarchical fashion. One possible mechanism for this would be the mutation driven de-differentiation of a progenitor leading to the establish of an independent CSC pool.

In a similar fashion to the IGROV-1 sub-populations (Section 4.4.4.3.3), the demonstrated presence of multiple pCSC populations within the IGROV-CDDP model (Section 4.4.4.3.4) may have contributed to this unexpected observation. It is most probable that both the HSP+ and HSP- cells contain a more stem-like sub-population. The possible CSC hierarchies would need to be investigated, before further statements about de-differentiation versus hierarchical stemness could be made.

The heterogeneity of pCSC sub-populations observed in the IGROV and IGROV-CDDP cell lines (Section 4.3) would appear to be representative of that seen in patient samples. For example, Silva et al. (2011) screened 13 patient samples for the presence of pCSC markers (CD24, CD44, CD90, CD117, CD133 and ALDH). They found that only 2 of 13 patients had 0 to 3 pCSC sub-populations while 11 of 13 had 4 to 6 pCSC sub-populations. Similarly, Curley

et al. (2009) found that 5 of 5 patient samples screened had 4 pCSC sub-populations based on the expression of CD24, CD44, CD133 and EpCAM.

The identification of hierarchies in OvCSCs is a substantial legacy of this project. However, the limitations of the CSC validations discussed above with respect to the validation of HSP+ and HSP- sub-populations need to be overcome if we are to fully understand the complexity of CSC biology within an ovarian cancer context. The first step might be: if more that one pCSC is observed in a model system, all possible overlaps are isolated and subjected to the SD assay rather than just picking one marker and clustering the diverse range of sub-populations into two groups based on this single marker expression.

6.4.1.3 The SK-OV-3 and 59M CD117+ pCSCs and non-pCSCs are not well suited to SD based CSC validation:

Due to time constraints, the malignant potential of the SK-OV-3 and 59M CD117+ pCSC and CD117- non-pCSC sub-populations were not validated in the mouse tumourgenicity assay. The differentiation and self-renewal potential of these sub-populations were examined via the SD assay. Both populations from the SK-OV-3 cell line did produce CD117+ pCSC and CD117- non-pCSCs. However, neither the pCSC nor the non-pCSC produced discrete CD117+/- sub-populations, as observed in the parent cell line (Section 6.3.5). It was not possible to determine if the CD117+/- sub-populations represent true differentiation and self-renewal without further experiments (discussed further in Section 6.4.5). Due to these limitations, it was not possible to demonstrate that either the pCSC or non-pCSC sub-population was more or less stem-like than one another. These limitations would not have been resolved by a larger number of cells. This is a not a screening limitation but rather a question that must be answered via the biology of the cell types detected. The different morphologies observed in the SK-OV-3 SD assay, were different between clones rather than within clones, so these observations can not be used to infer SD.

Both populations from the 59M cell line did produce CD117+ pCSC and CD117- non-pCSCs. The CD117+ pCSC clones all reproduced CD117+ and CD117- sub-populations as observed in the parent cell line (Section 6.3.6). This demonstration of differentiation and self-renewal potential means that the 59M CD117+ cells can be declared CSCs, pending further investigations into their malignant potential. The non-pCSC (CD117-) clones also reproduced CD117+ and CD117- sub-populations as observed in the parent cell line (Section 6.3.6). However, three of five of these clones had a high percentage of false positives in the CD117+

fraction. Further experiments would be required to demonstrate that these clones were actually producing CD117+ cells (in which case they are CSCs) or if they are attributable to false positives. These experiments will be discussed further in Section 6.4.5.

6.4.2 Cancer stem cell populations in the A2780 and A2780cis models.

6.4.2.1 Malignant potential:

The data described in Section 6.3.1.1 showed no difference in the malignant and differentiation potential of the A2780 ALDH+ pCSCs and the A2780 ALDH- non-pCSCs. Similarly, the data described in Section 6.3.2.1 showed no difference in the malignant and differentiation potential of the A2780cis ALDH+ pCSCs and the A2780cis ALDH- non-pCSCs. There was no significant difference between the tumour latency or tumour size produced by the ALDH- non-pCSCs and the ALDH+ pCSCs of either the A2780 or A2780cis models (Sections 6.3.1.1 and 6.3.2.1 respectively).

The A2780 cell line has been shown to produce poorly differentiated tumours (Molthoff et al. 1991; Shaw et al. 2004). Both Molthoff et al. and Shaw et al. injected 1 x 10^7 A2780 cells sub-cutaneously into the flanks of nude mice, and demonstrated that the resultant xenograft tumour morphology was that of an undifferentiated ovarian epithelial cancer. The A2780cis cell line was derived *in vitro* from the A2780 cell line. The tumours produced by both the ALDH+ and ALDH- sub-populations of both the A2780 and A2780cis models were high grade, with a poorly differentiated histology (Sections 6.3.1.1.2 and 6.3.2.1.2). This shows that both the ALDH+ pCSC and ALDH- non-pCSCs had the malignant potential to form tumours of the same histology as the parent cell line from which they were isolated. Both the pCSCs and non-pCSC from both the A2780 and A2780cis were able to efficiently form tumours at a cell density of 5 x 10^2 cells. The high malignant potential of both the ALDH- and ALDH+ sub-populations together with the ability of each sub-population to differentiate and self-renew (Sections 6.3.1.2 and 6.3.2.2), validated both the ALDH+ and ALDH- sub-populations of the A2780 and A2780cis cell lines as CSCs. The SD assay identified heterogeneity within the ALDH- sub-population. This will be discussed further in the next section (Section 6.4.2.2).

6.4.2.2 Differentiation and self-renewal potential:

The clonal analysis of the A2780 ALDH+ pCSCs via the SD assay, suggests that the ALDH+ sub-population is homogeneous, with respect to differentiation and self-renewal potential, when assessed for the ALDH+ pCSC marker (Section 6.3.1.2.2). All the clones tested demonstrated

the ability to self-renew and differentiate producing populations of both ALDH+ and ALDH- cells. On the other hand, the clonal analysis of the A2780 ALDH- non-pCSCs via the SD assay, suggests that the ALDH- sub-population is heterogeneous with respect to differentiation potential (Section 6.3.1.2.1). It was found that some of the ALDH- non-pCSC clones (A2780 ALDH_NegB) expressed the expected phenotype and did not exhibit the ability to differentiate and self-renew (Figure 6.3). However, other ALDH- non-pCSC clones (A2780 ALDH_NegA) expressed an unexpected phenotype, via exhibition of the CSC-like ability to differentiate and self renew (Figure 6.4). A2780 ALDH_NegA clones produced both ALDH- and ALDH+ sub-populations.

The proportion of the ALDH_NegA cells was 30.77 % +/- 23.08 % (Section 6.3.1.2.1). The error margin comes from the proportion of the clones which could not be classified as either ALDH_NegA or ALDH_NegB (Section 6.3.1.2.1). The frequency of the ALDH_NegB was 46.15 % +/- 23.08 % (Section 6.182). Considering these frequencies, one can assume that the A2780 ALDH- cells injected into mice were a mixture of approximately 42 % CSCs (ALDH_NegA) and 58 % non-CSCs (ALDH_NegB). This could explain the unexpected malignant potential of the ALDH- non-pCSCs observed in the mouse tumourgenicity study (Section 6.3.1.1).

In a similar fashion to the A2780 ALDH+ pCSCs, clonal analysis of the A2780cis ALDH+ pCSCs via the SD assay, suggests that the ALDH+ sub-population is homogeneous with respect to differentiation and self-renewal potential, when assessed for the ALDH+ pCSC marker (Section 6.3.2.2.2). All the clones tested demonstrated the ability to self-renew and differentiate producing populations of both ALDH+ and ALDH- cells. Interestingly, the clonal analysis of the A2780cis ALDH- non-pCSCs via the SD assay, found that the majority of the ALDH- sub-population (71.43 % +/- 28.57 %) exhibited the CSC-like ability to differentiate and self renew (Figure 6.9), by producing both ALDH- and ALDH+ sub-populations. A small fraction of ALDH- cells (28.57 % +/- 28.57 %) may have been ALDH_NegB cells (Section 6.3.2.2.1). The identification that the majority of the A2780cis ALDH- sub-population exhibit CSC-like differentiation and self-renewal, could explain the unexpected malignant potential of the ALDH- non-pCSCs observed in the mouse tumourgenicity study (Section 6.3.2.1).

Baba et al. (2008), were the first to use single cell clonal analysis as a method of assessing the self-renewal and differentiation capacity of CSCs within an ovarian cancer context. They plated single CD133+ or CD133- cells isolated from both PEO1 and A2780 cell lines and retested their ability to reconstitute the heterogeneous CD133+/-phenotype seen in the parent lineage.

They reported finding that the A2780 CD133- clones "led to the production of more CD133- progeny" while the CD133+ cells "either produced more CD133+ cell populations or produced heterogeneous cell populations", suggesting that only the CD133+ cells have the ability to self-renew and differentiate. In their supplementary material Figures S2A and S2B, the flow cytometry data presented indicates that some of the CD133- clones from the PEO1 cell line do produce some CD133+ cells. They did not comment on the possibility of further sub-populations within the CD133- fraction, as was described above in the A2780 ALDH- sub-population (Section 6.3.1). Presumably this is being actively explored. As it stands the SD assay is currently under-utilised in the CSC literature, presumably due to the technical difficulties in establishing the assay. However, such an assay is more high-throughput than mouse based validations and provides more detailed information compared to clonogenic based assays. As such, it is of great value to understanding the complex CSC networks identified in ovarian cancer patient samples (Curley et al. 2009; Silva et al. 2011).

6.4.2.3 A Revised Hypothesis:

Originally, it was hypothesised that ALDH positivity would mark CSCs and ALDH negativity would mark non-CSCs (Figure 6.22A). Sub-populations of ALDH+ pCSCs and ALDH- non-pCSCs were identified and isolated from the A2780 and A2780cis cell lines (Sections 4.0 and 5.0). It was shown that both the ALDH+ and ALDH- cells from both of these models were equally capable of forming tumours in NOD.SCID mice (Sections 6.3.1.1 and 6.3.2.1). However, it was demonstrated that the A2780 ALDH- sub-population consisted of two types of ALDH- cells. The ALDH_NegB type which exhibited non-CSC characteristics and the ALDH_NegA type which exhibited CSC characteristics (Section 6.3.1.2.1). Both the ALDH_NegA and ALDH+ clones, exhibited a differentiation and self-renewal potential, while the ALDH_NegB clones did not. This suggests that the ALDH_NegB clones are less stem-like (more differentiated) that the ALDH_NegA and ALDH+ clones. Interestingly, the ratio of ALDH- to ALDH+ cells produced by the ALDH_NegA clones is not significantly different to that observed for the parent population (Section 6.3.1.2.2). Whereas, the ratio of ALDH- to ALDH+ cells produced by the ALDH+ clones is significantly different to that observed for the parent population (Section 6.3.1.2.2). This suggests that the ALDH_NegA clones have an augmented potential to reconstitute the parent cell line compared to the ALDH+ clones, implying that the ALDH_NegA clones are more stem-like than the ALDH+ clones. This set of observations led to a revision of the original hypothesis (Figure 6.22A), which suggested a two

population CSC/non-CSC model, to a new hypothesis (Figure 6.22B), which suggested a three population CSC/progenitor/non-CSC model.

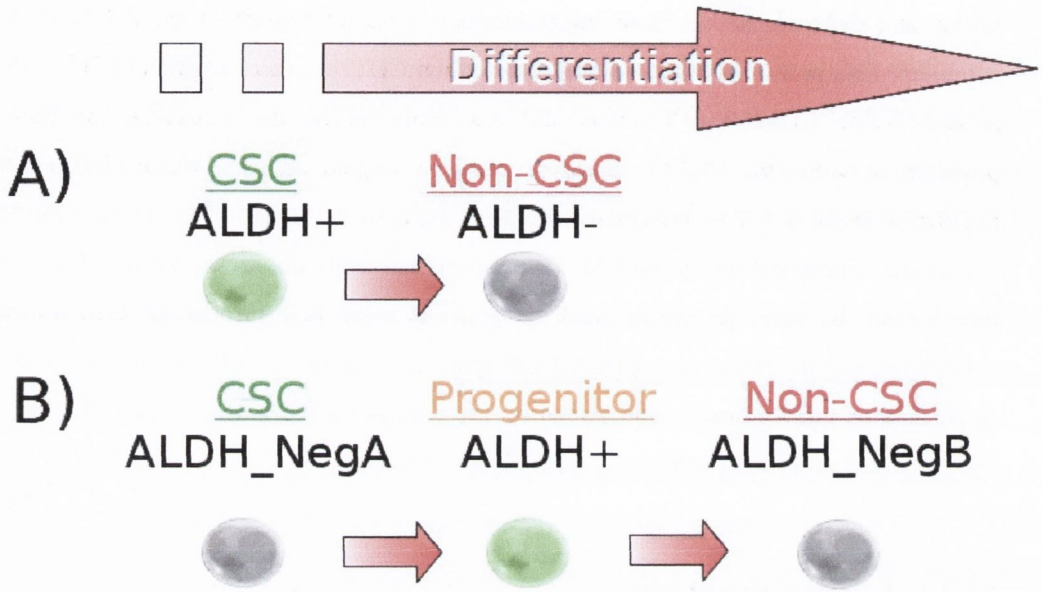

Figure 6.22: A Revised Hierarchical CSC Hypothesis - This diagram shows the original hypothesis (A) and the revised hypothesis (B). A) Shows a two step hypothesis of cancer stemness in in the A2780 and A2780cis models. The ALDH+ phenotype marks the CSC population and the ALDH- phenotype marks the non-CSC phenotype. B) Shows a three step hypothesis of cancer stemness in the A2780 and A2780cis models. The CSC and non-CSC sub-populations are indistinguishable based on ALDH expression alone. However, they can be functionally discriminated in the SD assay. ALDH_NegA cells are CSCs, ALDH+ cells are tumorigenic progenitors and ALDH_NegB cells are non-CSCs

The pCSC screen did identify both ALDH+/- and CD133+/- sub-populations within the A2780 cell line (Section 4.4.4.3.1). Due to logistical reasons, only the ALDH+/- sub-populations were brought forward for analysis in this project (discussed in Section 4.3.5). The revised hypothesis discussed above suggests that another pCSC marker, independent of ALDH, could further resolve the ALDH- sub-population into a CSC and non-CSC sub-population. Based on the sizes of the predicted CSC and non-CSC sub-populations (42 % and 58 % respectively), CD133 is not the marker in question. The size of the CD133+ population was shown to be 0.06 % +/- 0.02 % (Section 4.3.3.1.3). Therefore, it cannot be responsible for the ALDH_NegA and ALDH_NegB sub-populations.

Interestingly, there was a significant difference in the proportion of ALDH- cells produced by the A2780cis ALDH+ clones (98.79 % +/- 0.69 %) compared to the A2780 ALDH+ clones (52.61 % +/- 26.38 %; p-value = 0.03941). The A2780cis ALDH+ clones produced a lower proportion of ALDH- cells compared to the A2780 ALDH+ clones. The A2780cis model also had a lower proportion of ALDH_NegB clones compared to the A2780 model. This observation further supports the hypothesis of ALDH_NegA cells producing ALDH+ cells which in turn produce ALDH_NegB cells (Figure 6.22B), as opposed to a model of stochastic de-differentiation of ALDH- cells to ALDH+ cells (Figure 6.23).

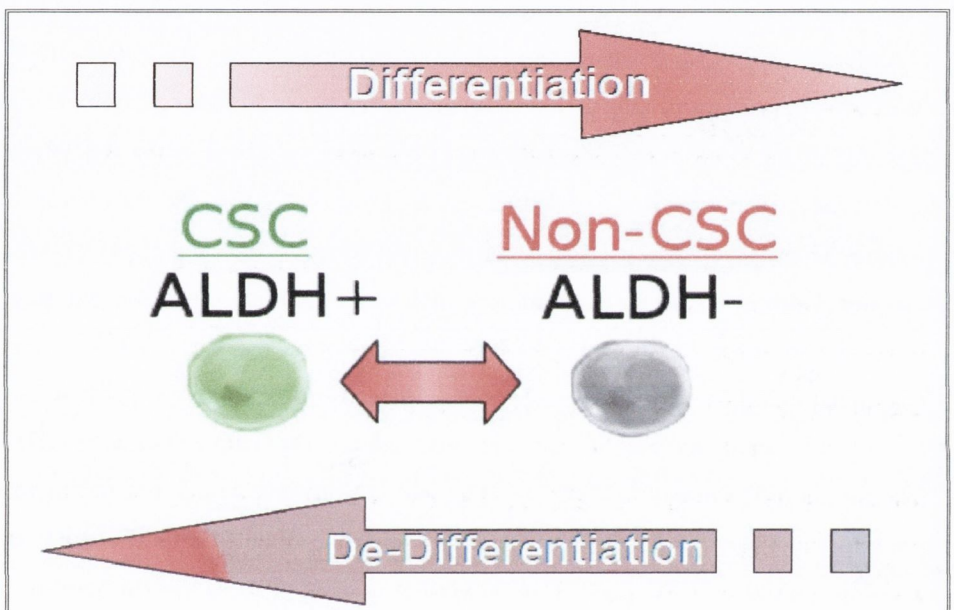

Figure 6.23: A Stochastic De-differentiation Hypothesis - This diagram shows a hypothesis of stochastic differentiation which could contribute to the ALDH_NegA phenotype observed in the A2780 and A2780cis SD validation assays. ALDH+ CSCs differentiate to produce ALDH- non-CSC. Due to malignant plasticity, non-CSCs are able to de-differentiate back to ALDH+ CSCs at a low frequency.

6.4.3 Two hypotheses regarding the CSC and non-CSC biology of acquired cisplatin resistance in Ovarian Cancer.

Two cell biology based hypotheses for the development of acquired cisplatin resistance have been developed based on the observations made during the CSC validation process described in this chapter.

First, as described above (Section 6.4.2.3), it was noted that the degree of differentiation of the A2780cis ALDH+ CSCs was significantly different to that of the A2780 ALDH+ CSCs. The A2780cis ALDH+ CSCs produced a much smaller proportion of suspected ALDH_NegB non-pCSCs. This suggests that acquired cisplatin resistance correlates with shift away from differentiation and towards self-renewal with respect to ALDH+ CSCs. High grade tumours are classified as such due to an absence of differentiation (Silverberg 2000). High grade tumours have a worse patient prognosis than low grade tumours (Silverberg 2000). It could be possible that one of the contributing mechanisms to cisplatin resistance in the A2780cis cell line is the maintenance of a higher proportion of less differentiated cells. The data herein supports such a model. There is evidence to suggest that radiotherapy alters the cancer stem cell division kinetics, causing a shift away from asymmetric division and thus differentiation, towards self-renewal symmetric divisions in glioblastoma multiforme (Gao et al. 2013). Gao et al found that fractioned radiation of 3 x 2 Gy led to a 6-fold expansion of the CSC pool: an enrichment which could not be attributed to CSC radioresistance alone. They showed that the CD133- non-pCSCs did not 'de-differentiate' to CD133+ cells and therefore deduced that the increase in the CSC pool post therapy was partly due to an increased ratio of self-renewal compared to asymmetric division within the CSC pool. They comment that "Radiation has furthermore been shown to activate the AKT/cyclin D1/Cdk4 pathway in human glioblastoma cells" and point out that this pathway "yields a significantly shorter cell-cycle time of 15 to 16 hours in human embryonic stem cells than in somatic cells due to an abbreviated G1 phase". Interestingly, Roccio et al. (2013) show via fluorescent tracking of the cell cycle that the G1 phase almost doubles during neural stem cell differentiation and suggested that stem cells can avoid differentiation if they cycle quickly through the G1 phase of cell division. It is possible that similar chemotherapy induced alterations to asymmetric division and differentiation are responsible for the difference in differentiation observed between the A2780 and A2780cis ALDH+ sub-populations (Sections 6.3.1 – 6.3.2).

Second, it was noted that the tumours produced by the A2780 derived ALDH+ and ALDH- sub-populations grew significantly faster than those produced by the A2780cis derived ALDH+

and ALDH- sub-populations (p-value = 0.001062; Sections 6.3.1.1 and 6.3.2.1). It was also noted upon post-mortem examination that tumours of A2780 origin seemed to have a richer blood supply than those produced of A2780cis origin. Although there was insufficient time to do it for this project, it is possible to stain the A2780 and A2780cis ALDH+/- tumour samples for a vascular marker (such as CD34, CD31 or von-Willebrand factor) and count the blood vessels to confirm a richer blood supply. Increased vasculature in the A2780 tumours would be an interesting observation as A2780 was found to have a CD133+ sub-population (Section 4.3.3.1.3), whereas A2780cis was found to be CD133- (Section 4.3.3.2.3). As discussed in Section 4.4.4.4.3, Kusumbe et al. (2009) found that CD133+ cells were not OvCSCs, but rather augmented tumourgenicity via the facilitation of angiogenesis. In addition to this, hypoxia has been demonstrated to facilitate cisplatin resistance in ovarian cancer (Selvendiran et al. 2009). Furthermore, preliminary experiments indicated a poor overlap between ALDH+ cells and CD133+ cells in the IGROV-CDDP cell line (Section 4.3.4.2). Perhaps the CD133+ phenotype is a sub-population of the ALDH_NegB phenotype, suggesting a restructuring of the cellular hierarchies upon acquired cisplatin resistance. The emergence of a fibroblast-like morphology in the A2780cis cell line which was absence in the A2780 cell line is consistent with such a theory. These findings taken together suggest that one of the contributing factors to acquired cisplatin resistance could be the loss of CD133+ and ALDH_NegB sub-populations accompanied by the gain of a fibroblast-like sub-population, resulting in the development of a less vascularised, more hypoxic tumour, which is more resistant to chemotherapy.

6.4.4 Tumourgenicity based validation of the IGROV-1 and IGROV-CDDP pCSC and non-pCSC sub-populations:

The *in vivo* tumourgenicity validation of the IGROV-1 and IGROV-CDDP sub-populations presented a challenge. The tumour latency of the resulting tumours was too long for the NOD.SCID model used in this project. There are multiple possible solutions to this challenge:

1) A pilot study could be used to identify a more appropriate cell number at which to carry out the validation assay. By injecting pairs of mice with a range of cells from 5×10^6 to 5×10^3 a more optimal cell concentration could be identified at which to compare the malignant potential of the IGROV-1 and IGROV-CDDP pCSC and non-pCSC sub-populations.

2) A pilot study could be used to identify the optimal injection vehicle. Ham's F12 media supplemented with 'high concentration' matrigel has been demonstrated to be an effective vehicle for the A2780 and A2780cis derived sub-populations (Sections 6.3.1.1

and 6.3.2.1). However, there may be a more optimal vehicle to support the growth of the IGROV-1 and IGROV-CDDP derived sub-populations. By injecting pairs of mice with 5×10^6 IGROV-1 and IGROV-CDDP cells in a range of injection vehicles a more optimal vehicle may be established for the comparison of the malignant potential of the IGROV-1 and IGROV-CDDP pCSC and non-pCSC sub-populations.

3) The IGROV-1 and IGROV-CDDP cells may not be adapted to grow in the mouse s.c. micro-environment. A pilot study could be used to identify the optimal injection location. 5×10^6 IGROV-1 and IGROV-CDDP cells could be injected i.p. into pairs of mice or they could be injected into the ovarian bursal membrane. Such a pilot study could identify the optimal injection site at which to compare the malignant potential of the IGROV-1 and IGROV-CDDP pCSC and non-pCSC sub-populations.

4) Different strains of mice might be better suited to longer latency experiments. For example, Szotek et al. (2006) injected 6 week old Swiss nude mice with cells for experiments which lasted for 14 weeks. The mice would have been 140 days old by the time the experiments ended. The Swiss nude mice may be better suited to validation experiments with long tumour latencies.

6.4.5 SD based validation of the SK-OV-3, 59M and A2780 pCSC and non-pCSC sub-populations:

The SD based validation of the SK-OV-3 and 59M sub-populations presented challenges. It was not possible to determine if the SK-OV-3 pCSCs and non-pCSC were capable of differentiation and self-renewal. Neither population created the discrete CD117+ and CD117- sub-populations observed in the parent cell line (Section 4.3.3.5.2). However, both the pCSCs and non-pCSC clones produced a cell population with a CD117 profile which traversed the positive/negative threshold set by the autofluorescence control (Section 6.3.5.1). Further experiments are required to determine if the CD117+ and CD117- tails produced via the SD assay are the same as the discrete populations observed in the parent cell line. If the CD117+ and CD117- cells produced by the CD117 pCSC and CD117 non-pCSC clones were isolated via cell sorting, microarray analysis could be used to determine if these CD117+ and CD117- cells are the same cell types as the CD117+ and CD117- cells isolated from the parent cell line. Microarray analysis could be used to measure the relative gene expression of SK-OV-3 isolated CD117+ and CD117- cells, relative to the CD117+ and CD117- cells produced via the SD assay. Hierarchical clustering analysis could then be used to match the most similar gene expression profiles in a

pairwise fashion. If all the CD117+ and CD117- expression sets clustered together the closest then these can be considered the most similar to one another, i.e. they are the same cell type. Once the similarity or dissimilarity of these cells is established, statements about the their self-renewal and differentiation potential can be made. Unfortunately, there was insufficient time to carry out these experiments within this project.

The 59M CD117- non-CSCs clones showed some differentiation and self-renewal. Two of five CD117- non-pCSC clones reconstituted the CD117 profile of the parent cell line (Section 6.3.6.1). It can be stated that these clones have a CSC-like differentiation and self-renewal potential. Three of five CD117- non-pCSC clones did produce some cells which resembled CD117+ cells. However, there was a high degree of false positives detected in the autofluorescence sample compared to the size of the CD117+ population identified in the anti-CD117 stained samples in each of these clones. Further experiments are required to determine if the CD117+ cells produced by these clones are true CD117+ cells or if they are attributable to a high false positive rate. As described above, microarray analysis could be used to resolve this uncertainty. However, as the 59M CD117+ pCSC have expressed a consistent phenotype in the SD assay (Section 6.3.6.1), there is an alternate experiment which could address this issue. The questionable CD117+ cells from the clones in question could be isolated and plated as single cells for a 2nd generation SD assay. If they are true CD117+ cells then they should differentiate and self-renew in a similar fashion to the CD117+ pCSCs from the 1st generation (Section 6.3.6.1). If they do not demonstrate such differentiation and self-renewal potential, it can be said that the original CD117- non-pCSC clones, from which they were derived, did not have the differentiation potential to produce CD117+ cells. Unfortunately, there was insufficient time to carry out these experiments within this project.

The A2780 and A2780cis ALDH- clones were classified as ALDH_NegA, ALDH_NegB and ALDH- (unclassified). These clones were described in Section 6.3.1.2.1. The ALDH- (unclassified) produced some events, which resembled ALDH+ cells. However, due to the 'noisier' ALDH profile it is not certain whether these are true ALDH+ cells or if they are artefacts. If they are true ALDH+ cells then these clones can be classified as ALDH_NegA CSCs. If they are artefacts then these clones can be classified as ALDH_NegB non-CSCs. As described above, micro array analysis or 2nd generation SD could be used to determine if these query ALDH+ cells are true ALDH+ cells.

6.4.6 Summary:

The experiments in this chapter set out to validate the differentiation self-renewal and malignant potential of the pCSC and non-pCSC sub-populations identified in the pCSC screen.

It was found that both the A2780 and A2780cis ALDH+ pCSC exhibited the functional characteristics of CSCs (Sections 6.3.1.2.2 and 6.3.2.2.2). However, the A2780 and A2780cis ALDH- non-pCSCs also exhibited CSC functional characteristics. Data from the SD assay suggested that the ALDH- non-pCSC sub-populations contain a heterogeneous mix of CSCs and non-CSCs (Sections 6.3.2.2.2 and 6.3.2.2.1).

The IGROV-1 and IGROV-CDDP HSP+ and HSP- populations all demonstrated differentiation and self-renewal potential and were declared CSCs. The IGROV-1 and IGROV-CDDP HSP+ and HSP- sub-populations were known to be heterogeneous for other pCSC markers, prior to the validation experiments (Sections 4.4.4.3.3 – 4.4.4.3.4). The validation of a CSC-like differentiation and self-renewal potential within both HSP+ and HSP- sub-populations suggests that the HSP based sub-populations are not at the top of a hierarchy of pCSCs sub-populations identified within these models.

The SK-OV-3 pCSC and non-pCSC as well as the 59M non-pCSC validation experiments highlighted an unexpected limitation of the SD assay. This data suggests that the SD assay is not well suited to assaying for the presence of small non-discrete sub-populations, unless the staining technique has a very low false positive rate. The 59M CD117+ pCSCs exhibited CSC-like functional characteristics of differentiation and self-renewal and were declared a CSC population(Section 6.3.6.1).

The experiments in this chapter set out to validate the differentiation self-renewal and malignant potential of the pCSC and non-pCSC sub-populations identified in the pCSC screen. Once validated it was intended to progress to the characterisation of CSC and non-CSC sub-populations with the intention of identifying novel therapeutic targets. However, several lines of functional based evidence suggested that the cellular organisation of the ovarian cancer models utilised in this study was more complicated than originally hypothesised. For these reasons, additional functional experiments were designed to further understand this cellular organisation. These experiments are described in the next chapter (Section 8.0).

Section6.0 – Validation of CSC

Validation of pCSC and non-pCSC sub-populations:- Primary findings

The A2780 and A2780cis ALDH+ pCSCs, demonstrated differentiation, self-renewal and malignant potential, these have been validated as CSCs.

The A2780 and A2780cis ALDH- non-pCSC, Demonstrated differentiation, self-renewal and malignant potential, these have not been validated as non-CSCs but are in fact CSCs. The SCP assay suggests that the ALDH- non-pCSC sub-population may be a heterogeneous mix of CSC and non-CSC cells.

The IGROV-1 and IGROV-CDDP HSP+ pCSC, Demonstrated differentiation, self-renewal potential, two of the three functional characteristics of CSCs. Demonstration of malignant potential was impeded due to incompatibility of the NOD.SCID model with long tumour latencies. These have been declared CSCs, pending further investigations into their malignant potential.

The IGROV-1 and IGROV-CDDP HSP- non-pCSC, demonstrated differentiation, self-renewal potential, two of the three functional characteristics of CSCs. Demonstration of malignant potential was impeded due to incompatibility of the NOD.SCID model with long tumour latencies. These have not been validated as non-CSCs but are in fact CSCs. Heterogeneity of the HSP- non-pCSC sub-population is believed to have contributed to the unexpected differentiation and self-renewal potential of this sub-population.

The SK-OV-3 CD117+ pCSC and CD117- non-pCSC, could not be validated for differentiation and self-renewal potential due to unexpected flow cytometry profiles upon retesting of the SCP assay derived clones. Time constraints prevented the validation of the malignant potential of these sub-populations.

The 59M CD117+ pCSCs, demonstrated differentiation, self-renewal and malignant potential, two of the three functional characteristics of CSCs. Time constraints prevented the validation of the malignant potential of these sub-populations. These have been declared CSCs, pending further investigation into their malignant potential.

The 59M CD117- non-pCSCs, would require additional 2nd generation SCP experiments to elucidate the differentiation and self renewal potential of this non-pCSC sub-population.

6.5 References:

Baba, T., P. A. Convery, N. Matsumura, R. S. Whitaker, E. Kondoh, T. Perry, Z. Huang, R. C. Bentley, S. Mori, and S. Fujii. 2008. "Epigenetic Regulation of CD133 and Tumorigenicity of CD133+ Ovarian Cancer Cells." *Oncogene* 28 (2): 209–218.

Bleau, Anne-Marie, Dolores Hambardzumyan, Tatsuya Ozawa, Elena I Fomchenko, Jason T Huse, Cameron W Brennan, and Eric C Holland. 2009. "PTEN/PI3K/Akt Pathway Regulates the Side Population Phenotype and ABCG2 Activity in Glioma Tumor Stem-like Cells." *Cell Stem Cell* 4 (3) (March 6): 226–235. doi:10.1016/j.stem.2009.01.007.

Charafe-Jauffret, E., C. Ginestier, F. Iovino, J. Wicinski, N. Cervera, P. Finetti, M.-H. Hur, et al. 2009. "Breast Cancer Cell Lines Contain Functional Cancer Stem Cells with Metastatic Capacity and a Distinct Molecular Signature." *Cancer Research* 69 (4) (February 3): 1302–1313. doi:10.1158/0008-5472.CAN-08-2741.

Chiba, Tetsuhiro, Kaoru Kita, Yun-Wen Zheng, Osamu Yokosuka, Hiromitsu Saisho, Atsushi Iwama, Hiromitsu Nakauchi, and Hideki Taniguchi. 2006. "Side Population Purified from Hepatocellular Carcinoma Cells Harbors Cancer Stem Cell-like Properties." *Hepatology (Baltimore, Md.)* 44 (1) (July): 240–251. doi:10.1002/hep.21227.

Clarke, Michael F, John E Dick, Peter B Dirks, Connie J Eaves, Catriona H M Jamieson, D Leanne Jones, Jane Visvader, Irving L Weissman, and Geoffrey M Wahl. 2006. "Cancer Stem Cells--perspectives on Current Status and Future Directions: AACR Workshop on Cancer Stem Cells." *Cancer Research* 66 (19) (October 1): 9339–9344. doi:10.1158/0008-5472.CAN-06-3126.

Corti, Stefania, Federica Locatelli, Dimitra Papadimitriou, Chiara Donadoni, Sabrina Salani, Roberto Del Bo, Sandra Strazzer, Nereo Bresolin, and Giacomo P Comi. 2006. "Identification of a Primitive Brain-derived Neural Stem Cell Population Based on Aldehyde Dehydrogenase Activity." *Stem Cells (Dayton, Ohio)* 24 (4) (April): 975–985. doi:10.1634/stemcells.2005-0217.

Curley, M.D., V.A. Therrien, C.L. Cummings, P.A. Sergent, C.R. Koulouris, A.M. Friel, D.J. Roberts, et al. 2009. "CD133 Expression Defines a Tumor Initiating Cell Population in Primary Human Ovarian Cancer." *Stem Cells* 27 (12): 2875–2883.

Elkin, Michael, and Israel Vlodavsky. 2001. "Tail Vein Assay of Cancer Metastasis." In *Current Protocols in Cell Biology*, 19.2.1–19.2.7. John Wiley & Sons, Inc. http://onlinelibrary.wiley.com.elib.tcd.ie/doi/10.1002/0471143030.cb1902s12/abstract.

Gao, Xuefeng, J Tyson McDonald, Lynn Hlatky, and Heiko Enderling. 2013. "Acute and Fractionated Irradiation Differentially Modulate Glioma Stem Cell Division Kinetics." *Cancer Research* 73 (5) (March 1): 1481–1490. doi:10.1158/0008-5472.CAN-12-3429.

Haraguchi, Naotsugu, Tohru Utsunomiya, Hiroshi Inoue, Fumiaki Tanaka, Koshi Mimori, Graham F Barnard, and Masaki Mori. 2006. "Characterization of a Side Population of Cancer Cells from Human Gastrointestinal System." *Stem Cells (Dayton, Ohio)* 24 (3) (March): 506–513. doi:10.1634/stemcells.2005-0282.

Ho, Maria M, Alvin V Ng, Stephen Lam, and Jaclyn Y Hung. 2007. "Side Population in Human Lung Cancer Cell Lines and Tumors Is Enriched with Stem-like Cancer Cells." *Cancer Research* 67 (10) (May 15): 4827–4833. doi:10.1158/0008-5472.CAN-06-3557.

Huang, Emina H, Mark J Hynes, Tao Zhang, Christophe Ginestier, Gabriela Dontu, Henry Appelman, Jeremy Z Fields, Max S Wicha, and Bruce M Boman. 2009. "Aldehyde Dehydrogenase 1 Is a Marker for Normal and Malignant Human Colonic Stem Cells (SC) and Tracks SC Overpopulation During Colon Tumorigenesis." *Cancer Research* 69 (8) (April 15): 3382–3389. doi:10.1158/0008-5472.CAN-08-4418.

Inaba, Mayu, and Yukiko M Yamashita. 2012. "Asymmetric Stem Cell Division: Precision for Robustness." *Cell Stem Cell* 11 (4) (October 5): 461–469. doi:10.1016/j.stem.2012.09.003.

Kusumbe, Anjali P, Avinash M Mali, and Sharmila A Bapat. 2009. "CD133-expressing Stem Cells Associated with Ovarian Metastases Establish an Endothelial Hierarchy and Contribute to Tumor Vasculature." *Stem Cells (Dayton, Ohio)* 27 (3) (March): 498–508. doi:10.1634/stemcells.2008-0868.

Londoño-Joshi, Angelina, Patsy Oliver, Yufeng Li, Choo Lee, Andres Forero-Torres, Albert LoBuglio, and Donald Buchsbaum. 2011. "Basal-like Breast Cancer Stem Cells Are Sensitive to anti-DR5 Mediated Cytotoxicity." *Breast Cancer Research and Treatment*: 1–9. doi:10.1007/s10549-011-1763-0.

Ma, Stephanie, Kwok Wah Chan, Terence Kin-Wah Lee, Kwan Ho Tang, Jana Yim-Hung Wo, Bo-Jian Zheng, and Xin-Yuan Guan. 2008. "Aldehyde Dehydrogenase Discriminates the CD133 Liver Cancer Stem Cell Populations." *Molecular Cancer Research: MCR* 6 (7) (July): 1146–1153. doi:10.1158/1541-7786.MCR-08-0035.

Molthoff, C F, J J Calame, H M Pinedo, and E Boven. 1991. "Human Ovarian Cancer Xenografts in Nude Mice: Characterization and Analysis of Antigen Expression." *International Journal of Cancer. Journal International Du Cancer* 47 (1) (January 2): 72–79.

Pan, Jing, Qi Zhang, Yian Wang, and Ming You. 2010. "26S Proteasome Activity Is Down-Regulated in Lung Cancer Stem-Like Cells Propagated In Vitro." *PLoS ONE* 5 (10) (October 11): e13298. doi:10.1371/journal.pone.0013298.

Price, J E. 1996. "Metastasis from Human Breast Cancer Cell Lines." *Breast Cancer Research and Treatment* 39 (1): 93–102.

Prochazka, M, H R Gaskins, L D Shultz, and E H Leiter. 1992. "The Nonobese Diabetic Scid Mouse: Model for Spontaneous Thymomagenesis Associated with Immunodeficiency." *Proceedings of the National Academy of Sciences of the United States of America* 89 (8) (April 15): 3290–3294.

Reya, T., S. J. Morrison, M. F. Clarke, and I. L. Weissman. 2001. "Stem Cells, Cancer, and Cancer Stem Cells." http://deepblue.lib.umich.edu/handle/2027.42/62862.

Roccio, Marta, Daniel Schmitter, Marlen Knobloch, Yuya Okawa, Daniel Sage, and Matthias P Lutolf. 2013. "Predicting Stem Cell Fate Changes by Differential Cell Cycle Progression Patterns." *Development (Cambridge, England)* 140 (2) (January 15): 459–470. doi:10.1242/dev.086215.

Salvatori, Luisa, Francesca Caporuscio, Alessandra Verdina, Giuseppe Starace, Stefania Crispi, Maria Rita Nicotra, Andrea Russo, et al. 2012. "Cell-to-Cell Signaling Influences the Fate of Prostate Cancer Stem Cells and Their Potential to Generate More Aggressive Tumors." *PLoS ONE* 7 (2) (February 6): e31467. doi:10.1371/journal.pone.0031467.

Selvendiran, Karuppaiyah, Anna Bratasz, M Lakshmi Kuppusamy, Mia F Tazi, Brian K Rivera, and Periannan Kuppusamy. 2009. "Hypoxia Induces Chemoresistance in Ovarian Cancer Cells by Activation of Signal Transducer and Activator of Transcription 3." *International Journal of Cancer. Journal International Du Cancer* 125 (9) (November 1): 2198–2204. doi:10.1002/ijc.24601.

Shaw, Tanya J, Mary K Senterman, Kerri Dawson, Colleen A Crane, and Barbara C Vanderhyden. 2004. "Characterization of Intraperitoneal, Orthotopic, and Metastatic Xenograft Models of Human Ovarian Cancer." *Molecular Therapy: The Journal of the American Society of Gene Therapy* 10 (6) (December): 1032–1042. doi:10.1016/j.ymthe.2004.08.013.

Silva, Ines A, Shoumei Bai, Karen McLean, Kun Yang, Kent Griffith, Dafydd Thomas, Christophe Ginestier, et al. 2011. "Aldehyde Dehydrogenase in Combination with CD133 Defines Angiogenic Ovarian Cancer Stem Cells That Portend Poor Patient Survival." *Cancer Research* 71 (11) (June 1): 3991–4001. doi:10.1158/0008-5472.CAN-10-3175.

Silverberg, S G. 2000. "Histopathologic Grading of Ovarian Carcinoma: a Review and Proposal." *International Journal of Gynecological Pathology: Official Journal of the International Society of Gynecological Pathologists* 19 (1) (January): 7–15.

Szotek, P. P., R. Pieretti-Vanmarcke, P. T. Masiakos, D. M. Dinulescu, D. Connolly, R. Foster, D. Dombkowski, F. Preffer, D. T. MacLaughlin, and P. K. Donahoe. 2006. "Ovarian Cancer Side Population Defines Cells with Stem Cell-like Characteristics and Mullerian Inhibiting Substance Responsiveness." *Proceedings of the National Academy of Sciences* 103 (30): 11154–11159.

Visvader, Jane E, and Geoffrey J Lindeman. 2012. "Cancer Stem Cells: Current Status and Evolving Complexities." *Cell Stem Cell* 10 (6) (June 14): 717–728. doi:10.1016/j.stem.2012.05.007.

Ward, B. G, K. Wallace, J. H Shepherd, and F. R Balkwill. 1987. "Intraperitoneal Xenografts of Human Epithelial Ovarian Cancer in Nude Mice." *Cancer Research* 47 (10): 2662–2667.

Yu, Chunyan, Zhi Yao, Jinlu Dai, Honglai Zhang, June Escara-Wilke, Xiaohua Zhang, and Evan T Keller. 2011. "ALDH Activity Indicates Increased Tumorigenic Cells, but Not Cancer Stem Cells, in Prostate Cancer Cell Lines." *In Vivo (Athens, Greece)* 25 (1) (February): 69–76.

Zhang, S., C. Balch, M.W. Chan, H.C. Lai, D. Matei, J.M. Schilder, P.S. Yan, T.H.M. Huang, and K.P. Nephew. 2008. "Identification and Characterization of Ovarian Cancer-initiating Cells from Primary Human Tumors." *Cancer Research* 68 (11): 4311.

Zhang, Shu, Curt Balch, Michael W Chan, Hung-Cheng Lai, Daniela Matei, Jeanne M Schilder, Pearlly S Yan, Tim H-M Huang, and Kenneth P Nephew. 2008. "Identification and Characterization of Ovarian Cancer-initiating Cells from Primary Human Tumors." *Cancer Research* 68 (11) (June 1): 4311–4320. doi:10.1158/0008-5472.CAN-08-0364.

Investigating the Predictions of the Revised ALDH_NegA/B Hypothesis.

Section 7.0 – The Revised ALDH_NegA/B Hypothesis

7.1 Introduction:

In this project a series of pCSC markers were used to identify and isolate pCSC and non-pCSC sub-populations form ovarian cancer cell lines. ALDH was one of the panel of markers used to screen for pCSCs. ALDH+ pCSCs were identified within the A2780, A2780cis, IGROV-1 and IGROV-CDDP cell lines (Section 4.3.1). ALDH+ pSSCs were also identified in the HIO-80 cell line (Section 4.3.1.7). For the reasons explained in Section 4.3.5, only the ALDH+ pCSC and ALDH- non-pCSC sub-populations from the A2780 and A2780cis cell lines were brought forward for isolation (Sections 5.3.1 and 5.3.2) and validation (Sections 6.3.1 and 6.3.2) in this project.

As discussed in Section 6.4.2.3, the original hypothesis suggested, that both the A2780 and A2780cis ALDH+ cells were CSCs and ALDH- cells were non-CSCs (Figure 6.22A). However, in light of the data presented in Section 6.3, this hypothesis has been rejected in favour of a hierarchical stemness hypothesis ('The Revised ALDH_NegA/B Hypothesis'; Figure 6.22B). This revised hypothesis suggests that ALDH_NegA CSCs produce ALDH+ progenitors, which in turn produce ALDH_NegB non-CSCs.

7.1.1 Predictions of the revised ALDH_NegA/B Hypothesis:

Four testable predictions were made based on the revised ALDH_NegA/B hypothesis. The detailed experiments which could be used to test each prediction will be discussed in Section 7.4.2. The basis of these predictions and requirements for testing will be described here;

1) ALDH_NegA cells are defined by their ability to produce ALDH+ cells. This is an assumption of the hypothesis rather than a prediction. However, it is predicted that ALDH_NegA cells can differentiate to produce both ALDH+ and ALDH_NegB cells. The differentiation of ALDH_NegA cells to ALDH_NegB cells is a testable prediction. This is based on the ALDH_NegA cells being considered the most stem-like of the three populations under the revised ALDH_NegA/B hypothesis. The most stem-like population is predicted to have the highest differentiation potential and should be able to differentiate in a stepwise fashion to produce ALDH+ and ALDH_NegB cells. This prediction can be tested via the SD assay and requires a pure population of ALDH_NegA cells and a method or marker for discriminating ALDH_NegA cells from ALDH+ and ALDH_NegB cells. In the previous chapter (Section 6.0), ALDH- cells were shown to produce ALDH- and ALDH+ cells. However, it is unknown if the ALDH- cells produced are ALDH_NegA, ALDH_NegB or a mixture of both.

2) It is predicted that ALDH+ cells can differentiate to produce ALDH_NegB but not ALDH_NegA cells. This based on ALDH+ cells being considered more stem-like than ALDH_NegB cells but less stem-like than ALDH_NegA cells. This prediction can be tested via the SD assay and requires a pure population of ALDH+ cells and a method or marker for discriminating ALDH+ cells from ALDH_NegA and ALDH_NegB cells. If the ALDH- cells produced by the ALDH+ cells only expressed the, as of yet unidentified ALDH_NegB, this would support the ALDH_NegA/B hypothesis. If it was a mixed population of ALDH_NegA and ALDH_B this would support the model of stochastic de-differentiation.

3) ALDH_NegB cells are defined by their inability to make ALDH_NegA and ALDH+ cells (reduced differentiation potential). This is an assumption of the hypothesis, as opposed to a testable prediction. However, as NegB cells are hypothesised to be non-CSCs they are predicted to have a reduced malignant potential, compared to ALDH+ and ALDH- cells. This is based on CSCs being considered the driving force for malignant potential in tumours (Clarke et al. 2006). Therefore, non-CSCs should have a reduced malignant potential compared to the more stem-like populations. Testing this prediction requires a pure population of ALDH_NegB cells and the mouse xenograft tumourgenicity assay. If ALDH_NegB cells were shown to have a reduced malignant potential compared to ALDH+ and ALDH_NegA cells this would support the ALDH_NegA/B hypothesis.

4) It is predicted that ALDH_NegA and ALDH+ cells can be force differentiated to produce ALDH_NegB cells. This is based on the observation that an appropriate morphogen can be used to force differentiate CSCs (Andrews 1984). Forced differentiation is used therapeutically, in the treatment of acute promyelocytic leukemia (Degos and Wang 2001). This prediction can be tested via tissue culture and flow cytometry and requires pure populations of ALDH_NegA and ALDH+ cells, an appropriate differentiation morphogen and a method or marker for discriminating ALDH_NegB cells from ALDH_NegA and ALDH+ cells.

Section 7.0 – The Revised ALDH_NegA/B Hypothesis

Pure populations of ALDH+ and ALDH- cells were were isolated from both the A2780 and A2780cis cell lines (Section 5.0). Pure populations of ALDH_NegB cells were derived clonally as by product of the SD assay. As described in Section 6.3.2.2.1, the ALDH_NegB cells derived from the A2780cis ALDH- SD assay did not produce as clear an ALDH_NegB phenotype as the A2780 ALDH- derived clones. These A2780cis ALDH_NegB cells were brought forward as 'suspected' ALDH_NegB cells, to have as a cisplatin resistant derived comparator to the cisplatin sensitive derived A2780 ALDH_NegB cells.

7.1.2 Aims:

There was one major aim driving the work presented in this chapter;

To validate one of the predictions set forth by the revised ALDH_NegA/B hypothesis (Section 7.1.1): to demonstrate that the ALDH_NegB clones clones had a reduced malignant potential compared to the ALDH+ and ALDH- populations. This aim consisted of two sub-units;

1) To investigate the malignant potential of A2780 ALDH_NegB clones, identified in the A2780 ALDH- SD assay (Section 6.3.1.2.1).
2) To investigate the malignant potential of the suspected A2780cis ALDH_NegB (unclassified) clones, identified in the A2780cis ALDH- SD assay (Section 6.3.2.2.1).

7.1.3 Hypotheses:

The work in this chapter was based on the ALDH_NegA/B hypothesis. The experiments described in Section 7.3 were specifically based on the hypothesis that the A2780 and A2780cis ALDH_NegB cells functionally identified via the SD assay (Sections 6.3.1.2.1 and 6.3.2.2.1), were less stem-like than the A2780 and A2780cis ALDH+ and ALDH- populations identified in Sections 4.3.1.1 and 4.3.1.2.

7.2 Materials and Methods:

7.2.1 Cell Culture and Sub-Culture:

Three sub-populations (ALDH-, ALDH+ and ALDH_NegB) from each of the A2780, A2780cis cell lines were used in the experiments described in this chapter;

1) The identification of ALDH- sub-populations within the A2780 and A2780cis cell lines was described in Sections 4.3.1.1 and 4.3.1.2 respectively. Their isolation was described in Sections 5.3.1 and 5.3.2 respectively. These populations were originally believed to be non-CSCs. Experiments described in this chapter (Section 7.3) in this chapter investigated the hypothesis that they are a heterogeneous mix of CSCs and non-CSCs
2) The identification of ALDH+ sub-populations within the A2780 and A2780cis was described in Sections 4.3.1.1 and 4.3.1.2 respectively. Their isolation was described in Sections 5.3.1 and 5.3.2 respectively. These populations were originally believed to be CSCs. Experiments described in this chapter (Section 7.3) investigated the hypothesis that they are cancer progenitor cells (CPCs).
3) The identification of ALDH_NegB sub-populations within the A2780 and A2780cis, via the SD assay was described in Sections 6.3.1.2.1 and 6.3.2.2.1 respectively. Due to the homogeneous nature of these ALDH_NegB clones (with respect to ALDH expression), these populations were also 'isolated' via the SD assay as described in Sections 6.3.1.2.1 and 6.3.2.2.1 respectively. Experiments described in this chapter (Section 7.3) investigated the hypothesis that they non-CSCs

These sub-populations were cultured in an identical fashion to that of their parent cell line (as described in Section 2.2).

7.2.2 Mouse Tumourgenicity Assay:

pCSCs and non-pCSCs were validated via the mouse tumourgenicity assay. Ethical approval was granted for these animal studies by the Trinity College Dublin ethics committee and the Irish Department of Health. The investigators who conducted the mouse tumourgenicity assay had passed the Laboratory Animal Science and Training (LAST) exam and were qualified to work with laboratory animals. The Trinity College Dublin Bio-Resources staff provided the practical training required to handle the mice and conduct the procedures described in Sections 7.2.2.1 – 7.2.2.7.

7.2.2.1 Housing
Mice were housed as described in Section 2.7.2.

7.2.2.2 Handling
Mice were handled as described in Section 2.7.3.

7.2.2.3 Ear-punching
For the purposes of identifying individual mice within each isolator, mice were ear-punched as described in Section 2.7.4.

7.2.2.4 Shaving
To aid with the injection of cells, mice were shaved at the injection site as described in Section 2.7.5.

7.2.2.5 Injecting
Mice were injected with cells as described in Section 2.7.6.

7.2.2.6 Euthanasia
When scientific or humane experimental end-points were reached, mice were euthanised as described in Section 2.7.7.

7.2.2.7 Post-mortem Inspection
Post-mortems were carried out as described in Section 2.7.8.

7.2.3 Single Cell Self-renewal and Differentiation Assay
pCSCs and non-pCSCs were validated via the Single Cell Self-renewal and Differentiation assay. Single cells were plated as described in Section 2.8.1. The resulting colonies were passaged as described in Section 2.8.2. Clones were retested for cancer stemness markers via flow cytometry. Clones exhibiting the ALDH_NegB phenotype were brought forward for further experiments.

7.2.4 Flow Cytometry:

7.2.4.1 ALDH Assay
The ALDH assay was carried out as described in Section 2.5.1.

7.2.4.2 HSP Assay
The HSP assay was carried out as described in Section 2.5.2.

7.2.4.3 CSP Assay
The CSP assay was carried out as described in Section 2.5.3.

7.3 Data:

The experiments described in this section investigate the malignant potential of A2780 ALDH_NegB and suspected A2780cis ALDH_NegB cells. The ALDH_NegB phenotype is defined as ALDH- SD assay-derived clones which do not produce any ALDH+ cells. Two A2780 ALDH_NegB clones (Clones D9 and F6) were randomly selected as a representative sample from the set of six clones identified as having the ALDH_NegB phenotype in the A2780 ALDH- SD assay (Section 6.3.1.2.1). No A2780cis ALDH- clones were confirmed as having the ALDH_NegB phenotype. However, two clones did have a possible ALDH_NegB phenotype (Clones C9 and G9). These clones did produce some ALDH+ cells but it could not be determined if these were true ALDH+ cells or false positives due to the 'nosier' ALDH profile of these clones (as described in Section 6.3.2.2.1). For the purpose of having a comparator derived from a cisplatin resistant source (A2780cis) to compare to the ALDH_NegB cells derived from a cisplatin sensitive source (A2780), these A2780cis C9 and G9 clones were brought forward for further analysis. The experiments described in Sections 7.3.1 and 7.3.2 compare the malignant potential of ALDH_NegB cells to that of ALDH+ and ALDH- cells.

7.3.1 A2780 ALDH_NegB Malignant Potential:

The A2780 ALDH_NegB cells are hypothesised to be less stem like than the ALDH+ and ALDH- sub-populations. The ALDH- sub-population is suspected to be composed of at least two cell types: the CSC-like ALDH_NegA cells and the non-CSC-like ALDH_NegB cells. The SD assay demonstrated that the ALDH_NegB cells have a reduced differentiation potential than the compared to the ALDH+ and ALDH_NegA cells (Section 6.3.1.2). ALDH+ and ALDH_NegA cells were shown to produce ALDH+ pCSC progeny, while the ALDH_NegB cells were shown to produce only ALDH- non-pCSC progeny (Section 6.3.1.2). This work which was described in the previous chapter is sufficient to demonstrate that the ALDH_NegB cells had a reduced differentiation and self-renewal potential when compared to the ALDH_NegA and ALDH+ cells (Section 6.3.1.2).

To investigate if this reduced differentiation potential translated into a reduced malignant potential, A2780 ALDH_NegA cells were injected sub-cutaneously into NOD.SCID mice. Four mice were injected with 5×10^2 ALDH_NegB cells. Two of these replicates were derived from

the D9 clone and two from the F6 clone (Figure 7.1). Four mice were injected with 5×10^3 ALDH_NegB cells. Two of these replicates were derived from the D9 clone and two from the F6 clone (Figure 7.1). All four mice injected with 5×10^2 ALDH_NegB cells developed tumours. Three of the four mice injected with 5×10^3 ALDH_NegB cells developed tumours. The ALDH_NegB cells did not exhibit any significant difference in tumour latency or size to either the ALDH+ or ALDH- sub-populations (Table 7.1). Unexpectedly, at 5×10^3 cells, the 'Clone F6' replicates had a significantly longer tumour latency (30 days versus 54 days) than the 'Clone D9' replicates (Table 7.1), suggesting that the are not the same cell types (discussed in Section 7.4.1). This difference was only observed when comparing the latency and size of the 5×10^3 replicates but not the 5×10^2 replicates of the two clones. This reflects the wider range of latencies observed in tumours derived from 5×10^2 cells compared to tumours derived from 5×10^3 cells.

Logarithmically, more 'Clone F6' cells produced significantly smaller or no tumours even when allowed a significantly longer latency than both the ALDH+ and ALDH- cells (Table 7.1). This shows that the ALDH_NegB Clone F6 cells have a reduced malignant potential compared to the ALDH+ and ALDH- cells and fit the criteria of non-CSCs. This is consistent with the predictions of the ALDH_NegA/B hypothesis. This significance is only observed when comparing 5×10^3 ALDH_NegB Clone F6 cells to either 5×10^2 ALDH+ or ALDH- cells. When comparing 5×10^3 ALDH_NegB Clone F6 cells to either 5×10^2 ALDH+ or ALDH- cells, the difference is non-significant. This is due to the one F6 clone which did produce a large xenograft tumour.

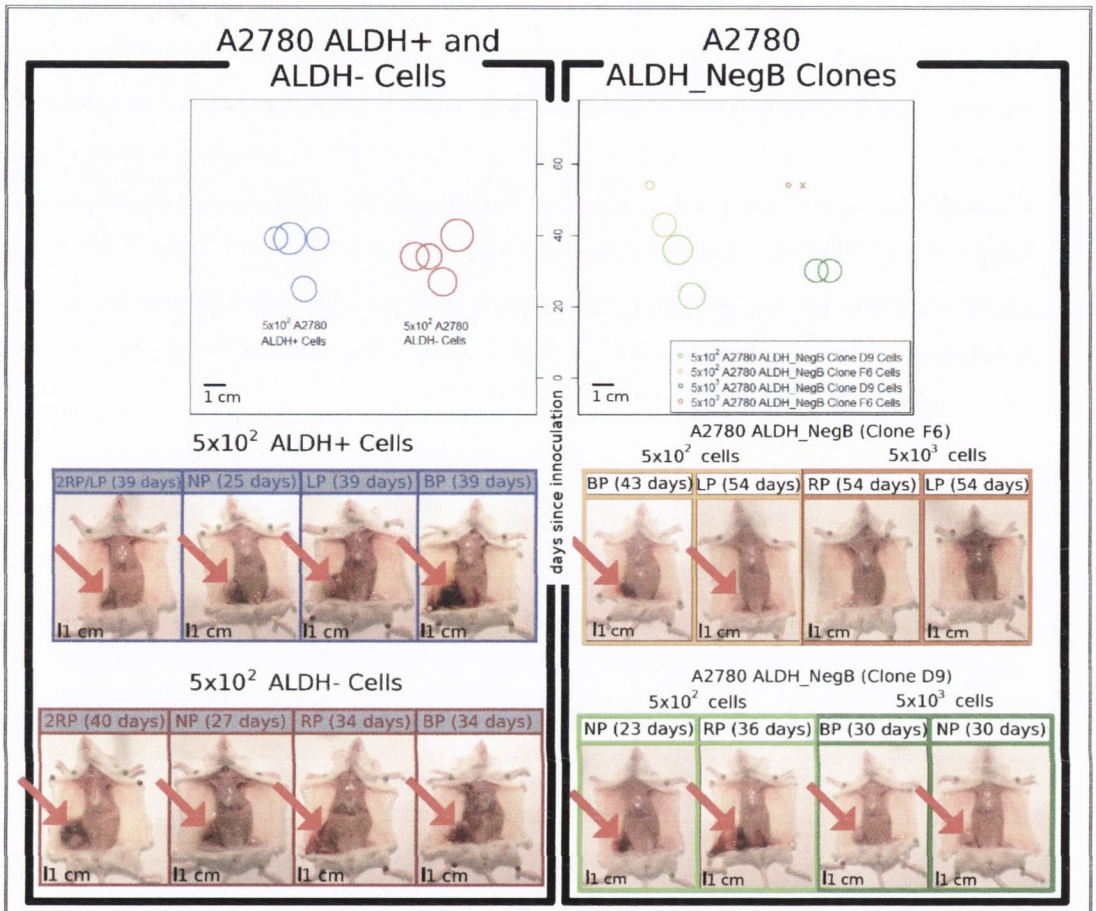

Figure 7.1: A2780 ALDH_NegB versus A2780 ALDH+ and A2780 ALDH- Mouse Tumourgenicity Experiments – The graphs show the tumour latency on the y-axis expressed in days compared to tumour size, expressed as the size of the circle points relative to the scale bar. Circle points mark the latency and size of tumours. Crosses mark the time at which animals, which did not develop tumours were euthanised. The photographs show a dissected view of each of the tumours/mice represented on the graphs and are colour coded to their respective points.

Table 7.1: A2780 Tumourgenicity Assay – Comparison of Tumour Latency and Sizes. This table shows the comparison of the tumour latency (latency) and tumour size (size) between the cell populations named in the title row and those in the title column. Cells shaded green indicate comparisons where both the tumour latency and tumour size are significantly different. Cells shaded yellow indicate where only the tumour latency was significantly different.

	ALDH+ 5×10^2	**ALDH- 5×10^2**	**ALDH_NegB Clone D9 5×10^2**	**ALDH_NegB Clone D9 5×10^3**
ALDH_NegB (Both Clones) 5×10^2	No significant difference in latency ($p = 0.6568$) or size ($p = 0.5371$).	No significant difference in latency ($p = 0.4961$) or size ($p = 0.2834$).	-	-
ALDH_NegB (Both Clones) 5×10^3	No significant difference in latency ($p = 0.4451$) or size ($p = 0.1245$).	No significant difference in latency ($p = 0.3306$) or size ($p = 0.08024$).	-	-
ALDH_NegB Clone F6 5×10^2	No significant difference in latency ($p = 0.193$) or size ($p = 0.4408$).	No significant difference in latency ($p = 0.1781$) or size ($p = 0.0.3611$).	No significant difference in latency ($p = 0.1588$) or size ($p = 0.3691$).	-
ALDH_NegB Clone F6 5×10^3	Both latency ($p = 0.0133$) and size ($p = 0.01961$) were significantly reduced compared to ALDH+ cells.	Both latency ($p = 0.004716$) and size ($p = 0.02576$) were significantly reduced compared to ALDH- cells.	-	The latency ($p = 0.00009$) but not size ($p = 0.08383$) was significantly reduced compared to 'Clone D9' cells.

7.3.2 A2780cis ALDH_NegB Malignant Potential

71.43 % (5/7) of A2780cis ALDH- clones were identified as ALDH_NegA clones (Section 6.3.2.2.1). 28.57 % (2/7) did not exhibit a clear ALDH_NegA phenotype (Section 6.3.2.2.1). Due to the 'nosier' ALDH profile it was not possible to determine if the ALDH+ cells in these clones were true ALDH+ cells or whether they were false positives. These 2 clones (C9 and G9), were brought forward for further experiments under the assumption that they were the A2780cis (cisplatin resistant model) counterparts to the A2780 (cisplatin sensitive model) ALDH_NegB clones. Further work is required to resolve this the true nature of this phenotype. The identification of a protein marker to differentiate between ALDH_NegA and ALDH_NegB cells would be the best approach. However, logarithmically more cells or additional replicates of the same clones may be able to resolve the 'suspected' A2780cis ALDH_NegB phenotype.

To investigate their malignant potential, A2780cis ALDH_NegB cells were injected sub-cutaneously into NOD.SCID mice. Four mice were injected with 5×10^2 ALDH_NegB cells. Two of these replicates were derived from the C9 clone and two from the G9 clone (Figure 7.2). Four mice were injected with 5×10^3 ALDH_NegB cells. Two of these replicates were derived from the C9 clone and two from the G9 clone. All mice injected with cells developed tumours. It took 5×10^2 ALDH_NegB cells a significantly longer latency than 5×10^2 ALDH- cells to generate tumours. This demonstrates that ALDH_NegB cells have a limited malignant potential compared to ALDH- cells (Table 7.2). This is consistent with the predictions of the ALDH_NegA/B hypothesis. There was no significant difference in tumour size or latency between the ALDH_NegB cells and ALDH+ cells (Table 7.2). There was no significant difference in tumour size or latency of the tumours produced by 5×10^3 cells compared to 5×10^2 cells of either ALDH- or ALDH+ cells (Table 7.2). There was no significant difference in the malignant potential of the to clones (Table 7.2). These experiments, through the demonstration of an increase in tumour latency, identify the A2780cis ALDH_NegB cells as having reduced stemness potential compared to the ALDH- cells, which are thought to be a mixed population of ALDH_NegA (pCSCs) and ALDH_NegB (non-pCSCs; Section 6.3.2.2.1).

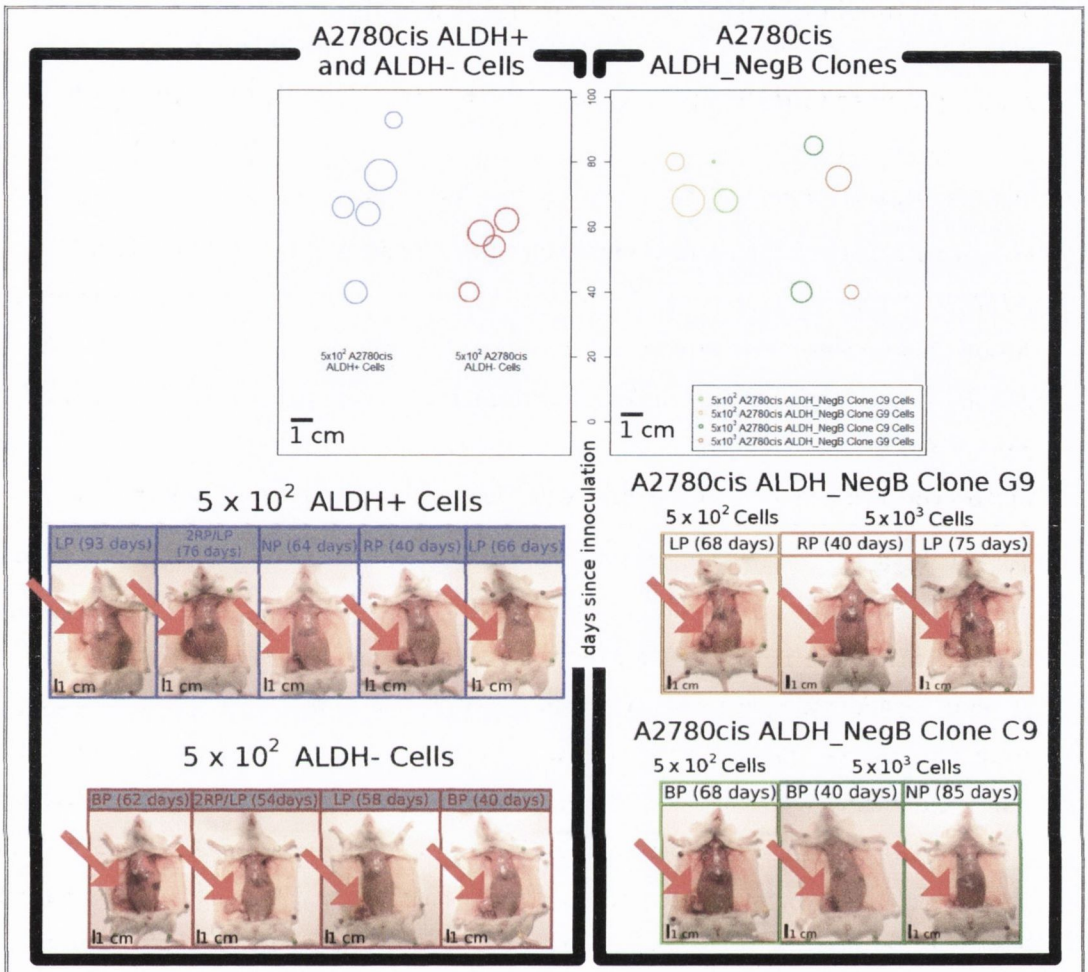

Figure 7.2: A2780cis ALDH_NegB versus A2780cis ALDH+ and A2780cis ALDH- Mouse Tumourgenicity Experiments – The graphs show the tumour latency on the y-axis expressed in days compared to tumour size, expressed as the size of the circle points relative to the scale bar. Circle points mark the latency and size of tumours. Crosses mark the time at which animals, which did not develop tumours were euthanised. The photographs show a dissected view of each of the tumours/mice represented on the graphs and are colour coded to their respective points.*

* Two of the images were unavailable (A2780cis ALDH_NegB 5 x 10^2 cells – clones G9 and C9).

Table 7.2: A2780cis Tumourgenicity Assay – Comparison of Tumour Latency and Sizes.
This table shows the comparison of the tumour latency (latency) and tumour size (size) between the cell populations named in the title row and those in the title column. Cells shaded yellow indicate comparisons where the tumour latency was significantly different.

	ALDH+ 5×10^2	**ALDH- 5×10^2**	**ALDH_NegB Clone D9 5×10^2**	**ALDH_NegB Clone D9 5×10^3**
ALDH_NegB (Both Clones) 5×10^2	No significant difference in latency ($p = 0.5337$) or size ($p = 0.5334$).	The latency ($p = 0.01547$) but not size ($p = 0.5892$) was significantly reduced compared to ALDH- cells.	-	-
ALDH_NegB (Both Clones) 5×10^3	No significant difference in latency ($p = 0.612$) or size ($p = 0.3094$).	No significant difference in latency ($p = 0.635$) or size ($p = 0.3422$).	-	-
ALDH_NegB Clone C9 5×10^2	-	-	No significant difference in latency ($p = 1.0$) or size ($p = 0.4731$).	-
ALDH_NegB Clone C9 5×10^3	-	-	-	No significant difference in latency ($p = 0.8878$) or size ($p = 0.9899$).

7.4 Discussion:

The results described above (Section 7.3) support the revised ALDH_NegA/B hypothesis by demonstrating that the ALDH_NegB cells have a reduced malignant potential within both the A2780 ('Clone F6' only) and the A2780cis model systems.

7.4.1 A2780 and A2780cis ALDH_NegB experiments:

It was shown that the F6 clone, at logarithmically higher cell numbers (5×10^3 compared to 5×10^2), had a significantly longer latency and smaller size than both the A2780 ALDH+ and the A2780 ALDH- cells (Section 7.3.1). This demonstrates a reduced malignant potential of A2780 ALDH_NegB Clone F6 cells compared with A2780 ALDH+ and A2780 ALDH- cells. The demonstration of reduced malignant potential (Section 7.3.1) and reduced differentiation potential (Section 6.3.1.2.1), validate this cell population as a non-CSC sub-population of the A2780 cell line.

Unexpectedly, the two clones selected to represent the A2780 ALDH_NegB sub-population exhibited a different malignant potential to one another. This difference was not statistically different when comparing both clones at 5×10^2 cells (Latency: p-value = 0.1588; Size: p-value = 0.3691). However, when comparing the clones at 5×10^3 cells it was noted that the F6 clone had a significantly longer latency (p-value = 0.00009). More A2780 ALDH_NegB clones need to be assessed to confirm which is the dominant phenotype within the A2780 ALDH_NegB population.

The difference in malignant potential suggests that the D9 clone is more stem-like than the F6 clone. However, this is not reflected in the differentiation potential of these two clones (Section 6.3.1.2.1). It is possible that these clones are not composed of the same cell type. Microarray analysis of this clone in conjunction with other sub-populations of the A2780 cell line could be used to confirm whether these were the same cell types or not. Microarray analysis could be used to measure the relative gene expression of A2780 ALDH+, ALDH- and ALDH_NegB Clone D9 and Clone F6 cells. Hierarchical clustering analysis could then be used to match the most similar gene expression profiles in a pairwise fashion. If the D9 and F9 clones paired closest in the hierarchy this would be evidence of the two clones being the same cell type. However, if the D9 clone paired more closely with one of the other populations, this would be evidence of it being more similar to that cell type than the F6 clone. It is possible for an A2780 ALDH_NegA clone to generate an A2780 ALDH_NegB phenotype in the SD assay.

Section 7.0 – The Revised ALDH_NegA/B Hypothesis

The production of ALDH+ cells is currently the only distinguishing feature between ALDH_NegA and ALDH_NegB cells in the SD assay. However, it is possible that the ALDH_NegA cells could proliferate in a self-renewal state only, in which case they would phenotypically resemble the ALDH_NegB clones. This would explain the perceived reduction in differentiation potential while maintaining the malignant potential, as was seen in the A2780 ALDH_NegB D9 clone.

The A2780cis ALDH_NegB cells showed a significantly longer latency (p-value = 0.01547) than the A2780cis ALDH- cells, to reach a tumour size which was not significantly different (p-value = 0.5892). No significant difference was observed between the A2780cis ALDH_NegB cells and the A2780cis ALDH+ cells (Latency: p-value = 0.5337; Size = 0.5334). This demonstrates a reduced malignant potential of A2780cis ALDH_NegB cells compared with ALDH- cells. This is consistent with the prediction of the A2780cis ALDH_NegA/B hypothesis and validates these A2780cis ALDH_NegB clones as non-CSCs isolated from the A2780cis cell line.

These findings support the revised hypothesis and highlight the power of using the SD assay in conjunction with the mouse tumourgenicity assay to validate pCSCs. Without the SD assay the ALDH_NegA and ALDH_NegB populations would not have been observed. While the data presented in Section 7.3 does support the ALDH_NegA/B hypothesis, it is important to bear in mind that these experiments were based on the progeny of a single cell. It takes at least 20 population doublings for a single cell to divide to produce 1 x 10^6 cells (2^{20} = 1,048,576). As such, genetic drift is a concern in these experiments. Clones had to be used for these experiments as it was the only available method with which to obtain a pure population of ALDH_NegB cells. It would be preferable to use ALDH_NegA and ALDH_NegB cells isolated directly from the parent cell line to validate the predictions of the ALDH_NegA/B hypothesis. If a cell surface marker could be identified to discriminate ALDH_NegA cells from ALDH_NegB cells, these cells could be isolated directly form their parent cell lines and compared without the possible influence of genetic drift in the results. The methods for identifying such markers is described in Section 7.4.2, along with the experiments required to validate the other predictions of the ALDH_NegA/B hypothesis.

While further experiments are needed to confirm the ALDH_NegA → ALDH+ → ALDH_NegB cancer stemnesss hierarchy, thus far, these data are the first direct evidence of a CSC hierarchy within ovarian cancer. Having said this, Silva et al. (2011) did put forward a putative ovarian cancer stemness hierarchy based upon indirect evidence. They put forward:

ALDH+/CD133+ → ALDH+ → ALDH-/CD133-. This was based upon findings of decreased tumourgenicity and spheroid growth from the ALDH+/CD133+ through the ALDH+ to the ALDH-/CD133- cells. They also reported that the xenograft tumours formed were retested via flow cytometry and indicated the self-renewal and differentiation potential of each population. ALDH+/CD133+ derived tumours were shown too be ALDH+/- and CD133+/-. While, ALDH+/CD133- derived tumours were reported as only producing CD133- cells. However, the data presented showed that these tumours contained 1.3 % CD133+ cells. Additionally, they presented data showing that ALDH-/CD133+ derived tumours produced an ALDH+ sub-population: A finding which supports the ALDH_NegA/B hypothesis presented in this chapter. Interestingly, this finding was not incorporated when Silva et al. put forward their putative ovarian cancer stemness hierarchy model.

7.4.2 Testing the Predictions of the Revised ALDH_A/B Hypothesis:

As described in Section 7.1.1, four testable predictions were made based on the ALDH_NegA/B hypothesis. Several of these experiments require a marker to discriminate between ALDH_NegA and ALDH_NegB cells so that these cell types can be isolated directly from the parent cell lines. An experiment designed to identify such possible markers will be described first in Section 7.4.2.1. After which the experiments designed to investigate the other predictions of the ALDH_NegA/B hypothesis will be discussed (Sections 7.4.2.2 – 7.4.2.5).

7.4.2.1 Identification of ALDH_NegA and ALDH_NegB markers:

Markers of ALDH_NegA and ALDH_NegB are defined as readily detectable proteins with differential expression between the ALDH_NegA and ALDH_NegB cell types. Cell surface proteins are readily detectable proteins. Fluorescently conjugated antibodies can be used to detect their presence/absence or relative expression level via flow cytometry while maintaining the viability of the cell. Microarray analysis can be used to assess differential gene expression between cell populations. With the exception of post-transcriptional regulation, gene expression is proportional to protein expression. Therefore, microarray analysis of ALDH_NegA and ALDH_NegB cells could be used to identify readily detectable proteins with differential expression between the ALDH_NegA and ALDH_NegB cell types. However, a pure population of ALDH_NegA cells is not available. Pure populations of ALDH_NegB cells are available via the SD assay (Section 6.3.2.2.1) and a mixture of approximately (42 %) ALDH_NegA and (58 %) ALDH_NegB cells are available in the from of ALDH- cells isolated directly from the parent cell lines via the ALDH assay (Section 5.3.1). ALDH_NegB clones could be compared

to ALDH- cells via microarray analysis. Genes which encode cell surface proteins and show a decreased expression in ALDH- cells relative to ALDH_NegB cells are putative markers of the ALDH_NegB cell type. Genes which encode cell surface proteins and show an increased expression in ALDH- cells relative to ALDH_NegB cells are putative markers of the ALDH_NegA cell type. Panels of antibodies raised against the putative markers could then be used to plate putative ALDH_NegA and ALDH_NegB cells as single cells in the SD assay. The clones which form could then be tested with the ALDH assay to determine which of the putative markers had successfully segregated the ALDH_NegA and ALDH_NegB phenotypes. Such markers could then be declared ALDH_NegA or ALDH_NegB markers.

7.4.2.2 ALDH_NegA cells are predicted to differentiate to produce both ALDH+ and ALDH_NegB cells:

To test this prediction, ALDH_NegA cells could be single cell plated via FACS, utilising novel markers (described in Section 7.4.2). These single cells would be allowed to grow into clones and then retested for the expression of ALDH_NegA, ALDH+ and ALDH_NegB markers, via flow cytometry. If all three cell types were present, this would indicate that ALDH_NegA cells have the self-renewal and differentiation potential to produce all the cell types detected via the ALDH assay. Such evidence would validate the prediction of the ALDH_NegA/B hypothesis.

7.4.2.3 ALDH+ cells are predicted to differentiate to produce ALDH_NegB but not ALDH_NegA cells:

ALDH+ cells have already been demonstrated to produce ALDH+ and ALDH- cells via the SD assay (Sections 6.3.1.2.2 and 6.3.2.2.2). However, it is unknown if these ALDH- cells are ALDH_NegA cells, ALDH_NegB cells or a mixture of both. The ALDH_NegA/B hypothesis predicts that ALDH+ cells have a reduced differentiation potential compared to ALDH_NegA cells and can differentiate to produce ALDH_NegB cells but not ALDH_NegA cells. To test this prediction, ALDH+ cells could be single cell plated via FACS for the SD assay. The clones produced could then be retested for the expression of ALDH_NegA, ALDH+ and ALDH_NegB markers, via flow cytometry. If only ALDH+ and ALDH_NegB cells were detected, this would indicate that ALDH+ cells are more differentiated than the ALDH_NegA but are still able to differentiate and self-renew to produce ALDH+ and ALDH_NegB cells. This would identify ALDH+ cells as progenitor cells in the middle of a CSC hierarchy. Such evidence would validate the prediction of the ALDH_NegA/B hypothesis. If it was found that ALDH+ cells produced both ALDH_NegA and ALDH_NegB cells this would support a model of de-differentiation as discussed in Section 6.4.2.3.

The process of isolating a sub-population and gauging its ability to derive clonal lineages to define a stemness hierarchy (discussed in Sections 7.4.2.2 – 7.4.2.3), was the approach used to interrogate the hierarchies within the now well mapped haematopoietic system. For example: the common lymphoid progenitors were identified in the murine system via fluorescence-activated cell sorting for $Lin^{-}/IL\text{-}7R^{+}/Thy\text{-}1^{-}/Sca\text{-}1^{lo}/c\text{-}kit^{lo}$ (CLP) cells. These CLP cells were shown to generate lymphoid lineage cells pro-B and pre-B cells when grown clonally under lymphoid differentiation conditions (IL-7 supplemented) on methylcellulose plates. Competitive reconstitution of lethally irradiated Ly5.1 mice with Ly5.2 congenic CLP cells and Ly5.1 synergenic bone marrow cells, demonstrated the lymphoid differentiation potential of CLPs under *in vivo* conditions (Kondo et al. 1997). Similar experiments also identified common myeloid progenitor cells (Akashi et al. 2000). These experiments, which proved successful in mapping the haematopoeitic system are analogous to the experiments suggested (Sections 7.4.2.2 – 7.4.2.3) for mapping the ovarian cancer stemness hierarchy.

7.4.2.4 ALDH_NegB Cells are predicted to have a reduced malignant potential when compared to ALDH+ and ALDH_NegA cells:

The investigation of the malignant potential of ALDH_NegB cells derived from the A2780 and A2780cis cell lines was described above (Section 7.3). As there was insufficient time to identify ALDH_NegA and ALDH_NegB markers, no direct comparison to ALDH_NegA cells could be made. Additionally a clonal source of ALDH_NegB cells had to be used. The experiments described above supported the revised ALDH_NegA/B hypothesis. This supports the need for further investigations.

Additional mouse tumourgenicity experiments with pure ALDH_NegA and ALDH_NegB cells isolated directly from the parent cell lines could exaggerate the differences seen between the various populations. For example; no significant difference was observed between ALDH+ and ALDH- cells (Sections 6.3.1.1.1 and 6.3.2.1.1) but a difference may be observed between ALDH+ and ALDH_NegA cells. The use of ALDH_NegB cells isolated directly from the parent cell line would be a better comparator to the ALDH+ and ALDH_NegA populations than the ALDH_NegB clones tested above, as the non clonal source would have been less exposure to genetic drift.

7.4.2.5 It is predicted that ALDH_NegA and ALDH+ cells can be force differentiated to produce ALDH_NegB:

To test this prediction requires knowledge of the molecular pathways up-regulated/down-regulated during differentiation of ALDH_NegA and ALDH+ cells to ALDH_NegB cells. Microarray analysis could be used to determine the relative gene expression of ALDH_NegB (differentiated) cells and ALDH_NegA/ALDH+ (undifferentiated) cells to identify which molecular pathways are up-regulated/down-regulated upon differentiation. Gene knock-down experiments could be used to determine which up-regulated/down-regulated pathways are sufficient to induce differentiation of the ALDH_NegA and ALDH+ cells. Any compound with the ability to induce similar activation/deactivation of such pathways could be used to force differentiate the ALDH_NegA and ALDH+ to the less malignant ALDH_NegB phenotype. Retinoic acid (RA), the ligand for, retinoic acid receptor, is routinely used to force differentiation pluripotent CSCs. The addition of RA to culture media induces the terminal differentiation of pluripotent NTera2 CSCs (Andrews 1984). The growth factors: bone morphogenic protein (BMP) and leukaemia inhibitory factor (LIF) are routinely used to maintain embryonic stem cells in an undifferentiated state. Addition/withdrawal of BMP and LIF can maintain embryonic stem cells in an undifferentiated/differentiated state respectively (Smith et al. 1988; Ying et al. 2003).

A panel of putative stimulatory and inhibitory agents could be assembled from the published literature. Morphogen concentration, and duration of incubation can be optimised via a matrix of dose response and incubation response experiments on ALDH_NegA and ALDH_NegB cells. The optimal dose and incubation duration could be identified, via 'real-time polymerase chain reaction' (RT-PCR) by detecting the up-regulation/down-regulation of downstream genes of the molecular pathways targeted. Such experiments could also identify if more than one morphogens are required to up-regulate/down-regulate all the pathways necessary for differentiation.

Once a panel of putative morphogens have been identified, each can be added to the culture media of ALDH_NegA and ALDH_NegB cultures. The cells of each culture can then be retested via RT-PCR, flow cytometry or fluorescent microscopy to detect a change in ALDH_NegA or ALDH+ phenotype to ALDH_NegB phenotype.

Identification of such factors for OvCSC differentiation would enable the establishment of model systems in which to study CSC differentiation mechanisms. There are very few such CSC models and no such OvCSC models. Such models would allow for the precise

characterisation of 'early' and 'late' mechanisms of differentiation. Such mechanisms would represent the most likely targets for CSC based therapies.

7.4.3 Summary:

This chapter introduced the testable predictions of the ALDH_NegA/B hypothesis (Section 7.1.1). Experiments were carried out to test one of these predictions and the data was presented in Section 7.3. The results of these experiments were discussed with respect to their support of the ALDH_NegA/B hypothesis (Section 7.4.1). Finally, further experiments designed to investigate the other predictions of the NegA/B hypothesis were described (Section 7.4.2).

Testing the ALDH_NegA/B Revised Hypothesis:- Primary findings

- A2780 ALDH_NegB cells ('Clone F6') have a reduced malignant potential compared to ALDH+ and ALDH- cells. This finding supports the revised ALDH_NegA/B hypothesis.
- The A2780 ALDH_NegB clones F6 and D9 exhibited significantly different malignant potential. Further experiments are required to determine if these clones are composed of the same cell types (discussed in Section 7.4.1).
- The A2780cis ALDH_NegB cells have a reduced malignant potential compared to ALDH- cells. This finding supports the revised ALDH_NegA/B hypothesis.

7.5 References:

Akashi, K, D Traver, T Miyamoto, and I L Weissman. 2000. "A Clonogenic Common Myeloid Progenitor That Gives Rise to All Myeloid Lineages." *Nature* 404 (6774) (March 9): 193–197. doi:10.1038/35004599.

Andrews, P W. 1984. "Retinoic Acid Induces Neuronal Differentiation of a Cloned Human Embryonal Carcinoma Cell Line in Vitro." *Developmental Biology* 103 (2) (June): 285–293.

Clarke, Michael F, John E Dick, Peter B Dirks, Connie J Eaves, Catriona H M Jamieson, D Leanne Jones, Jane Visvader, Irving L Weissman, and Geoffrey M Wahl. 2006. "Cancer Stem Cells--perspectives on Current Status and Future Directions: AACR Workshop on Cancer Stem Cells." *Cancer Research* 66 (19) (October 1): 9339–9344. doi:10.1158/0008-5472.CAN-06-3126.

Degos, L, and Z Y Wang. 2001. "All Trans Retinoic Acid in Acute Promyelocytic Leukemia." *Oncogene* 20 (49) (October 29): 7140–7145. doi:10.1038/sj.onc.1204763.

Kondo, M, I L Weissman, and K Akashi. 1997. "Identification of Clonogenic Common Lymphoid Progenitors in Mouse Bone Marrow." *Cell* 91 (5) (November 28): 661–672.

Silva, Ines A, Shoumei Bai, Karen McLean, Kun Yang, Kent Griffith, Dafydd Thomas, Christophe Ginestier, et al. 2011. "Aldehyde Dehydrogenase in Combination with CD133 Defines Angiogenic Ovarian Cancer Stem Cells That Portend Poor Patient Survival." *Cancer Research* 71 (11) (June 1): 3991–4001. doi:10.1158/0008-5472.CAN-10-3175.

Smith, Austin G., John K. Heath, Deborah D. Donaldson, Gordon G. Wong, J. Moreau, Mark Stahl, and David Rogers. 1988. "Inhibition of Pluripotential Embryonic Stem Cell Differentiation by Purified Polypeptides." , *Published Online: 15 December 1988; | Doi:10.1038/336688a0* 336 (6200) (December 15): 688–690. doi:10.1038/336688a0.

Ying, Qi Long, Jennifer Nichols, Ian Chambers, and Austin Smith. 2003. "BMP Induction of Id Proteins Suppresses Differentiation and Sustains Embryonic Stem Cell Self-renewal in Collaboration with STAT3." *Cell* 115 (3) (October 31): 281–292.

General Discussion

Section 8.0: General Discussion

8.8 Introduction:

This research was undertaken with the underlying hypothesis that recurrent chemoresistant ovarian cancer is driven by a small residual population of ovarian CSCs, which have adapted to chemotherapy. Currently, the development of CSC directed therapies against ovarian cancer (and other malignancies) is limited by the lack of models of ovarian CSCs. Once model systems are established it will facilitate the identification of therapeutically targetable CSC pathways and testing of anti-CSC chemotherapeutic agents.

To facilitate the investigation of the role of CSCs in each of these malignant processes this research aimed to identify, isolate and validate of CSCs from ovarian cancer sources. The system established during this research enables the identification of CSCs from any malignancy and produces the materials required to map differentiation and self-renewal pathways which facilitates the long-term aim of generating stable models. The results presented in this thesis reinforce the underlying hypothesis: as statistically significantly different proportions and 'types' of ovarian CSCs were observed between pair matched chemosensitive and chemo-adapted models. This suggests that CSCs and/or an altered structure of cellular differentiation within ovarian cancer play(s) a role in the acquisition of chemoresistant properties.

8.9 Viewing tumours as a malignant form of organogenesis can improve our understanding of the disease:

This thesis approached the study of cancer from the viewpoint that cancer is a malignant form of organogenesis and tissue homoeostasis, initiated and propagated through acquired genetic mutations.

In Section 1.3, cancer was described with respect to Hanahan and Weinberg's (2011) six 'hallmarks' of cancer: sustained proliferative signalling; evasion of growth suppressors; invasion and metastasis; replicative immortality; inducing angiogenesis; resistance to cell death. In a similar fashion to carcinogenesis, embryogenesis can be defined by analogues of four of these six 'hallmarks': Embryonic tissues, like cancerous tissues maintain a high state of cell proliferation, via self-sufficient autocrine and paracrine growth factor signalling (Leung 1987; Bohnsack and Hirschi 2004). Both carcinogenesis and embryogenesis give rise to tissues capable of replicative immortality. In embryogenesis this is achieved through the production and maintenance of SSC pools in highly regulated niches. In carcinogenesis this is achieved through CSC pools or aberrant telomerase expression, or a combination of the two (Blackburn

2005). Angiogenesis in embryogenesis, like carcinogenesis is among the first stages of development (Sherer and Abulafia 2001). Placental invasion of the uterine wall can be considered a 'healthy' analogue to the malignant invasion observed in cancerous growth and development (Holtan et al. 2009). Embryogenesis diverges from the six 'hallmarks' of cancer with respect to tumour suppressor evasion and anti-apoptotic attributes. Unlike cancer, these characteristics are highly regulated within the developing embryo (Brill et al. 1999). The similarities between carcinogenesis and embryo/organogenesis, presents a different way of viewing carcinogenesis and suggests new ways of treating tumours, as will be discussed below.

Germ cell teratocarcinomas have long been compared to malignant embryogenesis: Martin (1975) argued that both cell types were so similar that the pluripotent cells which were easily isolated and cultured from murine teratocarcinoma cells, could serve as a model for studying murine embryonic stem cells. The similarities between germ cell tumours and embryogenesis are probably best exemplified through the development of viable mice from chimeric mixtures of murine ES cells and murine pluripotent CSCs. It was demonstrated that such chimeric mice developed to term normally with complete tissues derived from both ES and CSCs (Mintz and Illmensee 1975). They generated a teratoma from a 6-day male mouse embryo, which had a black coat phenotype, by grafting the embryo under a testis capsule. The grafted embryo became disorganised, forming a teratoma, which metastasised to the renal node. This tumour was then passaged intraperitoneally, as ascites, for ~200 generations. The pluripotent tumour cells were then harvested and introduced into the inner cell mass of a blastocyst, with brown coat phenotype and implanted in a foster mother. Pregnancy ensued and live normal (mosaic black/brown coat) were born. This suggests that the embryonic environment is able to regulate the hyper proliferative growth of the pluripotent CSCs while adult tissues can not. The regulatory mechanisms in embryonic tissues are 'designed' to act on highly proliferative cells during normal growth and development, while adult tissues are not 'designed' to have highly proliferative cells during normal growth and development. It would be interesting to see if murine CSCs isolated from somatic tumours could also contribute to the formation of their normal tissue counterparts if introduced to a chimeric embryo. Such an experiment may require orthotopic transplantation into an embryo at a post-implantation stage of development. Therefore, such an experiment may be technically improbable.

These observations and lines of thought have an important bearing on possible future therapies against CSCs. It suggests that "weaponized" embryonic development regulators could be therapeutic in the treatment of cancer. This is especially true of gynaecological malignancies, as

several well studied, mechanisms are required to prevent the growth and development of female reproductive tissues in male embryos (Gustafson and Donahoe 1994). Interestingly, müllerian inhibiting substance (MIS), a growth factor which inhibits the growth of female reproductive system tissues in the male embryo, has been demonstrated to inhibit the proliferation of ovarian cancer cells (Szotek 2006). They showed that treatment of HSP cells isolated from two murine ovarian cancer cell lines were responsive to MIS. Treatment with 10 μg/ml MIS for 24 h induced an 86 % and 37 % reduction in proliferation in the HSP cells isolated from the MOVCAR7 and 4306 cell lines respectively. They linked this reduced proliferation to a functional MIS signalling pathway by showing that these cells express the MIS receptor II surface protein (via confocal microscopy), and expressed other key components: SMAD1, SMAD5, SMAD8, Alk2, Alk3 (via RT-PCR). In Section 7.0, the identification of a cancer stemness hierarchy was described. This lends weight to the malignant organogenesis viewpoint: demonstrating that ovarian cancer has structured forms of cellular differentiation – similar to that of somatic tissues. It may be possible to use differentiation morphogens, such as MIS, to force differentiate such hierarchies, which could have substantial therapeutic benefit to the patient. In particular, MIS may be useful in the forced differentiation of the HSP+ sub-populations isolated from the IGROV-1 and IGROV-CDDP models (Section 5.3).

Much cancer research focuses on genetic mutations and the ensuing molecular pathway dysregulation that exist in tumours. For example: the study of the links between genetic mutations and familial breast cancer led to discovery of the BRCA1 (Miki et al. 1994) and BRCA2 (Wooster et al. 1995) genes, which have improved the ability to screen for patients at risk of developing breast and ovarian cancers. Wooster et al. identified the BRCA2 gene by screening genomic DNA fragments (>300bp) containing putative coding sequences for genetic mutations. They screened at least one affected family member from 46 families with familial breast cancer. Each family in the study showed a genetic linkage for BRCA2 associated breast cancer and/or genetic linkage evidence against BRCA1 associated breast cancer. These approaches have greatly improved the understanding of cancer biology, leading to improved screening, which provides scope for proflactic therapies, such as salpingo-oophorectomies, which can reduce the risk of breast and ovarian cancer in patients who carry BRCA1 and BRCA2 mutations (Kauff et al. 2008). Research focused on genetic mutations have also led to the identification of directed anti-cancer therapies. For example: The discovery that CGP57148B (imatinib) selectively targets the BCR-ABL fusion protein has revolutionised the treatment of cronic myeloid leukemia and some subtypes of acute myeloid leukemia (Deininger

et al. 1997; Deininger et al. 2000; Buchdunger, O'Reilly, and Wood 2002). However, cancer can not be fully understood through the study of genetic mutations and molecular dysregulation at the tumour level. Cancer is a tissue malignancy as opposed to a molecular malignancy. To fully understand the function and dysfunction of a tissue one needs to understand the unique and diverse molecular mechanisms of each of the cell populations, which come together to make up the tissue and confer its function. As the results described in Section 4.0 show: ovarian cancer is made up of numerous sub-populations of different cell types. For example, as discussed in Section 4.4.4.3.4, the IGROV-CDPP ovarian cancer model may have up to 12 sub-populations related to cancer stemness. The results presented in Section 6.0 show that many of these sub-populations contribute differently to the self-renewal and differentiation capacities of the population as a whole. For example as shown in Section 6.3.1: A2780 ALDH_NegA and ALDH+ sub-populations do contribute to the differentiation capacity of the A2780 cell line while the ALDH_NegB sub-population does not. It is intuitive to consider that different sub-populations many also contribute differently to other properties of malignancy such as chemoresistance and metastasis.

It is important to recognise that cancerous tissues are made up of multiple populations of cell types, of which CSCs are only one sub-population. For example the field of circulating tumour cells focuses specifically on the specialised cell types which invade the circulatory system and establish distal metastasis. This thesis focused on the study of CSCs to understand the cellular composition of ovarian cancer, as based on the principles of the stem cell field, the CSC is the stem from which all other cancer cell types branch.

8.10 The experimental system established for this project systematically isolates ovarian CSCs and is readily transferable to patient samples and other malignancies:

Ovarian cancer disease progression follows closely that predicted by the CSC hypothesis. Approximately 70 % of cases generally respond well to first line therapy. However, recurrence is common and such recurrence is often refractory to further treatments, leading to poor clinical outcomes (Kikkawa et al. 2006). CSCs offer new therapeutic approaches to the treatment of ovarian cancer. The study of OvCSCs can lead to a better understanding of ovarian malignancy and to the design of better therapeutics with better clinical prognosis. As no models of OvCSC exist, OvCSCs must be identified and isolated from heterogeneous sources. The laboratory is

experienced in the study of CSCs, with most of the work being based upon established CSC model systems. This project was among the early attempts to isolate novel CSC populations in the laboratory. This meant that much of the methodologies utilised in this project had to be established and optimised during the course of this project (Section 3.0). A flow cytometric based pCSC screen was used to identify pCSC and non-pCSC across a diverse range of ovarian cancer models (Section 4.0). FACS was then used to isolate the most interesting of these pairs of pCSCs and non-pCSCs (Section 5.0). Isolated sub-populations were then brought forward to *in vivo* and *in vitro* validation experiments to validate them as CSC and non-CSC sub-populations (Section 6.0). This experimental design is very transferable to the study of other malignancies and patient samples. The only component of the entire system of investigation that has been specifically tailored to the study of OvCSCs is the panel of pCSC markers used (described in Section 1.9). To adapt this system to the study of CSCs in another malignancy, only requires the refinement of the pCSC markers used: the rest of the system can be applied as described in this thesis. To adapt this system to the study of CSCs in patient samples requires the establishment and optimisation of a technique of digesting the tumour samples into a viable single cell suspension. Once a single cell suspension has been acquired, the system of investigation can be applied to patient samples exactly as described in this thesis.

8.11 The data and materials produced in the screening and validation phases of this study identified models systems in which to study hierarchial cancer stemness and enabled the mapping of self-renewal and differentiation pathways within cancer stem cell hierarchies:

The future directions of individual experiments and sections were discussed in detail in the respective discussion sections of each chapter (Section 3.4, 4.4.5, 5.4, 6.4 and 7.4.2). As opposed to repeating these topics, this section will discuss the use of the data and materials produced in this project to enable future lines of investigation in the laboratory. As described above (Section 8.10), this project produced a system of investigation for the laboratory that enables several new studies of CSCs in other malignancies and patient samples. This project also produced enabling data and materials for future lines of investigation with respect to the ovarian cancer models used in this project.

The identification phase of this project identified multiple pCSC and non-pCSC sub-populations across several models of ovarian cancer (Section 4.3.5). Of all the models screened the IGROV-1 and IGROV-CDDP cell lines had the most diversity in pCSC sub-

populations (Section 4.3.5). These findings enable the use of the IGROV-1 and IGROV-CDDP model systems in further investigations, which will focus on the identification of the developmental relationships (if any) between the different CSC sub-populations identified within ovarian cancer. As these are a pair of cisplatin sensitive (IGROV-1) and cisplatin resistant (IGROV-CDDP) models the elucidation of the developmental relationships (hierarchies) of each CSC sub-population may lead to a better understanding of how different cell lineages may contribute to acquired cisplatin resistance in ovarian cancer (similar to that discussed in Sections 4.4.4.4.1). This finding of multiple sub-populations within one model system closely reflects the CSC heterogeneity observed in patient samples. As discussed in Section 6.4.1.2 Curley et al. (2009) and Silva et al. (2011) found that 100 % (n = 5) and 84.6 % (n = 13) respectively of patient samples had 4 or more pCSC sub-populations.

As described in Sections 4.3.1.1 and 4.3.1.2 several ALDH expression based sub-populations have been identified within the A2780 and A2780cis models: ALDH_NegA, ALDH+ and ALDH_NegB. The data described in Sections 6.3.1.2 and 6.3.2.2 suggest that these populations are organised into a hierarchical CSC lineage. This will be discussed further in Section 8.12. The analysis of this hierarchy led to the production of materials, which enable further lines of investigation within the laboratory. Both A2780 and A2780cis ALDH+ and ALDH- sub-populations were isolated via the work described in Section 5.0. Clones of ALDH_NegA CSCs which have differentiated and self-renewed to produce ALDH+ and ALDH- cells were produced via the SD assay described in Sections 6.3.1.2 and 6.3.2.2. Clones of ALDH+ CSCs which have differentiated and self-renewed to produce ALDH+ and ALDH- cells were also produced via SD assay described in Sections 6.3.1.2 and 6.3.2.2. Additionally, clones of ALDH_NegB non-CSCs were produced via the SD assay described in section Sections 6.3.1.2 and 6.3.2.2.. These materials have been stocked and can be used to enable future lines of investigation within the laboratory. Microarray gene expression analysis of these materials can be used to map the differentiation pathways which regulated the hypothesised differentiation of ALDH_NegA to ALDH+ to ALDH_NegB cells. Analysis of the differential gene expression of pure ALDH+ cells, isolated directly from the parent cell line, to ALDH+ clones which have differentiated and self-renewed via they SD assay should allow for the identification of the gene expression mechanisms involved in the differentiation of ALDH+ cells to ALDH- cells. As described in Section 7.4.2.5, comparison of the differential gene expression of ALDH_NegB clones to the pure ALDH- population isolated from the parent cell line should allow for the discovery of ALDH_NegA and ALDH_NegB markers. Once such markers have been identified

pure ALDH_NegA cells can be isolated from the parent cell line and compared (microarray) against the ALDH_NegA clones which have differentiated to produce ALDH+ cells. Such a comparison should identify the differentiation pathways involved in the differentiation of ALDH_NegA cells to ALDH+ and presumably ALDH_NegB cells. With such pathways identified, it should be possible to develop stable 'undifferentiated' CSC models of the ALDH_NegA and ALDH+ cell lines. For example the growth factors: bone morphogenic protein (BMP) and leukaemia inhibitory factor (LIF) are routinely used to maintain embryonic stem cells in an undifferentiated state. Addition/withdrawal of BMP and LIF can maintain embryonic stem cells in an undifferentiated/differentiated state respectively (Smith et al. 1988; Ying et al. 2003). Furthermore, the gene expression analysis should enable the identification of differentiation morphogens that allow for inducible differentiation of such models. For example the differentiation morphogen: retinoic acid is routinely used to force differentiate the Ntera2 cell line which is a pluripotent CSC model (Andrews 1984). Such models would emulate the teratocarcinoma models established in the 1980s (Andrews 1984). Such models would be a first in OvCSC biology and would greatly augment the rate at which the knowledge gap between somatic CSC biology and ES cell biology is closed. Additionally, any agent which could force differentiate the isolated OvCSCs, would be a potential therapy for the treatment of ovarian cancer.

8.12 CSC Hierarchies as opposed to CSC sub-populations may be better candidates for therapeutic targeting:

The data produced by the A2780 and A2780cis tumourgenicity (Sections 6.3.1.1 and 6.3.2.1) and SD (Sections 6.3.1.2 and 6.3.2.2.) experiments indicated the presence of an ALDH_NegA, ALDH+ and ALDH_NegB cellular hierarchy. Further experiments described in Section 7.0, confirmed ALDH_NegB cells as the least stem-like of the three sub-populations. The additional experiments required to fully understand the developmental relationships between these populations were described in Section 7.4.2. While other publications have started to identify more stem-like sub-populations within OvCSC populations (Silva et al. 2011), none have yet to publish evidence of the differentiation of one of these sub-populations directly leading to the production of the other. The data presented in this thesis has not yet demonstrated this either. However, the data and materials produced have the laboratory well positioned to carry out such experiments. The ALDH_NegA, ALDH+ and ALDH_NegB sub-populations could be the first step in the mapping of an OvCSC lineage. The identification of such sub-populations is a demonstration of the power the SD assay brings to the validation of CSCs, when used in

conjunction with the tumourgenicity assay. If this lineage is confirmed via future experiments, this system of investigation could be used to describe other lineages, marked by other CSC markers. This will facilitate the understanding of the various OvCSCs described in the literature and their roles in creating the different histologies and tissue characteristics seen in ovarian cancer. It will also facilitate the understanding of links between the different CSC sub-populations. It is important to establish if the various OvCSC sub-populations are developmentally linked or if they constitute independent CSC pools. Such information is important in the development of therapeutic strategies. As argued by Visvader and Lindeman (2012): the identification of multiple tumourigenic CSC populations within cancer complicates the task of directing therapies against them. As all independent CSC populations would need to be eliminated if the treatment was to be successful at removing the malignant potential of the tumour. However, if such CSC populations were linked in a hierarchical/developmental fashion, directing therapies against them may be a more simple affair. As demonstrated by Andrews (1984), it is possible for a single agent (retinoic acid; RA) to differentiate a highly undifferentiated pluripotent CSC population fully to a terminally differentiated state. As discussed in Section 1.13 RA is also used in the clinic to differentiate acute promyelocytic leukemia (Degos and Wang 2001). Understanding the cell biology of a tumour is key to deciding on the type of therapies which should be directed against it.

8.13 A 'Clonal Cancer Stemness' model of cancer predicts the failure of unilateral therapeutic approaches and suggests that alternative, multifaceted therapeutic approaches should be more successful:

Tumors are known to contain colonies of cells with divergent genetic mutations (Gerlinger et al. 2012). Cancer is also known to contain populations of different cell types attributable to differentiation (Marusyk et al. 2012). It is widely accepted that multiple genetic hits are required to establish a tumourigenic clone from a healthy somatic tissue (Hanahan and Weinberg 2011). These three observations can be united into one comprehensive model of tumourigenesis, which builds upon the model presented in Section 8.12. This model of 'clonal cancer stemness' may aid the development of more robust therapeutic approaches.

Given that multiple genetic mutations are required to transform a somatic cell into a tumourigenic clone, it can be stated that a lineage of cells exist along side the cancer cells

which is just one mutation away from becoming cancerous. In fact several such lineages should should exist which are 1 to 'n' mutations away from becoming cancerous (where 'n' is the number of genetic mutations it takes to transform a somatic tissue). If such pre-cancer mutations are occurring in SSCs (creating pre-CSCs), these cells should have the proliferative potential to maintain a pre-cancer lineage alongside the tumour proper. Such pre-cancer lineages could also accumulate divergent genetic mutations, such as chemoresistance, without be coming tumourigenic. If these pre-CSCs acquire an additional oncogenic mutation, the resulting novel CSC can seed the tumour with characteristics which do not appear to follow a stepwise acquisition of characteristics within the tumour. Divergent genetic mutations can lead to multiple clonal cell types within a tumour. For example some cells may acquire mutations which make them resistant to therapies that target cell proliferation. CSC differentiation can lead to cell heterogeneity within a tumour. Different cell types can confer different characteristics to the tumour. When these models are unified a 'clonal cancer stemness' model of tumourigenesis can be proposed. Such a model predicts failure of unilateral approaches to cancer therapy. However, multifaceted approaches could produce favourable outcomes.

Based on this 'clonal cancer stemness' model, a therapy directed against highly proliferative cells has multiple single point failures:

- A clonal lineage of cells, which has acquired chemoresistance via genetic mutation, can survive chemotherapy and result in chemoresistant disease with a dominant chemoresistant phenotype.
- The intrinsically resistant nature of CSCs may allow them to survive chemotherapy, adapt to the environmental stress and result in chemoresistant relapse.
- A dormant CSC population may also evade such a therapy, adapt to the environmental stress and result in chemoresistant relapse.

With so many points of failure in the anti-proliferation based therapy, a forced differentiation approach would at first appear to be a viable option. However, if it is possible for a spontaneous mutation to create a clonal lineage resistant to anti-proliferation drugs, then it is also possible for CSC clones to exist which are resistant to forced differentiation. So treating via forced differentiation will still leave a tumourigenic clone behind. One of the research interests of the laboratory is identification of such 'resistant to forced differentiation'. The study of two cell lines: NTera2 and 2102ep allows for the modelling of CSCs which are resistant to differentiation. The both cell lines are undifferentiated CSCs models. However, the NTera2

model (pluripotent) can be induced to differentiate via addition of retinoic acid to the culture media, whereas 2102ep cells (nullipotent) are resistant to this forced differentiation and do not differentiated in the presence of retinoic acid.

A combination of anti-proliferation and forced differentiation therapies would presumably be more successful, depending on the lower probability of clones being resistant to both therapeutic approaches. However there is still the problem of intrinsic resistance of dormant CSC pools. Harrison and Lerner (1991) demonstrated in mice that a single dose of 5-fluorouracil (5-FU; 1.5 mg/10 g body weight) can deplete both the myeloid and lymphoid compartments of the blood (~90 % reduction 4 days after treatment). However, the blood count would start to recover at about 8 days and be back to normal by 15 days. Mice treated with a second dose of 5-FU, one or eight days later, showed no reduction in the ability to reconstitute the blood cells. While mice treated with a second dose of 5-FU, three or five days later, showed a 75 % or 86 % reduced ability to reconstitute the blood cells. They suggest that the slow cycling haematopoietic stem cells (HSCs) are resistant to 5-FU due to their slow cell cycle. 5-FU is toxic during S-phase of the cell cycle. They suggest that the initial dose of 5-FU stimulates the HSCs to divide, allowing them to become sensitive to a second dose of 5-FU. Similar to this principle demonstrated by Harrison and Lerner it may be necessary to induce hyper proliferation of CSCs, before utilising the anti-proliferation and forced differentiation therapies. Such an approach should ensure all cells are actively dividing, making them more susceptible to the anti-proliferation therapy. The synergistic use of forced differentiation should overcome the intrinsically resistant nature of the CSC populations. This two stage (I: hyper-proliferation; II: anti-proliferation and forced differentiation) therapeutic strategy should only have one single point failure: namely a chemoresistant lineage that has acquired a resistance to forced differentiation.

Section 8.0: General Discussion

8.14 Summary:

This thesis described an approach to cancer research based upon a malignant organogenesis hypothesis. It focused on CSC biology as the method for understanding the malignant development of heterogeneous cells and tissues within cancer.

The experiments required to establish and optimise the CSC investigation model were described in Section 3.0. This investigation model was applied to the identification (Section 4.0), isolation (Section 5.0) and validation (Sections 6.0 and 7.0) of ovarian CSCs and non-CSCs. The data produced has given insight into the role of CSCs and possibly other sub-populations in the role of acquired chemoresistance in ovarian cancer (Sections 4.4.4.4.1 and 4.4.4.4.3). Multiple pCSCs and non-pCSC sub-populations were identified in the pCSC screen (Section 4.3.5). Sub-populations of interest were subsequently isolated (Section 5.0) and validated (Section 6.0). Two pairs of CSCs and non-CSCs were validated in a pair of cisplatin sensitive (A2780) and cisplatin resistant (A2780cis) models. Analysis of these CSC and non-CSC sub-populations has identified what could be the first cancer stemness hierarchy identified in ovarian cancer (Sections 6.0, 7.0). The materials produced from the isolation of CSCs and non-CSCs from cell lines, as well as the clones produced by the SD assay, has positioned the laboratory to be able to identify growth factors to maintain stemness in, or force differentiate ALDH_NegA and ALDH+ OvCSCs. Such growth factors could be used to generate a stable 'undifferentiated' OvCSC model which can be induced to differentiated *in vitro*. Such a model would be a first within the OvCSC field.

This thesis has presented the case for the study of CSCs. It applied the principles of CSC biology to the study of ovarian cancer. The data and materials produced have taken another step forward toward to the development of CSC directed cancer therapies, which are not susceptible to CSC driven relapse, metastasis and acquired chemoresistance.

Section 8.0: General Discussion

8.15 References:

Andrews, P W. 1984. "Retinoic Acid Induces Neuronal Differentiation of a Cloned Human Embryonal Carcinoma Cell Line in Vitro." *Developmental Biology* 103 (2) (June): 285–293.

Blackburn, Elizabeth H. 2005. "Telomerase and Cancer Kirk A. Landon - AACR Prize for Basic Cancer Research Lecture." *Molecular Cancer Research* 3 (9) (September 1): 477–482. doi:10.1158/1541-7786.MCR-05-0147.

Bohnsack, Brenda L, and Karen K Hirschi. 2004. "Red Light, Green Light: Signals That Control Endothelial Cell Proliferation During Embryonic Vascular Development." *Cell Cycle (Georgetown, Tex.)* 3 (12) (December): 1506–1511.

Brill, A, A Torchinsky, H Carp, and V Toder. 1999. "The Role of Apoptosis in Normal and Abnormal Embryonic Development." *Journal of Assisted Reproduction and Genetics* 16 (10) (November): 512–519.

Buchdunger, Elisabeth, Terence O'Reilly, and Jeanette Wood. 2002. "Pharmacology of Imatinib (STI571)." *European Journal of Cancer (Oxford, England: 1990)* 38 Suppl 5 (September): S28–36.

Curley, M. D., V. A. Therrien, C. L. Cummings, P. A. Sergent, C. R. Koulouris, A. M. Friel, D. J. Roberts, M. V. Seiden, D. T. Scadden, and B. R. Rueda. 2009. "CD133 Expression Defines a Tumor Initiating Cell Population in Primary Human Ovarian Cancer." *Stem Cells* 27 (12): 2875–2883.

Degos, L, and Z Y Wang. 2001. "All Trans Retinoic Acid in Acute Promyelocytic Leukemia." *Oncogene* 20 (49) (October 29): 7140–7145. doi:10.1038/sj.onc.1204763.

Deininger, M W, J M Goldman, N Lydon, and J V Melo. 1997. "The Tyrosine Kinase Inhibitor CGP57148B Selectively Inhibits the Growth of BCR-ABL-positive Cells." *Blood* 90 (9) (November 1): 3691–3698.

Deininger, M W, S Vieira, R Mendiola, B Schultheis, J M Goldman, and J V Melo. 2000. "BCR-ABL Tyrosine Kinase Activity Regulates the Expression of Multiple Genes Implicated in the Pathogenesis of Chronic Myeloid Leukemia." *Cancer Research* 60 (7) (April 1): 2049–2055.

Gerlinger, Marco, Andrew J. Rowan, Stuart Horswell, James Larkin, David Endesfelder, Eva Gronroos, Pierre Martinez, et al. 2012. "Intratumor Heterogeneity and Branched Evolution Revealed by Multiregion Sequencing." *New England Journal of Medicine* 366 (10): 883–892. doi:10.1056/NEJMoa1113205.

Gustafson, M L, and P K Donahoe. 1994. "Male Sex Determination: Current Concepts of Male Sexual Differentiation." *Annual Review of Medicine* 45: 505–524. doi:10.1146/annurev.med.45.1.505.

Hanahan, Douglas, and Robert A Weinberg. 2011. "Hallmarks of Cancer: The Next Generation." *Cell* 144 (5) (March 4): 646–674. doi:10.1016/j.cell.2011.02.013.

Harrison, D E, and C P Lerner. 1991. "Most Primitive Hematopoietic Stem Cells Are Stimulated to Cycle Rapidly after Treatment with 5-fluorouracil." *Blood* 78 (5) (September 1): 1237–1240.

Holtan, Shernan G, Douglas J Creedon, Paul Haluska, and Svetomir N Markovic. 2009. "Cancer and Pregnancy: Parallels in Growth, Invasion, and Immune Modulation and Implications for Cancer Therapeutic Agents." *Mayo Clinic Proceedings. Mayo Clinic* 84 (11) (November): 985–1000. doi:10.1016/S0025-6196(11)60669-1.

Kauff, Noah D, Susan M Domchek, Tara M Friebel, Mark E Robson, Johanna Lee, Judy E Garber, Claudine Isaacs, et al. 2008. "Risk-reducing Salpingo-oophorectomy for the Prevention of BRCA1- and BRCA2-associated Breast and Gynecologic Cancer: a Multicenter, Prospective Study." *Journal of Clinical Oncology: Official Journal of the American Society of Clinical Oncology* 26 (8) (March 10): 1331–1337. doi:10.1200/JCO.2007.13.9626.

Section 8.0: General Discussion

Kikkawa, Fumitaka, Akihiro Nawa, Kazuhiko Ino, Kiyosumi Shibata, Hiroaki Kajiyama, and Seiji Nomura. 2006. "Advances in Treatment of Epithelial Ovarian Cancer." *Nagoya Journal of Medical Science* 68 (1-2) (January): 19–26.

Leung, B S. 1987. "Perspective: Growth Factors in Normal and Abnormal Fetal Growth." *In Vivo (Athens, Greece)* 1 (6) (December): 363–368.

Martin, G R. 1975. "Teratocarcinomas as a Model System for the Study of Embryogenesis and Neoplasia." *Cell* 5 (3) (July): 229–243.

Marusyk, Andriy, Vanessa Almendro, and Kornelia Polyak. 2012. "Intra-tumour Heterogeneity: a Looking Glass for Cancer?" *Nature Reviews Cancer* 12 (5) (May 1): 323–334. doi:10.1038/nrc3261.

Miki, Y, J Swensen, D Shattuck-Eidens, P A Futreal, K Harshman, S Tavtigian, Q Liu, C Cochran, L M Bennett, and W Ding. 1994. "A Strong Candidate for the Breast and Ovarian Cancer Susceptibility Gene BRCA1." *Science (New York, N.Y.)* 266 (5182) (October 7): 66–71.

Mintz, B, and K Illmensee. 1975. "Normal Genetically Mosaic Mice Produced from Malignant Teratocarcinoma Cells." *Proceedings of the National Academy of Sciences of the United States of America* 72 (9) (September): 3585–3589.

Sherer, D.M., and O. Abulafia. 2001. "Angiogenesis During Implantation, and Placental and Early Embryonic Development." *Placenta* 22 (1) (January): 1–13. doi:10.1053/plac.2000.0588.

Silva, Ines A, Shoumei Bai, Karen McLean, Kun Yang, Kent Griffith, Dafydd Thomas, Christophe Ginestier, et al. 2011. "Aldehyde Dehydrogenase in Combination with CD133 Defines Angiogenic Ovarian Cancer Stem Cells That Portend Poor Patient Survival." *Cancer Research* 71 (11) (June 1): 3991–4001. doi:10.1158/0008-5472.CAN-10-3175.

Smith, Austin G., John K. Heath, Deborah D. Donaldson, Gordon G. Wong, J. Moreau, Mark Stahl, and David Rogers. 1988. "Inhibition of Pluripotential Embryonic Stem Cell Differentiation by Purified Polypeptides." , *Published Online: 15 December 1988; | Doi:10.1038/336688a0* 336 (6200) (December 15): 688–690. doi:10.1038/336688a0.

Szotek, P. P. 2006. "Ovarian Cancer Side Population Defines Cells with Stem Cell-like Characteristics and Mullerian Inhibiting Substance Responsiveness." *Proceedings of the National Academy of Sciences* 103 (30) (July 25): 11154–11159. doi:10.1073/pnas.0603672103.

Takahashi, Kazutoshi, Koji Tanabe, Mari Ohnuki, Megumi Narita, Tomoko Ichisaka, Kiichiro Tomoda, and Shinya Yamanaka. 2007. "Induction of Pluripotent Stem Cells from Adult Human Fibroblasts by Defined Factors." *Cell* 131 (5) (November 30): 861–872. doi:10.1016/j.cell.2007.11.019.

Visvader, Jane E, and Geoffrey J Lindeman. 2012. "Cancer Stem Cells: Current Status and Evolving Complexities." *Cell Stem Cell* 10 (6) (June 14): 717–728. doi:10.1016/j.stem.2012.05.007.

Wooster, R, G Bignell, J Lancaster, S Swift, S Seal, J Mangion, N Collins, S Gregory, C Gumbs, and G Micklem. 1995. "Identification of the Breast Cancer Susceptibility Gene BRCA2." *Nature* 378 (6559) (December 21): 789–792. doi:10.1038/378789a0.

Ying, Qi Long, Jennifer Nichols, Ian Chambers, and Austin Smith. 2003. "BMP Induction of Id Proteins Suppresses Differentiation and Sustains Embryonic Stem Cell Self-renewal in Collaboration with STAT3." *Cell* 115 (3) (October 31): 281–292.